Studies on Biodegradation and Biofiltration for Removal of Volatile Organic Compounds

THESIS

Submitted in partial fulfillment

of the requirements for the degree of

DOCTOR OF PHILOSOPHY

By

SMITA RAGHUVANSHI

Under the supervision of

Prof. B. V. Babu

BIRLA INSTITUTE OF TECHNOLOGY AND SCIENCE

PILANI (RAJASTHAN) INDIA

2009

BIRLA INSTITUTE OF TECHNOLOGY AND SCIENCE

PILANI, RAJASTHAN, INDIA

CERTIFICATE

This is to certify that the thesis entitled **"Studies on Biodegradation and Biofiltration for Removal of Volatile Organic Compounds"** and submitted by **Smita Raghuvanshi** ID. No. **2003PHXF408** for the award of Ph.D. Degree of the Institute embodies the original work done by her under my supervision.

Signature in full of the Supervisor _____

Name in capital block letters **Prof. B V BABU**

Designation Dean, Educational Hardware Division
Professor, Chemical Engineering Group
BITS Pilani, India

Date:

DEDICATED

TO

MY DEAR SISTER
who is responsible
for my being here
& MY PARENTS

ACKNOWLEDGEMENTS

I begin writing my acknowledgement by thanking my teacher, my Guide **Prof B V Babu**, Dean Educational Hardware Division for being my supervisor for my PhD. I thank him for his constant support throughout the PhD work from initial to the final level which enabled me to develop an understanding of the subject. I sincerely thank him for his encouraging words, showing his confidence in things which I could do, realizing me how to avoid doing small mistakes. I am thankful to him for making sure that all the required experimental facilities could be availed easily without which this work would have been impossible.

I thank the members of Doctoral Advisory Committee, Dr H K Mohanta, Assistant Professor and Mr Pratik N Sheth, Lecturer Chemical Engineering Group for their support and suggestions to carry out this work effectively.

My sincere thanks go to Prof L K Maheshwari, Vice-Chancellor, BITS Pilani for giving me the opportunity to carry out the PhD work in BITS Pilani. I am thankful to Prof V S Rao, Director (Hyderabad Campus); Prof K E Raman, Acting Director (Goa Campus); Prof R K Mittal, Deputy Director (Administration); Prof G Raghurama, Deputy Director (Academics) for providing the necessary infrastructure to carry out the work. I sincerely thank Prof Ravi Prakash, Dean Research and Consultancy Division for providing the necessary facility and always showing his concern towards the status of my PhD work. I am also thankful to Prof A K Sarkar, Dean Instruction Division and Faculty Division-I for his words of encouragement. I also thank my controlling officer Prof G Sundar, Dean Practice School Division.

My sincere thanks are due to the team of Research and Consultancy Division for providing the support and required information.

I very humbly thank Prof S K Verma, for giving time and being very patient in making me understand the procedure of bio-based experiments related to my PhD work. I also sincerely thank Dr A K Das for his time. I also thank Dr Arvind Kr Sharma, Group Leader Chemical Engineering Group for his initial help and support in carrying out the work. I also thank research scholars Narayan, Vishal and Shilpi for helping me in the bio-based experiments.

I extend my special thanks to Dr T N S Mathur, Dr Basudeb Munshi, Dr Madhushree Kundu, Mr Sushil Kumar, Mr Nikhil Prakash, Mr Ashish Gujrathi, Mr Amit Jain and Ms Priya C Sande for their support through out the work.

I would also take this opportunity to thank Mr Ashok Saini for his extended help and word of caution in carrying out the experimental work. Thanks are also due to Mr Jeevan, Mr Babu Lal Saini, Mr Jangvir, Mr Pramod, Sh Shankarmal ji, Sh Jamunadhar ji, Sh Mathuramji for their cooperation during my PhD work.

I also thank my friends Mathew, Shalini, Nitin for their moral support.

Words cannot describe my deep sense of gratitude for my mother, my father and my dear sister for their sacrifices to bring out best in me. They have showered their love, care, concern towards me. Their words of wisdom, encouragement and humbleness have made me a better person. I am very fortunate to thank my mother in law and sister in law Deepa, for their support in carrying out the work to completion. I also thank my brother in law, my Bhabhiji for their support towards the last phase of my work.

Now I thank the person without whom this work would not have been completed. I am fortunate to have by my side the love and care of my husband Suresh, who has been very encouraging and patiently helping me out in carrying out the experimental work and giving his full support in writing papers and Thesis. I sincerely thank him for always asking me to be focused on my work, the importance of being patient, virtue of doing things, realizing me not to repeat the mistakes. I say my utmost thanks to GOD for blessing me with a companion like him who shows that he cares for you by doing things. I also take this opportunity to thank our little daughter Namya for her cuteness, lovely smiles, her innocence which has brought bundles of joy in our life. I also would like to thank my sister`s son Vaibhav and my nephew Shaurya for their cute ways of bringing smiles on other`s face.

I pray to ALMIGHTY and thank him for being so kind, teaching me patience at every point of my life and giving me inner strength to take each work in a positive manner.

SMITA RAGHUVANSHI

ABSTRACT

The technological advancements in a day-to-day life and increased industrialization have affected the quality of air and water available for use. The major impact of industries on the environment is the emission of gaseous, liquid and particulate materials into the atmosphere which lead to air and water pollution. The polluted streams comprise of criteria pollutants and hazardous pollutants (as characterized by EPA). The criteria pollutants include sulfur dioxide (SO_2), nitrogen dioxide (NO_2), carbon monoxide (CO), ozone (O_3), suspended particulate matter (SPM), lead (Pb); while the hazardous air pollutants include Volatile Organic Compounds (VOCs), ammonia (NH_3), hydrogen sulfide (H_2S), etc. VOCs are the major pollutants released by the industries which contaminate the atmospheric air and the fresh water resources. VOCs are found to have adverse effects on human health even at very low concentrations. Certain VOCs such as toluene, methyl ethyl ketone (MEK), methyl iso butyl ketone (MIBK), isoprene, trichloroethylene, benzene and chloroform are carcinogenic in nature and other VOCs such as isopropyl alcohol (IPA), methyl acetate (MA), ethyl acetate (EA), butyl acetate (BA) also have serious health related affects on living beings. The petroleum hydrocarbons (benzene, toluene, etc.) are ground water pollutants which commonly result in leakage due to the or from storage tanks and spills. Thus, there is a need to control these emissions as they can cause serious damage to both humans and the environment.

The present work deals with the biodegradation and biofiltration studies for the removal of VOCs from water and air. The potential of microorganisms in consuming the VOCs as carbon source makes biodegradation an attractive option for the removal of pollutants from the waste water streams. Biofiltration is one of the bio-based techniques to prevent the air and water pollution. This process is cost effective and is efficient for the removal of VOCs over other physical and chemical methods. This study is focused on the batch biodegradation studies of VOCs such as MEK, MIBK, IPA, MA, EA and BA and biofiltration studies for the removal of MEK, MIBK, IPA and EA.

The exhaustive biodegradation experiments are carried out using acclimated mixed culture for the treatment of pollutants such as MEK, MIBK, IPA, MA, EA and BA. The batch experiments are carried out to study the effect of time on initial concentration and effect of time on biomass concentration. The concentration of VOCs is found decreasing with time which shows that the microorganisms consume the VOCs as they utilize it as a carbon source. The maximum value of specific growth rate is obtained as 0.391, 0.128, 0.210, 0.134, 0.137, and 0.141 h^{-1} for MEK, MIBK, IPA, MA, EA and BA at 400, 600, 400, 600, 500, and 500 mg L^{-1} of initial concentration respectively. The growth kinetic models such as Monod, Powell`s, Haldane, Luong and Edwards models are fitted with the obtained experimental data for a wide concentration range of 200 – 800 mg L^{-1}. The obtained results for different growth kinetic models indicate that the growth kinetics of acclimated mixed culture for biodegradation of MEK and IPA is better understood by Edward model but the biodegradation kinetics of MIBK, MA, EA and BA are better described by Luong model. The rate kinetic analysis is performed using zero-

order and three-half-order kinetic models. The three-half-order kinetic model is found suitable for the biodegradation of all VOCs used in the present study.

The continuous column studies are carried out for the removal of pollutants such as MEK, MIBK, IPA and EA on a laboratory scale biofilter column (of 5 cm diameter and 100 cm long). The 60 days phasewise studies on a biofilter column are carried out for the removal of MEK and MIBK. The operation time for the IPA and EA are 40 and 45 days respectively. It is observed that the removal efficiency at the initial period of acclimation is low which further increases with time and reaches to more than 90% removal efficiency for VOCs used in the present study. The bed height versus normalized concentration study is also carried out using all the VOCs in the present work. The industrial application of biofilter column is carried out by subjecting the column to shock loading conditions for a period of 16 days for MEK, 20 days for MIBK and 10 days for IPA and EA immediately after the 60 days of biofilter operation for MEK and MIBK, 40 days for IPA and 45 days for EA. The biofilter performance is also evaluated and discussed in terms of elimination capacity. The steady state values obtained for each phase of all VOCs are used in the estimation of the kinetic constants using Michaelis–Menten kinetic model. The coefficient of determination (R^2) obtained for MEK, MIBK, IPA, and EA are 0.99, 0.993, 0.996, and 0.991 respectively which are quite good and shows the applicability of Michaelis-Menten model for the biodegradation of MEK, MIBK, IPA, and EA. The obtained experimental data are also fitted with the Ottengraf-Van den Oever model.

The work also deals with the development of a mathematical model for the transient biofilter operated in a periodic and transient mode. The simulations results are obtained to understand the influence of various important parameters such as inlet VOC concentration, bed height and gas velocity on the biofilter column performance operated in the periodic mode. The standard deviation for MEK and butanol are obtained as 0.00242 and 0.000537 for the present model of periodic mode operated biofilter. A generalized mathematical model is proposed for the transient biofilter operated in continuous mode which incorporates the effects of gas biofilm resistances, possible extent of reaction in pores on biofilter, gas-phase mass transfer coefficient, and axial diffusion coefficient. The generalized mathematical model is validated with the available literature results and simulations are carried out to study the effect of significant parameters such as initial concentration, residence time (flow velocity) and bed height on the biofilter performance.

Keywords: *Volatile organic compounds; methyl ethyl ketone; methyl isobutyl ketone; isopropyl alcohol; methyl acetate; ethyl acetate; butyl acetate; biodegradation studies; growth kinetic models; rate kinetics; column studies; phasewise studies; shock loading conditions; transient biofilter; mathematical model.*

TABLE OF CONTENTS

LIST OF FIGURES

LIST OF PLATES

LIST OF TABLES

NOMENCLATURE

a	proportionality constant (biomass concentration^{-1} time^{-1})
A	interfacial area per unit volume, m^{-1}
A_b	biofilm surface area, m^2
A_T	cross sectional area of column, m^2
b	Langmuir adsorption equilibrium constant, m^3 g^{-1}
C	gas phase concentration, g m^{-3}
C_l	substrate concentration in liquid phase, g m^{-3}
C_b	substrate concentration in bulk gas, g m^{-3}
$C_{critical}$	critical inlet concentration, g m^{-3}
C_i	inlet gas phase concentration, g m^{-3}
C_e	outlet gas phase concentration, g m^{-3}
D	diffusion coefficient in the biofilm, m^2 s^{-1}
D_e	effective diffusion coefficient of pollutant in biolayer, m^2 s^{-1}
D_f	substrate diffusion coefficient in biofilm phase, m^2 s^{-1}
D_g	substrate diffusion coefficient in air, m^2 s^{-1}
D_L	dispersion coefficient, m^2 s^{-1}
D_s	substrate diffusion coefficient in solid phase, m^2 s^{-1}
D_v	dispersion coefficient in reactor, m^2 h^{-1}
D_w	substrate diffusion coefficient in aqueous phase, m^2 s^{-1}
E	cell concentration, g L^{-1}
h	Bed height, m
H	Henry`s constant, (-)
I	inhibitor in biodegradation kinetics, (-)
$IL_{critical}$	critical inlet load, g m^{-3} h^{-1}
J	diffusion flux into the biofilm, m^2 s^{-1}
k	mass transfer coefficient, s^{-1}
k_0	zero-order rate constant,

k_1	proportionality constant, s^{-1}
k_f	film transfer rate coefficient, m s^{-1}
$k_{ig\text{-}ads}$	overall mass transfer coefficient, s^{-1}
K	linear adsorption isotherm constant, m^3 g^{-1}
K_1	liquid phase mass transfer coefficient, m s^{-1}
K_{1a}	apparent first-order reaction parameter, s^{-1}
K_b	biofilm phase mass transfer coefficient, m s^{-1}
K_f	adsorption capacity constant for Freundlich isotherm, m^{3n} g^{-n}
K_I	inhibitor constant, g m^{-3}
K_m	Michael – Menten constant, g m^{-3}
K_s	substrate affinity constant, g m^{-3}
m	distribution coefficient for pollutant water system, (-)
m_c	moisture content of the packing material, (wt%)
n	adsorption constant for Freundlich isotherem, (-)
N	total number of biofilm subdivisions, (-)
N_P	number of packing material in the section, (-)
P	rate of product formation, Cell concentration $time^{-1}$
q	concentration of component in the solid media, g g^{-1}
q_s	saturation solid loading, g m^{-3}
r	mean radius, m
r_{max}	maximum degradation rate, g $m^{-3}s^{-1}$
r_X	rate of cell growth, kg cell m^{-3} s^{-1}
R_1	radius of particle, m
R_2	radius of particle + biofilm, m
R_3	radius of particle + biofilm + water film, m
R_4	radius of particle + biofilm + water film + gas film, m
R_S	rate of consumption of substrate in the support phase, g $m^{-3}s^{-1}$
R_{Sj}	degradation rate of component, j, g $m^{-3}s^{-1}$
S	substrate concentration in the biofilm, g m^{-3}
S_0	substrate concentration at zero time, g m^{-3}
S_{crt}	critical substrate concentration, g m^{-3}

S_f	aqueous phase substrate concentration in biofilm, g m^{-3}
S_{min}	threshold substrate concentration, g m^{-3}
S_w	aqueous phase substrate concentration in water film, g m^{-3}
t	time, s
v	Superficial gas velocity, m s^{-1}
V	volumetric gas flow rate, m^3 h^{-1}
V_0	interstitial gas velocity, m s^{-1}
V_1	superficial liquid velocity, m s^{-1}
V_m	maximum degradation rate, µg mL^{-1} h^{-1}
V_R	total reactor volume, m^3
U_g	superficial gas phase velocity, m h^{-1}
w	no. of biofilm subdivisions and biofilter stages, (-)
W	number of layer subdivisions, (-)
x	distance, m
X	cell concentration, kg cell m^{-3}
X_v	biofilm density, g m^{-3}
y	position along the biofilter height, m
z	distance from the inlet of the bed, m s^{-1}
Z	biofilm thickness where sorption volume is not counted, µm

Greek Symbols

α	fraction of bed covered by the biofilm, (-)
δ	Biofilm thickness, m
ε	bed porosity, (-)
μ	specific growth rate of microorganisms, h^{-1}
ν	Kinematic viscosity of water, m^2 s^{-1}
ρ_s	Density of adsorbent, kg m^{-3}
σ	Capacity ratio, (-)
τ	Dimensionless time, (-)
θ	position in the biolayer, (-)
ξ	Dimensionless superficial velocity, (-)

Subscripts

w	biofilter layer subdivisions : $1 \leq w \leq W$
n	biofilm and sorption volume subdivisions: $1 \leq n \leq N+1$
i	liquid phase concentration
f	biofilm concentration
g	gaseous phase concentration
i	initial

Superscripts

*	equilibrium
N	power exponent in biodegradation equation

Abbreviations

2,4,6 TCP	2,4,6- trichlorophenol
2,4-DCP	2,4-dichlorophenol
4-CP	4-chlorophenol
ACE	Acetone
CDR	Convection Diffusion Reaction
DMA	Di-methyl Amine
EA	Ethyl Acetate
EBRT	Empty Bed Residence Time
EC	Elimination Capacity
GAC	Granular Activated Carbon
GSIM	General Substrate Inhibition Models
HRT	Hydraulic Retention Time
IPA	Isopropyl Alcohol
LDFB	Linear Driving Force Biofiltration Model
MA	Methyl Amine
MEK	Methyl Ethyl Ketone
MIBK	Methyl Isobutyl Ketone

MLTSS	Mixed Liquor Total Suspended Solids
MTBE	Methyl Tert-Butyl Ether
MTBX	Methyl Ethyl Ketone, Toluene, *n*-Butyl Acetate, *o*-Xylene
ODEs	Ordinary Differential Equations
PAHs	Poly Aromatic Hydrocarbons
RE	Removal Effeciency
SCOD	Soluble Chemical Oxygen Demand
SEM	Scanning Electron Microscopy
SKIP	Sum Kinetics with Interaction Parameters
SRT	Solids Retention Time
STR	Stirred Tank Reactor
TBAB	Trickle Bed Air Biofilter
TCE	Trichloroethylene
THC	Total Hydrocarbon
TMA	Tri-methyl Amine
TSV	Total Sorption Volume
VOCs	Volatile Organic Compounds
VSS	Volatile Suspended Solids

CHAPTER – 1

INTRODUCTION

1.1. Air and water pollution

In the present age of the technological advancements, the quality of natural water and air are getting deteriorated. Improving the quality of the above is a much sought after topic of research. It has a great deal of practical significance also. The effect of increased industrialization has adverse impact on the environment thus leading to air pollution and water pollution. The major impact of industrial systems on the environment is the emissions of gaseous, liquid and particulate materials in the atmosphere which leads to air pollution. Air pollution is aggravated now-a-days because of economic development of societies across the world. The category of air emissions include the criteria pollutants given by the Environmental Protection Agency (EPA), USA which include sulfur dioxide (SO_2), nitrogen dioxide (NO_2), carbon monoxide (CO), ozone (O_3), suspended particulate matter (SPM) and lead (Pb) which are significant contributors in the deterioration of public health (USEPA, 1993). Another important category of pollutants is hazardous pollutants such as Volatile Organic Compounds (VOCs), ammonia (NH_3), hydrogen sulfide (H_2S), etc. which are responsible for major air and water pollution. Out of all listed hazardous pollutants, VOCs are the large group of organic compounds emitted into the atmosphere by a wide range of industries. In fact, VOCs are one of the major pollutants released by the industries which contaminate the atmospheric air and the fresh water resources.

1.2. Volatile organic compounds

VOCs are defined as organic chemical compounds which have high enough vapor pressures at normal conditions to significantly vaporize and enter into the atmosphere. As per the definition of EPA, VOC is an organic compound that participates in atmospheric photochemical reactions except those having negligible photochemical reactivity. The other definition given by EPA is that the VOCs are compounds which have a high vapor pressure and low water solubility. The Clean Air Act Amendments of 1990 (CAAA, 1990) has reported a list of 188 Hazardous Air Pollutants (HAPs). This list includes 82 VOCs which have vapor pressure ranging from 0.1 to 308 mm Hg at 25 ^{o}C. VOCs come from a variety of chemical classes which include aliphatic (methane, hexane, cyclo hexane), aromatic and chlorinated hydrocarbons (benzene, toluene, styrene, dichloromethane, trichloroethene), aldehydes (formaldehyde, acetaldehyde), esters (diethyl ether, methyl tert-butyl ether), alcohols (methanol, butanol) and ketones (methyl iso butyl ketone, methyl ethyl ketone, acetone).

VOCs are released into the atmosphere from various industries which include chemical, petrochemical, pharmaceutical, food processing, pulp and paper mills, color printing and coating, paint, rubber, fragrance, etc. (Devinny et al., 1999; Delhomenie et al., 2002; Hwang et al., 2003; Lu et al., 2004; Dehghanzadeh et al., 2005; Taghipour et al., 2008; Alvarez-Hornos et al., 2008). They are also released into the ambient air by sources such as motor vehicle exhaust, motor vehicle fuel evaporative losses, and tobacco smoke (Hinwood et al., 2006). Bulk of VOCs are released during petroleum storage and contaminate the quality of ground water. The VOCs released from these industries include methyl ethyl ketone (MEK), methyl isobutyl ketone (MIBK), aromatic

compounds (benzene, toluene, xylene), amines [triethyl amine (TEA), diethyl amine (DEA)], acetates [ethyl acetate (EA), methyl acetate (MA), butyl acetate (BA)], isopropyl alcohol (IPA), etc. It is reported in the National Emission Trends (NET) database prepared by US EPA that the total annual emissions of VOCs into the air is approximately two million tonnes nationally in 1999 (USEPA, 1995) from both the stationary and mobile sources. The Central Pollution Board (CPCB) of India has given the maximum emission limit of VOCs from the petrochemical plants as 0.1 g m^{-3}. The Minimal National Standards (MINAS) given by CPCB for VOCs emitted from stacks in rubber products manufacturing industries is 0.05 g m^{-3} (CREP, 2003).

1.2.1. Harmful effects of VOCs

The impact of a VOC on the environment depends upon the concentration and properties of individual compounds. However, majority of VOCs are found to have adverse effects on human health even at very low concentrations (0.1 g m^{-3}) (World Health Organization, 1990; 1993). Inhalation of low concentrations of VOCs can lead to headache, dizziness, nausea and cramps (Rene et al., 2005; Chang and Lu, 2003; Kim et al., 2008). The other harmful effects of VOCs are nose and throat discomfort, eye irritation, allergic skin reaction, fatigue and asthama exacerbation (Liu et al., 2002; Yoon and Park, 2002; Hwang et al., 2003). Odorous VOCs such as amines and esters cause serious discomfort in the working areas thus damaging public health as they lead to fatigue, skin reactions, etc. (Ho et al., 2008). Certain studies have reported that several VOCs such as toluene, methyl ethyl ketone, methyl iso butyl ketone, isoprene, trichloroethylene, benzene and chloroform are carcinogenic in nature. (Deshusses, 1994; Martin et al., 1998; Murata et

al., 1999; Yoon and Park, 2002). The exposure to VOCs can also lead to chronic health effects such as liver damage, kidney damage, and damage to central nervous systems.

VOCs contribute to tropospheric ozone production by reacting with oxides of nitrogen (NO_X) in the presence of sunlight which adversely affect the plants, animals and materials made up of natural and synthetic rubber, certain coatings and textiles (Derwent and Nelsen, 2002). The vast majority of VOCs have the potential to contribute to the global warming by absorbing infrared radiations (Bates et al., 2003). VOCs such as methane, non-methane hydrocarbons and chlorine containing substances are also identified as one of the sources of stratospheric ozone depletion besides, chlorofluorocarbons (CFCs) (Bates et al., 2003). The VOCs released from wastewater treatment plants or composting facilities cause green house effect and thus producing acid rain (Cohen, 2002). The petroleum hydrocarbons are common ground water pollutant as a result of leakage in storage tanks and spills (Goudar et al., 1999; Reardon et al., 2000).

Thus, there is a need to control these emissions as they can cause serious damage to both humans and the environment. The stricter air and water regulations have come up in recent years by various national and international pollution control boards which force industries to adapt better control technologies for the removal of VOCs from various polluted streams. Therefore there is a need for efficient pollution abatement techniques that can be used for the removal of VOCs from industrial effluent streams.

1.3. Abatement techniques for VOCs removal

1.3.1. Removal of VOCs from wastewater

The abatement techniques used for the treatment of VOCs from wastewater streams include the adsorption, absorption, stripping, pervaporation (membrane separation), biodegradation, etc.

Adsorption is an effective method for the removal of VOCs from wastewater streams. The wastewater is passed over the solid adsorbent and VOCs get adsorbed onto the adsorbents thus controlling water pollution. However, this technique is expensive as the cost of adsorbents is high and requires secondary treatment methods for regeneration and disposal of the used adsorbents.

In absorption and stripping operations, air or steam is passed through the wastewater. The VOCs are transferred from the concentrated wastewater to the less concentrated air streams in packed bed columns. The transfer efficiency depends on the contact area between the air and liquid. The absorption and stripping operations are carried out generally in oil and gas industries prior to the biological treatment to bring down the concentration range to the lower values.

The pervaporation is another method for the removal of VOCs which uses ceramic supported polymeric membranes. The method is costly over other methods as it needs expensive membranes

Now-a-days bio based technique named biodegradation is being used for the removal of VOCs from wastewater streams, where the VOCs get degraded by the microorganisms. Biodegradation is a technique in which microorganisms consume the organic compounds present in the wastewater as a sole carbon source and giving the end products such as

carbon-di-oxide, water and biomass. Hence it is well suited for the removal of VOCs from wastewater over the other methods.

1.3.2. Removal of VOCs from waste air streams

The VOC emissions in waste gas streams are a common problem due to the rapid industrialization. Thus, it requires efficient control techniques. The choice of technique depends on the total cost of operation, nature of compound being treated, the concentration, the flow rate and the mode of emissions of the gaseous waste streams (Devinny et al., 1999). The commonly used physicochemical air pollution control methods for removing VOCs in waste gas streams include processes such as thermal incineration, catalytic incineration, adsorption, absorption, condensation and membrane separation.

Thermal incineration and catalytic incineration are widely used techniques for the removal of waste gases. Thermal incineration involves the combustion of pollutants at temperatures ranging from 700 to 1400 ^{o}C. The catalytic incineration allows a temperature range between 300 to 700 ^{o}C with catalysts such as platinum and palladium. The costs involved with the thermal incineration are quite high as large amounts of fuel is involved to maintain the large temperature for the treatment of low concentrated pollutants. In the catalytic incineration, the cost of catalyst makes this method more expensive with the addition of fuel cost. The release of NO_X and some other gases during these methods may require further treatment of the secondary pollutants.

Adsorption is one of the most efficient methods for the treatment of low concentrated VOCs where vapors get adsorbed onto the surface of carbon or zeolites which are used as the adsorbents. The disadvantage of adsorption is that the bed is to be regenerated once it

has reached its adsorption capacity and thus lead to increased operating cost of the adsorption system. The cost of commercial adsorbents is also high and the disposal of the used adsorbent becomes a problem.

Absorption is another technique used for treating VOCs which requires the scrubbing solution (most commonly used is water) that mixes the gaseous pollutants with the solvent and removes it with its solution. Once the treatment has taken place, the additional treatment of the liquid phase is necessary to separate VOCs from the solvent. This is achieved by desorbing the pollutant at high temperatures and incinerating the vapors.

Condensation is generally a preferred technique when waste gas is highly concentrated with VOCs and having high boiling point values. The VOCs are partially recovered by simultaneous cooling and compressing the gaseous vapors. This technique is economical for the concentrated vapors where recycling of the streams are needed. The other side of the process is that if waste gas involves the mixed pollutant stream, additional separation techniques are required to separate the pollutants from the recycle stream which increases the cost of the process.

Membrane separation technique is relatively a newer technique which is used for the treatment of VOCs. In this process, compression and condensation is followed by a membrane system. The emission stream is compressed to approximately 310 to 1400 kPa, leading to higher vapor pressure on air-feed side than on the permeate side of the membrane. Thus pressure difference is created which is the driving force for the membrane separation process. The disadvantage of the process is that the process

requires treatment of the liquid permeate for final VOC disposal or recycling. The use of the costly membranes makes this process more expensive.

All these physico-chemical techniques are less effective, more expensive and require further secondary treatment methods before discharging into the atmosphere. Hence, there is a need to find a suitable control technique that can finally give the harmless end products without affecting the environment.

Biofiltration is one such technique in which degrading microorganisms are immobilized over a filter bed and degrade the organic pollutants (VOCs) into carbon-di-oxide, water and biomass. This process offers numerous advantages over other physical-chemical methods for the treatment of polluted gaseous streams contaminated with VOCs. This process is cost effective and is efficient for the removal of VOCs without generating any secondary pollutants.

1.4. Biological treatment methods

Biological based treatment methods are becoming more popular for the removal of VOCs from wastewater and polluted air over other treatment methods. These processes do not require external energy and utilize the capacity of microorganism to degrade a wide range of VOCs. Microorganisms (bacteria and fungi) act as catalyst and are able to utilize VOCs as a source of available carbon for further cell growth, the reaction of which is given by Eq. (1.1).

$$\mathrm{VOC} + \mathrm{O_2/Air} \xrightarrow{\text{microorgan isms}} \mathrm{CO_2} + \mathrm{H_2O} + \text{biomass} \qquad (1.1)$$

Biological treatment methods (for waste gases and wastewater) are considered to be efficient and cost effective for the treatment of contaminants as compared to other

physical or chemical treatment methods (Wright, 2005; Rene and Swaminathan, 2007). Biological treatment techniques such as biodegradation, biofiltration are the viable options for the removal of VOCs from wastewater and waste gaseous streams (Neal and Loehr, 2000).

1.4.1. Biodegradation

Biodegradation of VOCs is one of the most promising techniques for the removal of pollutants from wastewater streams. The potential of microorganisms in degrading these organic compounds into harmless biomass makes it an attractive alternative for the removal of VOCs (Nwaeke and Okpokwasili, 2003). The selection of microbial culture for the degradation of a particular VOC plays an important role in the successful use of this method. Several studies have been reported for the biodegradation of various volatile organic compounds using different microorganisms and are listed in Table 1.1.

The use of pure strain may lead to the formation of toxic intermediates and do not have the ability to completely mineralize the organic pollutants (Buitron and Gonzalez, 1996). The use of mixed culture for the biodegradation has an advantage over the pure strains. The advantage achieved by the mixed culture is the interaction between all the species present which enhance the biodegradation of VOCs (Kim et al., 2002). The biodegradation ability of the microorganisms can be further enhanced by use of the acclimated mixed culture (Buitron et al., 1998). The acclimation is a step that leads to the growth of trained community of microorganism that can easily degrade a particular organic compound and enhance the rate of biodegradation for the same.

Table 1.1. Studies on biodegradation of VOCs reported in the literature

S No	VOC	Type of microorganism species used	Reference
1.	Phenol	*Pseudomonas cepacia G4*	Folsom et al. (1990)
		Pseudomonas putida (MTCC 1194)	Kumar et al. (2005)
		Mixed culture	Saravanan et al. (2008)
2.	Trichloroethylene	*Pseudomonas cepacia G4*	Folsom et al. (1990)
3.	Chlorobenzene	*Pseudomonas* strain JS6	Pettigrew et al. (1991)
4.	Toluene	*Pseudomonas* strain JS6	Pettigrew et al. (1991)
5.	MEK and MIBK	Mixed culture	Geoghegan et al. (1997)
6.	Benzene, toluene, and phenol	*Pseudomonas putida*	Reardon et al. (2000)
7.	2,4- dichlorophenol	Mixed culture	Quan et al. (2003)
8.	2,4,6-trichlorophenol	Acclimated mixed culture	Snyder et al. (2006)

1.4.2. Biofiltration

Biofiltration is a relatively new environmental pollution control technology used in the treatment of wastewater and gaseous streams contaminated with biologically degradable compounds (Devinny et al., 1999). It is different from other biological treatment methods as in this technique, there is a separation between the microorganisms and the treated waste. This technique is different than the other reported methods as in this technique, microbial biomass is static (immobilized to the packing material) and the treated fluid is mobile (i.e it flows through the packing material) (Cohen, 2002). Biofilter is also defined as a packed bed column in which a microbial community grown on the packing surface carries out the biodegradation of the VOCs (Devinny et al, 1999). Contaminants pass into a wet biofilm layer surrounding the support particles and are aerobically degraded to carbon dioxide, water and biomass. The technique incorporates all the basic processes such as adsorption, absorption, degradation and desorption of gas-phase contaminants. It takes the advantage of metabolic and physiological flexibility, as well as the high adaptability of the populations of microbial species.

The performance of biofilter column majorly depends on the selection of microbial culture and packing material. The Table 1.2 lists the studies of various microbial cultures for the biofiltration of VOCs. The packing material should have the following properties: (i) it should provide a high surface area for the growth of microbial species; (ii) it should be porous in nature to promote the homogeneous distribution of polluted gases throughout the bed; and (iii) it should have good water retention capacity. The variety of materials used as packing include compost (Rene et al., 2005), soil, peat (Yoon and Park, 2002), coal (Chang et al., 2001), granular activated carbon (Ho et al., 2008), and other

porous media such as polyurethane foam (Moe and Irvine, 2001) and polypropylene pall rings (Cox et al., 2001) which are capable of adsorbing compounds and support microbial growth. The use of peat or coal as a packing material suffers from certain disadvantages such as not being able to provide enough nutrients or indigenous ecosystem for the microbial growth. The drawbacks of compost include the development of back-pressure due to gradual compaction with time, and aging effects due to microbial mineralization. Hence, there is a need to develop an innovative packing material which has the advantages over the above mentioned shortcomings. The performance of a biofilter operation also depends on the other significant parameters such as inlet load of VOCs, empty bed resistance time (EBRT), nutrient composition and its flow rate, temperature and moisture content.

1.4.3. Modeling aspects

The modeling in the bio-based techniques includes the estimation of growth kinetic constants using kinetic models such as Monod and Haldane models. The kinetic models such as Michaelis–Menten model, Ottengraf – Van den Oever model are used for the estimation of several biokinetic constants in order to understand the behavior of microorganisms in the biofiltration experiments as reported by Mathur and Mazumdar (2008) and Chan and Peng (2008). In addition, generalized biofiltration models are also developed in various studies as reported by Zarook et al. (1997) and Spigno et al. (2003). These developed models predict the concentration profiles with time and also useful in validating the experimental data generated though the experiments.

Table 1.2. Studies on removal of VOCs by biofiltration reported in the literature

S No	VOC	Type of microorganism species used	Reference
1.	MEK	*Rhodococcus sp.*	Amanullah et al. (2000)
2.	MIBK	*Cladosporium resinae, C. sphaeraspermum, Exophiala lecanii-corni, Phanerochaete chrysosporium*	Qi et al. (2002)
3.	EA	*Rhodococcus fascians*	Hwang et al. (2003)
4.	BA	*Cladosporium resinae, C. sphaeraspermum, Exophiala lecanii-corni,*	Qi et al. (2002)
5.	BTX (Benzene, Toluene, Xylene)	*Phanerochaete chrysosporium*	Oh et al. (1998)
6.	2,4,6-trichlorophenol	Acclimated mixed culture	Snyder et al. (2006)
7.	2,4- dichlorophenol	Mixed culture	Quan et al. (2003)

1.5. Need and importance of the present study

The studies on biodegradation of volatile organic compounds are limited to compounds such as phenol (Banerjee et al., 2001; Abuhamed et al., 2004; Saravanan et al., 2008), trichlorophenol (Andreoni et al., 1998; Aranda et al., 2003; Snyder et al., 2006), trichloroethylene (Nelson et al., 1986; Folsom et al., 1990), and aromatic compounds such as benzene (Pettigrew et al., 1991; Reardon et al., 2000), toluene (Pettigrew et al., 1991; Reardon et al., 2000). These studies were mainly focused on the biodegradation using pure culture. The use of pure strain may lead to the formation of toxic intermediates and do not have the ability to completely mineralize the organic pollutants (Buitron and Gonzalez, 1996). The use of mixed culture for the biodegradation has an advantage over the pure strains. The advantage achieved by the mixed culture is the interaction between all the species present which enhance the biodegradation of VOCs (Kim et al., 2002). The biodegradation ability of the microorganisms can be further enhanced by use of the acclimated mixed culture (Buitron et al., 1998). There is a lack of biodegradation studies for VOCs removal using mixed acclimated culture. Such studies also lacked in the kinetic aspects which are needed in order to understand the mechanism of biodegradation.

The biofiltration experiments are carried over the past two decades for variety of toxic compounds such as benzene (Abumaizar et al., 1998; Yoon and Park, 2002), toluene (Abumaizar et al., 1998; Auria et al., 2000; Moe and Irvine, 2001; Acuna et al., 2002), xylene (Abumaizar et al., 1998; Bibeau et al., 2000; Chang et al., 2001), ketones (Deshusess, 1994; Deshusses et al., 1997), amines (Ho et al., 2008), ethanol (Arulneyam and Swaminathan, 2000; Cox et al., 2001). These experiments were carried out either for one month, two months or six months and the effect of initial concentration of VOCs

were studied and removal efficiencies were calculated. The studies were mainly carried out using the packing materials such as peat, coal or compost. The microorganisms used were mainly pure cultures or mixed cultures obtained from the local wastewater treatment plants without acclimatization. But the studies on other toxic compounds such as ethyl acetate, isopropyl alcohol are scarce. The biofiltration needs to be studied in terms of shock loading conditions (changing inlet loads of VOCs in a gap of few days) so that it can be chosen as an industrial waste gas treatment technique. Also the effect of certain important parameters such as bed height and shock loading conditions on the performance of biofiltration were not studied.

The modeling of the biofiltration column was carried out by several researchers such as Deshusses, (1994); Zarook et al. (1997); Amanullah et al. (2000); Spigno et al. (2003). They made certain assumptions in their models such as neglecting the effects of gas biofilm resistances and radial dispersion. In most of the cases, the biodegradation kinetics was explained using the Monod kinetic model only. Also very few studies have been reported on the kinetic analysis using the Michaelis-menten model and Ottengraf-van den Oever model (Chan and Su, 2008; Mathur and Mazumdar, 2008).

Hence the present study is aimed at addressing some of these key aspects in biodegradation, biofiltration and in the modeling studies. The work includes the biodegradation studies for the removal of VOCs such as methyl ethyl ketone, methyl isobutyl ketone, isopropyl alcohol, butyl acetate, ethyl acetate and methyl acetate. The biodegradation kinetics are needed and carried out in the present work in order to understand the mechanism of degradation of VOCs using acclimated mixed culture. The kinetic data obtained from the batch experimental studies are helpful in the estimation of

the growth kinetic and the rate kinetic constants. This information helps in the determination and prediction of the potential risk which a VOC has on biodegradation in the natural environment. The kinetic constants such as maximum specific growth rate, saturation constant, inhibition constant, maintenance rate are useful in the selection of the microorganisms and the design of the biofilter column on large scale. The phenomenon of biofiltration can be well understood by carrying out exhaustive experiments on a lab scale biofilter column for long duration and for different VOCs of industrial importance. The experimental studies on biofiltration are needed to understand the behavior of microorganisms in the degradation of these VOCs and stability of biofilter column for the removal of higher inlet loads.

As the biofiltration process consists of complex interactions between physical, chemical and biological processes, a thorough understanding of the biofiltration process is required for the design of an industrial biofilter column. The various processes involved can be expressed in the form of mathematical equations using the mass and energy balances, microbial growth and rate kinetics, chemical and biochemical reactions, and stoichiometry. The determination of kinetic parameters is important in order to understand the kinetic behavior of biofilter system which is also helpful in the prediction of the efficiency (elimination capacity) of a biofilter column at a given operating condition. It is difficult to predict experimentally the behavior of biofiltration process under different conditions. Thus mathematical model can be used to understand the characteristics of biofiltration column under different conditions. It also helps to understand the relationship between various parameters such as surface area of filter bed, biological activity, biofilm thickness, etc. The mathematical models reported in literature

have not incorporated the effects of important aspects such as radial dispersion of air flow, gas biofilm resistances, possible extent of reaction in pores, gas-phase mass transfer coefficient, and axial diffusion coefficient in the performance of biofiltration process. These parameters are essential to incorporate in order to enhance the understanding of biofiltration process using a generalized mathematical model for a biofilter column.

1.6. Objectives

Based on the background of this field and the associated limitations of the existing literature, the objectives of the present study are formulated as:

To understand the physical aspects in modeling of biofilter for the removal of volatile organic compounds (VOCs).

To improve the existing models by incorporating the effects of radial dispersion of airflow, gas biofilm resistances, possible extent of reaction in pores on biofilter, gas-phase mass transfer coefficient, and axial diffusion coefficient which were reportedly neglected.

To carry out experiments for the removal of VOCs using:

Biodegradation studies

Biofiltration studies

To validate the proposed models with the actual experimental data obtained from the experiments and the data reported in the literature.

1.7. Organization of thesis

These mentioned objectives are achieved by carrying out an exhaustive literature survey on the removal of VOCs using biodegradation and biofiltration which is given in Chapter – 2. Chapter- 3 deals with the details of the experimental set up both for the batch studies (biodegradation) and the continuous studies (biofiltration). Various growth kinetic models and rate kinetic models obtained from the biodegradation studies and the improved mathematical model for biofilter column by incorporating the limitations of earlier studies are discussed in the Chapter-4. Chapter-5 includes the detailed results obtained by carrying out the biodegradation studies for VOCs and continuous biofiltration studies. The results are discussed based on a detailed parametric study. This chapter also includes the validation of proposed kinetic models from the results obtained by biodegradation studies. Validation of improved mathematical model from the experimental and modeling results reported in the literature is discussed in this chapter. Chapter-6 presents the conclusions of this study.

CHAPTER – 2

LITERATURE REVIEW

In this chapter, the literature on batch biodegradation studies, column studies and theoretical studies on biofiltration for the removal of various organic pollutants present in waste water and waste gaseous streams is presented in sections 2.1, 2.2 and 2.3 respectively. In the section 2.4, the existing gaps of research are discussed and scope of the present work is described in section 2.5.

2.1. Batch biodegradation studies

Klecka and Maier (1985) conducted batch experiments to examine the kinetics of pentachlorophenol by the enrichment culture. The batch experiments were carried out for an initial concentration range of pentachlorophenol from 200 – 2000 μg L^{-1}. It was observed that the rate of degradation of pentachlorophenol increased with time due to the growth of microorganisms. The inhibition was observed for the concentration more than 800 μg L^{-1}. The obtained results were then used for obtaining the kinetic constants using the Haldane`s model. The maximum specific growth rate (μ_m), substrate affinity constant (K_S) and substrate inhibition constant (K_I) were obtained as 0.074 h^{-1}, 60 μg L^{-1} and 1375 μg L^{-1}, respectively.

Dwyer et al. (1986) studied the phenol degradation by immobilized methanogenic consortium. The study focused on the development of proper immobilization technique for the biodegradation of phenol, survival of phenol degrading culture at higher

concentrations, and the development of kinetic model for the understanding of the rate kinetics. The kinetic analysis was performed using the inhibition models such as Andrews and Edwards model for the data generated through experiments. The scanning electron microscope showed three distinct kind of bacterial growth on the agar plates. The maximum degradation rate (V_m) for the immobilized culture was found to be 12 µg mL^{-1} h^{-1}, substrate affinity constant (K_S) obtained was 46 µg mL^{-1} and the substrate inhibition constant (K_I) reported as 1720 µg mL^{-1}.

Folsom et al. (1990) carried out batch studies for the degradation of phenol and trichloroethylene (TCE) by using a pure strain of bacteria known as *Pseudomonas cepacia G4*. TCE is considered to be a significant pollutant which migrate from soils and pollute the groundwater. The kinetics of the biodegradation of phenol and TCE, and the inhibition effect in the presence of these two compounds were also studied. The inhibition effect of high concentration of phenol was modeled using Haldane`s inhibition model and μ_m and K_S were obtained as 466 nmol min^{-1} and 8.5 µM respectively. The μ_m and K_S values for the degradation of TCE were obtained as 8 nmol min^{-1} and 3 µM respectively. They concluded that the *Pseudomonas cepacia G4* strain was able to degrade these pollutants.

Pettigrew et al. (1991) studied the biodegradation of chlorobenzene and toluene using *Pseudomonas JS6* strain. The study focused on finding the possibility of the degradation of mixtures of chloro- and methyl-substituted hydrocarbons. The study was carried out in a bioreactor and strain *JS6* was used for the degradation of benzene, toluene and chlorobenzene. Based on the experimental results, they concluded that the simultaneous

removal of chlorobenzene and toluene was possible. They also provided the pathway for the degradation of such compounds using strain JS6.

The biodegradation of methyl ethyl ketone (MEK) and methyl iso butyl ketone (MIBK) was carried out by Geoghegan et al. (1997) in a bioreactor with an enrichment culture obtained from the wastewater treatment plant of a pharmaceutical industry. The experiments were performed using 200 mg L^{-1} each of methyl ethyl ketone and methyl iso butyl ketone. The experiments were also performed by doubling the concentration of MEK or MIBK to 400 mg L^{-1} and maintaining the concentration of other compound as constant. The step-wise increase in the concentration of these two compounds was also carried out to observe the degradation effect of one compound over the other. The specific growth rate of 0.19 h^{-1} and 0.20 h^{-1} were obtained with methyl ethyl ketone (MEK) and methyl iso butyl ketone (MIBK) as single carbon substrate. However, the simultaneous utilization of MEK and MIBK as mixtures showed the specific growth rate of 0.21 h^{-1} for the enriched culture.

Kanaly and Harayama (2000) carried out a review on the biodegradation study of poly aromatic hydrocarbons (PAHs) which is considered to be toxic on human health. PAHs are released into atmosphere from petroleum refining sectors and from the transport activities. The study focused on various pathways for the degradation of PAHs using different bacterial strains such as *Pseudomonas paucimobilis, Sphingomonas yanoikuyae, Alcaligenes denitrificans, etc.* They presented various mechanisms of the degradation of PAHs combined with other hydrocarbons in the mixtures.

Reardon et al. (2000) studied the growth kinetics of *Pseudomonas putida* F1 for the biodegradation of benzene, toluene, and phenol individually and also their mixtures. The

rates of biodegradation were measured for the batch cultures. The SKIP (Sum kinetics with interaction parameters) model was used to study the biodegradation kinetics of mixtures of benzene, toluene and phenol. They also observed that the presence of toluene acts as the inhibitor in the consumption of other substrates such as benzene and phenol.

Peyton et al. (2002) studied the degradation of phenol by carrying out the batch experiments using five different cultures obtained from diverse saline environments. The obtained batch experimental data were tested with the Monod and Haldane models. The specific growth rate obtained was in the range of 0.22 to 0.32 $h^{-1}$for the five cultures with an initial phenol concentration of 50 mg L^{-1}. It was observed that the specific growth rate decreases on increasing the phenol concentration suggesting the role of inhibition at higher concentration of phenol.

Kumar et al. (2005) carried out the biodegradation of phenol and catechol using the bacterial strain *Pseudomonas putida* (MTCC 1194) in the shake flasks for concentration range of 0 – 1000 mg L^{-1} for phenol and 0 – 500 mg L^{-1} for catechol. They studied the acclimatization phase for both the compounds, effect of initial concentration on the degradation behavior of phenol and catechol and the growth kinetics. It was found that the well acclimatized culture of *Pseudomonas putida* (MTCC 1194) degraded the phenol and catechol in 162 h and 94 h respectively. The lag phase was found to increase with an increase in the initial concentration of phenol and catechol. The growth kinetics were estimated using the Monod model. The maximum specific growth rate and substrate affinity constants were reported as 0.216 h^{-1} and 20.59 mg L^{-1} for phenol and 0.143 h^{-1} and 9.66 mg L^{-1} for catechol. The inhibition effect was found to be apparent and hence

the results were fitted to the Haldane model. The biokinetic constants were estimated with a coefficient of determination (R^2) of 0.99.

Okpokwasili and Nweker (2005) studied the microbial growth and biodegradation kinetic models for various chemical contaminants. The study examined various kinetic models for the prediction of microbial removal of organic contaminants from the environment. The study gave an overview of the kinetic models such as Monod's, Andrews, Bungay's weighted model, general substrate inhibition models (GSIM) and sum kinetic models for the estimation of specific growth rates and degradation of organic substances. They concluded that the models need to be understood in detail for any bio based treatment processes.

The removal of acetone and methyl iso butyl ketone (MIBK) in a pilot scale activated sludge system was investigated by Quesnel and Nakhla (2006). The biodegradation was carried out by using the aerobic thermophilic bacterial consortium. The analysis was carried out in terms of mixed liquor total suspended solids (MLTSS), hydraulic retention time (HRT) and solids retention time (SRT). They found a substantial removal of acetone and MIBK throughout the experiments which showed a better performance than that of activated sludge system. The results were based on single substrate removal which followed the first order biodegradation kinetics. The kinetic rates obtained for the removal of rate obtained as 1.7 day^{-1} and 2.23 day^{-1} for acetone and MIBK removal.

The biodegradation kinetics of 2,4,6- trichlorophenol (2,4,6 TCP) using an acclimated mixed culture was investigated by Snyder et al. (2006). The acclimated mixed culture developed was used as an inoculum for bench scale experiments in a 4 L stirred-tank reactor (STR) with 2,4,6-TCP as the sole carbon source. The rate of degradation was

modeled with the zero-order kinetics. Biodegradation rates were compared for four operating conditions including two different initial 2,4,6-TCP concentrations and two different initial biomass concentrations. It was concluded that the lower biomass concentration gave a high zero-order specific degradation rate.

Shainkaya and Dilek (2007) investigated the biodegradation kinetics of 2,4-dichlorophenol (2,4-DCP) using two different mixed cultures: Culture M, which was acclimated to mixture of 4-chlorophenol (4-CP) and 2,4-DCP, and the other culture (Culture 4), which was acclimated only with 4-CP. The batch experiments were conducted in 500 mL Erlenmeyer flasks at 200 rpm and at 27 ^{o}C. The study also focused on the degradation ability of pure strain which was isolated from the mixed culture for degrading 2,4-DCP. It was concluded that the culture 4 degraded the 2,4-DCP up to 80 mg L^{-1} within 30 h and culture M completely degraded 2,4-DCP after 20 h. The self inhibition effect of 2,4-DCP was also observed at higher concentrations. The biokinetic constants such as substrate affinity constant (K_S) and inhibition constant (K_I) were obtained as 13.77 mg L^{-1} and 44.46 mg L^{-1} respectively culture M and 7.72 mg L^{-1} and 22.81 mg L^{-1} respectively for culture 4 using the Haldane model.

Saravanan et al. (2008) conducted batch studies for the degradation of phenol for concentration ranging from 100 - 800 mg L^{-1} using a mixed culture obtained from a local sewage treatment plant. The effect of initial concentration on phenol biodegradation and the effect of initial phenol concentration on the growth of microbial culture were studied. The inhibition effect was observed when the concentration of phenol is more than 500 mg L^{-1}. The growth kinetic data were fitted using the substrate inhibition models such as Haldane and Han–Levenspiel substrate models and the corresponding biokinetic

constants were evaluated. It was found that the Han-Levenspiel model fitted the experimental data for growth kinetics better than the Haldane`s model with the root mean square error obtained as 0.0211 as compared to 0.2020 obtained using the Han-Levenspiel model.

~

2.2. Column studies on biofiltration

Fortin and Deshusses (1999) carried out the experimental studies on the gas phase biotrickling filters for the removal of gasoline additive methyl tert-butyl ether (MTBE) which is of a great environmental concern. The work focused on the microbiological aspects of the process culture and on the steady-state performance of the biotrickling filter. It also involved the study of the dynamic behavior of the biotrickling filters under simulated field conditions. It was observed that the biotrickling filters adapted rapidly to the new conditions, and new steady state conditions were obtained within 15 hours of biofilter operation. It was concluded that the process was mostly limited by the biological reaction rather than by mass transfer which was important in order to understand the mechanism of biotrickling filters.

Bibeau et al. (2000) carried out the biofiltration studies for the removal of xylene vapors. The column was packed with peat balls which were specifically designed for the biofiltration experiments. Three types of microbial strains namely Strain *Drummond A, Drummond B and Drummond C* were used as the microbial culture. The operating parameters varied were temperature, pressure drop, and bacterial count. The performance of biofilter was assessed in terms of elimination capacity, conversion yields and carbon dioxide production. The results obtained highlighted that the elimination capacity (EC) of

60 g $m^{-3}h^{-1}$ was achieved when an inlet load of xylene was maintained as 110 g $m^{-3}h^{-1}$. This study revealed that a greater stability of biofilter column was achieved after 2 months of biofilter operation.

Chang et al. (2001) studied the performance of a trickle-bed air biofilter (TBAB) for the removal of ethyl acetate (EA) and xylene which are produced during polyurethane and epoxy manufacture respectively. Coal was used as the packing material and activated sludge was used as the microbial culture. The parameters such as soluble chemical oxygen demand (SCOD), volatile suspended solids (VSS) and pressure drop across the biofilter column were measured. The results obtained for EA and total hydrocarbon (THC) removal confirmed the suitability of TBAB during the manufacture of polyurethane. The results obtained for the removal of EA, xylene and THC during epoxy manufacture revealed that the performance of the TBAB was relatively poor due to the lack of volatile organic compound sources.

The treatment of ethanol vapors in biotrickling filters was investigated by Cox et al. (2001). Two reactors were operated in parallel, one at ambient temperature of 22 ^{o}C and the other at a high temperature of 53 ^{o}C. After a short adaptation phase, the removal of ethanol was similar in both the reactors. It was found from the obtained experimental results that the process was limited by biodegradation in the biofilm. The high-temperature biotrickling filter exhibited a higher degree of ethanol mineralization to CO_2. Hence, a lower rate of biomass accumulation was observed. Plating and cultivation of biofilm samples showed that the high-temperature biotrickling filter hosted a process culture composed of both mesophilic and thermophilic microorganisms, whereas the

ambient-temperature reactor lacked microorganisms capable of growing at high temperature.

The impact of nitrogen limitations on two toluene-fed biofilters were assessed by Moe and Irvine (2001) over a 97-day period operation. The biofilters were packed with the polyurethane foam medium and contained different initial levels of nitrate nitrogen. The investigation determined the effect of nutrient limitation on biofilter performance during both continuous flow and unsteady-state conditions. Packing medium samples were periodically removed and analyzed to quantify changes in nitrate-nitrogen content over time. The elemental analysis of biomass samples was conducted to determine the differences between biofilters operated with different initial nutrient levels. They observed that the consumption of nutrients by microbial culture and production of biomass affected the performance of biofiltration. The operation of biofilter under shock loading conditions found to increase the stability of biofilter column.

Yoon and Park (2002) studied the effects of parameters such as incoming gas concentration, empty bed residence time (EBRT), and column temperature for the removal of VOCs such as isoprene, dimethyl sulfide, chloroform, benzene, trichloroethylene, toluene, *m-xylene,* o-xylene and styrene. The biofilter column was made up of glass and packed with peat which was operated for 101 days of biofilter operation. It was found that the degradation of VOCs by microorganisms was affected by various environmental factors such as moisture content, temperature and pH. The maximum removal rate was achieved as 3977 g m^{-3} h^{-1} at 32 ^{o}C. The removal efficiency of aromatic compounds such as benzene, toluene, and xylene were obtained in the range

of 93-94%. The microbial cell concentration was increased to 100-fold from the initial value and reached to $1.12X10^{8}$ cells (g of dry peat)$^{-1}$ showing a good microbial growth.

Acuna et al. (2002) carried out experimental investigations using the sterile peat as biofilter medium for the removal of toluene for a period of 120 days. Four different concentrations of a nutrient solution were used in their study and the toluene consumption rate and CO_2 production were measured. The scanning electron microscopy (SEM) observations on biofilm formation were carried out to understand the influence of nutrient concentration on microbial distribution. It was observed that the toluene consumption rates were delayed in a peat biofilter medium amended with high nutrient concentration. The performance of the biofilter column increased gradually and reached higher values than those obtained with lower nutrient concentration. The results obtained in their study confirmed the achievement of early start-up period and high elimination capacity during the steady state operation of the biofilter column.

Spigno et al. (2003) assessed the performance of a biofilter column for the removal of hexane using a fungi named as *Aspergillus niger*. They investigated for the best operational conditions in terms of pollutant concentration and nutrients addition for the achievement of better removal efficiency. The acclimation period of 2 weeks was observed by the fungus used and the average elimination capacity was achieved as 150 g $m^{-3}h^{-1}$. It increased with the organic load until a maximum load was achieved as 300 g m^{-3} h^{-1}.The fungal development onto the support medium was monitored by SEM observations of expanded clay particles from the biofilters.

The performance of a trickle-bed air biofilter packed with coal and activated sludge was examined for the treatment of isopropyl alcohol (IPA) and acetone (ACE) mixtures under

different gas flow rates and inlet concentrations by Chang and Lu (2003). It was observed that the elimination capacities of isopropyl alcohol and acetome increased during pseudo-steady-state conditions but the removal efficiencies decreased with increased inlet carbon loading. The removal efficiency of isopropyl alcohol was achieved higher as compared to acetone. This indicated that IPA was the preferred substrate in the IPA and ACE mixtures. It was found that more than 90% removal efficiencies were achieved with inlet carbon loadings of IPA and ACE below 80 and 53 g m^{-3} h^{-1}, respectively.

Hwang et al. (2003) investigated the microbial degradation of ethyl acetate and toluene mixtures by conducting the biofiltration experiments. Three strains named as AC_6, TO_3 and B_5 were selected, identified and studied in a shake-flask culture to obtain the sufficient microbial culture for carrying out the biofiltration experiments. It was observed that the strain B_5 was a better choice for inoculation into biofilters than strains AC_6 and TO_3 as it grew rapidly under a low concentration of ethyl acetate.

Dehghanzadeh et al. (2005) carried out the biological treatment of waste gas which was contaminated with styrene vapor in a three-stage bench-scale biofilter. Yard waste compost mixed with shredded hard plastics in a 25:75 v/v ratio was inoculated with thickened municipal activated sludge. The performance was evaluated for regular operation of biofilter column which lasted for 420 days for an inlet concentration varying from 0.5 to 3.0 g m^{-3}, with respect to height of the biofilter column. It was found that the maximum elimination capacity obtained was 45 $gm^{-3}h^{-1}$ at a loading rate of 60 $gm^{-3}h^{-1}$ under steady state conditions. The elimination capacity was reduced from 39 to 27 g m^{-3} h^{-1} by the reduction of retention time from 60 s to 30 s. The concentration profile along the bed height indicated the dominance of first-order kinetics.

A compost-based biofilter unit inoculated with a mixed microbial population was used to treat the toluene vapors from a synthetic and real gas stream by Rene et al. (2005). The biofilter was operated continuously for a period of 8 months at different flow rates in the range of 0.024– 0.144 m^3 h^{-1}, with toluene concentrations ranging from 0.1 to 2.3 g m^{-3}. The biofilter performance along the column height and for various shock loading conditions were observed. The removal efficiencies were obtained in the range from 40 to 95% and elimination capacities ranged from 3.5 to 128 g $m^{-3}h^{-1}$ depending on the initial loading rates. The stability of the biofilter column was examined for a sudden change in inlet concentration of toluene from 1.5 to 2.3 g m^{-3} and around 92 % of the removal efficiency was obtained. The study also revealed the potential of biofilter column to handle the industrial gas mixtures with operation using a real sample from a pharmaceutical industry. The removal efficiencies of 60–90% for toluene and 60–80% for benzene from the gas mixture were achieved for an inlet pollutant concentration of 0.25 to 1.3 g m^{-3}.

A biofilter using granular activated carbon immobilized with *Paracoccus sp.* CP_2 was applied for the elimination of 10–250 ppm of trimethylamine (TMA), dimethylamine (DMA), and methylamine (MA) by Ho et al. (2008). The parameters such as effect of pH and effect of glucose on tri methyl amine removal were studied. The obtained results indicated that the system effectively treated methyl amine (>93%), di methyl amine (>90%), and tri methyl amine (>85%) under high loading conditions. The kinetic parameters such as maximum degradation rate (V_m) of *Paracoccus sp.* CP2 were obtained as 1.4, 1.2 and 0.9 g-N $kg^{-1}day^{-1}$ for methyl amine, dimethyl amine and trimethyl amine

respectively using Michaelis–Menten equation. It was also concluded that among the three different amines treated, TMA was the most difficult to degrade.

Biodegradation kinetics for the removal of ethyl acetate and amyl acetate using a composite bead biofilter were investigated by Chan and Su (2008). The microbial growth rate of ethyl acetate was greater than that of amyl acetate in the inlet concentration range of 100–400 ppm. The substrate affinity constant (K_s) values of ethyl acetate and amyl acetate were obtained as 16.26 and 12.65 ppm, respectively. The maximum reaction rate (V_m) values of ethyl acetate and amyl acetate were obtained as 4.08 and 3.53 g C h^{-1} kg^{-1} packed material, respectively. It was concluded that the biochemical reaction rate of ethyl acetate was greater than that of amyl acetate in the inlet concentration range of 100–400 ppm, and ethyl acetate was degraded by microbial culture easily than the amyl acetate.

Mathur and Mazumdar (2008) performed experiments for the removal of mixtures (MTBX) comprised of methyl ethyl ketone (MEK), toluene, *n*-butyl acetate and *o*-xylene emitted from the paint industry in a coal based bio-trickling filter. The experiments were divided into five phases lasting for 149 days by changing the flow rate and inlet loading of MTBX. The performance of the biofilter column was evaluated in terms of removal efficiency, elimination capacity, pressure drop along the bed length and microbial concentration. The kinetic constants were evaluated to understand the kinetic behavior of biotrickling filters. The results showed that the rate of biodegradation followed the order of *n*-butyl acetate, MEK, toluene and *o*-xylene. A maximum elimination capacity of 184.86 g m^{-3} h^{-1} was obtained at a MTBX load of 278.27 g m^{-3} h^{-1} with an empty bed residence time of 42.4 s in phase V. The maximum removal rate (r_{max}) values of MEK, toluene, butyl acetate, xylene (MTBX) were calculated as 0.085, 0.033, 0.16 and 0.024 g

m^{-3} h^{-1} respectively. The MTBX concentration profiles along the depth were also determined by using convection-diffusion reaction (CDR) model. It was observed that at low concentration and low flow rate, the model was in good agreement with the experimental values for MEK, toluene and *n*-butyl acetate, but for *o*-xylene the model results deviated from the experimental results.

Alvarez-Hornos et al. (2008) investigated the operation of two biofilter columns for the removal of high concentration of ethylbenzene vapors: one packed with the soil amendment granular high mineralized peat (35% organic content) locally available and the other packed with the fibrous peat (95% organic content) inoculated with a two-month conditioned culture. The effect of operating conditions such as inlet load and empty bed residence time (EBRT) were studied to assess the performance of two different packing materials. The Ottengraf–van den over model was used to analyze the experimental data obtained at 127 s for both the packing materials. The results showed that the maximum elimination capacity was achieved for the soil amendment biofilter of about 45 g m^{-3} h^{-1} for an inlet load of 55 g m^{-3} h^{-1} and about 120 g m^{-3} h^{-1} for an inlet load of 135 g m^{-3} h^{-1} for the fibrous peat biofilter. The zero-order kinetic constant (K_0) was obtained as 120 g m^{-3} h^{-1} for the fibrous peat and 44 g m^{-3} h^{-1} for soil amendment biofilter using the Ottengraf–van den oever model. The critical inlet concentration ($C_{critical}$) was obtained as 5.2 g m^{-3} and 2 g m^{-3} for fibrous peat and soil amendment biofilter respectively.

2.3. Theoretical studies on biofiltration

Deshusses et al. (1994, 1995a, b) developed the first model which described the transient behavior of biofilter. The basic modeling was carried out by dividing the biofilter height into several layers, denoted by *w*. Each layer was further divided into three main sections of gas phase, biofilm phase and liquid sorption volume. The mass balance over the gas phase was given by Eq. (2.1):

$$\frac{V_R \varepsilon}{W}\frac{dC}{\partial t} = V\left(C_{w-1} - C_w\right) - J_{\mathrm{W}}\frac{AV_R}{W} \tag{2.1}$$

where ($V_R\varepsilon$/W) is the volume of each gaseous subdivision, (AV_R/W) is the interfacial area, *W* is the total no. of layers and *w* is the layer considered $1 \le w \le \mathrm{W}$.

The mass balance over the biofilm was given by Eq. (2.2):

$$\frac{AV_R}{W}\frac{Z}{N}\frac{dS_{n,w}}{dt} = D\frac{AV}{W}\left(\frac{S_{n-1,w} - S_{n,w}}{Z/N} - \frac{S_{n,w} - S_{n+1,w}}{Z/N}\right) - R_{\mathrm{S_{j,n,w}}}\frac{AV_R}{W}\frac{Z}{N} \tag{2.2}$$

where (AV_{R} /*W*) (*Z*/*N*) is the volume of one biofilm subdivision, (AV_{R}/W) is its cross section and R_{Sj} is the rate of biodegradation and is given by Eq. (2.3):

$$R_{S_{n,w}} = \frac{r_{\max} S_{n,w}}{K_m\left(1 + I_{n,w}/K_I\right) + S_{n,w}} \tag{2.3}$$

The mass balance over the sorption volume was given by Eq. (2.4):

$$\frac{TSV}{W}\frac{dS_{n,w}}{dt} = D\frac{AV}{W}\left(\frac{S_{4,w} - S_{5,w}}{Z/N}\right) \tag{2.4}$$

TSV is the total sorption volume represented by difference between the volume of water in the system and that of the biofilm given by Eq. (2.5):

$$TSV = V_R\left(1-\varepsilon\right)mc - V_R AZ \tag{2.5}$$

The equations were solved using the SimuSolv program which is an interactive mathematical modeling tool for simulating physical systems defined by algebraic and

differential equations. The model results were validated using the MEK and MIBK column results and dynamic response of the biofilter column was evaluated by Deshusses et al. (1994, 1995a, b). Based on the results obtained, it was concluded that the biodegradation of MEK and mixtures of MEK and MIBK were subjected to the overall limitation by the biodegradation rate.

Amanullah et al. (2000) carried out the equilibrium and kinetic studies of methyl ethyl ketone (MEK) by carrying out the biofiltration experiments and the theoretical studies. The work dealt with different modes of operation which included adsorption in compost and granular activated carbon (GAC), the reaction rate and selectivity of microorganisms for MEK biodegradation, and the role of adsorption capacity of the support medium on biofilter dynamics were investigated. The equations were solved by using the linear driving force biofiltration model (LDFB). The gas phase substrate balance was given by Eq. (2.6):

$$\frac{\partial C}{\partial t} = D_L \frac{\partial^2 C}{\partial t} - V_0 \frac{\partial C}{\partial z} - \frac{1-\varepsilon}{\varepsilon}\left[k\left(q^* - q\right)\right] \tag{2.6}$$

The initial condition was given by Eq. (2.7):

$$C(z,0) = 0 \tag{2.7}$$

The boundary conditions were given by Eqs. (2.8) and (2.9):

$$D_L \frac{\partial C}{\partial z} = -V_0\left(C\ |_{0-} - C\ |_{0+}\right) \tag{2.8}$$

$$\left.\frac{\partial C}{\partial z}\right|_{z=1} = 0 \tag{2.9}$$

The support phase substrate balance was given by Eq. (2.10):

$$\frac{\partial q}{\partial t} = -k\left(q^* - q\right) - R_S \tag{2.10}$$

The initial condition was given by Eq. (2.11):

$$q(z,0)=0 \tag{2.11}$$

The linear and Langmuir isotherms for compost and GAC were given by Eqs. (2.12) and (2.13):

$$q^{*} = KC \tag{2.12}$$

$$\frac{q^{*}}{q_S} = \frac{bC}{1+bC} \tag{2.13}$$

The biodegradation reaction was given by Eq. (2.14):

$$R_S = \frac{r_{\max} q}{K_m + q} \tag{2.14}$$

The partial differential equations from (2.6) – (2.14) were transformed into dimensionless form and then discretized in space using the method of orthogonal collocation. The resulting set of ordinary differential equations were solved using the Gear`s multistep method given in MATLAB. They concluded that the adsorption of MEK was linear in the entire range of concentrations using compost while in case of GAC as adsorbent, the adsorption isotherm was highly non-linear. They could explain the biofilter dynamics using the LDFB model.

A mathematical model was developed for biofilter design and the performance of biofilter column was predicted for the purification of contaminated gas streams by Den and Pirbazari (2002). The model considered a spherical adsorbent particle, a biofilm of constant thickness, external liquid film with defined thickness and a hydrodynamic gas layer. The model incorporated the important aspects such as mass transfer, biodegradation, and adsorption processes. The mass balance of the hydrodynamic gas film was given by Eq. (2.15):

$$\frac{\partial C}{\partial t} + V\frac{\partial C}{\partial r} = D_g \frac{1}{r^2}\frac{\partial}{\partial r}\left(r^2 \frac{\partial C}{\partial r}\right) \tag{2.15}$$

The initial and boundary conditions were given by Eqs. (2.16), (2.17), and (2.18):

$$C(r, t=0) = 0 \tag{2.16}$$

$$D_g \frac{\partial C(r=R_3, t)}{\partial r} = k_f \left(S_{g,l} - S_{l,f}\right) \tag{2.17}$$

$$C(r \to \alpha, t) = C_b \tag{2.18}$$

The mass balance for the external liquid film was given by Eq. (2.19):

$$\frac{\partial S_w}{\partial t} = D_w \frac{1}{r^2}\frac{\partial}{\partial r}\left(r^2 \frac{\partial S_w}{\partial r}\right) \tag{2.19}$$

The initial and boundary conditions were given by Eqs. (2.20), (2.21), and (2.22):

$$S_w(r, t=0) = 0 \tag{2.20}$$

$$D_w \frac{\partial S_w(r=R_2, t)}{\partial r} = D_f \frac{\partial S_f(r=R_2, t)}{\partial r} \tag{2.21}$$

$$S_w(r=R_3, t) = \frac{C(r=R_3, t)}{H} \tag{2.22}$$

The mass transfer within the biofilm was given by Eq. (2.23):

$$\frac{\partial S_f}{\partial t} = D_f \frac{1}{r^2}\frac{\partial}{\partial r}\left(r^2 \frac{\partial S_f}{\partial r}\right) - X_v \frac{\mu_m S_f}{K_s + S_f} \tag{2.23}$$

The initial and boundary conditions were given by Eqs. (2.24), (2.25) and (2.26):

$$S_f(r, t=0) = 0 \tag{2.24}$$

$$D_f \frac{\partial S_f(r=R_1, t)}{\partial r} = D_S \rho_s \frac{\partial q(r=R_1, t)}{\partial r} \tag{2.25}$$

$$S_f(r=R_2, t) = S_w(r=R_2, t) \tag{2.26}$$

The mass balance for the adsorbent phase was given by Eq. (2.27):

$$\frac{\partial q}{\partial t} = \frac{D_S}{r^2}\frac{\partial}{\partial r}\left(r^2\frac{\partial q}{\partial r}\right) \tag{2.27}$$

The initial and boundary conditions were given by Eqs. (2.28), (2.29) and (2.30):

$$q(r, t=0) = 0 \tag{2.28}$$

$$\frac{dq(r=0,t)}{dr} = 0 \tag{2.29}$$

$$q_s = q(r=R_1, t) = K_f S_{f,s} n \tag{2.30}$$

The partial differential equations from Eqs. (2.15) – (2.30) were discretized into ordinary difference equations (ODEs) by using the backward difference formula with time derivatives written in the dimensionless form and solved by using an implicit finite difference scheme. The ODEs were solved iteratively. The model results were validated by carrying out the experiments using trichloroethylene as a pollutant. The developed model was in good agreement with the experimental results under different operating conditions.

Spigno et al. (2004) developed a simple model to fit the experimental data considering certain assumptions such as the formation of biolayer only on the exterior surface of the particles and considered that no reactions occurred in the pores; the pollutant and oxygen at the biolayer / air interface were in equilibrium and was given by Henry`s law and the biofilm density was considered as constant. The mass balance of the pollutant in the gas phase was given by Eq. (2.31):

$$\frac{D_v \partial^2 C}{\partial h^2} - \frac{v \partial C}{\partial h} + D_e \alpha A \frac{\partial S}{\partial \theta}\Big|_{\theta=0} = 0 \tag{2.31}$$

The Eq. (2.31) was solved with the boundary conditions given by Eqs. (2.32) and (2.33):

$$At\ h = 0;\ \ \frac{D_v}{v}\frac{\partial C}{\partial h} = C - C_0 \tag{2.32}$$

$$At\ h = 1;\ \ \frac{\partial C}{\partial h} = 0 \tag{2.33}$$

The mass balance of the pollutant in the biological phase was given by Eq. (2.34):

$$\frac{D_e \partial^2 S}{\partial \theta^2} - \frac{X_v \mu^* S}{Y\left(K_S + S + \frac{S}{K_I}\right)} = 0 \tag{2.34}$$

The boundary conditions for solving Eq. (2.34) were given by Eqs. (2.35) and (2.36):

$$0 \le h \le H\ \ ;\theta = 0;\ S = \frac{C}{m} \tag{2.35}$$

$$0 \le h \le H\ \ ;\theta = \delta;\ \frac{\partial S}{\partial \theta}\Big|_{\theta=\delta} = 0 \tag{2.36}$$

Eqs. (2.31) - (2.36) were solved in dimensionless form using computer code developed using gPROMS according to the method-of-lines family of numerical methods. The modeling results were validated by carrying out the biofiltration experiments using hexane as pollutant.

Certain researchers have focused on the kinetic modeling of biofiltration system in recent years in order to understand the degradation of VOCs using microbial culture. One such work was carried out by Park et al. (2004) who carried out the kinetic modeling on biofiltration such as first order reaction model, Ottengraf model, Ottengraf-van den Oever model and van Lith et.al model. All the models were fitted with the experimental data obtained by carrying out the biofiltration for the removal of toluene. They studied the Ottengraf model (Ottengraf, 1986) which was proposed in 1986 and given by Eq. (2.37):

$$\ln\left(\frac{C_e}{C_i}\right) = \frac{H}{mV_0} K_{1a} \tag{2.37}$$

The value of the constant K_{1a} was calculated by plotting the graph between ln (C_e/C_i) and (H/mV_0). Ottengraf-Van den Oever model (1983) was used to obtain the removal efficiency for toluene using Eq. (2.38):

$$\left(\frac{C_e}{C_i}\right) = \left(1 - \frac{aH}{U_g}\sqrt{\frac{K_0 D_e}{2C_i}}\right)^2 \tag{2.38}$$

They also studied the Van Lith et al. (1990) model which related the elimination capacity (EC) of the biofilter column with the inlet and outlet concentration and time. The model is represented by Eq. (2.39):

$$EC = \frac{2}{t} X (C_i - \sqrt{C_i}\sqrt{C_e}) \tag{2.39}$$

Eq. (2.39) was solved by plotting the graph between the obtained elimination capacity and [C_i- (C_i X C_e)] for different flow rates. They mentioned that such models help in the prediction of removal efficiencies and the elimination capacities which further are useful in the design of biofilter column at industrial scale.

Chmiel et al. (2005) studied the periodic operation of biofilters. The mass balance equation for the gas phase was given by Eq. (2.40):

$$\frac{\partial C}{\partial t} = D_L \frac{\partial^2 C}{\partial x^2} - V\frac{\partial C}{\partial x} - \frac{1-\varepsilon}{\varepsilon} k_{ig-ads}\left(q^* - q\right) \tag{2.40}$$

The initial and boundary equations were given by Eqs. (2.41), (2.42) and (2.43):

$$C(x,,0) = 0 \tag{2.41}$$

$$\left.\frac{\partial C}{\partial x}\right|_{x=H} = 0 \tag{2.42}$$

$$D_L \left.\frac{\partial C}{\partial x}\right|_{x=0} = -V\left(C\ |_{0-} - C\ |_{0+}\right) \tag{2.43}$$

The mass balance and the initial conditions for the solid phase were given by Eqs. (2.44) and Eq. (2.45):

$$\frac{\partial q}{\partial t} = k_{ig-ads}\left(q^* - q\right) - r_S \tag{2.44}$$

$$q(x,,0) = 0 \tag{2.45}$$

The rate of biodegradation (r_s) was given by Eq. (2.46):

$$r_S = \mu \frac{q^N}{K_m + q} \tag{2.46}$$

The set of Eqs. (2.40) – (2.46) were solved using the gPROMS codes. The results were obtained for the concentration versus time and were validated with the MEK and *n*-butanol. It was concluded that the use of appropriate biodegradation kinetic equation was helpful in obtaining a good agreement between predicted and the experimental results.

A mathematical model which accounted for bioreaction and mass transfer was developed to study the degradation of contaminant present in waste water in biofilter by Agarwal and Ghoshal (2008). The developed model was then used to predict the dynamics of biofiltration operation using different parameters such as inlet substrate concentration, liquid phase mass transfer coefficients, particle size, Henry`s constant, growth and half saturation constants. The mass balance equation for the substrate in the liquid phase was given by Eq. (2.40):

$$\left(V_0 A C_1\right)_y - \left(V\ A C_1\right)_{y+dy} - K_1\left(C_1 - C_{1i}\right) N_P A_b = A_T dy \varepsilon \frac{\partial C_1}{\partial t} \tag{2.40}$$

The initial and boundary conditions to solve this equation were given by Eqs. (2.41) and (2.42):

$$At\ t = 0; C_1 = 0; for\ all\ y \tag{2.41}$$

$$At\ y = 0; C_1 = C_{10} \tag{2.42}$$

The mass balance equation for the substrate in the biofilm phase and initial conditions were given by Eqs. (2.43) and (2.44):

$$K_b(S - S_i)N_P A_b - rV_b N = V_b N \frac{\partial S}{\partial t} \tag{2.43}$$

$$At\ t = 0; S = 0; for\ all\ y \tag{2.44}$$

The rate of biodegradation was given by Monod kinetics. Eqs. (2.40) – (2.44) were solved using the POLYMATH software. The developed model was validated with the data available in the literature.

2.4. Existing gaps for research

The reported studies for the biodegradation of VOCs are limited to certain specific compounds such as phenol, trichlorophenol, dichlorophenol, benzene, toluene, xylene, dichlorobenzene, and trichloroethylene. Very few studies have reported the biodegradation of other widely used compounds such as methyl ethyl ketone, methyl isobutyl ketone, isopropyl alcohol, esters etc. These compounds are used as solvents in petrochemical, rubber, pulp and paper industries, etc. These compounds are also considered as toxic, hazardous, carcinogenic and mutagenic and hence are harmful when released into the atmosphere. The few experimental studies carried out using pure strain for the biodegradation of these compounds are not sufficient to understand the mechanism of biodegradation. The use of pure strain may lead to the formation of toxic intermediates and do not have the ability to completely mineralize the organic pollutants.

The use of mixed culture for the biodegradation has an advantage over the pure strains. There is a lack of biodegradation studies for VOCs removal using mixed acclimated culture. Past studies on biodegradation growth kinetics are mainly focused on Monod kinetic model which do not give the complete insight of the mechanism of biodegradation because it does not include the substrate inhibition effect. Some studies have reported the application of Haldane model which considers the effect of substrate inhibition. But it is not sufficient to explain the growth kinetics of all compounds (Edwards, 1970; Luong, 1986). Other substrate inhibition models such as Luong model and Edward model are not studied in the previous works.

The literature on biofiltration experimental studies suggested that very few researchers have carried out the biofiltration experiments (continuous column studies) for the removal of certain high priority toxic VOCs such as MEK, MIBK, IPA and ethyl acetate etc. Biofiltration experiments for these compounds are needed to understand the effect of significant parameters such as bed height, inlet load, and stability of the biofilter column. Biofiltration column studies are essential to in collecting the experimental data for the design of biofilter column at pilot plant scale as well as at an industrial scale.

The modeling of biofilter column is always considered to be quite challenging task as it incorporates the microbial degradation which is quite complex to understand. The existing literature on the modeling of biofilter column point out good attempts have been made in understanding the modeling aspects of biofiltration column. Few studies have focused on the kinetic modeling (Michaelis–Menten model, Ottengraf – Van den Oever model, etc.) of biofilter column which is useful in the estimation of bio-kinetic constants that are required for the design of biofilter column. The mathematical models

for biofiltration column, which are available in the literature, neglected some of the important physical aspects of biofiltration process. The effect of radial dispersion is excluded in several studies reported in the literature. Many studies have not incorporated the effect of gas biofilm resistances and the adsorption of VOCs on the uncovered portion of the packing material by biofilm in the modeling of biofilter column. Because of the complexity of substrate inhibition growth kinetic models, most of the studies have described the growth kinetics by the Monod model only in the modeling of biofiltration column.

2.5. Scope of the present study

There is a need to carry out the batch studies for the biodegradation of volatile organic compounds such as methyl ethyl ketone, methyl isobutyl ketone, isopropyl alcohol and esters in order to understand the mechanism of biodegradation. In this study, biodegradation experiments are performed using acclimated mixed culture. Data obtained using biodegradation experiments are fitted with various growth kinetic models such as Monod, Haldane, Luong and Edward model. The obtained growth kinetic models help in the understanding of the behavior of microorganisms in degrading the VOCs. The rate kinetic data are tested with zero-order and three-half-order rate kinetic models.

There is a lot of scope to carry out the biofiltration column studies for the removal of organic pollutants such as methyl ethyl ketone, methyl isobutyl ketone, isopropyl alcohol and ethyl acetate by changing various important parameters such as air flow rate and inlet concentration to study their effects. The biofiltration experiments (column studies) are carried out to get an idea about the adaptability of the microorganisms in the

changed operating conditions and thus obtaining the required removal efficiency. Such studies will thus help in the estimation of required parameters needed for the design of the biofilter column on bench scale and on industrial scale.

The work also deals with the development of the Michaelis-Menten kinetic model and the Ottengraf-Van den Oever model from the biofiltration experiments carried out for the removal of methyl ethyl ketone, methyl isobutyl ketone, isopropyl alcohol and ethyl acetate for the estimation of biokinetic constants. The present work also includes the development of the mathematical model for the biofilter column incorporating the limitations of the earlier studies. The performance of the developed model is tested with the available data from the literature and with the data generated in the present study.

CHAPTER – 3

EXPERIMENTAL STUDIES

The present chapter deals with the details of experimental work carried out for the batch biodegradation studies for removal of methyl ethyl ketone (MEK), methyl isobutyl ketone (MIBK), isopropyl alcohol (IPA), methyl acetate (MA), ethyl acetate (EA) and butyl acetate (BA) from liquid phase and continuous column biofiltration experiments for the treatment of MEK, MIBK, IPA and EA present in air stream.

3.1. Biodegradation studies for the removal of VOCs used in present study

3.1.1. Batch experimental setup for biodegradation studies

The batch biodegradation studies are carried out for various VOCs such as MEK, MIBK, IPA, MA, EA, and BA in 250 mL conical flasks in the BOD incubator shaker (Mac Scientific, New Delhi, India) at 150 rpm which is maintained at 37 ^{o}C. The conical flasks are sealed with the stoppers to avoid the loss of VOCs during shaking. The photograph of the batch experimental setup is shown in Plate 3.1. This is basically a rotary shaker.

3.1.2. Experimental procedure for biodegradation studies

3.1.2.1. Chemicals and their properties

The VOCs used in the biodegradation studies are MEK, MIBK, IPA, MA EA, and BA. The properties of the above mentioned VOCs are listed in Table 3.1.

Plate 3.1. Photograph of batch experimental setup for biodegradation study

Table 3.1. Properties of VOCs used in the present study (Kirk-Othmer, 2005; World Health Organization, 1990 and 1993)

Compounds	Molecular formulae	Molecular weight, g mol^{-1}	Boiling point, ^{o}C	Vapor pressure at 20 ^{o}C, kPa	Solubility in water at 20 ^{o}C	OSHA, permissible exposure limit (PEL), ppm	Short term exposure limit (STEL), ppm
MEK	C_4H_8O	72.10	79.6	10.3	290 g L^{-1}	200	300
MIBK	$C_6H_{12}O$	100.16	115.8	2.0	19 g L^{-1}	100	75
IPA	C_3H_8O		82	4.39	Miscible in water	400	400
MA	$C_3H_6O_2$	74.08	56	13.33	Appreciable	No information	250
EA	$C_4H_8O_2$	88.11	77	23.06	Partially soluble in cold and hot water	400	No information
BA	$C_4H_8O_2$	116.16	126.5	1.3	Partially soluble in cold water	No information	No information

3.1.2.2. Preparation of minimal salt medium (MSM)

The media, Minimal Salt Medium (MSM), is prepared using different salts in 1 L of distilled water. The compositions of different salts used in the biodegradation study for MEK, MIBK, IPA and MA, EA and BA are given in Table 3.2. 100 ml of MSM is taken in 250 ml Erlenmeyer flask and is autoclaved. Autoclaving is carried out at 130 ^{o}C in the pressure cooker in order to kill all the impurities present.

3.1.2.3. Microorganism culture conditions

The source for the sludge obtained for the enrichment of culture is the activated sludge taken from the secondary clarifier section of Sewage Treatment Plant of BITS Pilani. One such sample is shown in Plate 3.2. The sludge is mixed thoroughly with water. It is allowed to settle for 3 hours at room temperature (away from sunlight) in order to separate the supernatant and the sludge. This first settling is carried out in order to remove the dissolved impurities from sludge and hence the time given for this settling is more. The supernatant which include the dissolved impurities is discarded off and sludge is retained including microbial culture. Ten grams of sludge obtained from first settling is taken and again thoroughly mixed with 100 mL of distilled water in a beaker. The shaking is carried out gently and then sludge is allowed to settle for short time (1 min) in order to screen out the stones or other particles. The second settling was carried out to collect microbial culture in the supernatant. Fifty milliliters of supernatant is then taken in a 50 mL centrifuge tube. The centrifugation is carried out for 2 minutes at 10,000 rpm at 4 ^{o}C in a Centrifuge (Remi Cooling Centrifuge, India) as shown in plate 3.3. After centrifugation for 2 minutes, a clear pellet is obtained. The liquid is not readily poured off as doing so can mix up the pellet obtained and the liquid. The portion of the upper liquid

is removed carefully from the top of the centrifuge tube without disturbing the pellet. Then the pellet is taken out with the help of loop and transferred in the 250 mL flask in an aseptic environment in the Laminar hood chamber (Model no. HS-42, Atlantis, New Delhi India) as shown in Plate 3.4.

3.1.2.4. Enrichment procedure for utilizing VOCs used in present study

The culture enrichment is carried out in the laminar hood chamber. A loop full of sludge obtained after centrifugation is added to 100 mL of autoclaved MSM. Stock glucose solution is prepared by dissolving 10 g of glucose in 100 ml of distilled water. One mL of stock glucose solution is also added in the 100 mL of autoclaved solution to make the concentration of glucose to 1000 mg L^{-1}. The solution is then kept in the BOD incubator rotary shaker at 37 ^{o}C for 48 hours. The growth of microbial culture is measured by optical density value in a UV-VIS Spectrophotometer (Model 119- Systronics, India) as shown in Plate 3.5 having the cuvette of path length 10 mm. The value of optical density obtained for microbial culture is 0.1 which is an indicative measure of sufficient microbial culture. The enrichment of culture is carried out for a period of 18 days for MEK, MIBK & IPA and 21 days for MA, BA, & EA by decreasing the amount of glucose from 1000 mg L^{-1} to 0 mg L^{-1} with a decrement of 200 mg L^{-1} in every 3 days and increasing VOCs concentration accordingly.

MEK and MIBK concentration are increased from 0 µL to 60 µL (corresponds to 480 mg L^{-1}) with an increment of 20 µL (corresponds to 160 mg L^{-1}) after first 3 days and then 10 µL (corresponds to 80 mg L^{-1}) from 4^{th} to 18^{th} day. The final acclimated cultures are obtained only with 480 mg L^{-1} of MEK and MIBK (no glucose) which are then used for the corresponding biodegradation studies. The final acclimated culture showed an

extensive growth in MEK and MIBK respectively which substantiates the fact that both are biodegradable compounds as reported in the literature (Bridie et al. 1979; Price et al. 1974).

IPA concentration is increased from 0 µL to 60 µL (corresponds to 444.44 mg L^{-1}) with an increment of 20 µL (corresponds to 148.15 mg L^{-1}) after first 3 days and then 10 µL (corresponds to 74.075 mg L^{-1}) from 4^{th} to 18^{th} day. MA concentration is increased from 0 µL to 70 µL (corresponds to 652.44 mg L^{-1}) with an increment of 20 µL (corresponds to 186.41 mg L^{-1}) after first 3 days and then 10 µL (corresponds to 93.205 mg L^{-1}) from 4^{th} to 21^{st} day. Similarly, EA and BA concentration are increased from 0 µL to 70 µL (corresponds to 630.06 mg L^{-1} for EA and 616.19 for BA) with an increment of 20 µL (corresponds to 180.02 mg L^{-1} for EA and 176.06 for BA) after first 3 days and then 10 µL (corresponds to 90.01 mg L^{-1} for EA and 88.03 for BA) from 4^{th} to 21^{st} day. The final acclimated culture is obtained only with 444.44 mg L^{-1} of IPA, 652.44 mg L^{-1} of MA, 630.06 mg L^{-1} of EA and 616.19 mg L^{-1} of BA and respectively. The final acclimated culture thus obtained is used for carrying out the biodegradation study.

Table 3.2. Composition of MSM for different VOCs used in biodegradation study

S No	Constituents	Composition for MEK, MIBK and IPA in one L of distilled water (g)	Composition for MA, EA and BA in one L of distilled water (g)
1.	K_2HPO_4	0.8	-
2.	KH_2PO_4	0.2	0.4
3.	$CaSO_4.2H_2O$	0.05	0.05
4.	$MgSO_4.7H_2O$	0.5	0.5
5.	$(NH_4)_2SO_4$	1.0	1.0
6.	$FeSO_4.7\ H_2O$	0.01	0.01
7.	KNO_3	-	0.3
8.	$NaHCO_3$	-	0.02

Plate 3.2. Photograph of activated sludge used for the acclimated culture growth

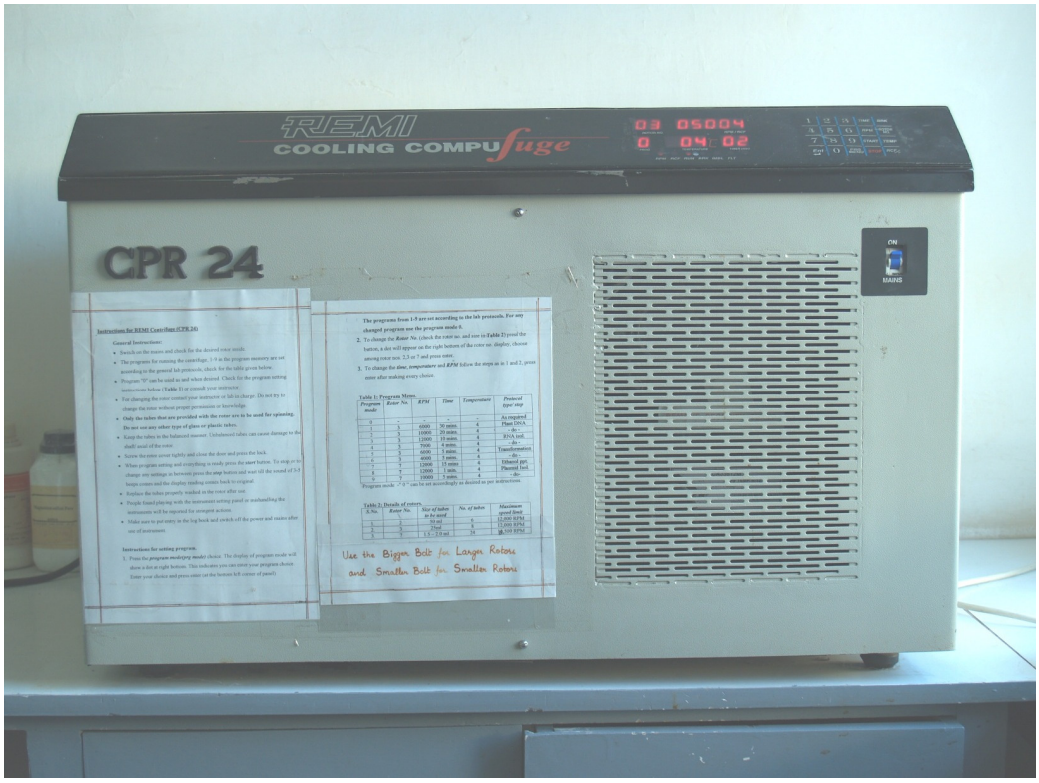

Plate 3.3. Photograph of centrifuge used in present study

Plate 3.4. Photograph of laminar hood chamber (HS-42, Atlantis, India) used in the present study

Plate 3.5. Photograph of UV-VIS Spectrometer used in the present study

3.1.2.5. Biodegradation study

The biodegradation study is carried out for MEK, MIBK, IPA, MA, EA and BA for varying concentration range using the acclimated culture obtained from the enrichment procedure. The range of different parameters used in the biodegradation study of MEK, MIBK, IPA, MA, EA and BA are given in Table 3.3. The biodegradation study is carried out individually in 250 ml Erlenmeyer flasks.

In these experiments, 100 mL of MSM is autoclaved and added with known amount of acclimated mixed culture obtained from the enrichment procedure. Known amount of VOCs are added in autoclaved MSM to maintain the required concentration. The amount of pre cultured suspension added for the biodegradation study effects the growth of the culture. The lag time decreases if more amount of pre cultured suspension than required is taken. The amount of acclimated mixed culture used for the biodegradation study of MEK, MIBK and IPA is 5 mL while 10 mL of acclimated mixed culture is used for the study of MA, EA and BA. The amount of MEK added is 25, 37, 50, 62, 75 and 87 µl (based on density and boiling point of MEK) to maintain 200, 300, 400, 500, 600 and 700 mg L^{-1} of MEK concentration respectively. The amount of MIBK and IPA added are 25, 38, 50, 63, 75, 88 µL and 27, 40, 54, 68, 82, 95 µl to maintain 200, 300, 400, 500, 600 and 700 mg L^{-1} of MIBK and IPA concentration respectively. The amount of BA added is 11.36, 22.73, 34.08, 45.44, 56.8, 68.16, 79.52, 90.88 µl to maintain 100, 200, 300, 400, 500, 600, 700 and 800 mg L^{-1}. Similarly, the amounts of EA and MA are varies from 11.11, 22.22, 33.33, 44.44, 55.55, 66.66, 77.77 µL and 10.73, 21.46, 32.19, 42.92, 53.65, 64.37, 75.10, 85.9 µL respectively to maintain the EA and MA concentration to 100, 200, 300, 400, 500, 600, 700 and 800 mg L^{-1}.

The 250 mL conical flasks used in the biodegradation study are sealed with stoppers to minimize VOCs loss during shaking. The flasks are kept in the rotary shaker which is maintained at 37 ^{o}C and at 150 rpm throughout the biodegradation process. The samples are collected at different intervals for different concentrations ranging from 200 to 700 mg L^{-1} for MEK, MIBK and IPA and 100 to 800 mg L^{-1} for BA, EA and MA based on visual observation (turbidity). The flasks are briefly opened for taking out the samples in the laminar hood chamber. It is done quickly (less than 20 s time) in order to minimize the VOCs loss. The loss of VOCs is neglected during the collection of the sample is as this is insignificantly small. The time interval for the collection of samples is different for different samples. The time is not before 2 hours for MEK, 4 hours for MIBK, 7 hours for IPA, 5 hours for MA, 3 hours for EA and 4 hours for BA samples to be taken out and the final time is decided by observing the constant value of biomass concentration for 2 or 3 consecutive samples.

Table 3.3. Range of parameters investigated in biodegradation study

S No	VOCs	Initial concentration range, mg L^{-1}	Temperature (^{o}C)	Time (h)
1.	MEK	200-700	37	0-67
2.	MIBK	200-700	37	0-58
3.	IPA	200-700	37	0-18
4.	MA	200-800	37	0-24
5.	EA	200-800	37	0-18
6.	BA	200-800	37	0-36

3.1.2.6. Analytical methods

The optical density (OD) of the microbial culture is measured at 540 nm with respect to MSM using UV-VIS Spectrophotometer (Model 119- Systronics, India). The path length for the optical density measurements is 10 mm. The samples collected from the biodegradation study are then centrifuged at 10000 rpm for 2 minutes to separate biomass and supernatant (aqueous microbial culture solution) (Saravanan et al. 2008). Dry weight of biomass is obtained from a known volume of microbial culture. The calibration curve is prepared in terms of optical density value versus biomass concentration as shown in Fig. 3.1. The concentrations of VOCs in aqueous samples (supernatant) are measured using a gas chromatograph (Model 5765, Nucon Engineers, India) with a poropak column (2m length, 1/8 in i.d.) and flame ionization detector as shown in Plate 3.6. The temperatures of injection port, detector port and oven are maintained at 150 ^{o}C, 150 ^{o}C and 200 ^{o}C, respectively for MEK, MIBK and IPA and at 130 ^{o}C, 130 ^{o}C and 200 ^{o}C, respectively for MA, EA and BA. Nitrogen at 2.5 kg cm^{-2} is used as the carrier gas at the flow rate of 24 mL min^{-1} and hydrogen is used as the fuel. All the experiments and measurements are carried out twice and the arithmetic averages are taken for the calculations and data analysis. The calibration plots are prepared in terms of area versus volume of VOCs such as MEK, MIBK, IPA, MA, EA and BA as shown in Figs. 3.2, 3.3, 3.4, 3.5, 3.6, and 3.7 respectively.

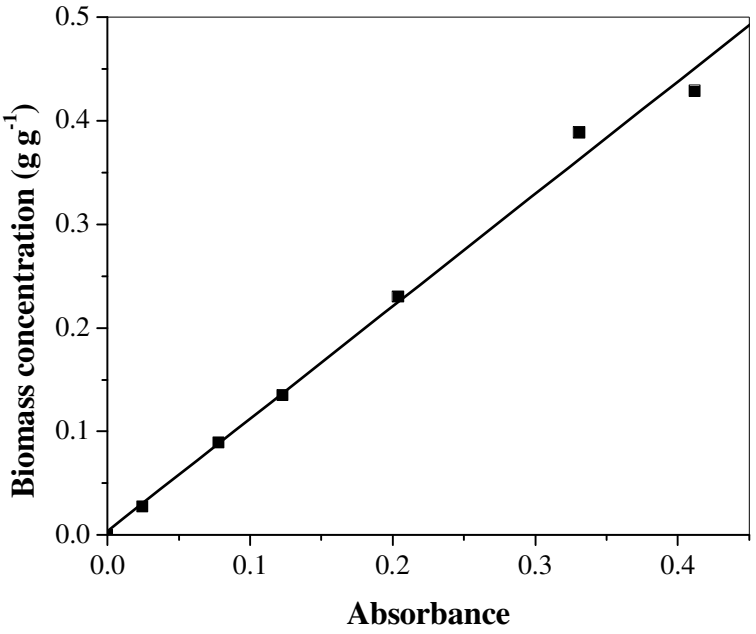

Fig. 3.1. Calibration curve for biomass concentration in liquid phase

Plate 3.6. Photograph of Gas chromatograph (NUCON 5765) used in present study

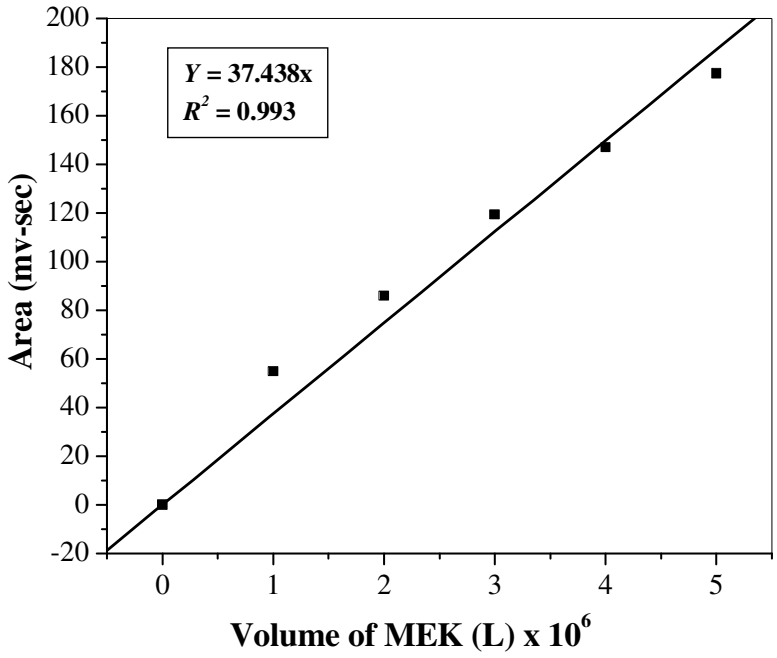

Fig. 3.2. Calibration plot for liquid phase concentration of MEK

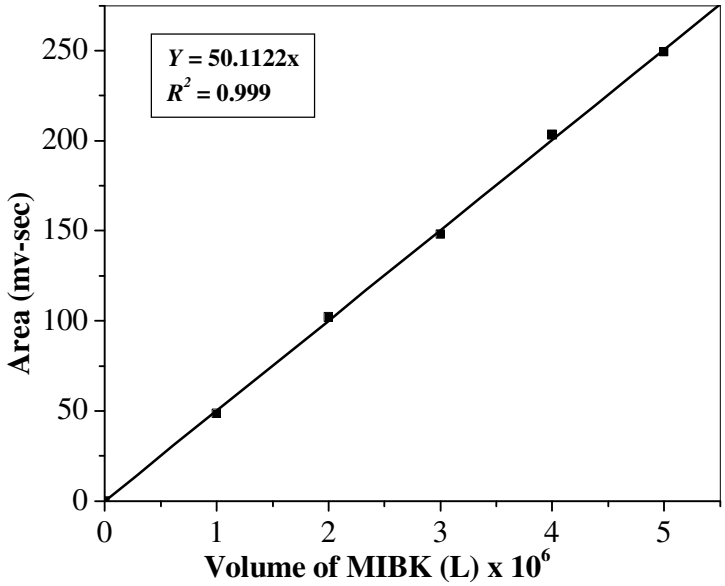

Fig. 3.3. Calibration plot for liquid phase concentration of MIBK

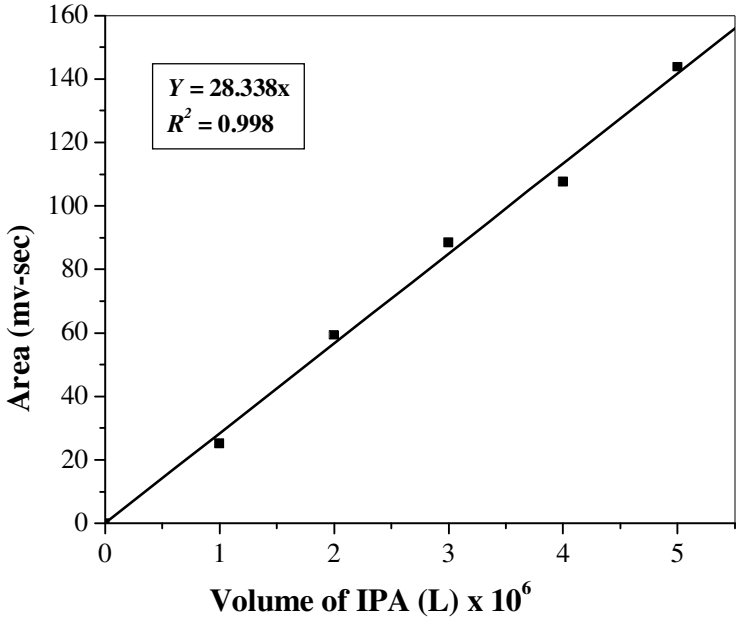

Fig. 3.4. Calibration plot for liquid phase concentration of IPA

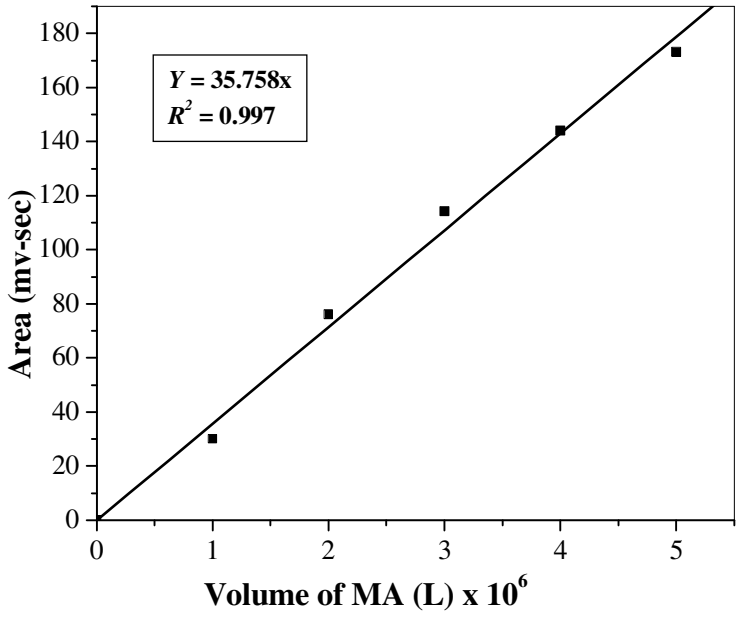

Fig. 3.5. Calibration plot for liquid phase concentration of MA

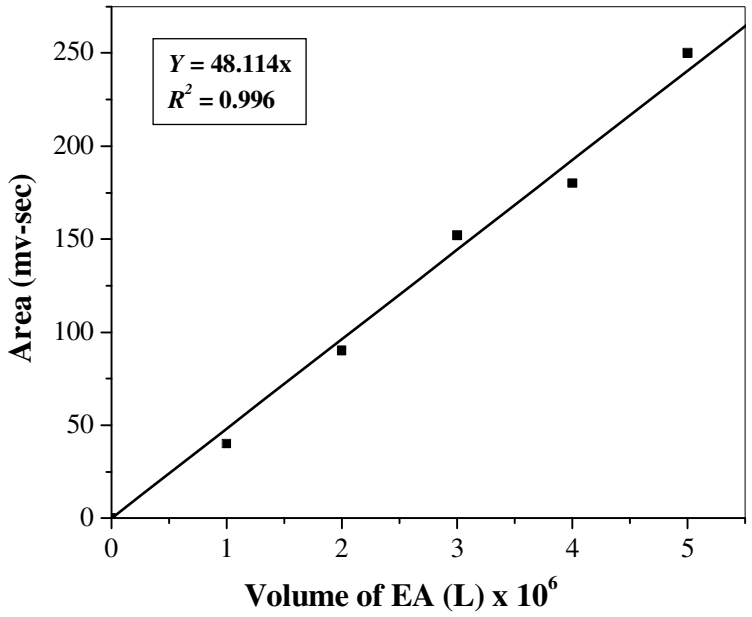

Fig. 3.6. Calibration plot for liquid phase concentration of EA

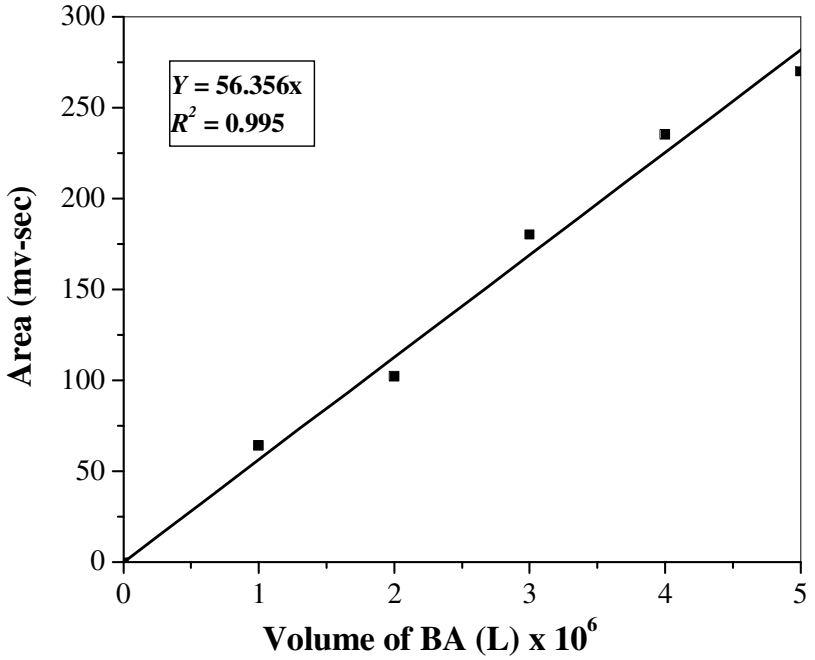

Fig. 3.7. Calibration plot for liquid phase concentration of BA

3.2. Continuous column studies for biofiltration of VOCs

3.2.1. Biofilter column setup

The schematic diagram and the photograph of the biofilter column setup used in this study are shown in Fig. 3.8 and in Plate 3.7 respectively. The biofilter column is made up of a perspex tube of 1 m length and 5 cm inner diameter. The length of the column which is packed is 0.70 m. The coal and matured compost is used as the packing material (hybrid bed) in the present system. The set-up is comprised of different sampling bottles for VOC, air and mixture of VOC and air. The air is passed into the VOC sampling bottle to obtain the air-VOC vapor mixture. The air-VOC vapor mixture of the organic compound and the air stream (from the air sampling bottle) is then passed separately into the mixture sampling bottle. Finally, VOC enriched stream is passed into the biofilter column in an up flow mode of operation. The packing material is supported by a stainless steel mesh installed at the bottom of the column to maintain a proper radial distribution of the VOC vapors. The moisture content in the bed is maintained periodically by sprinkling fresh minimal salt medium (MSM) from the top of the biofilter column as shown in Fig 3.8. The MSM provides the necessary mineral for the development of biofilm and helps in the growth of microorganisms in the biofilter column. The column has 6 sampling ports at every 10 cm from the bottom in the 0.7 m packed column height. The inlet port for the inlet of solvent vapors is at 0.1 m from bottom of the column and the outlet sampling port is at 0.2 m from top of the column as shown in Fig. 3.8. The air and VOC flow rates are maintained using air rotameters (Japsin, NewDelhi, India).

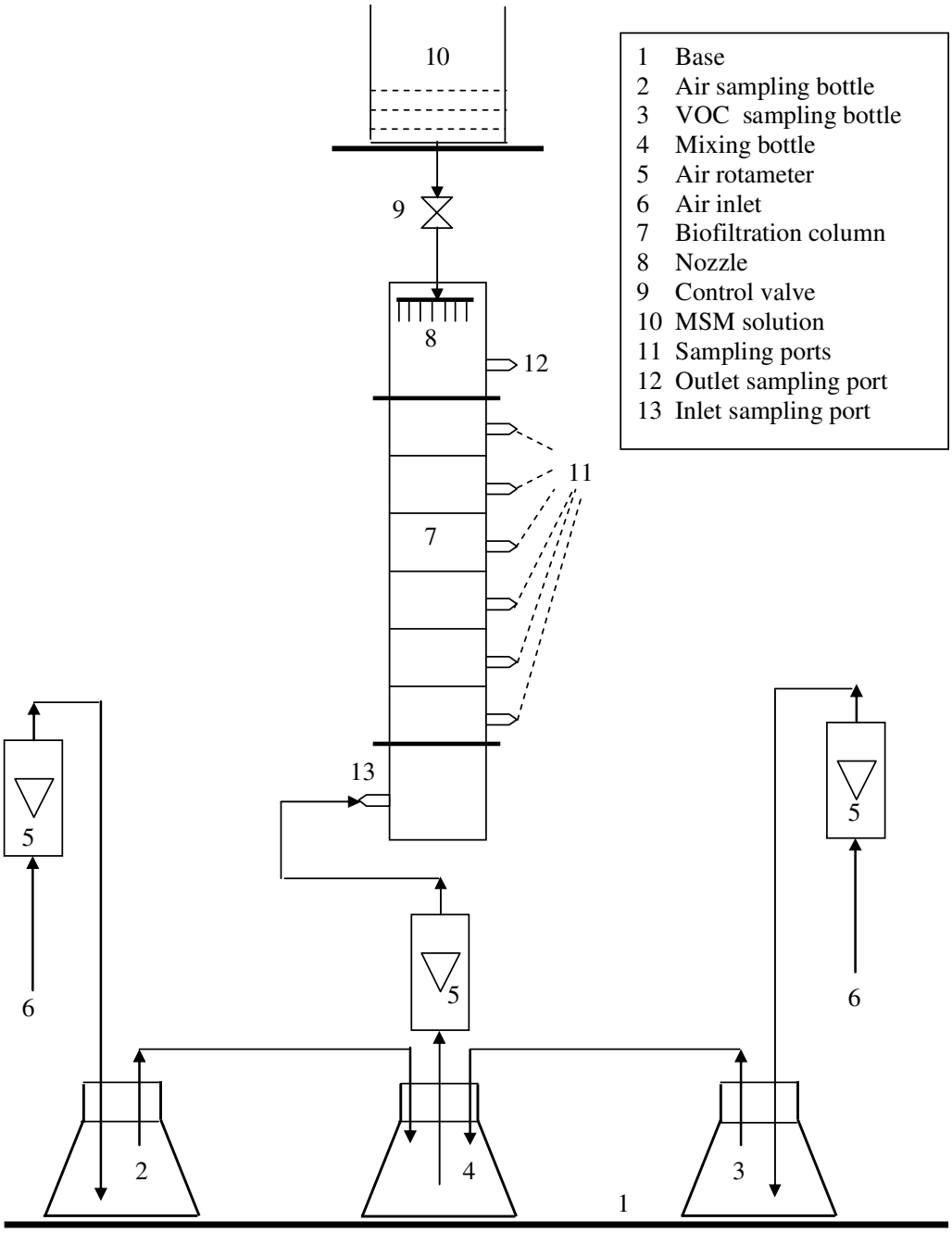

Fig. 3.8. Schematic diagram of biofilter set-up

Plate 3.7. Photograph of biofilter column for biofiltration

3.2.2. Experimental procedure for biofiltration studies

3.2.2.1. Development of seeding culture for biofiltration study

The seeding culture is prepared in the similar manner as the procedure discussed in Section *3.1.2.3.* The final acclimated culture which is obtained only with the respective VOC is used as the seeding culture in the biofiltration study.

3.2.2.2. Preparation of packing material for biofilter column

The column is packed with the mixture of matured compost and coal in the ratio of 2:1 (W/W) (200 g of matured compost and 100 g of coal) for the biofiltration study of MEK, MIBK, IPA and EA. The matured compost is obtained from The JRD Tata Foundation for Research in Yoga, Naturopathy & Ayurvedic Sciences, Chitrakut, UP (India). The matured compost is derived from cow dung and subjected to anaerobic digestion. The coal is obtained from the local market. It is sieved through 8 – 10 mm mesh screen and final coal size is obtained as 2.36 mm for the study. The coal is washed with normal water and then with distilled water. The washed coal is kept in the oven which is maintained at a temperature of 100 ^{o}C for 1 day for removing the moisture content by heating.

3.2.2.3. Packing of biofilter column

The biofilter column is packed with the prepared packing material of coal and compost which is mixed with 200 mL of acclimated mixed culture obtained from the shake flask processes for MEK and MIBK study. The mixture is then transferred into the column. The packing height of the column is 70 cm. The acclimated culture is again transferred to the packed column thrice (100 mL each) in order to thoroughly mix the packing used with the acclimated culture. The entire amount of 500 mL of the total acclimated culture

(seeding culture) which corresponds to 0.25 g of microbial culture is used for the study of MEK and MIBK. The leachate collected at the bottom of the column is also transferred to the packed column for one week during start up operation. Similar procedure is followed for the packing of columns using IPA and EA for the biofiltration study. The total amount of acclimated culture (seeding culture) used for the biofiltration study of IPA and EA are 700 mL which corresponds to 0.35 g of microbial culture. The moisture content of the packing material is obtained as 60.2% and 64.5 % on wet weight basis for the MEK and MIBK study respectively. The moisture content obtained for IPA and EA are 65% and 63% respectively on wet basis.

3.2.2.4. Biofilter operating conditions

The operating conditions for various phases of biofilter operation for MEK, MIBK, IPA and EA are given in Table 3.4, 3.5, 3.6, and 3.7 respectively. The phase I is the acclimation phase which is 20 days for the biofiltration study of MEK and MIBK and 10 days for the study of IPA and EA. The phase II, III, IV and V for MEK & MIBK and phase II, III, IV for IPA & EA are distributed in 10 days each for the biofiltration study. The continuous experiments are carried out by varying the flow rates of air and VOCs to get different initial concentrations and residence times. The air flow rates ranged from 0.18 to 0.3 $m^3 h^{-1}$ with equivalent EBRT from 16.5 to 27.4s for the biofiltration of MEK, MIBK, IPA and EA. The biofiltration experiments are also carried out for the shock loading conditions. The operating conditions for shock loading conditions for MEK which is carried out for a period of three weeks and MIBK which is studied for 20 days are given in Table 3.8 and Table 3.9 respectively. The operating conditions for shock

loading conditions for IPA and EA which is carried out for a period of ten days are given in Tables 3.10 and 3.11 respectively.

3.2.2.5. Analytical methods

The gaseous phase concentration is measured in the gas phase using a Gas Chromatograph (GC) (Model 5700 series, Nucon Engineers, India) with a poropak column (2m length, 1/8 in i.d.) and flame ionization detector. The temperatures of the injection port, detector port and oven for MEK, MIBK, and IPA are maintained at 150 ^{o}C, 150 ^{o}C and 200 ^{o}C, respectively. The temperatures of injection port, detector and oven ports are maintained at 130 ^{o}C, 130 ^{o}C and 200 ^{o}C, respectively for EA. Nitrogen is used as the carrier gas at the flow rate of 24 mL min^{-1} and hydrogen is used as the fuel. Calibration curves are prepared between areas and VOC concentration for the MEK, MIBK, IPA, and EA as the procedure reported by Lodge (1989) and shown in Figs. 3.9, 3.10, 3.11, and 3.12 respectively. The calibration curve is prepared by injecting a known amount of VOC into the gas chromatograph from the sealed bottle equipped with a Teflon septum, according to the standard procedure. The air samples are drawn from various sampling ports by using a gas tight syringe and are transferred into the GC through 2mL sampling loop.

The microbial concentration is measured in the units of colony forming units CFU g^{-1} of packing material after the acclimation period of 20 days and after the phase V (at the end of 60 days of biofilter operation) for the MEK and MIBK study. The microbial concentration is measured after phase I (10 days acclimation period for IPA and 15 days acclimation period for EA) and after the end of phase IV for IPA and EA respectively. One gram of moist packing material (comprised of coal and compost) is taken from the

top of the biofilter column. Initially, 100 ml of 0.8% NaCl stock solution is prepared by dissolving 0.8 g of NaCl in 99.2 g of distilled water. Then this solution is sterilized. 9 mL of 0.8% sterilized NaCl solution is taken and added to 1 g of packing material. This solution is shaken vigorously in a shaker for 15 min and serially diluted with sterilized water. Then the plating is carried out in the nutrient agar media in the petri dishes in the aseptic conditions. The petri dishes are incubated in the BOD incubator (Macro Scientific, India) for 2 days at 30 ^{o}C. The colonies are counted to study the microbial concentration.

The performance of the biofilter is evaluated in terms of the percentage removal efficiency and the elimination capacity of the biofilter bed which are given in Eq. (3.1) and (3.2).

$$RE = \frac{C_{gi} - C_{g0}}{C_{gi}} \times 100 \tag{3.1}$$

$$EC = \frac{Q\left(C_{gi} - C_{g0}\right)}{V} \tag{3.2}$$

where Q is the flow rate ($m^3\ h^{-1}$), V the volume of the filter bed (m^3), EC is the Elimination capacity ($g\ m^{-3}\ h^{-1}$), RE is the percentage removal efficiency and C_{gi} and C_{g0} are the inlet and exit VOCs concentration ($g\ m^{-3}$).

Table 3.4. Operating conditions for biofiltration study for MEK

Phase	Operating time (days)	Air flow rate, Q, (m^3 h^{-1})	Inlet concentration range, C_{gi} (g m^{-3})	Inlet loading (g m^{-3} h^{-1})	EBRT (s)
I (Acclimation)	20	0.24	0.15 – 0.25	26.37-43.13	20.6
II	10	0.18	0.45 – 0.6	59.46 – 77.66	27.4
III	10	0.24	1.19 – 1.33	207.97–232.59	20.6
IV	10	0.30	0.75 – 0.88	163.93-194.05	16.5
V	10	0.21	1.51 – 1.64	231.33-248.90	23.5

Table 3.5. Operating conditions for biofiltration study for MIBK

Phase	Operating time (days)	Air flow rate, Q (m^3 h^{-1})	Inlet concentration range, C_{gi} (g m^{-3})	Inlet loading (g m^{-3} h^{-1})	EBRT (s)
I (Acclimation)	20	0.21	0.07 – 0.09	10 -14	23.5
II	10	0.24	0.251 – 0.26	44 – 46	20.6
III	10	0.18	0.5 – 0.51	66 – 68	27.4
IV	10	0.3	0.71 – 0.73	156 -159	16.5
V	10	0.21	0.45 – 0.46	69 – 71	23.5

Table 3.6. Operating conditions for biofiltration study for IPA

Phase	Operating time (days)	Air flow rate, Q, ($m^3\ h^{-1}$)	Inlet concentration range, C_{gi} (g m^{-3})	Inlet loading (g $m^{-3}\ h^{-1}$)	EBRT (s)
I (Acclimation)	10	0.18	0.04 – 0.051	5.24.-6.68	27.4
II	10	0.24	0.101 – 0.115	17.64 – 20.08	20.6
III	10	0.21	0.352 – 0.365	53.78-55.77	23.5
IV	10	0.30	0.162 – 0.173	35.36–37.76	16.5

Table 3.7. Operating conditions for biofiltration study for EA

Phase	Operating time (days)	Air flow rate, Q, ($m^3\ h^{-1}$)	Inlet concentration range, C_{gi} (g m^{-3})	Inlet loading (g $m^{-3}\ h^{-1}$)	EBRT (s)
I (Acclimation)	15	0.18	0.05 – 0.063	6.54.-8.25	27.4
II	10	0.30	0.131 – 0.145	28.59 – 31.65	16.5
III	10	0.21	0.231 – 0.240	35.29-36.67	23.5
IV	10	0.24	0.18– 0.193	31.43–33.70	20.6

Table 3.8. Operating conditions for biofilter operation for shock loading conditions for MEK

Days of biofilter operation	Air flow rate, Q (m^3 h^{-1})	Inlet concentration, C_{gi} (g m^{-3})	Inlet loading (g m^{-3} h^{-1})	EBRT (s)
1 – 4	0.24	0.45 – 0.47	79.1 – 82.2	20.6
5 – 8	0.24	1.2 – 1.23	209.5–214.8	20.6
9 – 12	0.3	0.75 – 0.77	163.5-168.3	16.5
13- 16	0.3	1.50 – 1.52	328.7-331	16.5

Table 3.9. Operating conditions for biofilter operation for shock loading conditions for MIBK

Days of biofilter operation	Air flow rate, Q (m^3 h^{-1})	Inlet concentration range, C_{gi} (g m^{-3})	Inlet loading (g m^{-3} h^{-1})	EBRT (s)
1 - 5	0.21	0.6	92 - 94	23.5
6 – 10	0.21	0.25	37 – 39	20.6
11 – 15	0.3	0.81	175 – 177	27.4
16 - 20	0.3	0.41	88 - 91	16.5

Table 3.10. Operating conditions for biofilter operation for shock loading conditions for IPA

Days of biofilter operation	Air flow rate, Q (m^3 h^{-1})	Inlet concentration range, C_{gi} (g m^{-3})	Inlet loading (g m^{-3} h^{-1})	EBRT (s)
1 – 3	0.21	0.6	45.83 - 55	23.5
4 – 6	0.21	0.25	69.85 –75.09	20.6
7 – 10	0.3	0.81	26.19 -30.12	27.4

Table 3.11. Operating conditions for biofilter operation for shock loading conditions for EA

Days of biofilter operation	Air flow rate, Q (m^3 h^{-1})	Inlet concentration range, C_{gi} (g m^{-3})	Inlet loading (g m^{-3} h^{-1})	EBRT (s)
1 - 3	0.21	0.25 – 0.27	38.19 – 41.25	23.5
4 – 6	0.24	0.28 – 0.3	48.89 – 52.39	20.6
7 – 10	0.18	0.18 – 0.195	23.57 – 25.14	27.4

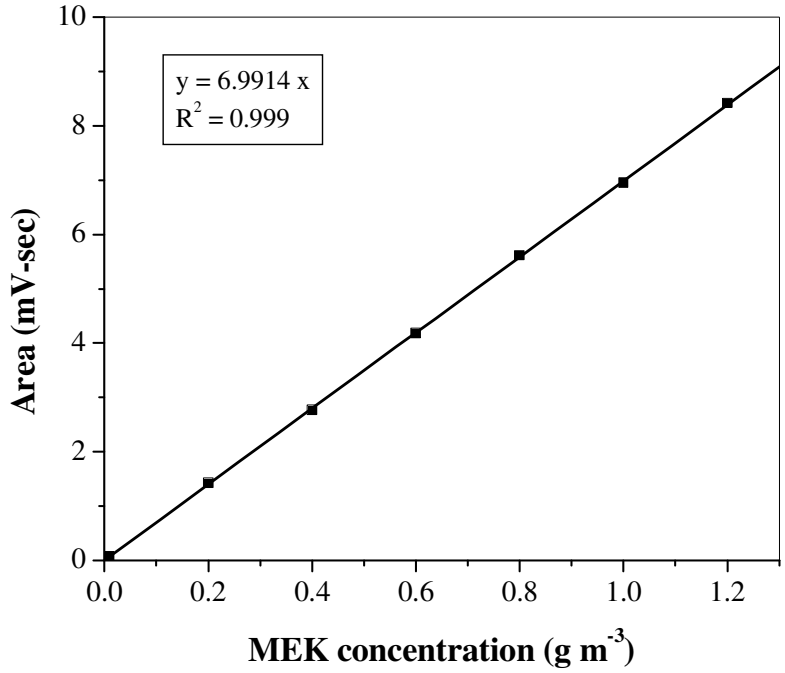

Fig. 3.9. Calibration plot for gas phase concentration of MEK

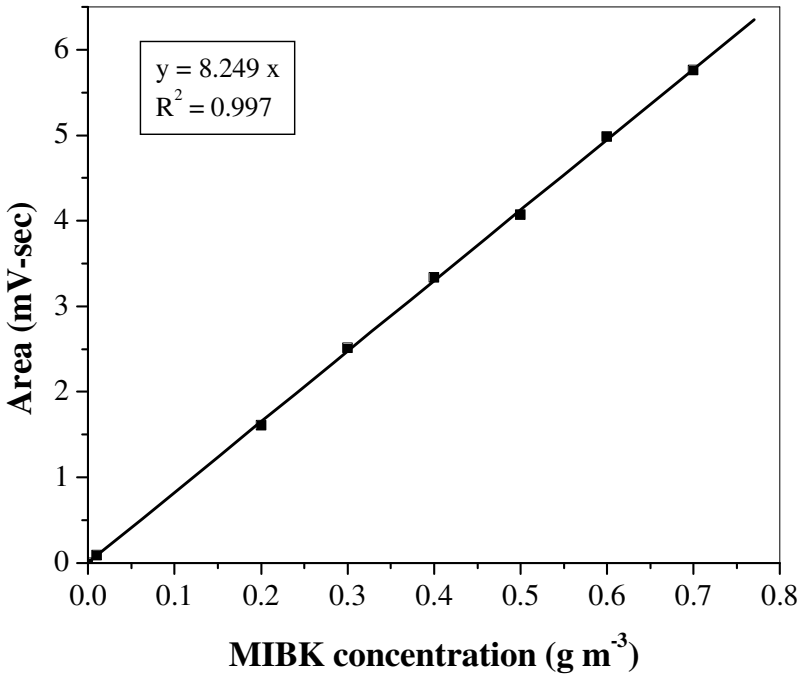

Fig. 3.10. Calibration plot for gas phase concentration of MIBK

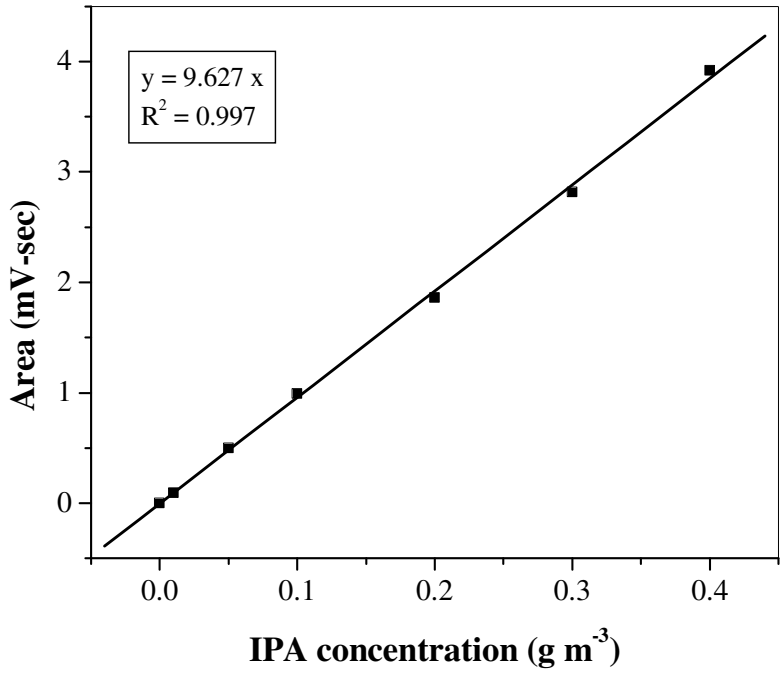

Fig. 3.11. Calibration plot for gas phase concentration of IPA

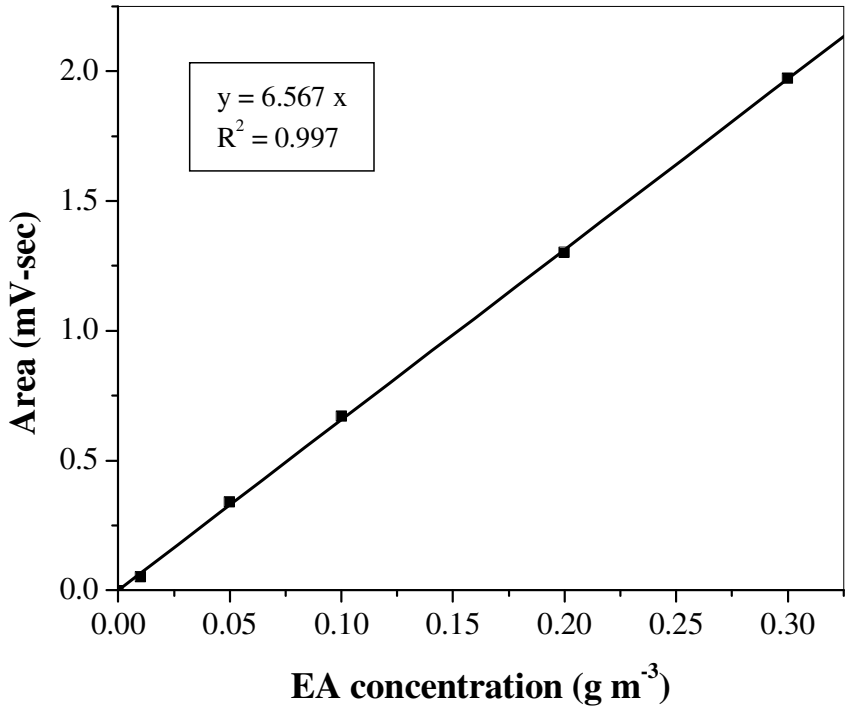

Fig. 3.12. Calibration plot for gas phase concentration of EA

CHAPTER – 4

MATHEMATICAL MODELING AND SIMULATION

This chapter describes various growth kinetic models and rate kinetic models for biodegradation studies reported in the literature. It also includes the Michaelis Menten and Ottengraf model for explaining the kinetic behavior in the biofiltration column systems. An improved mathematical model for the design of biofilter system proposed in the present work is also described in this chapter.

4.1. Growth kinetic models for biodegradation

The biological treatment is a promising alternative to attenuate the environmental impact caused by VOCs due to the potential characteristic of the microbial culture as agents for the degradation of carbon compounds. The carbon substrates are most often utilized by the microorganisms under the carbon and energy controlled environmental conditions. The growth is a result of catabolic and anabolic enzymatic activities. Therefore, processes such as substrate utilization or growth-associated product formation, can also be quantitatively described on the basis of the growth kinetic models. The relationship between the specific growth rate (μ) of a population of microorganisms and the substrate concentration (S) is a valuable tool in the biodegradation processes (Okpokwasili and Nweke, 2005). This relationship is expressed by a set of empirically derived rate laws which are considered as theoretical kinetic models. The kinetic models are helpful in the

understanding of mechanism of biodegradation of the biological processes and predicting the VOCs concentration in various treatment systems. Various biodegradation growth kinetic models such as Monod model (Monod, 1949), Powell model (Powell, 1967), Haldane model (Andrew, 1968), Luong model (Luong, 1986) and Edwards model (Edwards, 1970) are reported in the literature are used to explain the behavior of biodegradation process. A brief description of these models is given in the following sections.

4.1.1. Monod model

During the last half century, the concepts of microbial growth kinetics have been dominated by the relatively simple empirical model proposed by Monod (Monod, 1949). Monod model is extensively used for explaining the growth kinetics of several VOCs such as MEK, MIBK, IPA, phenol, butanol etc. (Deshusses, 1994; Kumar et al., 2005). Monod`s model relates growth rate (μ) with the concentration of a single growth-controlling substrate by two parameters; the maximum specific growth rate (μ_m) and substrate affinity constant (K_S) as given by Eq. (4.1).

$$\mu = \mu_m \frac{S}{K_s + S} \tag{4.1}$$

where, μ is a specific growth rate (h^{-1}), and S is the substrate concentration (mg L^{-1}). Eq. (4.1) is a non linear equation and on linearizing Eq. (4.2) is obtained.

$$\frac{1}{\mu} = \frac{K_s}{\mu_m}\left(\frac{1}{S}\right) + \frac{1}{\mu_m} \tag{4.2}$$

A graph plotted between ($1/\mu$) and ($1/S$) by using the log phase data for a given initial concentration gives a straight line. The intercept of the line gives the value of μ_m and the slope gives the value of K_s.

Monod model describes the rate at which the biomass is expected to grow. Therefore it explains that the pollutant (VOC) degradation is first-order at low concentration as given by Eq. (4.3).

$$\text{when } S \to 0; \mu = \frac{\mu_m}{K_S} S \tag{4.3}$$

At high concentration, the equation becomes zero-order as given by Eq. (4.4).

$$\text{when } S \to \infty; \mu \to \mu_m \tag{4.4}$$

The growth rate increases linearly at low VOC concentration and becomes constant at high concentration of VOC as given by Eq. (4.5)

$$\text{when } S \to K_S; \mu = \frac{\mu_m}{2} \tag{4.5}$$

Monod model is a simple model, and describes only the dependence of biodegradation rate on biomass concentration (Okpokwasili and Nweke, 2005). The limitation of classical Monod`s equation is that it does not account for the fact that cells may need substrate or may synthesize product even when they do not grow. Also it is not valid for those substrates which limit growth at low substrate concentration

The original Monod equation was modified by Powell (1967) which takes into account of some of the limitations of Monod model.

4.1.2. Powell`s model

The original Monod equation is modified by introducing the terms of maintenance, expressed as the threshold substrate concentration (S_{min}) and maintenance rate (m). The maintenance rate describes the substrate required for non-growth functions. This lead to the modified equation proposed in various studies by Powell (1967) as given by Eq. (4.6):

$$\mu = (\mu_{max} + m)\frac{S}{K_S + S} - m \tag{4.6}$$

Kinetic constants of this model cannot be obtained accurately using graphical method as there are three unknown parameters in the model equation (Eq. 4.6). Monod and Powell models do not consider the self inhibition effect which is exhibited during the biodegradation of many organic pollutants. It is well established in earlier studies that if the substrate concentration (VOC concentration) is much higher than the affinity constant values, substrate inhibition models need to be studied (Kotturi et al., 1991; Kumaran and Paruchuri, 1997; Dapena-Mora, 2007).

4.1.3. Haldane model

The Haldane model is used when the substrate inhibits its degradation at higher concentrations of substrate. In such cases, Monod derivatives provide the corrections for the substrate inhibition by incorporating the substrate inhibition constant (K_I). The Haldane`s model is one of the most widely used inhibition models for explaining the kinetic behavior of microorganisms during biodegradation (Sokol, 1986; Tang and Fan, 1987; Deshusses, 1994; Goudar and Delvin, 2001; Peyton et al., 2002; Saravanan et al., 2008). The Haldane`s equation is given by Eq. (4.7).

$$\mu = \frac{\mu_m S}{K_s + S + \left(S^2 / K_I \right)} \tag{4.7}$$

Some of the studies reported that it is a modified Monod relation which incorporates the inhibitory effects of substrate concentration (Snape et al., 1995). The inhibition term (S^2/K_I) as given in Eq. (4.7) is small in magnitude at low values of substrate concentration (*S)* and increases at high values of substrate concentration. The increase in the value of (S^2/K_I) causes a decrease in the value of μ. It is also to be noted that the high values of K_I corresponds to the decreasing effect of substrate concentration. The maximum value of specific growth rate, (μ_m) can be found by differentiating Eq. (4.7) with respect to *S* and equating it to zero. Thus the value of *S* corresponding to μ_m is given by Eq. (4.8) which is also called the critical substrate concentration (S_{crt}).

$$S_{crt} = \sqrt{K_s K_I} \tag{4.8}$$

In Haldane`s model, only the substrate utilization term is considered and the effect of biomass production upon the utilization of substrate is neglected (Monterio et al., 2000).

4.1.4. Luong model

The growth of microbial culture can be inhibited in different ways. Inhibition of microbial growth can be caused by the presence of inhibitors, higher substrate concentration and product formation. The product inhibition occurs when the concentration of product is increased to such levels at which the growth rate decreases and ultimately ceases to exist. In Haldane model, the analysis of growth curve implies that the cell would grow indefinitely which does not happen in real situations. Above certain substrate concentration limit, the microorganisms cease to grow. Luong (1986) proposed the substrate inhibition model to account for the inhibitory effect of substrate on

growth rate. The model incorporates a term S_m (mg L^{-1}) representing critical inhibitor concentration, above which the growth is completely inhibited. The model is based on the assumption that the substrate will act as an inhibitor at higher concentration and behave as activator at lower concentrations of VOCs. The inhibitory effect of VOC at higher concentration for mixed culture is given by Eq (4.9).

$$\mu = \frac{\mu_m S}{K_S + S}\left(1 - \frac{S}{S_m}\right)^n \tag{4.9}$$

Non-linear regression on experimental data to be carried out to find out the kinetic constants for Eq. (4.9).

4.1.5. Edwards model

Edward (1970) discussed various reasons for the substrate inhibition which affects the microbial growth. The reasons could be the formation of intermediates, or products; changed activity of one or more enzymes; dissociation of one or more enzymes or formation of metabolic aggregates. The study also focused on the development of inhibition models which can explain the highly complicated nature of microorganisms in the degradation of organic compounds and can suggest a mechanism of biodegradation at high substrate concentration. They tested the experimental data to study the substrate inhibition effects with five different sets of inhibition models. Each of these models was derived from the Haldane model. The Edward model given below contains four unknown parameters (μ_m, K_S, K_I and K) and is given by Eq. (4.10):

$$\mu = \mu_m \frac{S}{S + K_S + \left(\frac{S^2}{K_I}\right)\left(1 + \frac{S}{K}\right)} \tag{4.10}$$

where K is a positive constant which appear in the Edward model.

Models used in this study are Monod, Powell, Haldane, Luong and Edwards model.

4.2. Rate kinetic models

In waste water treatment processes such as biodegradation, it is necessary to model the rates of growth, substrate utilization and product formation. The environmental processes involve different types of microbial species having different growing rates, different nutrients and temperature requirements. However in many cases, all the microbial species can be combined together into a group called biomass and can be described by rate equations.

Thus in the biodegradation processes, several kinetic approaches for describing the transformation of organic compounds into biomass by suspended microorganisms are being evaluated. The rate of disappearance of substrate is dependent on the substrate concentration. The substrate concentration which changes with time can be described by zero-order, first-order and second-order rate kinetics.

In the batch growth, it is observed that the quantity of biomass and the concentration increases exponentially with respect to time. Such phenomena can be explained by the fact that all cells have the same probability to multiply. Therefore the overall rate of biomass formation is proportional to the biomass itself. Thus, the first-order rate kinetics is given by Eq. (4.11)

$$r_x = kX \tag{4.11}$$

where r_X is the rate of cell growth (kg cell $m^{-3}s^{-1}$), X is the cell concentration (kg cell m^{-3}), and k is a kinetic constant (s^{-1}).

$$\frac{dX}{dt} = kX \tag{4.12}$$

where *dX/dt* is the rate of change of cell concentration with respect to time (kg cell m^{-3} s^{-1}). On solving this equation, Eq (4.13) is obtained.

$$\ln X = kt + \ln X_0 \tag{4.13}$$

where X_0 is the initial cell concentration at time, $t = 0$.

Robinson and Tiedje (1983) have found that Monod kinetics, though deterministic in nature are more suitable to continuous than to batch culture systems. This is due to the linear approximation ($\Delta s/\Delta t$) of the differential equation which becomes highly inaccurate and impractical as the time intervals between the measurements increases.

According to Paris et al. (1981), the second order kinetics depends either on the substrate concentration and biomass or substrate concentration and time. Larson (1980) has considered that the biomass concentration is directly proportional to time and arrived at the second order differential equation. The integrated form of the model equation produces a sigmoidal curve and does not allow for the metabolism without growth.

The kinetics proposed in earlier studies such as Monod, first-order and second-order kinetics have the limitation that they do not take into account the biomass growth. Therefore, it is found that both the first-order and second-order kinetics are not widely preferred and are not sufficient to explain the biodegradation rate kinetics. These conceptual and mathematical difficulties led to single deterministic model known as three-half-order kinetic model which was proposed by Brunner and Frocht (1984). The model was based on the assumption of first-order model with the introduction of an additional term for explaining the biomass formation given by Eq. (4.14)

$$\frac{dS}{dt} = -k_1 S - aES \tag{4.14}$$

where, k_1 is the proportionality constant (time^{-1}), E is the cell concentration (g L^{-1}) and a is the proportionality constant (biomass concentration^{-1} time^{-1}).

Eq. (4.14) is solved by describing E as a function of time (t). The function which relates E with time is given by Eq. (4.15)

$$aE = k_2 t \tag{4.15}$$

Eq. (4.15) assumes linear growth and the units of k_2 is ([time^2]$^{-1}$). On substitution of Eq. (4.15), into Eq. (4.14), Eq. (4.16) is obtained.

$$\frac{dS}{dt} = -k_1 S - k_2 St \tag{4.16}$$

The integration of Eq. (4.16) yields Eq. (4.17).

$$S = S_0 e^{-k_1 t - (k_2/2)t^2} \tag{4.17}$$

S_0 is the substrate concentration at zero time.

The three-half model accounts for the rate of product formation (P) which is expressed by Eq. (4.18)

$$\frac{dP}{dt} = -\frac{dS}{dt} + k_0 \tag{4.18}$$

On integrating Eq. (4.18), Eq. (4.19) is obtained and is referred as three-half order model.

$$P = S_0 - S + k_0 t \tag{4.19}$$

Substitute Eq. (4.17) into Eq. (4.19) yields Eq. (4.20).

$$P = S_0 \left(1 - e^{-k_1 t - \left(k_2 t^2\right)/2}\right) + k_0 t \tag{4.20}$$

Eq. (4.20) is non linear and is solved by nonlinear regression method. Eq. (4.20) is rearranged to get Eq. (4.21).

$$Y = -k_1 - \frac{k_2 t}{2} \tag{4.21}$$

where

$$k_2 = {aE}/{t} \tag{4.22}$$

$$Y = \frac{1}{t}\left(\frac{\ln\left(S_0 - P + k_0 t\right)}{S_0}\right) \tag{4.23}$$

k_1 and k_2 are found by plotting Y against t which gives a straight line using the log phase data. P is the rate of product formation (CO_2) which is directly related to the change in biomass concentration. As the three-half order model included the term to explain biomass formation which can be measured in terms of P. k_0 and S_0 are zero-order rate constant and substrate concentration at zero time, respectively. Eq. (4.23) contains four unknown parameters and is highly non-linear. In this equation, S_0 and k_0 can be obtained by the zero-order kinetics which is represented by differential and integral form as given by Eqs. (4.24) and (4.25) respectively.

$$\frac{dS}{dt} = -k_0 \tag{4.24}$$

$$S = S_0 - k_0 t \tag{4.25}$$

4.3. Kinetic models for biofiltration

4.3.1. Michaelis-Menten kinetic model

The determination of kinetic parameters is important in order to understand the kinetic behavior of a continuous biofilter system and thus relating it to the biodegradation rate kinetics. In the present study, Michaelis–Menten kinetic model is used to calculate the kinetic constants for the biofiltration process. It is assumed that at the steady state, the

growth rate of microorganisms is balanced by its own decay rate, resulting in the biological equilibrium of the system. The kinetic constants remain constant over that period. The kinetic constants are calculated using Eq. (4.26):

$$\frac{V/\ Q}{C_{gi} - C_{go}} = \frac{K_S}{r_{max}} \frac{1}{C_{ln}} + \frac{1}{r_{max}} \tag{4.26}$$

where C_{gi} and C_{g0} are the inlet and outlet concentrations of the pollutant (VOC) (g m^{-3}). V is the volume of the filter bed (m^3), r_{max} is the maximum degradation rate per unit filter volume (g m^{-3} h^{-1}), K_S is the saturation constant (g m^{-3}) in gas phase, C_{ln} is the log mean concentration difference as shown in Eq. (4.27).

$$C_{ln} = \frac{C_{gi} - C_{g0}}{\ln\left(C_{gi} / \ C_{g0}\right)} \tag{4.27}$$

4.3.2. Ottengraf-Van den Oever model

According to Ottengraf-Van den Oever (1983), the diffusion limitation occurs in the wet biolayer. This also means that the biolayer is not fully active and the depth of penetration in the biolayer is smaller than the biofilm thickness (δ). Thus the conversion rate is controlled by the rate of diffusion. The zero-order with diffusion limitation kinetics is proposed by Ottengraf-Van den Oever (1983) and is given by Eq. (4.28):

$$\mathrm{EC} = \mathrm{IL}\left(1 - \left(1 - K_1\sqrt{\frac{\mathrm{EBRT}}{\mathrm{IL}}}\right)^2\right) \tag{4.28}$$

$$\text{Where, } K_1 = \sqrt{\frac{K_0 D_e a}{2m\delta}} \tag{4.29}$$

in which K_0 is the zero-order kinetic constant, D_e is the effective diffusion coefficient of respective VOC in the biofilm (m^2 h^{-1}), m is the Henry`s coefficient for VOC in water, a is the interfacial area per unit volume (m^{-1}), and δ is the biofilm thickness (μm). The gas

phase concentration of the VOC at the outlet of the biofilter column is obtained by Eq. (4.30):

$$\frac{C_{g0}}{C_{gi}} = \left[1 - \mathrm{EBRT}\frac{K_1}{\sqrt{C_{gi}}}\right]^2 \tag{4.30}$$

The zero-order with reaction limitation kinetics proposed by Ottengraf-Van den Oever is given by Eq. (4.31):

$$\mathrm{EC} = K_0 \tag{4.31}$$

The critical inlet concentration (C_{critical}) is defined as the limiting inlet concentration at which the biodegradation mechanism changes from diffusion-controlled to reaction-rate controlled and is given by Eq. (4.32):

$$\mathrm{C}_{\mathrm{critical}} = \frac{1}{4}\left(\frac{K_0}{K_1} + K_1 EBRT\right)^2 \tag{4.32}$$

The critical inlet load is calculated by using Eq. (4.33)

$$IL_{\mathrm{critical}} = \frac{C_{\mathrm{critical}}\mathrm{X}Q}{V} \tag{4.33}$$

4.4. Mathematical modeling of biofilter column

The mathematical modeling of biofiltration column is carried out in order to predict the performance of a biofilter column under different operating conditions. In the present study, two models are developed for the biofiltration study.

4.4.1. Modeling of biofilter column operated in periodic mode

The periodic operated model proposed by Chmiel et al., (2005) is validated in the present study for different VOCs used. In periodic mode of operation, biofilm is less developed

due to nutrient shortage. The Linear Driving Force (LDF) approach is being applied, which focuses on the adsorption phenomena to approximate the pollutant inter-phase transport. It is seen that some of the specific parameters concerning with the biofilm are not well known. This approach is being applied in the present study. The set of equations (2.40 – 2.46) are solved using the MATLAB software version 6.1. The results are validated with the present experimental data collected for MEK and MIBK and the data reported in the literature.

4.4.2. Development of generalized biofilter model

The model proposed in this study describes transport, physical and biological processes that occur during biofiltration. As air passes through the biofilter, various phenomena such as convection, dispersion, adsorption, diffusion, and reaction affect the level of pollutant (VOC) removal. The model is based on the following assumptions:

1. Isothermal operation and the ideal gas law apply for gas phase.
2. An axially dispersed plug flow is assumed for gas flow through the packed bed.
3. The frictional pressure drop is assumed to be negligible.
4. Oxygen limitation does not occur in the adsorbed phase reaction.
5. The rate of biodegradation depends on the concentrations of pollutant and oxygen.
6. Transport of pollutant and oxygen within the bioflim occurs through diffusion only.
7. The biofilm thickness and density are constant throughout the biofilter.
8. There is no net biomass accumulation in the biofilter bed.
9. The packing material is not entirely covered by the biofilm. The exposed patches of solid are in direct contact with air stream.

The amount of VOCs depleted from the gas phase is calculated using the mass balance equation and is given by Eq. (4.34):

$$\frac{\partial C_i}{\partial t} = D_L \frac{\partial^2 C_i}{\partial Z^2} - V \frac{\partial C_i}{\partial Z} - \left(\frac{1-\varepsilon}{\varepsilon}\right)\left(-\alpha A_s D_i \left.\frac{\partial S_i}{\partial X}\right|_{x=0}\right) + (1-\alpha) K_{ig-ads}\left(q^* - q\right) \qquad (4.34)$$

The first term on the R.H.S of Eq. 4.34 explains the transport due to dispersion; second term indicates the transport by convection (change in concentration due to velocity); third term means degradation of pollutants because of microorganisms and the last term explains the removal of pollutants by adsorption.

The amount of oxygen depleted from the gas phase is calculated using the mass balance equation and is given by Eq. (4.35):

$$\frac{\partial C_0}{\partial t} = D_L \frac{\partial^2 C_0}{\partial Z^2} - V \frac{\partial C_0}{\partial Z} - \left(\frac{1-\varepsilon}{\varepsilon}\right)\left(-\alpha A_s D_0 \left.\frac{\partial S_0}{\partial X}\right|_{x=0}\right) \qquad (4.35)$$

Similarly, the first term on the R.H.S of Eq. 4.35 means the movement of oxygen along the bed height; second term means the transport of oxygen by convection; third term means the interfacial equilibrium and transport of oxygen on the biofilm surface.

The following initial conditions are considered for solving Eqs. (4.34) and (4.35):

$$C_i(z,0) = 0 \qquad (4.36)$$

$$C_o(z,0) = 0 \qquad (4.37)$$

The boundary conditions for solving Eqs. (4.34) and (4.35) are given by:

$$D_L \left.\frac{\partial C_i}{\partial Z}\right|_{z=0} = -V\left(C_i\big|_{0^-} - C_i\big|_{0^+}\right) \qquad (4.38)$$

$$\left.\frac{\partial C_i}{\partial Z}\right|_{z=L} = 0 \qquad (4.39)$$

$$D_L \left.\frac{\partial C_0}{\partial Z}\right|_{z=0} = -V\left(C_0\big|_{0^-} - C_0\big|_{0^+}\right) \tag{4.40}$$

$$\left.\frac{\partial C_0}{\partial Z}\right|_{z=L} = 0 \tag{4.41}$$

Eq. 4.38 means that for any time t; at z = 0; concentration of VOC should be equal to its initial concentration and Eq. 4.39 explains that there is no change in VOC concentration at the end of the column.

The mass balance for VOC and oxygen in the biofilm is given by Eqs. (4.42) and (4.43):

$$\frac{\partial S_i}{\partial t} = D_i \frac{\partial^2 S_i}{\partial x^2} - R_{i,bf} \tag{4.42}$$

$$\frac{\partial S_0}{\partial t} = D_o \frac{\partial^2 S_o}{\partial x^2} - R_{0,bf} \tag{4.43}$$

The initial conditions are given by Eqs. (4.44) and (4.45):

$$S_i(z, x, 0) = 0 \tag{4.44}$$

$$S_o(z, x, 0) = 0 \tag{4.45}$$

The boundary conditions are given by Eqs.(4.46) to (4.49):

$$S_i\big|_{x=0} = C_i \big/ m_{1,i} \tag{4.46}$$

$$-\alpha A_s D_i \left.\frac{\partial S_i}{\partial x}\right|_{x=\delta} = k_{i,1-ads}\left(q^*_{i,g-ads} - q_i\right) \tag{4.47}$$

$$S_0\big|_{x=0} = C_0 \big/ m_0 \tag{4.48}$$

$$\left.\frac{\partial S_0}{\partial x}\right|_{x=\delta} = 0 \tag{4.49}$$

The balance of VOC in the adsorbent phase is given by Eq. (4.50):

$$\frac{\partial q_i}{\partial t} = \alpha k_{i,1-ads}\left(q^*_{i,g-ads} - q_i\right) + (1-\alpha)k_{i,g-ads}\left(q^*_{1,g-ads} - q_i\right) - R_{ads} \tag{4.50}$$

The initial condition for solving Eq. (4.50) is given by Eq. (4.51):

$$q_i(z,0) = 0 \tag{4.51}$$

The biodegradation in the biofilm with oxygen limitation is given by Eqs. (4.52) and (4.53):

$$R_{i,\mathrm{bf}}\left(S_i, S_O\right) = \frac{r_{\max,i} S_i}{k_{\mathrm{m,i}}\left(1 + \dfrac{S_i^2}{K_{\mathrm{I},i} k_{\mathrm{m,i}}}\right) + S_i} \frac{S_{\mathrm{O}}}{k_{\mathrm{O,i}} + S_{\mathrm{O}}} \tag{4.52}$$

$$R_{O,\mathrm{bf}}\left(S_i, S_O\right) = \frac{r_{\max O,i} S_i}{k_{\mathrm{m,i}}\left(1 + \dfrac{S_i^2}{K_{\mathrm{I},i} k_{\mathrm{m,i}}}\right) + S_i} \frac{S_{\mathrm{O}}}{k_{\mathrm{O,i}} + S_{\mathrm{O}}} \tag{4.53}$$

The proposed mathematical model incorporates the effects of gas biofilm resistances, possible extent of reaction in pores on biofilter, gas-phase mass transfer coefficient, and axial diffusion coefficient which were neglected in earlier studies.

4.4.2.1. Dimensionless form of model equations

The mass balance equations are converted to dimensionless form in order to get simplified solution because the explicit finite difference technique has been used to solve these equations. The non-dimensionalization forms of some of the terms used in the present models are given by Eqs. (4.54) to (4.62).

Dimensionless substrate concentration:

$$X_{\mathrm{i}} = \frac{C_{\mathrm{i}}}{C_{\mathrm{i0}}} \tag{4.54}$$

Dimensionless time:

$$T = \frac{vt}{L} \tag{4.55}$$

Dimensionless height:

$$Z = \frac{z}{L} \tag{4.56}$$

Peclet No.:

$$Pe = \frac{Lv}{D_{\mathrm{L}}} \tag{4.57}$$

Biolayer substrate concentration:

$$Y_i = \frac{m_{1\mathrm{i}} S_{\mathrm{i}}}{C_{\mathrm{i0}}} \tag{4.58}$$

Dimensionless biolayer thickness:

$$X = \frac{x}{\delta} \tag{4.59}$$

Dimensionless super substrate concentration:

$$Z_{\mathrm{i}} = \frac{m_{2\mathrm{i}} q_{\mathrm{i}}}{C_{\mathrm{i0}}} \tag{4.60}$$

Dimensionless oxygen concentration:

$$X_0 = \frac{C_{\mathrm{O}}}{C_{\mathrm{O,0}}} \tag{4.61}$$

Dimensionless biolayer oxygen concentration:

$$Y_O = \frac{m_{\mathrm{O}} S_{\mathrm{O}}}{C_{\mathrm{O,0}}} \tag{4.62}$$

The dimensionless form of Eq. (4.34) is given by Eq. (4.63):

$$\frac{\partial X_i}{\partial t} = \frac{1}{Pe}\frac{\partial^2 X_i}{\partial Z^2} - \frac{\partial X_i}{\partial Z} - \left(\frac{1-\varepsilon}{\varepsilon}\right)\left(-\frac{\alpha A_s L D_i}{\delta V}\frac{\partial Y}{\partial X}\bigg|_{x=0}\right) + \frac{(1-\alpha)LK_{ig-ads}}{m_{2,j}V}\left(X_i - Z_i\right) \tag{4.63}$$

The dimensionless form of Eq. (4.35) is given by Eq. (4.64):

$$\frac{\partial X_O}{\partial t} = \frac{1}{Pe}\frac{\partial^2 X_O}{\partial Z^2} - \frac{\partial X_O}{\partial Z} + \left(\frac{1-\varepsilon}{\varepsilon}\right)\left(-\frac{\alpha A_s L D_O}{m_O \delta V}\frac{\partial Y_O}{\partial X}\bigg|_{x=0}\right) \tag{4.64}$$

The dimensionless form of initial conditions and boundary conditions to solve Eqs. (4.63) and (4.64) respectively are given by Eqs. (4.65) & (4.66) and Eqs (4.67) to (4.70):

$$X_i(Z,0) = 0 \tag{4.65}$$

$$X_O(Z,0) = 0 \tag{4.66}$$

$$\frac{\partial X_i}{\partial Z}\bigg|_{X=0} = -Pe\left(X_i|_{0^-} - X_i|_{0^+}\right) \tag{4.67}$$

$$\frac{\partial X_O}{\partial Z}\bigg|_{X=0} = -Pe\left(X_O|_{0^-} - X_O|_{0^+}\right) \tag{4.68}$$

$$\frac{\partial X_i}{\partial Z}\bigg|_{z=1} = 0 \tag{4.69}$$

$$\frac{\partial X_O}{\partial Z}\bigg|_{z=1} = 0 \tag{4.70}$$

The dimensionless form of Eq. (4.42) is given by Eq. (4.71):

$$\frac{\partial Y_i}{\partial T} = \frac{D_i L}{V\delta^2}\frac{\partial^2 Y_i}{\partial X^2} - \frac{r_{\max,i} L}{V}\frac{Y_i}{k_{mi}\left(1+\dfrac{C_{i,O}Y_i^2}{m_{1,i}^2 k_{1,i} k_{m,i}}\right)} + \frac{C_{i,0}}{m_i}Y_i\frac{Y_O}{\dfrac{k_{O,i}m_O}{C_{O,0}} + Y_O} \tag{4.71}$$

The dimensionless form of Eq. (4.43) is given by Eq. (4.72):

$$\frac{\partial Y_O}{\partial T} = \frac{D_O L}{V\delta^2}\frac{\partial^2 Y_O}{\partial X^2} - \frac{r_{\max O,i} L}{V}\frac{Y_i\dfrac{C_{i,0}}{m_i}}{k_{mi}\left(1+\dfrac{C_{i,O}Y_i^2}{m_{1,i}^2 k_{1,i} k_{m,i}}\right)} + \frac{C_{i,0}}{m_i}Y_i\frac{Y_O}{\left(k_{O,i} + \dfrac{C_{O,0}}{m_O}Y_O\right)} \tag{4.72}$$

The dimensionless form of initial conditions and boundary conditions to solve Eqs. (4.71) and (4.72) are given by Eqs. (4.73) & (4.74) and Eqs. (4.75) to (4.78):

$$Y_i(Z,X,0) = 0 \tag{4.73}$$

$$Y_O(Z,X,0) = 0 \tag{4.74}$$

$$Y_i\big|_{x=0} = X_i \tag{4.75}$$

$$\left.\frac{\partial Y_i}{\partial X}\right|_{X=1} = \frac{m_{1,i}}{\alpha m_{2,i}} \frac{k_{i,1-ads}\delta}{A_S D_i}\left(X_i - Z_i\right) \tag{4.76}$$

$$Y_O\big|_{x=0} = X_O \tag{4.77}$$

$$\left.\frac{\partial Y_O}{\partial X}\right|_{z=1} = 0 \tag{4.78}$$

The dimensionless form of Eq. (4.50) is given by Eq. (4.79):

$$\frac{\partial Z_i}{\partial T} = \frac{(1-\alpha)LK_{ig-ads}}{V} + \frac{\alpha LK_{i,1-ads}}{V}\left(X_i - Z_i\right) - \frac{LK_{rxn,i}}{V}\left(\frac{C_{g,0}}{m_2}\right)^{n-1} {Z_i}^n \tag{4.79}$$

The dimensionless form of initial condition to solve Eq. (4.79) is given by Eq. (4.80):

$$Z_i(Z,0) = 0 \tag{4.80}$$

4.5. Solution techniques

In the present study, the linear and nonlinear growth kinetic models are fitted by method of linear and nonlinear least squares using a professional graphics software package ORIGIN (version 6). It uses the linear and nonlinear curve fit tool available in this software. It has a flexibility to build the user defined mathematical equations which has different constant values and can be used to fit the experimental data. The results

obtained are useful to obtain the constants used in various models with error estimation in terms of coefficient of determination.

The preceding set of partial differential equations in dimensionless form (Eq. 4.63 – 4.80) is discretized using finite difference technique. Finite difference technique has been successfully applied to solve such type of partial differential equations in other studies by Babu and Chaurasia (2003a; 2003b; 2004a; 2004b; 2004c; 2004d), Babu and Gupta (2005), Gupta and Babu (2009), and Babu and Sheth (2006). A mathematical algorithm to solve these coupled equations is developed and implemented into a computer program using MATLAB (v.6.1) software (Appendix I to IV).

The standard deviation, s.d., was calculated for comparing the model and experimental results is and given as:

$$\text{s.d.} = \sqrt{\sum \frac{(C_{\exp} - C_{\mathrm{mod}\,el})^2}{N-1}} \tag{4.81}$$

CHAPTER – 5

RESULTS AND DISCUSSION

The results obtained on biodegradation studies for the removal of methyl ethyl ketone (MEK), methyl isobutyl ketone (MIBK), isopropyl alcohol (IPA), methyl acetate (MA), ethyl acetate (EA) and butyl acetate (BA) are discussed in this chapter. The detailed results on biofiltration studies for the treatment of polluted gases containing VOCs such as MEK, MIBK, IPA and EA are presented. The mechanism of biodegradation of different VOCs is explained with the help of growth kinetic studies and rate kinetic models. The generalized mathematical model for biofiltration column is presented and validated with experimental data and modeling data reported in the literature.

5.1. Batch studies on MEK, MIBK, IPA, MA, EA, and BA

The biodegradation studies are carried out for the removal of MEK, MIBK, IPA, MA, EA, and BA from wastewater. The effect of various important parameters, such as initial concentration of VOC, operating time and biomass concentration is studied. Various growth kinetic models and rate kinetic models are used to understand the mechanism of biodegradation and to obtain the kinetic parameters which are helpful in the design of biofiltration column.

5.1.1. Substrate utilization

The rate of biodegradation is greatly affected by the initial concentration of VOCs. Figs. 5.1 – 5.3 show the change in MEK, MIBK and IPA concentration ranging from 200 – 700 mg L^{-1} with increase in time for biodegradation using the acclimated mixed culture. The time required for the complete consumption of MEK is obtained as 14 h, 15 h, 24 h, 30 h, 34 h and 36 h for 200, 300, 400, 500, 600 and 700 mg L^{-1} of initial MEK concentration (Fig. 5.1). It is observed from Fig. 5.2 that the acclimated mixed culture degraded MIBK in 13 h, 17 h, 23 h, 25 h, 27 h and 29 h for 200, 300, 400, 500, 600 and 700 mg L^{-1} of initial MIBK concentration. Fig. 5.3 show that the maximum concentration of IPA (700 mg L^{-1}) is degraded in 28 h and takes 14 h, 18 h, 21 h, 24 h, and 26 h for the degradation of 200, 300, 400, 500, and 600 mg $L^{-1}$of initial IPA concentration, respectively.

Figs. 5.4, 5.5, and 5.6 show the concentration profiles of MA, EA and BA, respectively for an initial concentration ranging from 200 to 800 mg L^{-1}. It is observed from Fig. 5.4 that the methyl acetate gets degraded by acclimated mixed culture within 39 h for the maximum initial MA concentration of 800 mg L^{-1}. It is found that the acclimated mixed culture completely utilized EA in 15 h, 22 h, 26 h, 32 h, 35 h, 36 h and 38 h for 200, 300, 400, 500, 600, 700 and 800 mg L^{-1} of initial EA concentration (Fig. 5.5). The time required for complete biodegradation of 200 and 800 mg L^{-1} of initial BA concentration is 14 h and 36 h, respectively (Fig. 5.6).

In all studies of biodegradation, for the above six VOCs, biomass concentration and concentration of the compounds are measured till all the compounds are fully consumed by the acclimated mixed culture. Figs. 5.1 – 5.6 show that the concentration of different

compounds decreases with time which indicates the consumption of compounds by microbes as they utilize it as a carbon source for their growth (Devinny et al. 1999). The results obtained from Figs. 5.1 – 5.6 indicate that at initial VOCs concentration values of 100 – 300 mg L^{-1}, the time taken by microorganisms to start degradation of VOCs is less. This also confirms the presence of small lag phase for lower values of initial VOCs concentration. As the initial VOCs concentration is increased over 300 mg L^{-1}, the time taken by microorganisms to start utilizing the VOCs as food source also increased. The increase in initial VOCs concentration is attributed to the increase in lag time. This may be due to the fact that the longer lag time corresponds to the ability of mixed culture to acclimate itself to increase in VOCs concentration and is attributed to substrate inhibition. Longer lag time corresponding to an increase in initial concentration of VOCs is also reported for mixed culture by Saravanan et al. (2008). The results obtained for biodegradation studies indicate that higher initial concentration of VOCs, more is the time taken by microorganisms for complete degradation of VOCs. The increase in biodegradation time with increase in initial concentration of VOCs may be due to the increase in lag time which delays in the total time for biodegradation.

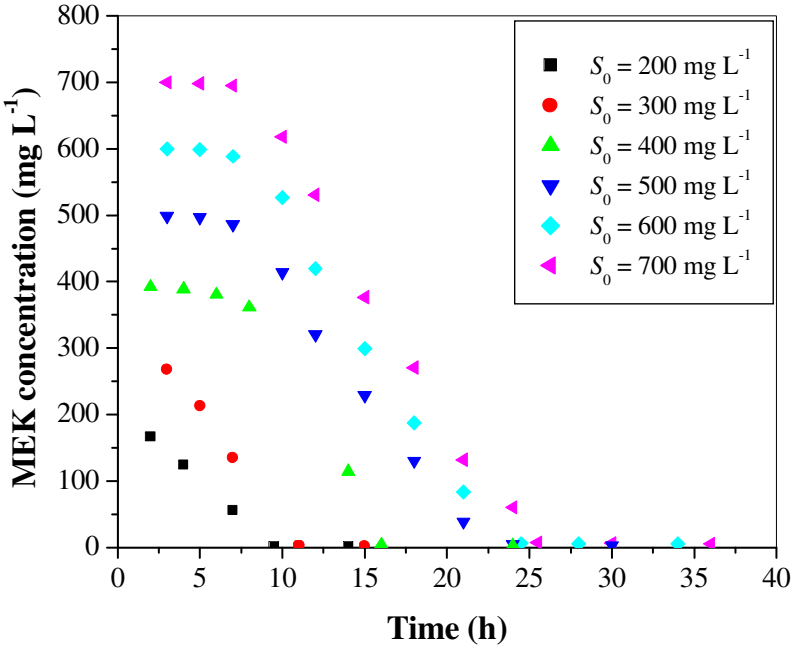

Fig. 5.1. Variation of MEK concentration with time using acclimated mixed culture

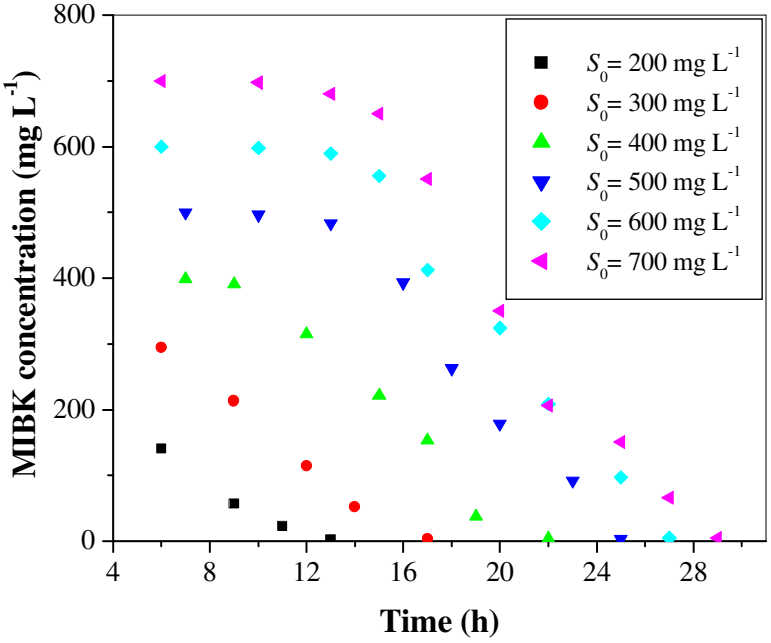

Fig. 5.2. Variation of MIBK concentration with time using acclimated mixed culture

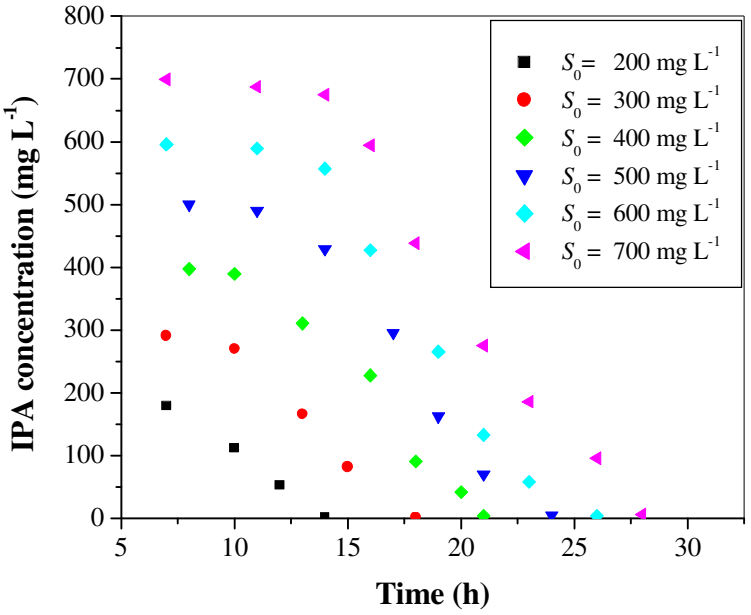

Fig. 5.3. Variation of IPA concentration with time using acclimated mixed culture

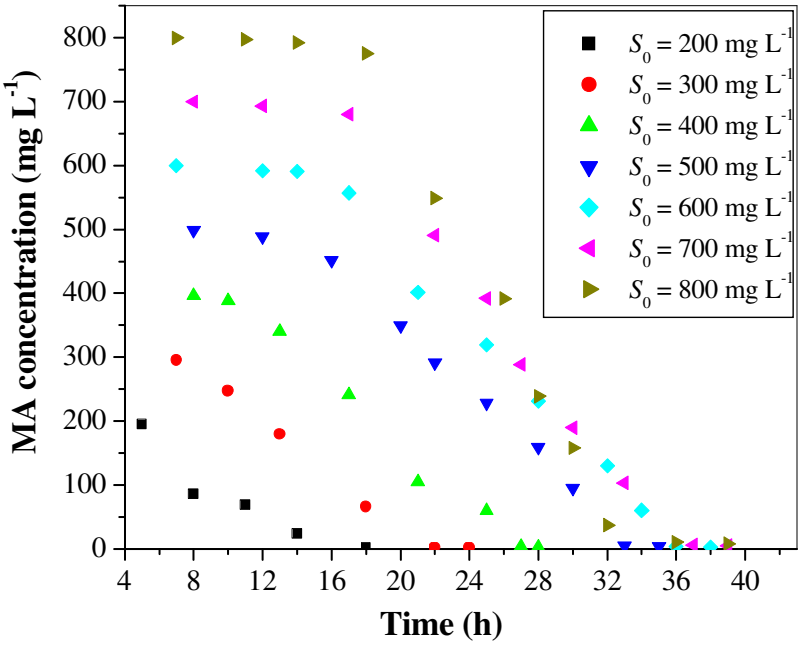

Fig. 5.4. Variation of MA concentration with time using acclimated mixed culture

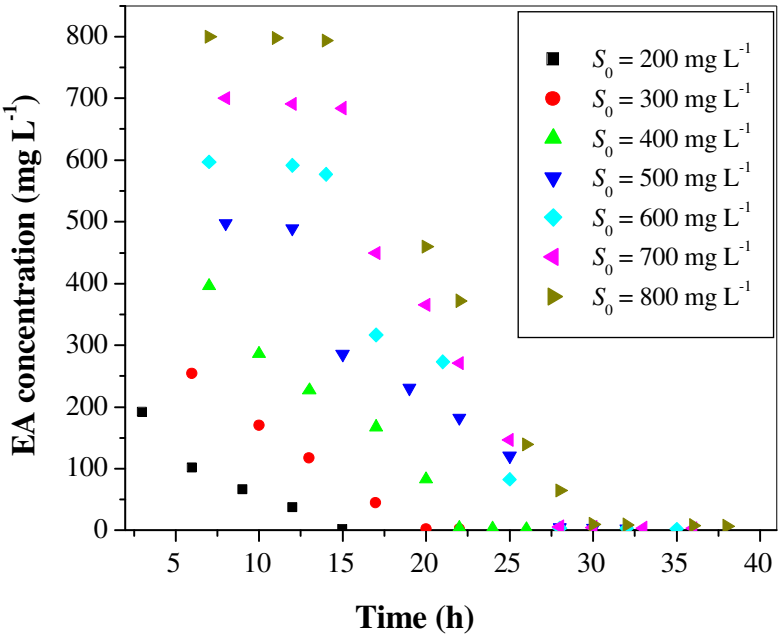

Fig. 5.5. Variation of EA concentration with time using acclimated mixed culture

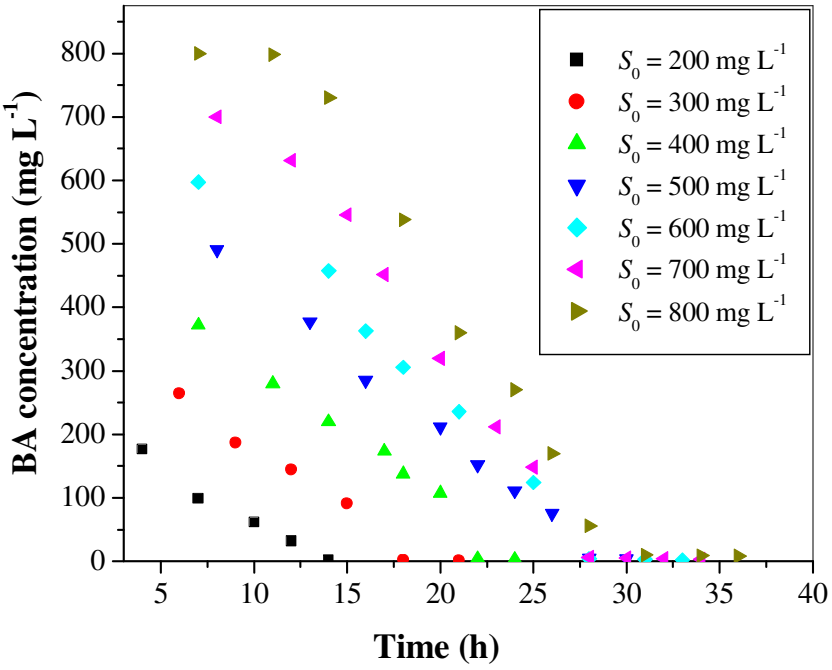

Fig. 5.6. Variation of BA concentration with time using acclimated mixed culture

5.1.2. Microbial growth profiles

The biomass concentration profile of the acclimated mixed culture (as OD_{540}) at different times for the initial concentration ranging from 200 to 700 mg L^{-1} is observed for MEK, MIBK and IPA. The biomass concentration is calculated using the calibration curve (optical density vs. biomass concentration) for each compound as given in Chapter-3 (Fig. 3.1). The values of maximum biomass concentration are obtained as 0.368, 0.451, 0.5, 0.475, 0.462, and 0.451 g L^{-1} for the initial MEK concentrations of 200, 300, 400, 500, 600, and 700 mg L^{-1}, respectively as shown in Fig. 5.7. The biomass concentration increased with an increase in the initial MEK concentration from 200 to 400 mg L^{-1} and thereafter decreasing trend is observed. The maximum values of biomass concentration are achieved as 0.172, 0.21, 0.257, 0.294, 0.286, and 0.28 g L^{-1} for the initial MIBK concentrations ranging from 200 – 700 mg L^{-1}, respectively (Fig. 5.8). The biomass concentration shows an increasing trend for an increase in initial MIBK concentration from 200 to 500 mg L^{-1} then it decreases with an increase in initial MIBK concentration. The values of biomass concentration are obtained as 0.104, 0.137, 0.155, 0.151, 0.143, and 0.139 g L^{-1} for 200 – 700 mg L^{-1} of IPA concentration as shown in Fig. 5.9. The biomass concentration increased with an increase in initial IPA concentration from 200 to 400 mg $L^{-1}$and then the decreasing trend is observed.

Figs. 5.10 – 5.12 show the profiles of biomass concentration versus time for MA, EA, and BA, respectively. The values of maximum biomass concentration are obtained as 0.25, 0.289, 0.302, 0.432, 0.435, 0.401 and 0.321 g L^{-1} for initial MA concentration of 200, 300, 400, 500, 600, 700 and 800 mg L^{-1}, respectively (Fig. 5.10). The values of maximum biomass concentration increases from 0.225 – 0.45 g L^{-1} for initial EA

concentration from 200 – 500 mg L^{-1} then it decreases with an increase in initial concentration up to 800 mg L^{-1} and obtained as 0.36 g L^{-1} (Fig. 5.11). It is observed from Fig. 5.12 that the maximum value of biomass concentration is obtained as 0.465 g L^{-1} for 500 mg L^{-1} of initial BA concentration.

Figs. 5.7 - 5.12 shows the growth curve where all the three phases such as lag, log stationary and decay phases are observed. It is observed that, initially, with an increase in time, there is no increment in the biomass concentration for higher concentration range of VOCs (beyond 400 mg L^{-1} for MEK, MIBK, IPA and EA while) giving the lag phase. The lag phase is observed beyond 300 and 200 mg L^{-1} MA and EA respectively. This is due to the reason that the microbial culture takes some time for acclimation to the new environment. This can also be explained by the fact that at higher concentration of VOCs, the substrate inhibition effect predominates. In log phase, the biomass concentration is increased exponentially where most of the substrate (VOC) is utilized by the microorganisms for their growth. The log phase is obtained earlier for the lower range of initial concentration for all VOCs. The log phase data for biodegradation are used for the evaluation of kinetic parameters. The biomass growth rate at this phase is maximum and constant which depends on the microbial species and the environmental conditions. Once the whole VOC available as food is utilized by the microorganisms, the growth of biomass eventually stops and the growth rate gradually decreases with an increase in the time of biodegradation and this phase is known as stationary phase. In most cases the stationary phases in practically absent (Figs 5.7 to 5.12) which means that the mixed culture is very sensitive. After this phase, the death rate of microorganisms increases and the number of living cells decreases. This is an indicative measure of death phase.

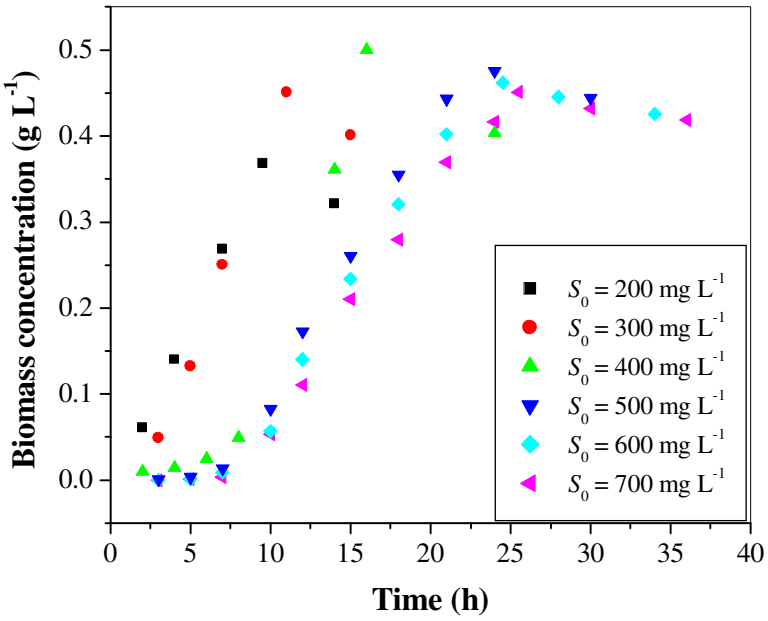

Fig. 5.7. Variation of biomass concentration with respect to time for different initial MEK concentration

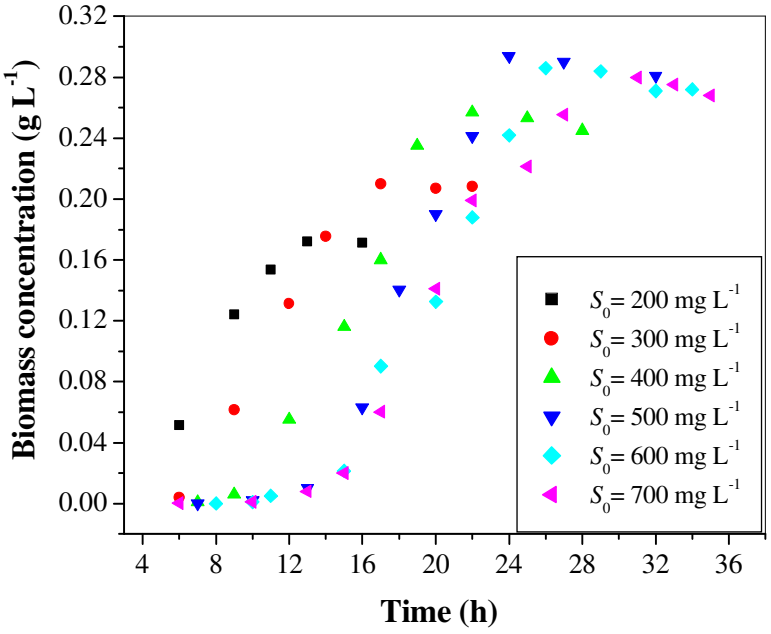

Fig. 5.8. Variation of biomass concentration with respect to time for different initial MIBK concentration

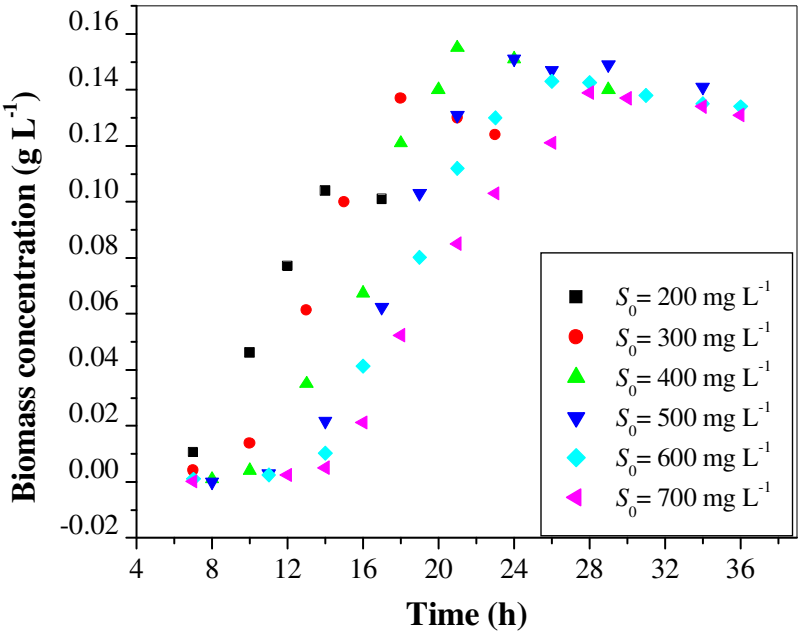

Fig. 5.9. Variation of biomass concentration with respect to time for different initial IPA concentration

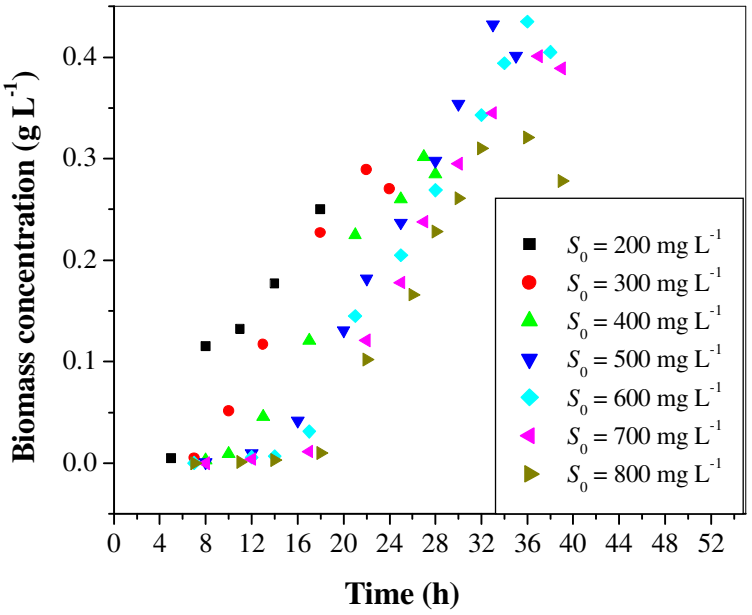

Fig. 5.10. Variation of biomass concentration with respect to time for different initial MA concentration

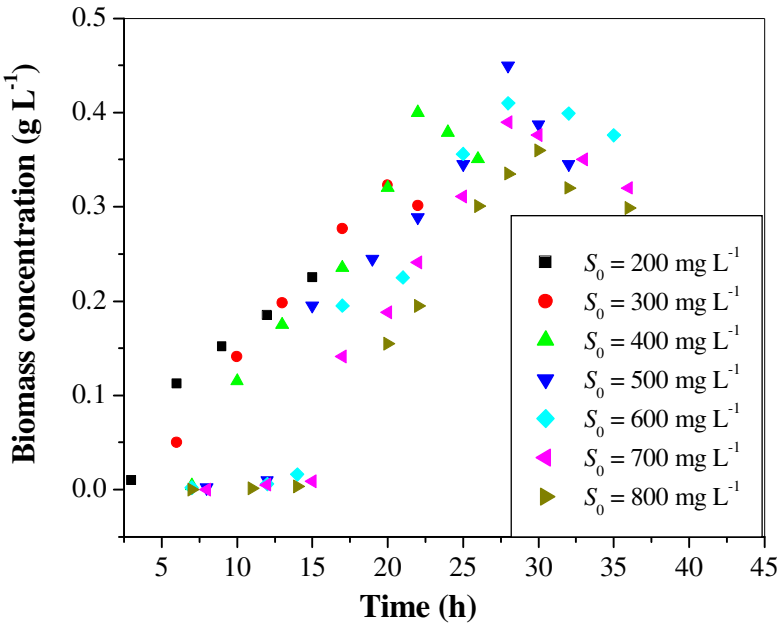

Fig. 5.11. Variation of biomass concentration with respect to time for different initial EA concentration

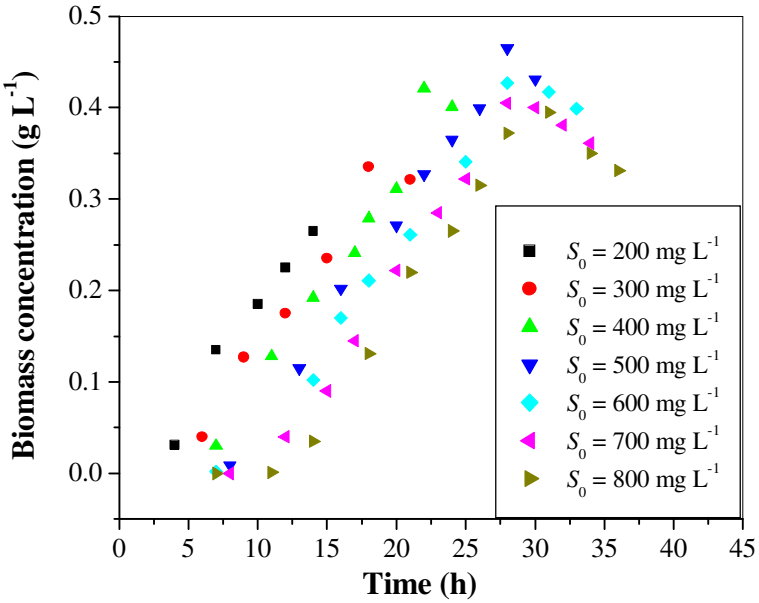

Fig. 5.12. Variation of biomass concentration with respect to time for different initial BA concentration

5.1.3. Specific growth rate

In the batch biodegradation study, the contaminant (VOC) degradation leads to the formation of biomass. The amount of biomass increases exponentially with respect to time during log phase. The increase in biomass concentration depends on the depletion of substrate concentration. As contaminant degradation is the result of the microbial activity, the kinetics of contaminant degradation is closely related to the specific growth rate of microorganisms. In general, the growth rate of the microorganisms at a given time in the log phase is proportional to the number of microorganisms present at that time. The obtained biomass concentration and substrate concentration at different time intervals for various initial concentrations of VOCs are used to calculate the specific growth rate and given by Eq. (5.1).

$$\mu = \frac{1}{x}\frac{dx}{dt} \tag{5.1}$$

where, μ is the specific growth rate (h^{-1}), x is the biomass concentration (g L^{-1}) at time t (h), and dt is the change in time (h). After integration, Eq. (5.1) becomes Eq. (5.2):

$$\ln x = \ln x_0 + \mu t \tag{5.2}$$

where, x_0 is the initial biomass concentration (g L^{-1}) at $t = 0$. A plot of ln x versus t gives a straight line with ln x_0 as its intercept and μ as the slope. The specific growth rate for different values of initial concentration of MEK, MIBK, IPA, MA, EA and BA are calculated using the data obtained for log phase. The plots of ln x versus t for different initial concentration values of MEK, MIBK, IPA, MA, EA and BA are shown in Figs. 5.13 – 5.18 respectively. The log phase data are considered for the estimation of specific growth rate and data for other phases such as lag, stationary and death phases are ignored

as there is no growth of biomass in these phases. The values of specific growth rate for different compounds are reported in Table 5.1.

It is observed that the specific growth rate of MEK is higher than the MIBK at same initial concentration (Table 5.1). This indicates that MEK can be degraded faster than the MIBK. The specific growth rate of IPA is obtained less than MEK but higher than the MIBK. Out of MA, EA and BA (same series compounds), the specific growth rate is increasing in the order of MA, EA and BA. This may be due to increase in the molecular weight of compounds for the same series of acetates.

The obtained values of specific growth rates in batch biodegradation study are used to evaluate the growth kinetic models and estimate their respective model parameters for different VOCs such as MEK, MIBK, IPA, MA, EA and BA. The different growth kinetic models are discussed in the following sections.

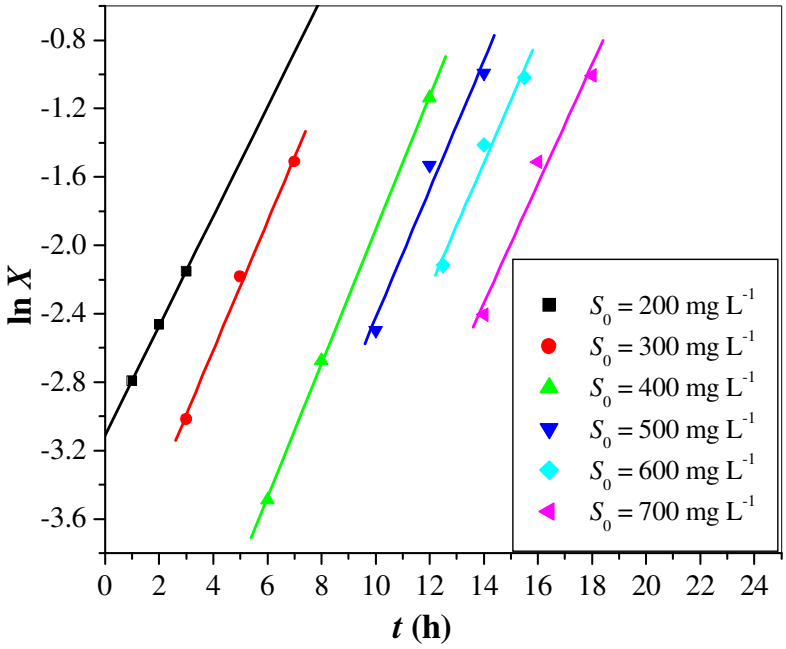

Fig. 5.13. Plot for calculation of specific growth rates for MEK

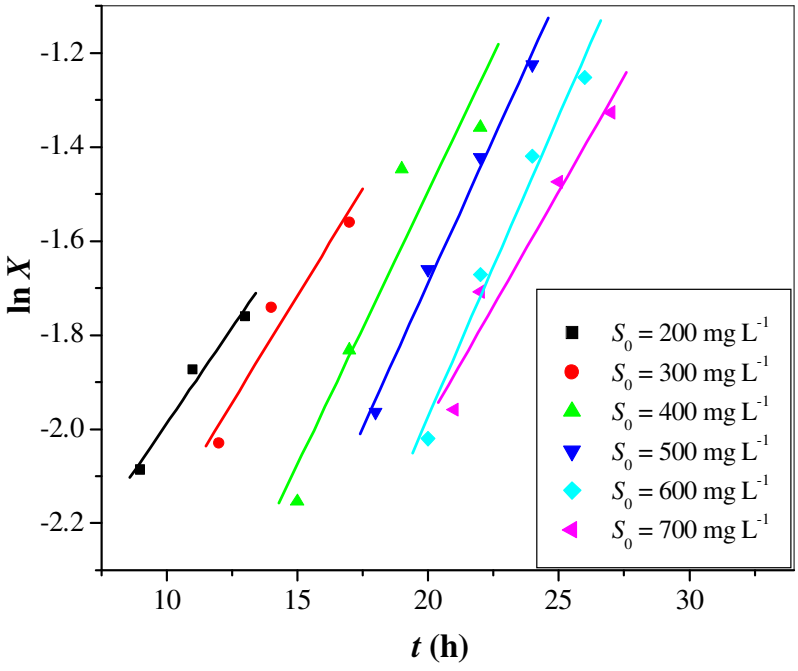

Fig. 5.14. Plot for calculation of specific growth rates for MIBK

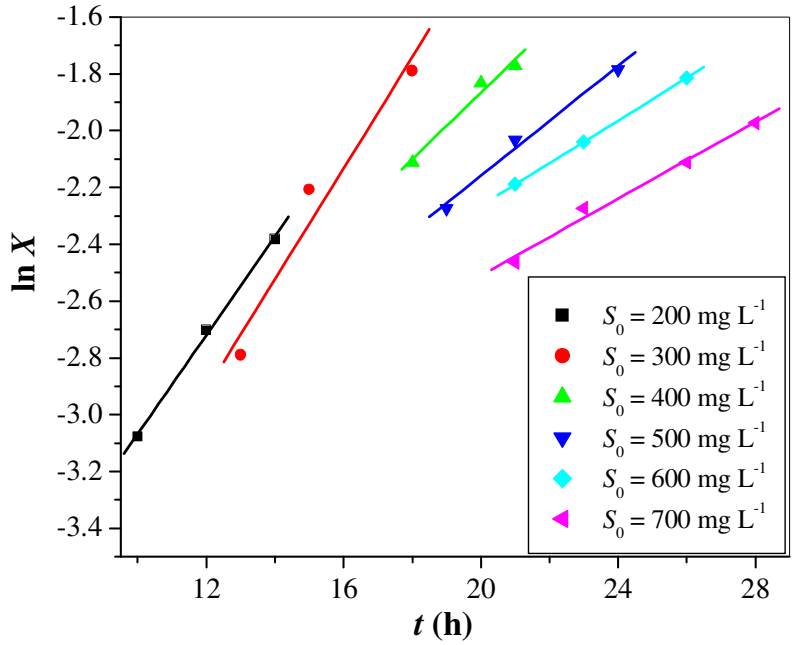

Fig. 5.15. Plot for calculation of specific growth rates for IPA

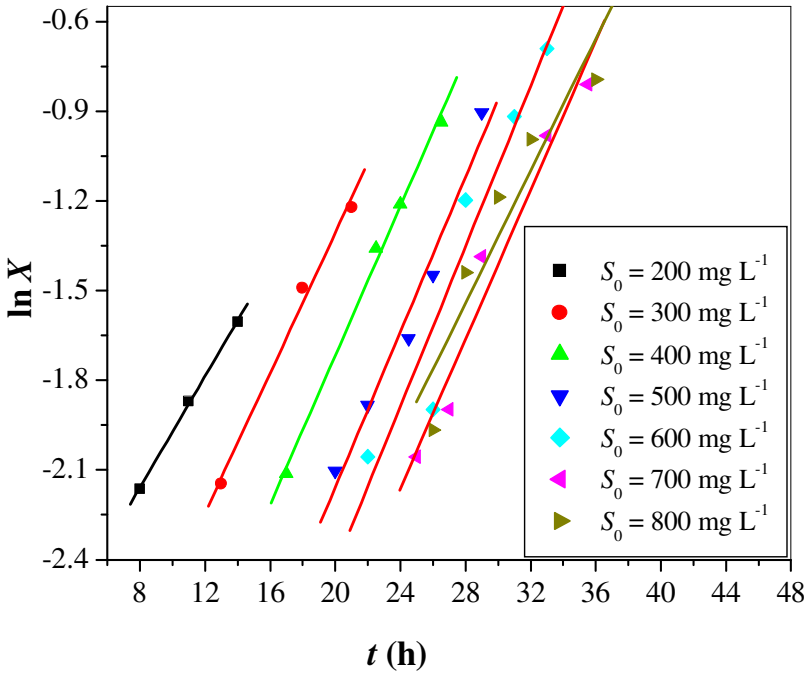

Fig. 5.16. Plot for calculation of specific growth rates for MA

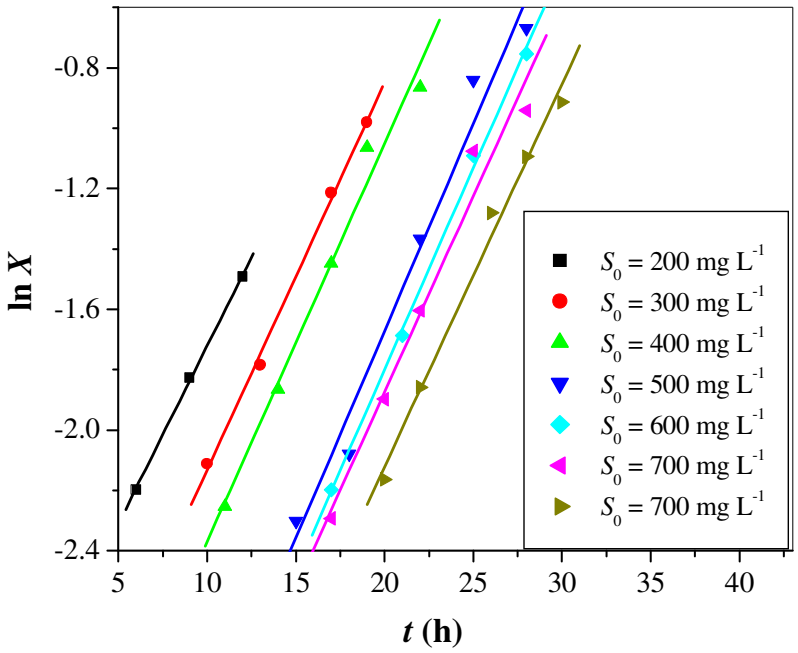

Fig. 5.17. Plot for calculation of specific growth rates for EA

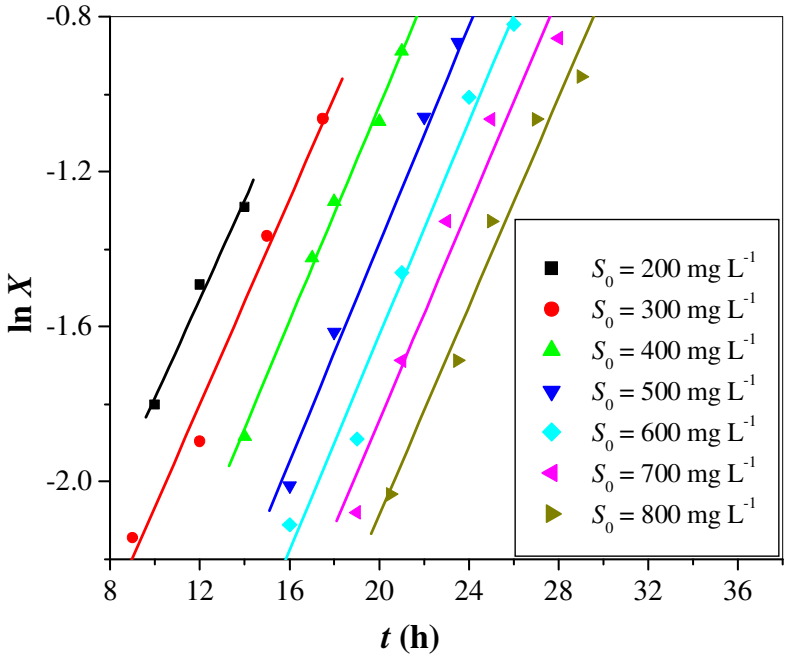

Fig. 5.18. Plot for calculation of specific growth rates for BA

Table 5.1. Specific growth rate for different compounds used in biodegradation studies

S No	Initial Concentration, S_0, (mg L^{-1})	Value of specific growth rate (Experimental), μ, (h^{-1})					
		MEK	**MIBK**	**IPA**	**MA**	**EA**	**BA**
1	200	0.319	0.082	0.154	0.093	0.118	0.128
2	300	0.376	0.091	0.195	0.117	0.129	0.132
3	400	0.391	0.116	0.210	0.125	0.132	0.136
4	500	0.375	0.123	0.202	0.130	0.137	0.141
5	600	0.366	0.128	0.182	0.134	0.134	0.138
6	700	0.349	0.098	0.153	0.125	0.130	0.137
7	800	-	-	-	0.111	0.127	0.135

5.1.4. Growth kinetic models

The contaminant degradation leads to the formation of biomass. As contaminant degradation is the result of the microbial activity, the kinetics of contaminant degradation is closely related to the kinetics of microbial growth. The relationship between the specific growth rate (μ) of a population of microorganisms and the substrate concentration (S) is a valuable tool in the biodegradation processes which is also known as growth kinetic model. Several relationships have been proposed to state the growth dynamics of a microbial population that is limited solely by the concentration of a single substrate. As acclimated culture was used for the biodegradation of VOCs in the present study, it is required to test the data obtained for biodegradation of VOCs with different growth kinetic models available in the literature so as to know which one is the best suited out of all the reported growth kinetic models. Various theoretical models such as Monod kinetic model (Monod, 1949), Powell kinetic model (Powell, 1967), Haldane model (Andrew, 1968), Luong model (Luong, 1986) and Edwards model (Edwards, 1970) are reported in the literature and are used in the present study to express the growth kinetics of different VOCs.

5.1.4.1. Monod model

The linearized Monod equation is solved by plotting the graph between ($1/\mu$) and ($1/S$) by using the log phase data for each of the VOCs which gives a straight line. The intercept of the straight line gives the value of maximum specific growth rate (μ_m) and the slope gives the value of substrate affinity constant (K_s). The values of μ_m are obtained as 0.39 h^{-1}, 0.142 h^{-1} and 0.193 h^{-1} for MEK, MIBK and IPA respectively while the values of K_s are obtained as 28.799 mg L^{-1}, 131.54 mg L^{-1} and 21.205 mg L^{-1} respectively and are

reported in Tables 5.2 to 5.4. The obtained values of coefficient of determination (R^2) are 0.271, 0.497 and 0.46 for MEK, MIBK and IPA respectively. The values of μ_m obtained for MA, EA and BA are 0.139 h^{-1}, 0.138 h^{-1} and 0.142 h^{-1} while the values of K_s are obtained as 71.366 mg L^{-1}, 26.315 mg L^{-1} and 20.627 mg L^{-1} respectively for MA, EA and BA and are listed in Tables 5.5 to 5.7. The obtained values of coefficient of determination (R^2) are 0.468, 0.464 and 0.682 for MA, EA and BA respectively. Experimentally calculated and predicted values using the Monod model for the specific growth rate are compared and are shown in Figs. 5.19, 5.20, 5.21, 5.22, 5.23, and 5.24 for MEK, MIBK, IPA, MA, EA, and BA respectively. Tables 5.8 to 5.10 report the experimental and predicted values of specific growth rate using Monod model for the concentration range from 200 – 700 mg L^{-1} for MEK, MIBK and IPA respectively. Experimental and predicted values of specific growth rate for MA, EA, and BA for the concentration range from 200 – 800 mg L^{-1} are listed in Tables 5.11, 5.12 and 5.13.

These lower values of R^2 indicate that the Monod model do not confirm well to the obtained experimental data of all the VOCs used in the present study. The specific growth rate is decreased above the initial concentration of 400, 600, 400, 600, 500, and 500 mg L^{-1} for MEK, MIBK, IPA, MA, EA, and BA respectively which is an indicative of self-inhibition of VOCs (Figs. 5.19 to 5.24). The obtained value of K_s using Monod model is much smaller than the lowest concentration of different VOCs used in the present study which is also indicative of the self-inhibition of MIBK (Deshusses, 1994). The self-inhibition effect of substrate is not incorporated in the Monod model. This may be one of the reasons of poor fitting of the experimental kinetic data with this model.

5.1.4.2. Powell model

The Powell model (Eq. 4.6) involves the maintenance term and three kinetic constants which cannot be estimated accurately using graphical method. So the three kinetic constants for MEK, MIBK, IPA, MA, EA, and BA are obtained by log phase data by the method of non-linear least squares using data regression and are listed in Tables 5.2 – 5.7. The obtained values of coefficient of determination (R^2) are 0.558, 0.533, 0.538, 0.579, 0.484, and 0.691 for MEK, MIBK, IPA, MA, EA, and BA respectively which are higher than the obtained values of R^2 for Monod model and shows that Powell models fits the experimental data slightly better than the Monod model (Tables 5.2 – 5.7). This may be due to the incorporation of maintenance rate in Powell model. Although the values of R^2 obtained using Powell model are higher than the Monod model it still indicates that the present experimental kinetic data do not confirm well to the Powell model (Figs. 5.19 – 5.24). Experimental and predicted values of specific growth rate using Powell model for MEK, MIBK, IPA, MA, EA, and BA for the different concentration range are listed in Tables 5.8, 5.9, 5.10, 5.11, 5.12 and 5.13 respectively.

Except Monod model, other models are non-linear and have more than two parametric constants including maximum specific growth rate and substrate affinity constant. So, the initial guesses are needed for these parameters to obtain the parameters from inhibition models. Monod and Powell models do not consider the self inhibition effect which is exhibited during the VOCs biodegradation process at initial higher concentration. It was well established in earlier studies (Dapena-Mora et al., 2007) that if the substrate concentration is much higher than the substrate affinity constant values, substrate inhibition models are better than the Monod model. The values of substrate affinity

constant (K_s) obtained for MEK, MIBK, IPA, MA, EA, and BA using Powell model are 5.176, 2.344, 5.610, 15.674, 1.920, and 2.1741 mg L^{-1} which are quite lesser than the initial concentration of different VOCs (200 – 800 mg L^{-1}). As the affinity constant values obtained using the Monod and Powell models show significant inhibition effect, it is important to get an accurate inhibition growth kinetic model to define the relationship between the specific growth rate and substrate concentration. In the present study, as acclimated culture was used for the biodegradation of different VOCs, it is essentially required to test the data obtained for VOCs biodegradation with different inhibition growth kinetic models available in the literature.

5.1.4.3. Haldane model

As the substrate concentration is increased, the time to start degrading the VOCs by microbes increases, and the rate for biodegradation of VOCs decreases. This phenomenon is called substrate inhibition which is better explained by Haldane model. The three-parameter Haldane model (Eq. 4.7) is solved by the method of non-linear least squares. The bio-kinetic constants for Haldane model of MEK, MIBK, IPA, MA, EA, and BA degradation by acclimated mixed culture are evaluated using the log phase data and are listed in Tables 5.2, 5.3, 5.4, 5.5, 5.6, and 5.7 respectively. The estimated values of coefficient of determination (R^2) using Haldane model are 0.956, 0.702, 0.788, 0.905, 0.939, and 0.869 for MEK, MIBK, IPA, MA, EA, and BA respectively. The value of coefficient of determination (R^2) indicates that Haldane model fit the experimental kinetic data quite well for MEK (R^2 = 0.956), MA (R^2 = 0.905), and EA (R^2 = 0.939) but do not confirm well for MIBK (R^2 = 0.702), IPA (R^2 = 0.788) and BA (R^2 = 0.869). Haldane model is found to be better in describing the experimental kinetic data than the Monod

and Powell model for all VOCs used in the present study. The experimental and predicted specific growth rate values for different VOCs are plotted in Figs. 5.19 to 5.24 and reported in Tables 5.8 to 5.13.

Substrate inhibition constant (K_I) obtained are 595.96, 51.996, 69.14, 220.28, 1457.7, and 4970.1 mg L^{-1} for MEK, MIBK, IPA, MA, EA, and BA respectively. The obtained values of substrate inhibition constant are low for MIBK and IPA which indicate that MIBK and IPA are more toxic for the growth of microbial culture than the MEK, MA, EA, and BA. Similar trends were reported by Sahinkaya and Dilek (20007) for MIBK.

Critical concentration is obtained using Haldane model as 455.46, 520.95, 383.98, 495.57, 468.25, and 526.24 mg L^{-1} for MEK, MIBK, IPA, MA, EA, and BA respectively. Above the critical concentration, the VOCs show inhibitory effect and the growth rate falls (Tomei et al., 2004). Experimentally obtained values of MEK, MIBK, IPA, MA, EA, and BA concentration at which the specific growth rate decreases are 400, 600, 400, 600, 500, and 500 mg L^{-1} respectively which are similar to the obtained values of critical concentrations using Haldane model.

5.1.4.4. Luong model

Luong model also explains the substrate inhibition effect. So the experimental growth data sets of various VOCs are fitted with the Luong model. The bio-kinetic constants are evaluated with application of Luong model for different VOCs using log phase data and are listed in Tables 5.2 – 5.7. Experimentally found specific growth rate at different initial concentration of MEK, MIBK, IPA, MA, EA, and BA is fitted with Luong model and are shown in Figs 5.19 – 5.24. The obtained values of coefficient of determination (R^2) using Luong model are 0.978, 0,904, 994, 0.983, 0.957, and 0.914 for MEK, MIBK,

IPA, MA, EA, and BA respectively which are higher than the obtained values of coefficient of determination (R^2) for Monod, Powell, and Haldane models (Tables 5.2 – 5.7). This shows that the Luong model fits the experimental growth data better than the Monod, Powell, and Haldane models. The experimental and predicted specific growth rate values using Luong model for different VOCs used in the present study are reported in Tables 5.8 to 5.13.

The obtained value of maximum VOCs concentration (S_m) at which the culture ceased to grow is 5976.9, 762.193, 1107, 898.23, 1189.7, and 864.39 for MEK, MIBK, IPA, MA, EA, and BA respectively according to Luong model. Hence the acclimated culture can grow in the presence of MEK, MIBK, IPA, MA, EA, and BA, if the concentration of substrate is maintained as lower than the maximum substrate concentration (S_m). The obtained maximum concentration of VOCs (S_m) is usually less than the critical exposure limit and short exposure limit of different VOCs as given in Table 3.1. This indicates that the obtained acclimated culture for different VOCs can be used to degrade the substrate (VOCs) from the various effluent streams of different industries.

5.1.4.5. Edwards model

The Edwards model explains the substrate inhibition for wider concentration range. The experimental specific growth data for log phase at different initial VOCs concentration for various VOCs are used for estimating the kinetic parameters of Edward model and listed in Tables 5.2 – 5.4. The obtained value of coefficient of determination (R^2) indicated that the Edward model explains the mechanism of biodegradation of MEK (R^2 = 0.989) and IPA (R^2 = 0.989) better than the Haldane model and Luong model. The coefficient of determination (R^2) for the biodegradation of MIBK, MA, EA, and BA are

obtained as 0.786, 0.946, 0.944, and 0.892 respectively which are lesser than the estimated values of coefficient of determination using Luong model but higher than the Haldane model (Tables 5.2 – 5.7). Hence, biodegradation of MIBK, MA, EA and BA can be explained using Edward model but not as good as Luong model. The experimental and predicted specific growth rate values using Edward model for different VOCs are plotted in Figs. 5.19 to 5.24 and reported in Tables 5.8 to 5.13.

The positive constant of Edward model, *K*, estimated is 40.57, 3.145, 4.26, 428.9, 4696, and 241.82 for MEK, MIBK, IPA, MA, EA, and BA respectively. Higher value of the positive constant, *K*, is obtained which indicates that Haldane model is not suitable for different VOCs used in present study as compared to Edwards model (Edwards, 1970).

The obtained results for different growth kinetic models indicate that the growth kinetics of acclimated mixed culture for biodegradation of MEK and IPA is better understood by Edward model but the biodegradation kinetics of MIBK, MA, EA, and BA are described by Luong model. These results also show that the acclimated mixed culture can be used for the treatment of MEK, MIBK, IPA, MA, EA, and BA from effluent streams using biodegradation method.

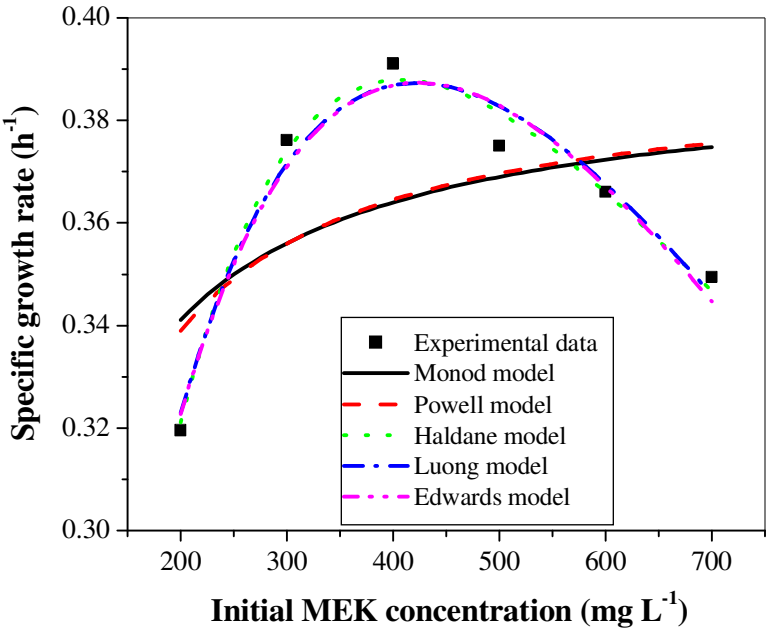

Fig. 5.19. Experimental and predicted specific growth rate values for different growth kinetics models at different initial MEK concentrations

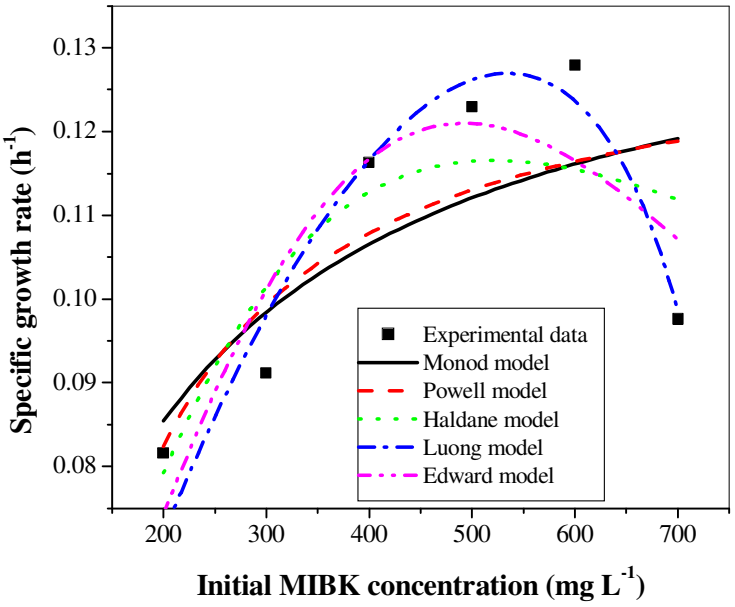

Fig. 5.20. Experimental and predicted specific growth rate values for different growth kinetics models at different initial MIBK concentrations

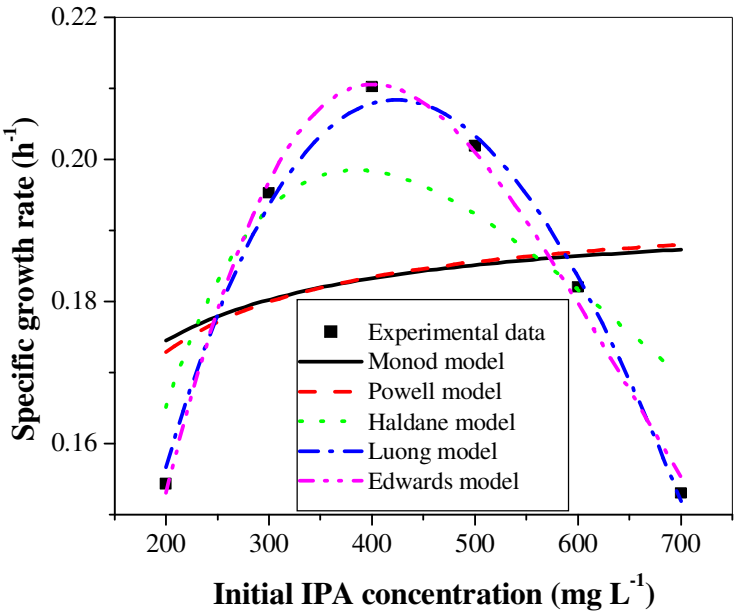

Fig. 5.21. Experimental and predicted specific growth rate values for different growth kinetics models at different initial IPA concentrations

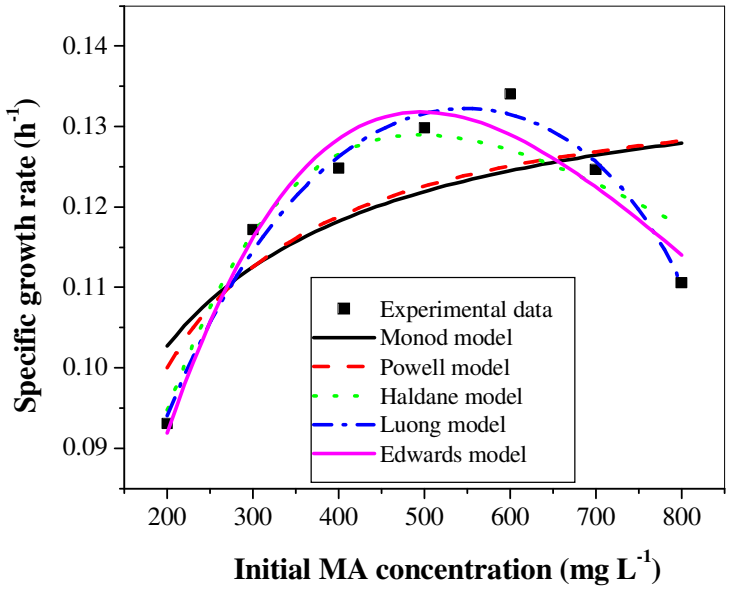

Fig. 5.22. Experimental and predicted specific growth rate values for different growth kinetics models at different initial MA concentrations

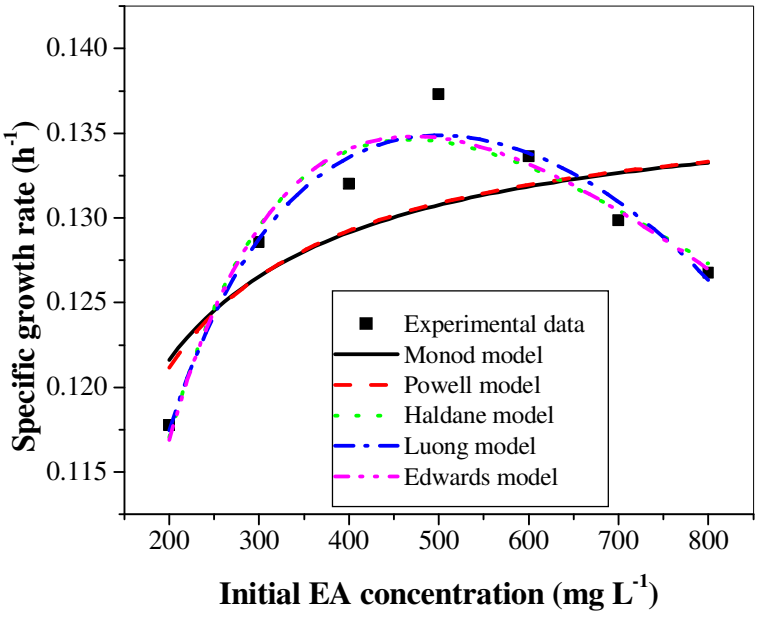

Fig. 5.23. Experimental and predicted specific growth rate values for different growth kinetics models at different initial EA concentrations

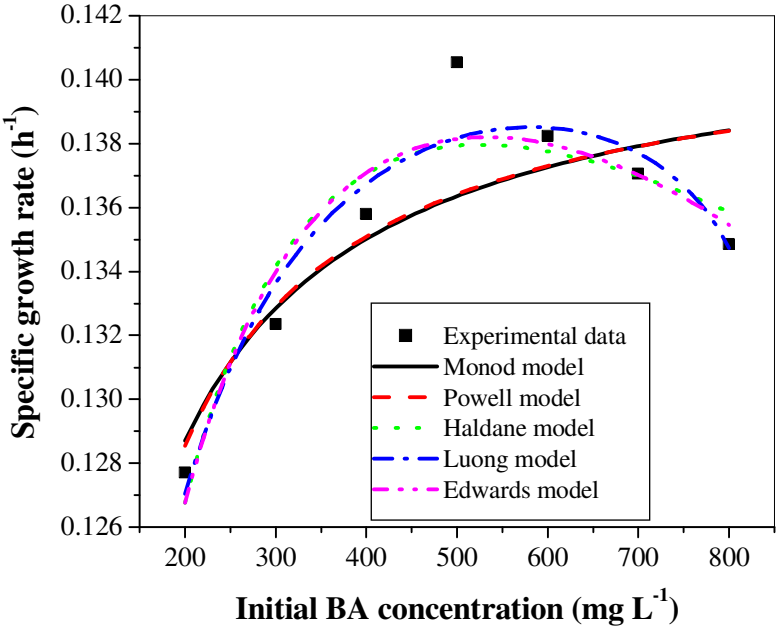

Fig. 5.24. Experimental and predicted specific growth rate values for different growth kinetics models at different initial BA concentrations

Table 5.2. Growth kinetic parameters for MEK biodegradation obtained from different growth models

S No	Model	μ_m (h^{-1})	K_s (mg L^{-1})	K_I (mg L^{-1})	S_m (mg L^{-1})	K	m	n	R^2
1	Monod	0.305	49.98	-	-	-	-	-	0.522
2	Powell	0.303	5.176			-	2.136	-	0.558
3	Haldane	0.721	348.09	595.96	-	-	-	-	0.956
4	Luong	2.167	1210.3	-	5976.9	-	-	8.497	0.978
5	Edward	0.533	250.18	19367		40.57		-	0.989

Table 5.3. Growth kinetic parameters for MIBK biodegradation obtained from different growth models

S No	Model	μ_m (h^{-1})	K_s (mg L^{-1})	K_I (mg L^{-1})	S_m (mg L^{-1})	K	m	n	R^2
1	Monod	0.142	131.54	-	-	-	-	-	0.497
2	Powell	0.134	2.344	-	-	-	4.296	-	0.533
3	Haldane	2.452	5219.49	51.996	-	-	-	-	0.702
4	Luong	1.718	4052.11	-	762.193	-	-	0.377	0.904
5	Edward	1.298	3188.62	23818.57	-	3.145	-	-	0.786

Table 5.4. Growth kinetic parameters for IPA biodegradation obtained from different growth models

S No	Model	μ_m (h^{-1})	K_s (mg L^{-1})	K_I (mg L^{-1})	S_m (mg L^{-1})	K	m	n	R^2
1	Monod	0.193	21.21	-	-	-	-	-	0.458
2	Powell	0.194	5.610	-	-	-	0.73	-	0.538
3	Haldane	2.404	2132.5	69.14	-	-	-	-	0.788
4	Luong	4.555	4141.2	-	1107	-	-	1.47	0.994
5	Edward	2.037	2314.3	13137	-	4.26	-	-	0.995

Table 5.5. Growth kinetic parameters for MA biodegradation obtained from different growth models

S No	Model	μ_m (h^{-1})	K_s (mg L^{-1})	K_I (mg L^{-1})	S_m (mg L^{-1})	K	m	n	R^2
1	Monod	0.139	71.366	-	-	-	-	-	0.468
2	Powell	0.138	15.674	-	-	-	0.48	-	0.519
3	Haldane	0.709	1114.9	220.28	-	-	-	-	0.905
4	Luong	0.268	335.86	-	898.23	-	-	0.24	0.983
5	Edward	0.453	733.37	1114.4	-	428.9	-	-	0.946

Table 5.6. Growth kinetic parameters for EA biodegradation obtained from different growth models

S No	Model	μ_m (h^{-1})	K_s (mg L^{-1})	K_I (mg L^{-1})	S_m (mg L^{-1})	K	m	n	R^2
1	Monod	0.138	26.315	-	-	-	-	-	0.464
2	Powell	0.137	1.920	-	-	-	1.59	-	0.484
3	Haldane	0.221	150.42	1457.7	-	-	-	-	0.939
4	Luong	0.182	97.906	-	1189.7	-	-	0.23	0.957
5	Edward	0.212	139.93	1907.5	-	4696	-	-	0.944

Table 5.7. Growth kinetic parameters for BA biodegradation obtained from different growth models

S No	Model	μ_m (h^{-1})	K_s (mg L^{-1})	K_I (mg L^{-1})	S_m (mg L^{-1})	K	m	n	R^2
1	Monod	0.142	20.627	-	-	-	-	-	0.682
2	Powell	0.142	2.1741	-	-	-	1.07	-	0.691
3	Haldane	0.167	55.719	4970.1	-	-	-	-	0.869
4	Luong	0.153	38.654	-	864.39	-	-	0.03	0.914
5	Edward	0.157	45.587	33683	-	241.82	-	-	0.892

Table 5.8. Experimental and predicted values of specific growth rate for MEK biodegradation using different growth kinetic models

S No	S_0 (mg L^{-1})	Exp. μ (h^{-1})	Value of predicted Specific growth rate, μ (h^{-1})				
			Monod	Powell	Haldane	Luong	Edward
1	200	0.319	0.24402	0.24147	0.23439	0.23013	0.23052
2	300	0.376	0.26144	0.26163	0.27068	0.2779	0.27139
3	400	0.391	0.27112	0.27184	0.2837	0.29881	0.28815
4	500	0.375	0.27728	0.27801	0.2844	0.30156	0.28899
5	600	0.366	0.28155	0.28214	0.27871	0.29233	0.27962
6	700	0.349	0.28467	0.2851	0.26985	0.27554	0.26423

Table 5.9. Experimental and predicted values of specific growth rate for MIBK biodegradation using different growth kinetic models

S No	S_0 (mg L^{-1})	Exp. μ (h^{-1})	Value of predicted Specific growth rate, μ (h^{-1})				
			Monod	Powell	Haldane	Luong	Edward
1	200	0.0816	0.08541	0.08236	0.07925	0.07204	0.07427
2	300	0.09112	0.09850	0.09954	0.10165	0.09750	0.1013
3	400	0.11628	0.1064	0.10801	0.11302	0.11665	0.11688
4	500	0.12291	0.11211	0.11310	0.1160	0.12620	0.12094
5	600	0.12788	0.11620	0.11650	0.1153	0.1230	0.11650
6	700	0.09761	0.11918	0.11889	0.11187	0.0984	0.1071

Table 5.10. Experimental and predicted values of specific growth rate for IPA biodegradation using different growth kinetic models

S No	S_0 (mg L^{-1})	Exp. μ (h^{-1})	Value of predicted Specific growth rate, μ (h^{-1})				
			Monod	Powell	Haldane	Luong	Edward
1	200	0.154	0.1745	0.17291	0.16516	0.15670	0.15315
2	300	0.195	0.1803	0.18004	0.19337	0.19401	0.19741
3	400	0.210	0.1834	0.18358	0.19833	0.20806	0.21059
4	500	0.202	0.1852	0.18555	0.19267	0.20379	0.20166
5	600	0.182	0.1864	0.1870	0.18187	0.18394	0.18019
6	700	0.153	0.18734	0.18803	0.16964	0.15196	0.15540

Table 5.11. Experimental and predicted values of specific growth rate for MA biodegradation using different growth kinetic models

S No	S_0 (mg L^{-1})	Exp. μ (h^{-1})	Value of predicted Specific growth rate, μ (h^{-1})				
			Monod	Powell	Haldane	Luong	Edward
1	200	0.093	0.10244	0.09309	0.09476	0.09416	0.09189
2	300	0.117	0.11229	0.10731	0.11665	0.11469	0.11609
3	400	0.125	0.11796	0.1147	0.12654	0.12646	0.12843
4	500	0.130	0.12164	0.11922	0.12892	0.13188	0.13174
5	600	0.134	0.12422	0.12227	0.12702	0.13187	0.12892
6	700	0.125	0.12614	0.12447	0.12287	0.12602	0.1224
7	800	0.111	0.12762	0.12612	0.11767	0.11098	0.114

Table 5.12. Experimental and predicted values of specific growth rate for EA biodegradation using different growth kinetic models

c	S_0 (mg L^{-1})	Exp. μ (h^{-1})	Value of predicted Specific growth rate, μ (h^{-1})				
			Monod	Powell	Haldane	Luong	Edward
1	200	0.118	0.12195	0.12058	0.11697	0.11712	0.11719
2	300	0.129	0.12687	0.12602	0.12945	0.12835	0.12976
3	400	0.132	0.12948	0.12875	0.1339	0.13306	0.1344
4	500	0.137	0.1311	0.13039	0.13444	0.13426	0.13504
5	600	0.134	0.1322	0.13149	0.13295	0.13314	0.13351
6	700	0.130	0.133	0.13228	0.13038	0.13018	0.13074
7	800	0.127	0.13361	0.13287	0.12724	0.12544	0.12727

Table 5.13. Experimental and predicted values of specific growth rate for BA biodegradation using different growth kinetic models

S No	S_0 (mg L^{-1})	Exp. μ (h^{-1})	Value of predicted Specific growth rate, μ (h^{-1})				
			Monod	Powell	Haldane	Luong	Edward
1	200	0.128	0.12872	0.12897	0.12663	0.12721	0.12674
2	300	0.132	0.13286	0.13328	0.13402	0.13381	0.13397
3	400	0.136	0.13504	0.13545	0.13691	0.13694	0.13706
4	500	0.141	0.13637	0.13675	0.13778	0.13839	0.13812
5	600	0.138	0.13728	0.13762	0.13761	0.13872	0.13796
6	700	0.137	0.13794	0.13825	0.13684	0.13795	0.13699
7	800	0.135	0.13843	0.13872	0.1357	0.13501	0.13543

5.1.5. Biodegradation rate kinetics

A plot of substrate concentration versus time gives a straight line with zero-order constants, S_0 and k_0 as intercept and slope respectively (Figs. 5.25 – 5.30). Three-half-order rate constants, k_1 and k_2 are found by plotting Y against t which gives a straight line using the log phase data (Figs. 5.31 – 5.36). The zero-order constants and three-half-order constants are evaluated for MEK, MIBK, IPA, MA, EA, and BA and listed in Tables 5.14, 5.15, 5.16, 5.17, 5.18, and 5.19 respectively. The coefficient of determination (R^2)obtained for zero-order kinetics are found in the range of 0.968 – 0.998, 0.983 – 0.995, 0.956 – 0.998, 0.935 – 0.998, 0.944 – 0.996, and 0.929 – 0.999 for MEK, MIBK, IPA, MA, EA, and BA respectively at various initial concentration values and reported in Tables 5.14 – 5.19. The value of S_0 and k_0 are found increasing with increase in initial concentration of different VOCs (Tables 5.14 – 5.19).

The obtained value of three-half-order rate constants, (k_1 and k_2), were found decreasing with an increase in the initial concentration of different VOCs used in the present study (Tables 5.14 – 5.19). The obtained values of coefficient of determination (R^2) for three-half-order kinetics are ranging from 0.967 – 0.995, 0.968 – 0.997, 0.986 – 0.996, 0.956 – 0.999, 0.978 – 0.995, and 0.951 – 0.996 at various initial concentration values for MEK, MIBK, IPA, MA, EA, and BA respectively. The values obtained for coefficient of determination (R^2) for zero-order and three-half-order kinetics indicates that the three-half-order kinetic model is suitable to explain the biodegradation rate kinetics for different VOCs using acclimated mixed culture over a wide range of operating conditions. This may be due to the fact that the three-half-order model

incorporates an additional term for explaining the biomass formation during biodegradation of VOCs.

Tables 5.14 to 5.16 shows that the values of constant k_1 and k_2 are decreasing with increase in initial concentration of MEK, MIBK and IPA. The values of k_1 and k_2 are decreasing with increase in the concentration for all the VOCs used in present study. This signifies that the change in biomass concentration with time has insignificant effect on the rate of disappearance of substrate. The order of magnitude of k_1 and k_2 is very small. This indicates that both zero-order and three-half-order kinetics are suitable for fitting the obtained experimental rate kinetic data. It is found that in the present study, in most of the cases, three-half-order kinetic fits the data well as compared to the zero-order kinetics for the VOCs.

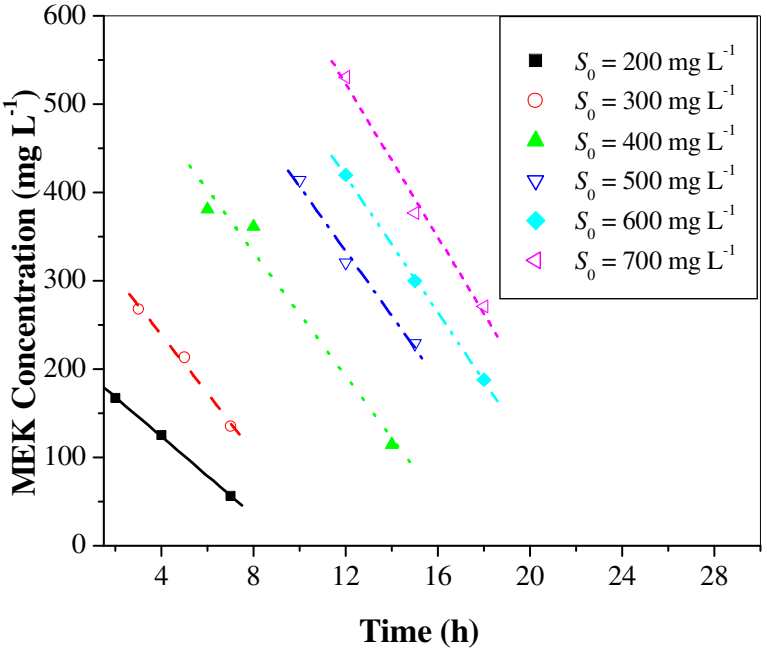

Fig. 5.25. Zero-order kinetics for biodegradation of MEK at different initial MEK concentrations

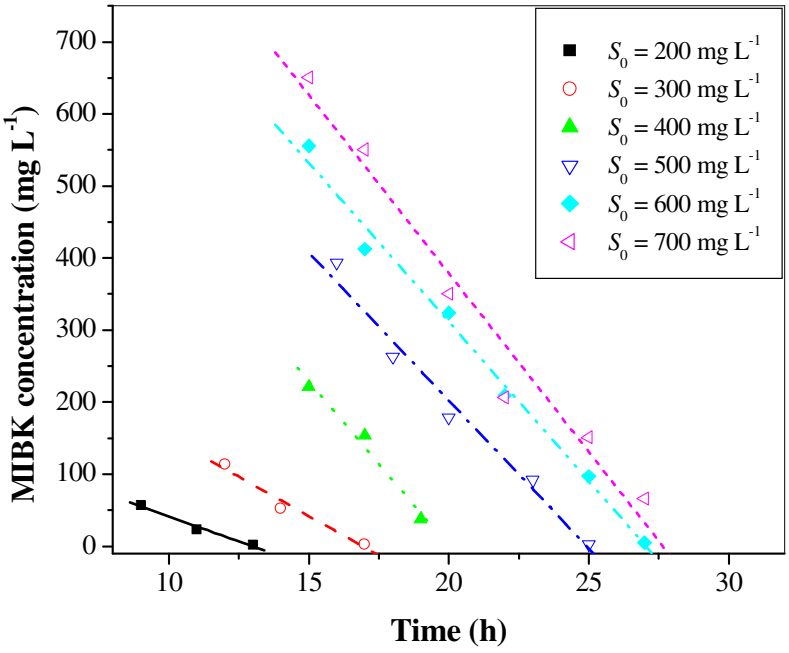

Fig. 5.26. Zero-order kinetics for biodegradation of MIBK at different initial MIBK concentrations

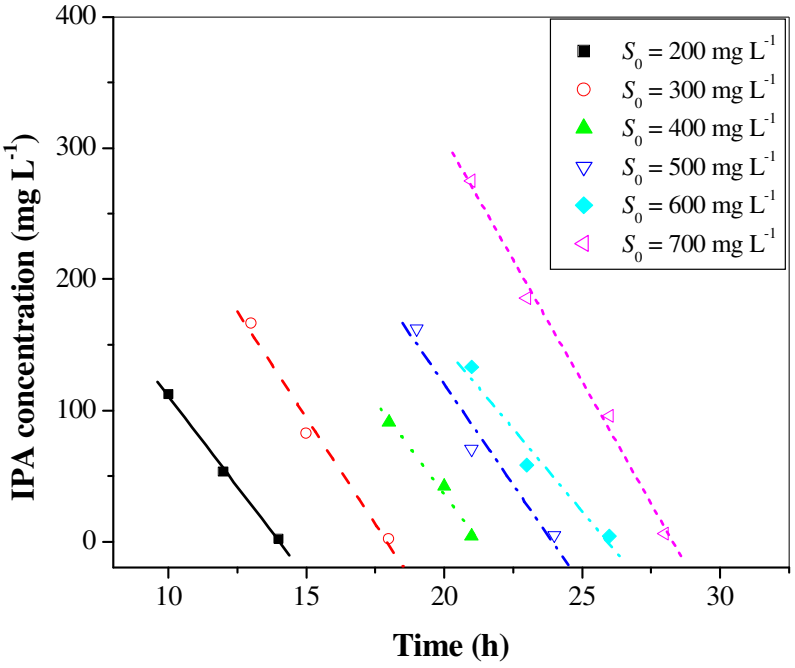

Fig. 5.27. Zero-order kinetics for biodegradation of IPA at different initial IPA concentrations

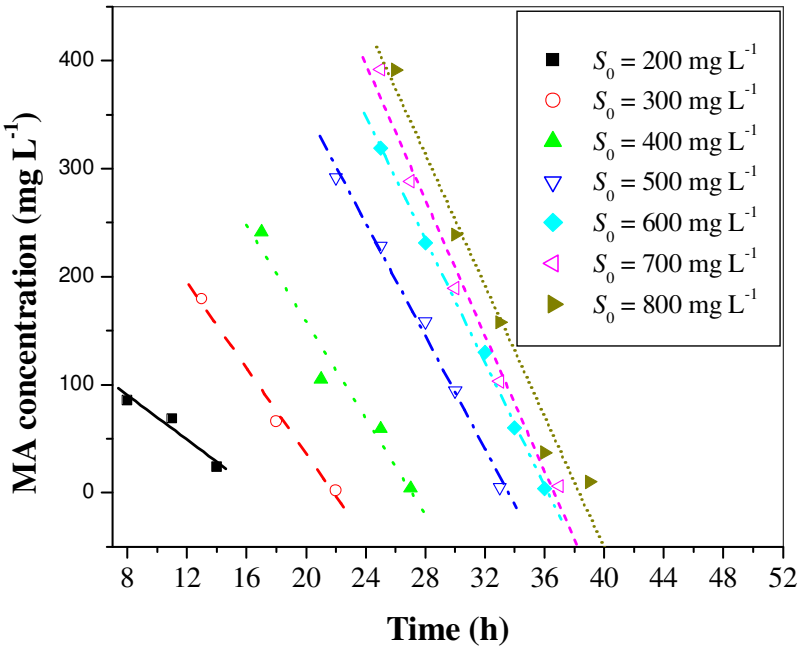

Fig. 5.28. Zero-order kinetics for biodegradation of MA at different initial MA concentrations

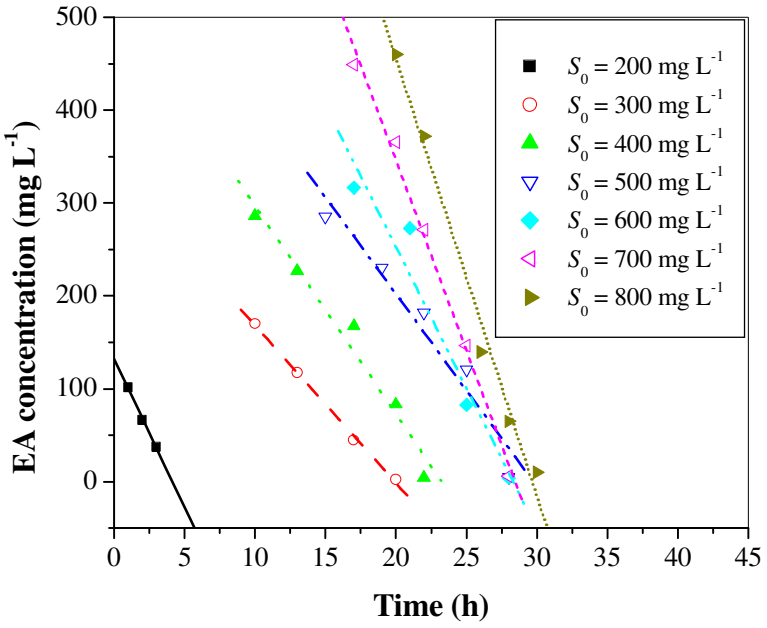

Fig. 5.29. Zero-order kinetics for biodegradation of EA at different initial EA concentrations

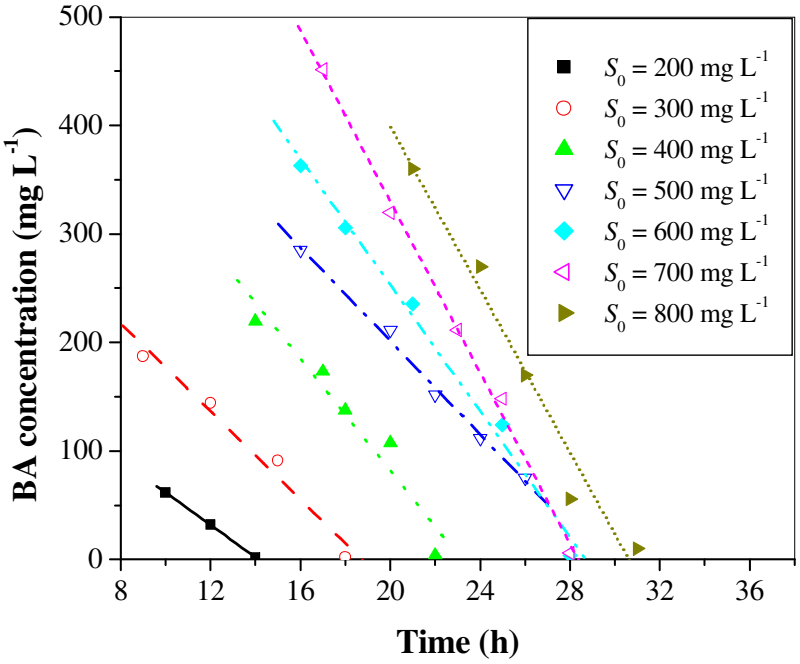

Fig. 5.30. Zero-order kinetics for biodegradation of BA at different initial BA concentrations

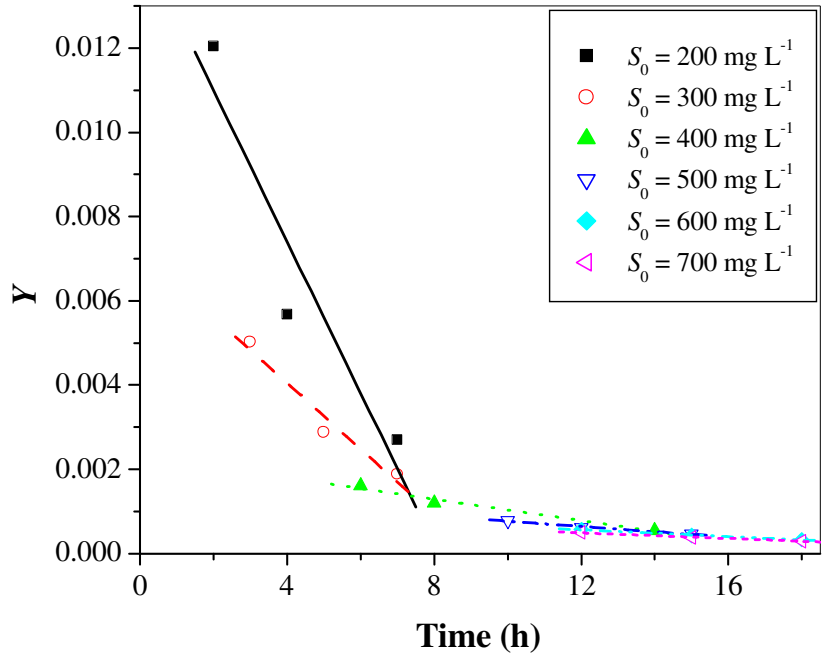

Fig. 5.31. Three-half-order kinetics for biodegradation of MEK at different initial MEK concentrations

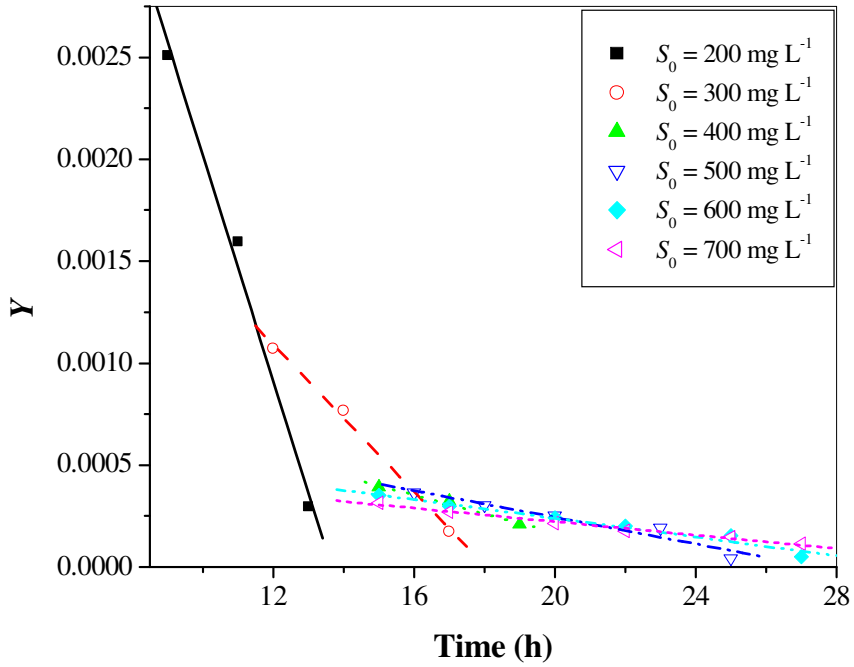

Fig. 5.32. Three-half-order kinetics for biodegradation of MIBK at different initial MIBK concentrations

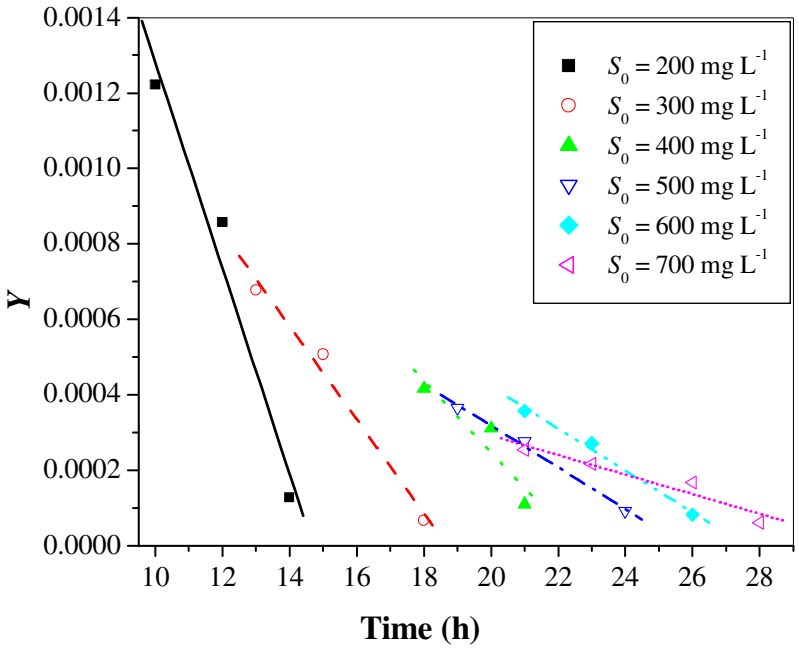

Fig. 5.33. Three-half-order kinetics for biodegradation of IPA at different initial IPA concentrations

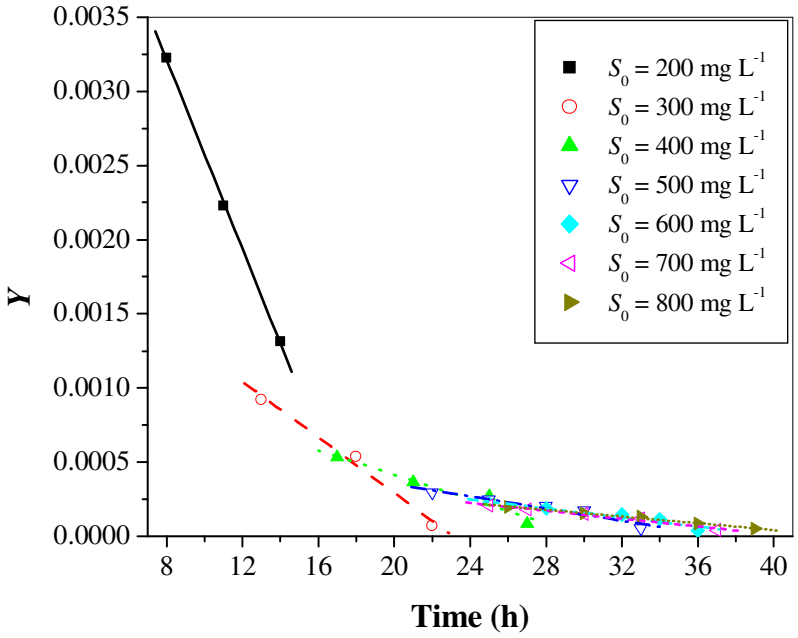

Fig. 5.34. Three-half-order kinetics for biodegradation of MA at different initial MA concentrations

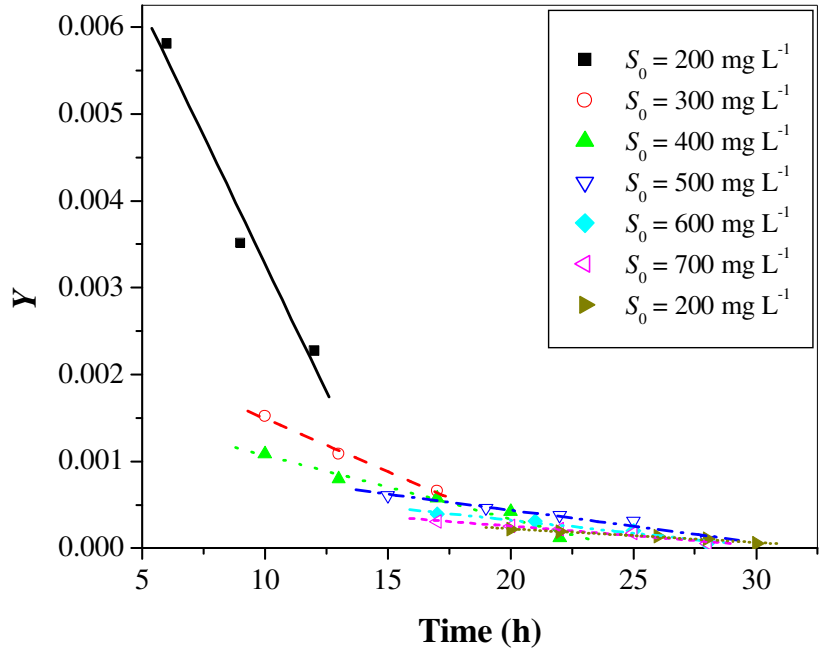

Fig. 5.35. Three-half-order kinetics for biodegradation of EA at different initial EA concentrations

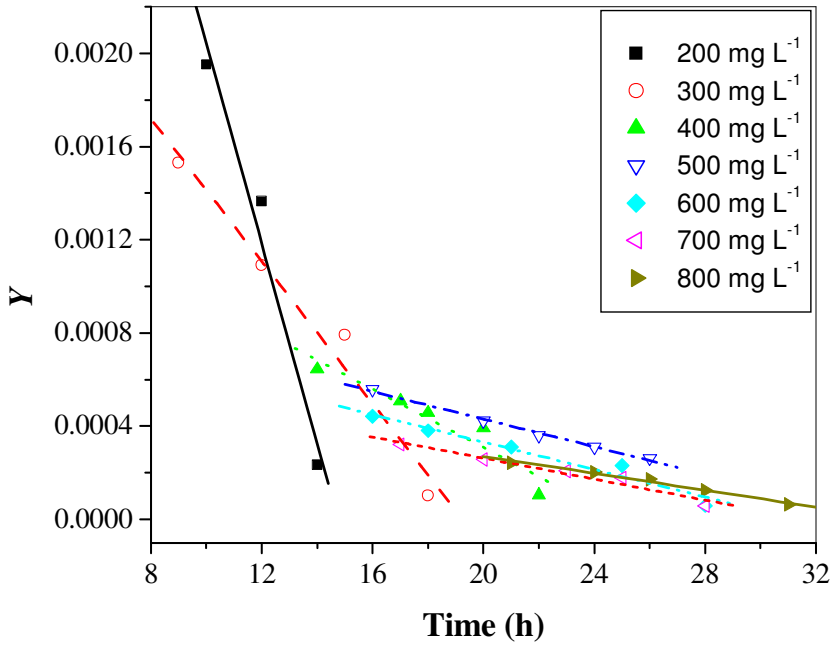

Fig. 5.36. Three-half-order kinetics for biodegradation of BA at different initial BA concentrations

Table 5.14. Parameters of zero-order and three-half-order kinetic models at different initial MEK concentrations

S No	Initial MEK Concentration, S_0(mg L^{-1})	Zero-order kinetics			Three-half-order kinetics		
		k_0	S_0	R^2	$k_1 \times 10^4$	$k_2 \times 10^4$	R^2
1	200	22.306	212.51	0.998	2.43	18.0	0.967
2	300	33.183	371.07	0.990	1.20	7.83	0.988
3	400	35.108	613.03	0.968	0.39	1.27	0.990
4	500	36.577	772.21	0.984	0.23	0.61	0.992
5	600	38.645	881.97	0.998	0.18	0.40	0.995
6	700	43.348	1042.8	0.988	0.15	0.34	0.993

Table 5.15. Parameters of zero-order and three-half-order kinetic models at different initial MIBK concentrations

S No	Initial MIBK Concentration, S_0(mg L^{-1})	Zero-order kinetics			Three-half-order kinetics		
		k_0	S_0	R^2	$k_1 \times 10^4$	$k_2 \times 10^3$	R^2
1	200	13.79	179.07	0.991	5.53	7.55	0.995
2	300	21.77	368.43	0.983	1.81	3.26	0.997
3	400	45.92	917.98	0.988	0.460	1.09	0.990
4	500	40.97	1021.9	0.989	0.327	0.898	0.968
5	600	44.14	1194.1	0.995	0.229	0.697	0.983
6	700	49.49	1368.5	0.983	0.165	0.552	0.993

Table 5.16. Parameters of zero-order and three-half-order kinetic models at different initial IPA concentrations

S No	Initial IPA Concentration, S_0(mg L^{-1})	Zero-order kinetics			Three-half-order kinetics		
		k_0	S_0	R^2	$k_1 \times 10^4$	$k_2 \times 10^4$	R^2
1	200	27.56	386.51	0.998	0.67	2.73	0.990
2	300	32.41	580.59	0.982	0.386	1.24	0.991
3	400	28.30	602.29	0.984	0.358	0.95	0.986
4	500	30.71	734.74	0.956	0.236	0.55	0.996
5	600	25.23	653.74	0.956	0.255	0.56	0.995
6	700	37.18	1050.3	0.992	0.135	0.259	0.989

Table 5.17. Parameters of zero-order and three-half-order kinetic models at different initial MA concentrations

S No	Initial MA Concentration, S_0(mg L^{-1})	Zero-order kinetics			Three-half-order kinetics		
		k_0	S_0	R^2	$k_1 \times 10^5$	$k_2 \times 10^4$	R^2
1	200	10.28	172.47	0.935	9.60	3.18	0.999
2	300	19.83	432.73	0.990	3.61	0.94	0.992
3	400	22.36	605.40	0.954	2.06	0.41	0.973
4	500	26.08	875.42	0.990	1.26	0.21	0.966
5	600	28.48	1031.9	0.998	1.02	0.15	0.956
6	700	31.41	1150.6	0.980	0.91	0.13	0.986
7	800	30.07	1162.1	0.972	0.82	0.11	0.995

Table 5.18. Parameters of zero-order and three-half-order kinetic models at different initial EA concentrations

S No	Initial EA Concentration, S_0(mg L^{-1})	Zero-order kinetics			Three-half-order kinetics		
		k_0	S_0	R^2	$k_1 \times 10^4$	$k_2 \times 10^4$	R^2
1	200	32.12	132.53	0.996	1.53	5.89	0.986
2	300	16.98	338.25	0.996	0.45	1.22	0.995
3	400	22.43	521.31	0.968	0.30	0.73	0.985
4	500	20.76	617.21	0.948	0.20	0.37	0.978
5	600	30.42	860.95	0.944	0.15	0.30	0.981
6	700	40.93	1164.4	0.990	0.12	0.22	0.979
7	800	47.10	1396.3	0.986	0.09	0.16	0.992

Table 5.19. Parameters of zero-order and three-half-order kinetic models at different initial BA concentrations

S No	Initial BA Concentration, S_0(mg L^{-1})	Zero-order kinetics			Three-half-order kinetics		
		k_0	S_0	R^2	$k_1 \times 10^4$	$k_2 \times 10^3$	R^2
1	200	14.94	211.21	0.999	1.06	4.29	0.984
2	300	20.28	379.88	0.970	0.49	1.52	0.986
3	400	25.77	597.36	0.929	0.26	0.63	0.951
4	500	21.53	632.17	0.992	0.17	0.30	0.996
5	600	29.06	834.18	0.990	0.15	0.29	0.978
6	700	39.44	1118.6	0.996	0.12	0.23	0.977
7	800	37.55	1149.5	0.964	0.11	0.18	0.993

5.2. Biofilter column studies on MEK, MIBK, IPA, and EA

In the present study, the biofiltration experiments are carried out using the matured compost and coal as packing material and acclimated culture as seeding culture. This study is carried out to estimate the acclimation period for different VOCs such as MEK, MIBK, IPA, and EA. The effects of time in the biofilter performance for different values of operating parameters such as inlet VOC concentration, air flow rate, and shock loading is studied. The present work also includes the effect of column height on bulk phase concentration of VOCs. The performance of biofilter is investigated in terms of the removal efficiency and elimination capacity.

5.2.1. Effect of time on biofilter performance

5.2.1.1. Biofilter performance for MEK removal

Fig. 5.37 shows the profiles of inlet and outlet concentration and removal efficiency of MEK at various air flow rates during 60 days of biofilter operation. The biofiltration experiments are divided into 5 phases (Phase I to Phase V). The operating conditions for the biofilter operation during the entire biofiltration process are given in Table 3.4. During the phase I (acclimation period), the inlet concentration is ranging from 0.15 to 0.25 g m^{-3} and air flow rate is maintained as 0.24 m^3 h^{-1} for 20 days of biofilter operation. It is observed from Fig. 5.37 that the removal efficiency at the initial period of acclimation is low (45%) which further increases with time leading to a maximum removal efficiency of 94%. At early stages of biofiltration, the microbial population in the biofilter column is less as it takes some time for the microbes to get acclimated with the actual operating conditions. In the later half of phase I, the removal efficiency increased because of the increase in microbial growth in the coal-compost biofilter. The

microbial concentration is measured in the biofilter column after phase I as per the procedure given in section (2.5.2). The microbial concentration is obtained as $2.48X10^{6}$ CFU g^{-1} after phase I which is comparable with the values of microbial concentration reported in the literature of around $1.06X10^{7}$ CFU g^{-1} after 40 days of acclimation period given by Rene et al. (2005) for toluene removal. The acclimation period of 20 days is also consistent with the reported acclimation periods from few days to several weeks depending on the nature of the packing material and culture media as reported by Dehghanzadeh et al. (2005).

In phase II, the inlet concentration is increased from 0.25 to 0.45 g m^{-3} and inlet air flow rate is decreased to 0.18 m^{3} h^{-1}. The removal efficiency is decreased from 94% achieved during phase I to 76% with sudden change in the operating conditions in phase II (Fig. 5.37). Initially, the removal efficiency is decreased but it gradually increases with increase in operating time and reaches to a steady state value of 95% at the end of this phase as shown in Fig. 5.37. The sudden decrease in the removal efficiency during this phase is due to an increase in the initial MEK concentration. The increase in the removal efficiency is achieved with an increase in the operating time due to an increase in the microbial population in new environment. Though the inlet concentration of MEK is more in phase II, the maximum removal efficiency obtained is more than that in phase I. This may be due to the increase in Empty Bed Residence Time (*EBRT*) from 20.6 to 27.4 s with a decrease in the air flow rate from 0.24 to 0.18 $m^{3}h^{-1}$ for phase I to phase II respectively.

The phase III lasted for 10 days from 31 to 40 days. In this phase, MEK inlet concentration is increased from an initial range of 0.45 - 0.6 g m^{-3} to a final range of 1.19

- 1.33 g m^{-3} and the gas flow rate is maintained at 0.24 m^3 h^{-1}. The MEK concentration is increased suddenly in order to study the adaptability of microbial culture in degrading MEK at a high inlet concentration. The removal efficiency suddenly decreased during this phase from 95% (achieved in phase-II) to 67%. Subsequently, it increases gradually and reaches to a maximum value of 73% (Fig. 5.37). The removal efficiency obtained in phase III is less than that obtained in other phases. This may be due to the fact that the microbial population is exposed to a very high inlet concentration which can lead to the self inhibition effect and affect the growth of the microbial culture. This can also be justified by the lower value of *EBRT* (20.6 s) in this phase. Due to the lower value of *EBRT*, the microbial culture gets less contact time for the degradation of MEK.

The performance of the biofilter column is checked in phase IV by further reducing the MEK inlet concentration. The inlet MEK concentration during phase IV is in the range of 0.75 to 0.89 g m^{-3} and the gas flow rate is increased to 0.3 m^3 h^{-1}. The removal efficiency increased from 73% (maximum in phase III) to 78% (initial value in phase IV) as shown in Fig. 5.37. Although the conditions in phase IV are changed, there is still an increase in the removal efficiency which may be due to the less value of initial MEK concentration. The self inhibition effect is also reduced in phase IV by decreasing the inlet MEK concentration from phase III. The removal efficiency increases with an increase in time and reaches to a maximum value of 85% on the 50^{th} day of biofilter operation. The maximum value of removal efficiency in phase IV is higher than that in phase III but less than that in phase II. This may be due to the fact that the initial MEK concentration in phase IV is more than that in phase II and less than the phase III. The decrease in the removal efficiency as compared to phase II can also be justified by the

fact that the EBRT for this phase is 16.5 s which is lesser than that in all other phases. So there is no sufficient contact time between microbial culture and MEK for the biodegradation.

The phase V is lasted for 51 to 60 days of biofilter operation. In this phase, MEK concentration is further increased to a higher value ranging from 1.51 - 1.64 g m^{-3} and the air flow rate is decreased to 0.21 m^3 h^{-1}. The removal efficiency is decreased from 85% (maximum of phase IV) to 70% (initial value of phase V) as shown in Fig. 5.37. Then the removal efficiency increases with an increase in the operating time during phase V and reached to a maximum value of 76%. The decrease in removal efficiency can be justified with a higher initial MEK concentration which provides a strong self inhibition effect. The increase in EBRT from 16.5 s (phase IV) to 23.5 s (phase V) increases the contact time between microbial culture and MEK which enhance the biodegradation. Because of higher concentration of MEK, self inhibition effect predominates and the removal efficiency decreases during phase V.

In the present study, the RE is obtained as 95% achieved during II phase (after 30 days) by the use of compost and coal filter bed and acclimated mixed culture for an inlet MEK load of 59.46 – 77.66 g m^{-3} h^{-1}. Mathur and Mazumdar (2008) showed a removal efficiency of around 99% after 40 days of biofilter operation for the removal of MEK using coal as the packing material for a low inlet load of 13.62 g m^{-3} h^{-1}. Similar phase-wise studies are carried out for the removal of MEK by Cai et al. (2004) using a trickle bed air biofilter. As compared with the systems reported by previous studies, the time taken to achieve maximum removal efficiency in the present study is less for higher inlet

loads. This may be due to the significant increase in microbial concentration inside the biofilter column.

It is observed from Fig. 5.38 that with the increase in inlet load from 26 g m^{-3} h^{-1} to 194 g m^{-3} h^{-1}, elimination capacity increases. But there is a sudden decrease in the elimination capacity value for inlet load of 208 g m^{-3} h^{-1}. This may be due to the sudden increase in the inlet load (concentration of VOC) which results in self inhibition for the growth of microbial culture which affects the degradation of MEK. Later on, while giving the same inlet load for some more time, results in the increase in the elimination capacity. This may be due to the acclimation of microbial culture in the new environment (increased concentration). This also establishes the fact that the developed biofilm under higher inlet load conditions is more stable and can be utilized for MEK removal under shock loading conditions.

The microbial concentration is measured after 60 days of biofilter operation. It is increased from $2.48X10^{6}$ CFU g^{-1} to $1.54X10^{8}$ CFU g^{-1} of packing material which shows a significant increase in the microbial concentration from phase I to phase V. Hence the column showed a considerable increase in the microbial concentration which is needed for the degradation of MEK.

5.2.1.2. Biofilter performance for MIBK removal

The performance of biofilter for MIBK removal is evaluated by conducting the experiments at different inlet loads and various air flow rates during 60 days of biofilter operation which are divided into 5 phases (Phase I to Phase V) and shown in Fig. 5.39. The operating conditions for the biofilter operation at different phases are reported in Table 3.5. In the acclimation period (phase I) of 20 days, the inlet MIBK concentration is

ranging from 0.07 to 0.096 g m^{-3} and air flow rate is maintained as 0.21 m^3 h^{-1}. The removal efficiency is found less (30.23%) at the initial time of acclimation. The maximum removal efficiency obtained in the acclimation period is 91.6% after 20 days of biofilter operation (Fig. 5.39). The obtained value of microbial concentration is $1.84X10^6$ CFU g^{-1} which is more and responsible for high removal efficiency at the end of acclimation period.

After 20 days of biofilter operation, the initial concentration is increased from 0.096 (Phase I) to 0.251 g m^{-3} for the next 10 days (phase II). The *EBRT* is maintained at 20.6 s during this period. Due to the sudden increase in the inlet concentration of MIBK, the removal efficiency first decreased to around 65% and then started to increase with time and reached to 85 – 88% during phase II (Fig. 5.39). The increase in the removal efficiency is achieved with an increase in the operating time as microbial population gets some time to the new environment to degrade the higher concentration of MIBK as compared to phase I. The maximum removal efficiency obtained in phase II is less than that in phase I. This may be due to the increase in initial MIBK concentration from 0.096 (phase I) to 0.251 g m^{-3} (phase II) and decrease in *EBRT* from 23.5 (phase I) to 20.6 s (phase II).

Phase III lasted for 31 to 40 days of biofilter operation with the air flow rate maintained at 0.18 m^3 h^{-1} (*EBRT* = 27.4 s) and the inlet MIBK concentration is maintained in the range of 0.502 – 0.518 g m^{-3}. The steady state removal efficiency achieved during this phase is around 85% and is comparable with the removal efficiency achieved during phase II (Fig. 5.39). In phase III, the inlet MIBK concentration is very high as compared to inlet MIBK concentration in phase II and EBRT is less as compared to phase II. This

indicates that the maximum removal efficiency in phase III could be lower than the phase II but it is found comparable with phase II. This shows that the microbial culture developed till 40 days is well developed and getting adapted to the change in the high inlet MIBK concentration.

Phase IV lasted from 41 to 50 days during which the inlet concentration is maintained at higher range of 0.71 to 0.73 g m^{-3}as compared to phase II and III. The air flow rate is maintained at 0.3 m^3 h^{-1} with *EBRT* of 16.5 s. The inlet MIBK concentration is high and the *EBRT* is also reduced thus the removal efficiency is decreased in the range of 72–78%. This removal efficiency leads to the outlet MIBK concentration of 0.17 g m^{-3} which is higher than that of the exposure limit (0.1 g m^{-3}). This indicates that at higher air flow rate and at higher concentration of MIBK, the column performance is not so good. Hence it is recommended that biofilters cannot be operated at higher flow rate and at higher MIBK concentration (Devinny et al., 1999). The self inhibition effect also plays an important role at higher substrate concentration which may also be one of the reasons for the reduced *RE*.

In the phase V, the MIBK concentration is decreased from the range of 0.71 – 0.73 g m^{-3} to a range of 0.45 - 0.46 g m^{-3} and *EBRT* is increased to 23.5 s. A high removal efficiency of around 91 – 93% is achieved as shown in Fig. 5.39. The maximum *RE* is obtained during this phase. This may be due to the fact that the biofilm is well developed by now and able to degrade the MIBK when concentration is increased to some medium range. The maximum removal efficiency obtained in this phase can also be justified with an increase in *EBRT* which provides sufficient contact time for biodegradation. This can also be justified with the increased value of microbial concentration obtained after phase V.

As per the studies reported in the literature, the microbial concentration along the column decreases from bottom to top in up flow mode of biofilter operation and increases with an increase in time of the biofilter operation (Taghipour et al., 2008; Rene et al., 2005).

It is observed from Fig. 5.40 that with the increase in inlet load from 10 g m^{-3} h^{-1} to 159 g m^{-3} h^{-1}, elimination capacity increases. This indicates that the self inhibition effect is not obtained up to the MIBK inlet load of 159 g m^{-3} h^{-1} and microbes are more MIBK with increase in concentration of MIBK.

It is found that the microbial concentration is increased from 1.84X10 ^{6} CFU g^{-1} to 2.36X10^{8} CFU g^{-1} of packing material with an increase in operation time from 20 to 60 days. This shows a significant growth after 60 days of biofilter operation. In the present study, the microbial concentration is measured at the top of the column at different time intervals. Based on the earlier studies reported in the literature as mentioned above, it is assumed that the microbial concentration is more in the bottom section of the biofilter as compared to the top section at any given time of operation. Hence the higher removal efficiency obtained in the phase V is due to the increase in microbial concentration.

5.2.1.3. Biofilter performance for IPA removal

The effect of operating time on outlet concentration and removal efficiency of IPA at various air flow rates is studied during 40 days of biofilter operation and is shown in Fig. 5.41. The total operating time is divided into 4 phases which include the acclimation phase of 10 days (phase I). The operating conditions for the 40 days of biofilter operation are given in Table 3.6. In phase I, the inlet concentration is maintained in the range of 0.04 – 0.051 g m^{-3} and air flow rate is kept constant at 0.18 m^{3} h^{-1} for the initial 10 days of biofilter operation. The removal efficiency increases from 40.23% to 91.25%

with an increase in the operation time of biofilter column from 2 to 10 days respectively (Fig. 5.41). The obtained maximum removal efficiency is 91.25% after 10 days of biofilter operation which indicates that there is sufficient microbial growth inside the biofilter column. This fact can also be justified with the obtained large value of microbial concentration as $8.6X10^5$ CFU g^{-1}. Hence, the acclimation phase is kept as 10 days for the IPA removal.

The inlet IPA concentration is increased from 0.051 to 0.101 g m^{-3} and air flow rate is increased from 0.18 to 0.24 m^3 h^{-1} in phase II of biofilter operation. A sudden decrease in removal efficiency from 91.25% (phase I) to 70.32% (phase II) is observed with sudden change in operating conditions from phase I to phase II. The increase in operating time further increases the removal efficiency and reaches to 93.22% after 20 days of biofilter operation (Fig. 5.41). Though the inlet IPA concentration and air flow rate are higher in phase II as compared to phase I, maximum removal efficiency during the phase II is more than that in phase I. This may be due to the increase in microbial concentration.

The phase III lasted for 10 days from 21 to 30 days. In this phase, inlet IPA concentration is increased from 0.115 to 0.352 g m^{-3} and air flow rate is decreased from 0.24 to 0.21 m^3 h^{-1}. The removal efficiency is decreased from 93.22% (phase II) to 65.4% (phase III) and further increases with an increase in operating time and reaches a steady state value of 85.22%. The maximum removal efficiency obtained in phase III is less than that in phase I and phase II. Though the EBRT is increased from 20.6 to 23.6 s, the removal efficiency is decreased in phase III. This may be due to the high inlet IPA concentration which leads to the predominant self inhibition effect.

The performance of biofilter is investigated by decreasing the inlet IPA concentration in the range of 0.162 – 0.173 g m^{-3} and air flow rate is increased to 0.3 m^3 h^{-1}. The removal efficiency decreased from 85.22% (maximum in phase III) to 74.33% (initial value in phase IV) as shown in Fig. 5.41. The removal efficiency further increased with an increase in operating time and reaches to a maximum value of 90% after 40 days of biofilter operation. The maximum value of removal efficiency in phase IV is higher than that in phase III but less than that in phase II and phase I. This may be due to the fact that the initial MEK concentration in phase IV is more than the phase II and less than that in phase III. The decrease in the removal efficiency as compared to phase II can also be justified by the fact that the EBRT for this phase is 16.5 s which is lesser than the all other phases. So there is no sufficient contact time between microbial culture and IPA for the biodegradation.

Elimination capacity is found increasing from 3 g m^{-3} h^{-1} to 48 g m^{-3} h^{-1} with the increase in inlet load from 5 g m^{-3} h^{-1} to 56 g m^{-3} h^{-1} and shown in Fig. 5.42. This indicates that the self inhibition effect is not obtained up to the IPA inlet load of 56 g m^{-3} h^{-1}. The microbes available in biofilm are showing increase in consumption of IPA with increase in IPA inlet load.

In the present study, the maximum removal efficiency is obtained as 93.22% after 20^{th} day of biofilter operation. The microbial concentration is estimated after 40 days of biofilter operation and is increased from $8.6X10^5$ CFU g^{-1} to $9.54X10^7$ CFU g^{-1} of packing material with an increase in operation time from 10^{th} day to 40^{th} day of biofilter operation. Hence the biofilter column showed a sufficient increase in the microbial concentration which is required for the degradation of IPA.

5.2.1.4. Biofilter performance for EA removal

The performance of biofilter in terms of removal efficiency is obtained for EA removal by performing the experiments at different inlet concentrations and air flow rates during 45 days of biofilter operation. The total duration of biofilter operation is divided into 4 phases (Phase I to Phase IV) as shown in Fig. 5.43. The operating conditions for the biofilter operation at different phases are reported in Table 3.7. The inlet EA concentration is ranging from 0.05 – 0.063 g m^{-3} and air flow rate is kept constant at 0.18 m^3 h^{-1} in the initial 15 days (acclimation period or phase I) of the biofilter operation. The removal efficiency is found to be 50.23% at 2^{nd} day of acclimation period. The removal efficiency increases with operation time and the maximum value of removal efficiency obtained in the acclimation period is 90.12% on 15^{th} day of biofilter operation (Fig. 5.43). The value of microbial concentration is obtained as $3.64X10^6$ CFU g^{-1} which is sufficient for the degradation of EA inside the biofilter column.

After the acclimation period (phase I), the initial concentration is increased from 0.063 (Phase I) to 0.131 g m^{-3} (phase II) for the next 10 days (16^{th} – 25^{th} day of biofilter opearation). The *EBRT* in the phase II is maintained constant as 16.5 s. As shown in Fig.5.43, the removal efficiency at initial time of phase II is decreased to around 68.23% and reaches to the steady state value of 86 – 87% at the end of this phase. The decrease in removal efficiency can be justified with the fact that the microbes take some time to get acclimatized in new environment. As the microbes get into the new environment, the removal efficiency increases with an increase in the operating time. The maximum removal efficiency obtained in phase II is less than that in phase I. This may be due to the

increase in initial EA concentration in phase II and decrease in *EBRT* from 23.5 (phase I) to 16.5 s (phase II).

Phase III lasted for 10 days during 26th to 35th day of biofilter operation with an inlet EA concentration ranging from 0.231 – 0.239 g m^{-3} and air flow rate maintained at 0.21 m^3 h^{-1} (*EBRT* = 23.5 s). The removal efficiency achieved during this phase ranges from 73.22 – 92.11%. The maximum removal efficiency obtained in phase III is 92.11% which is more than that in phase I and Phase II (Fig. 5.43). Though in phase III, the inlet EA concentration is higher as compared to inlet EA concentration in phase I and II, the maximum removal efficiency is more as compared to phase I and II. This may be due to the increase in *EBRT* from 16.5 s (phase II) to 23.5 s (phase III). Though the value of *EBRT* for phase I is higher than that in phase III, the maximum removal efficiency is found less than that in phase III. This indicates that the microbial culture developed till 35 days is well acquainted and getting adapted to degrade EA at high initial concentration.

During the operation of biofilter column from 36th to 45th day in phase IV, the inlet concentration is decreased in the range of 0.18 – 0.193 g m^{-3} and air flow rate is increased to 0.24 m^3 h^{-1} (EBRT = 20.6 s). The removal efficiency increases from 76.1% to 94.11% with an increase in operating time from 36th day to 45th day of biofilter operation (Fig. 5.43). The maximum removal efficiency obtained in phase IV is 94.11% which is higher as compared to all other phases of biofilter operation for EA removal. This may be due to the decrease in initial EA concentration. The increased value of maximum removal efficiency in phase IV can also be justified with the obtained value of microbial concentration which increases from 3.64X10^6 CFU g^{-1} to 5.12X10^8 CFU g^{-1} of packing

material with an increase in operation time from 15 to 45 days. This indicates that there is a sufficient growth of microbial culture inside the biofilter column at the end of phase IV. The obtained elimination capacity at different inlet loads is plotted and shown in Fig. 5.44. Elimination capacity is found increasing from 4 g m^{-3} h^{-1} to 34 g m^{-3} h^{-1} with the increase in inlet load from 7 g m^{-3} h^{-1} to 37 g m^{-3} h^{-1}. The self inhibition effect is observed at inlet load of 26 g m^{-3} h^{-1} of EA. Later on, while giving the same inlet load for some more time, results in the increase in the elimination capacity and provides a stable biofilm.

It is observed that the biofilter seems to reach a steady state very quickly at each phase studied for all VOCs. This may be due to the well acclimated culture used for the biofiltration studies. This reduces the sensitivity of the mixed culture in the biofiltration studies.

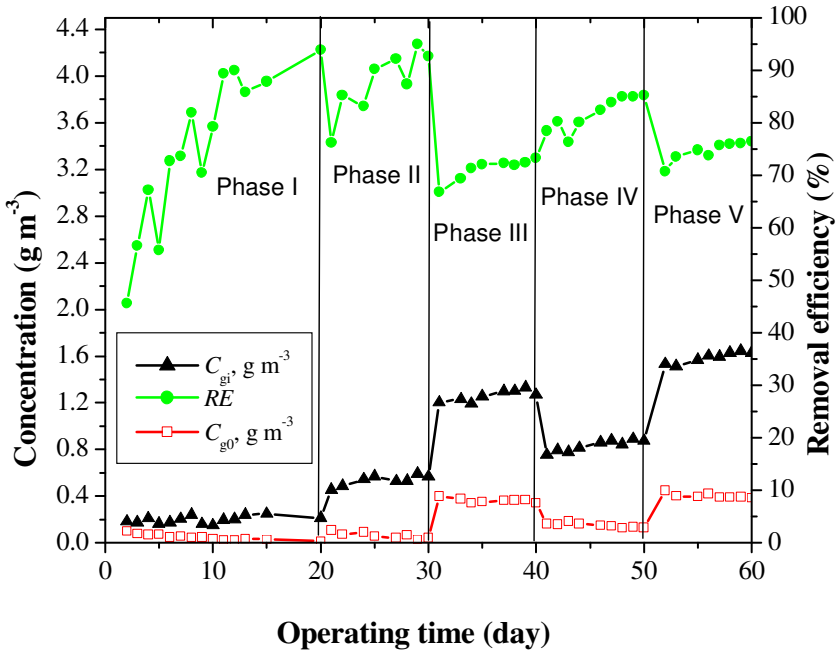

Fig. 5.37. Performance of biofilter with change in air flow rate and inlet MEK concentrations

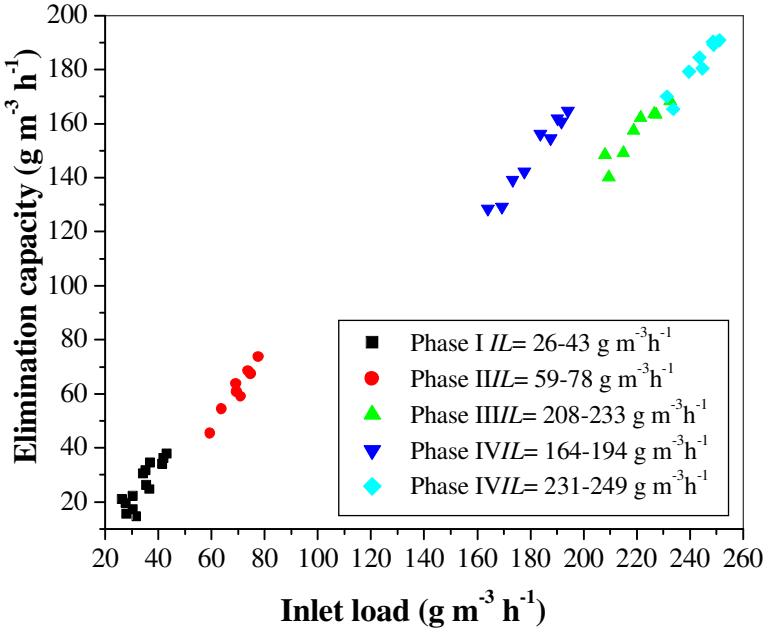

Fig. 5.38. Variation of elimination capacity with change in inlet loads of MEK

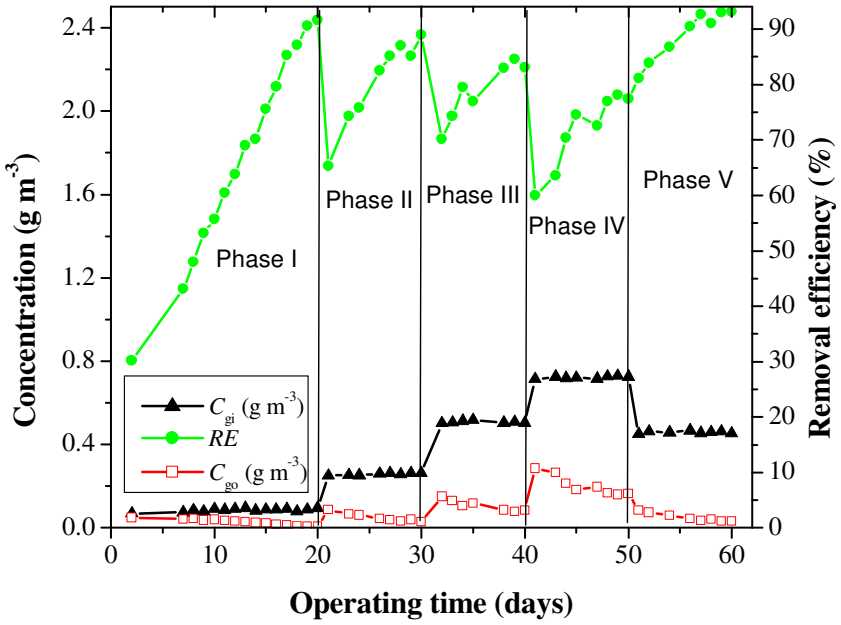

Fig. 5.39. Performance of biofilter with change in air flow rate and inlet MIBK concentrations

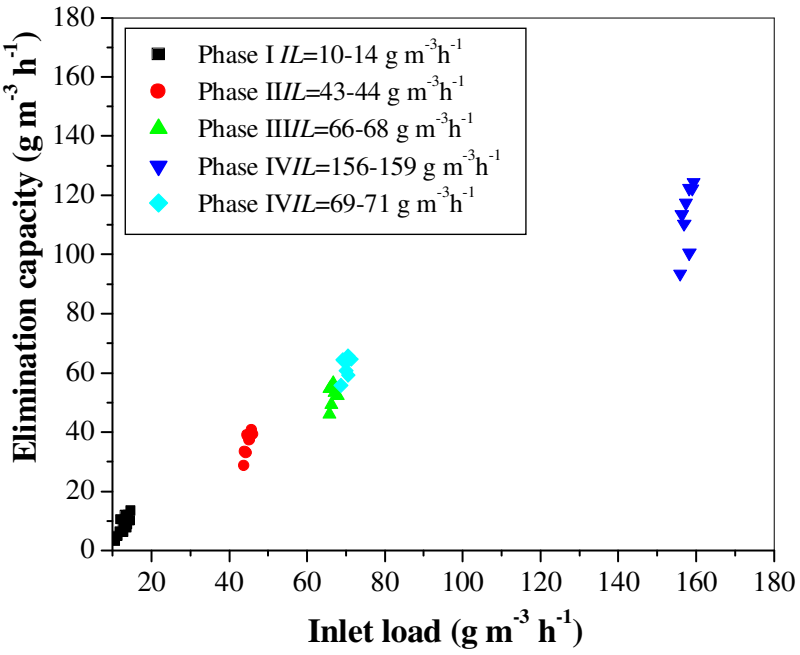

Fig. 5.40. Variation of elimination capacity with change in inlet loads of MIBK

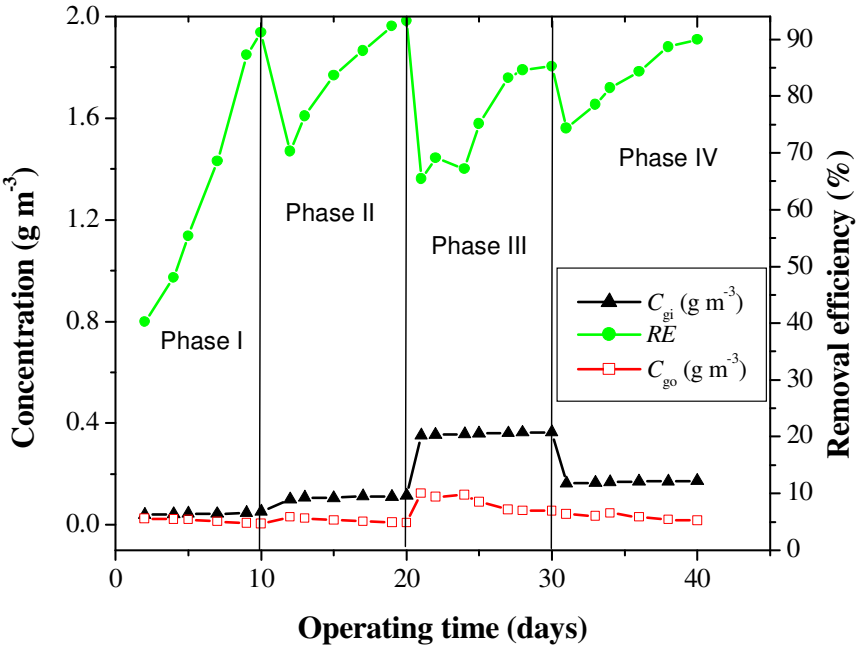

Fig. 5.41. Performance of biofilter with change in air flow rate and inlet IPA concentrations

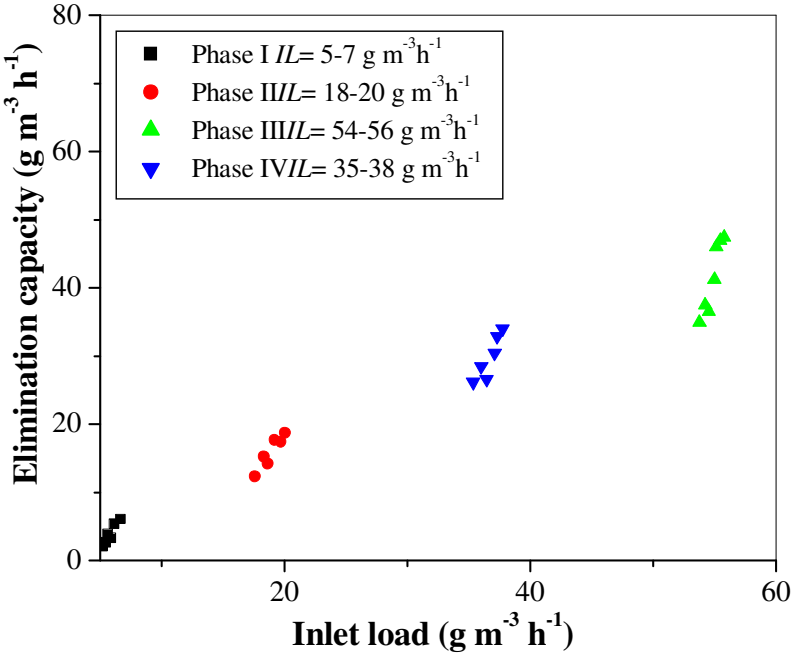

Fig. 5.42. Variation of elimination capacity with change in inlet loads of IPA

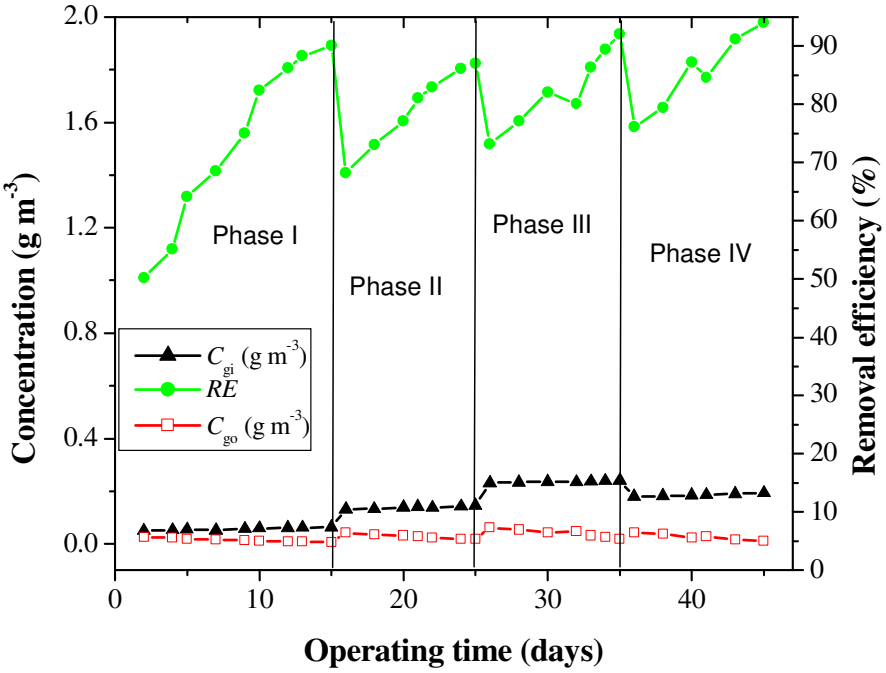

Fig. 5.43. Performance of biofilter with change in air flow rate and inlet EA concentrations

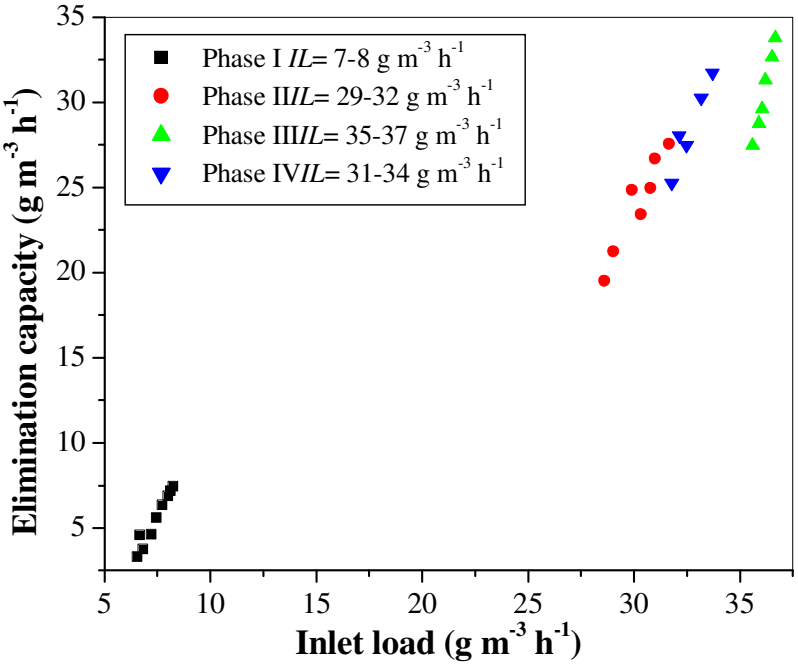

Fig. 5.44. Variation of elimination capacity with change in inlet loads of EA

5.2.2. Bed height versus normalized concentration

To understand the dynamics of biofiltration, the normalized concentration (ratio of outlet concentration, C_{g0}, to inlet concentration, C_{gi}) profiles for MEK, MIBK, IPA, and EA removal are obtained at different heights of the biofilter column and are shown in Figs. 5.45, 5.46, 5.47, and 5.48 respectively. Fig. 5.45 shows the profile of normalized MEK concentration versus bed height at five different operating conditions which are obtained from five different phases during 60 days of biofilter operation (Table 3.4). Almost 50% of MEK removal takes place at the bottom of the biofilter column (first 20 cm of the bed height) due to the presence of higher concentration of microbial population at that zone. The remaining MEK removal takes place at the other heights in the remaining part (i.e 50%) of the biofilter column. Fig. 5.46 shows the profiles of normalized MIBK concentration at different air flow rates (Q = 0.21, 0.24, 018 and 0.3 $m^3\ h^{-1}$) and inlet MIBK concentration (0.087, 0.259, 0.467, 0.518 and 0.721 g m^{-3}). It is observed from Fig. 5.46 that around 75% of MIBK removal takes place at the first 20 cm from the bottom of the biofilter column. This may be due to the higher concentration of microbial population in the bottom part of the biofilter column. When MIBK concentration is maintained at 0.518 g m^{-3}, at the flow rate of 0.18 $m^3\ h^{-1}$, the C_{g0}/C_{gi} is obtained as 0.778 which is quite high showing that the pollutant (VOC) is getting enough retention time to be degraded by the microbial culture. The change in normalized concentration along the bed height is estimated for the initial IPA concentration of 0.051, 0.115, 0.365, and 0.173 g m^{-3} and corresponding air flow rates are 0.18, 0.24, 0.21, and 0.3 $m^3\ h^{-1}$ as shown in Fig. 5.47. Almost 80% removal is observed at the bottom 20 cm of biofilter column for 0.051 g m^{-3} of initial IPA concentration. Approximately 60%, 50% and 40% removal is

obtained for 0.115, 0.365, and 0.173 of initial IPA concentration within first 20 cm height from the bottom of biofilter column. Fig. 5.48 shows the profiles of normalized concentration versus height of biofilter column for the removal of EA at different operating conditions. The initial EA concentrations are 0.063, 0.145, 0.24, and 0.193 g m^{-3} and respective air flow rates are 0.18, 0.3, 0.21, and 0.24 m^3 h^{-1}. It is found that the value of normalized concentration reaches to 0.22, 0.57, 0.52, and 0.53 for 0.063, 0.145, 0.24, and 0.193 g m^{-3} of initial EA concentration respectively within the bottom 20 cm height of biofilter column. The obtained value of normalized concentration is higher for 0.145 g m^{-3} of initial EA concentration which may be due to the lower value of *EBRT* (16.5 s).

It is observed from Figs. 5.45 – 5.48 that the decrease in normalized concentration is large for initial 50% height of the biofilter column but it is less in the remaining part of the column. The increase in inlet VOCs concentration, C_{g0} / C_{gi}, increases at the same height of the biofilter column. This may be due to the fact that more amount of VOC is available for the same quantity of microbial culture in the column. Hence some of the VOC is still unutilized by microbes which lead to an increase in the outlet concentration of VOC. Similar trends are reported for toluene removal under different operating conditions (Rene et al., 2005), for the removal of VOCs in a peat-packed biofilter (Yoon and Park, 2002), for the removal of VOCs in trickle-bed biofilters (Rihn et al., 1997), for the removal of ethylbenzene vapors using biofiltration (Álvarez-Hornos et al., 2008), for the removal of MEK, toluene, *n*-butyl acetate, and *o*-xylene in a biotrickling filter (Mathur and Majumder, 2008), for the combined removal of BTEX (benzene, toluene, ethyl benzene, and *o*-xylene) in a compost and GAC (Granular Activated Carbon) packed

biofilters (Mathur et al., 2007), and for the removal of butyl acetate by trickle-bed air biofilter (Lu et al., 2004).

5.2.3. Response to shock loads on the biofilter column

This study is important in order to use the biofilter column for industrial purpose where the inlet load varies on a daily basis. The industrial application of biofilter column is more justified when lab scale column undergoes sudden change in pollutant loads and response to such change in inlet loads is calculated in terms of removal efficiency and elimination capacity of the biofilter column. In the present work, the stability of the biofilter column is assessed by subjecting the column to shock loading conditions for a period of 16 days for MEK, 20 days for MIBK and 10 days for IPA and EA immediately after the 60 days of biofilter operation for MEK and MIBK, 40 days for IPA and 45 days for EA (Figs. 5.49 – 5.56). The procedure for shock loading conditions is taken from the literature (Atoche and Moe, 2004; Kim et al., 2008) and the days of operation of shock loading is fixed based on their normal days of operation proportionately. The operating conditions for shock loading operation for MEK, MIBK, IPA, and EA removal are reported in Tables 3.8, 3.9, 3.10, and 3.11 respectively.

It can be observed from Fig. 5.49 that during the first four days, when inlet concentration is maintained in the range of 0.45 to 0.47 g m^{-3} at a flow rate of 0.24 m^3 h^{-1}, the removal efficiency is obtained in the range of 89 to 91%. For the MEK inlet load ranging from 79 to 82 g m^{-3} h^{-1}, the corresponding elimination capacity obtained is in the range of 71 to 73 g m^{-3} h^{-1}. The high values of removal efficiency and elimination capacity obtained indicate that once the biofilter is acclimated with the microbial culture, it can show very high degradation rates for lower pollutant concentration. For the next four days, the inlet

concentration is increased in the range of 1.2 – 1.23 g m^{-3} and the removal efficiency obtained is in the range of 80-82% which is still showing relatively better removal efficiency. The inlet MEK load is in the range of 210 to 215 g m^{-3} h^{-1} and the elimination capacity calculated in this phase is ranging from 168 to 174 g m^{-3} h^{-1}. When inlet concentration is further decreased to 0.75 – 0.77 g m^{-3} (maintaining a constant flow rate of 0.3 m^3 h^{-1}) from 9th to 12th day, the removal efficiency is increased in the range of 83 to 86% showing that the biofilter is performing better for lower to medium inlet loads of MEK. On further increase in the inlet concentration in the range of 1.5 to 1.52 g m^{-3} (flow rate of 0.3 m^3 h^{-1}), for next four days, the removal efficiency decreased in the range of 70 to 73% (Fig. 5.49). The inlet load vs elimination capacity is shown in Fig. 5.50. The elimination capacity is increased from increase in inlet load of 79 to 331 g m^{-3} h^{-1}.

The inlet concentration of pollutant MIBK is maintained at 0.6 g m^{-3} for the first 5 days at a flow rate of 0.21 m^3 h^{-1}, and the RE obtained is in the range of 80 to 86% (Fig. 5.51). When the inlet MIBK concentration is decreased to 0.25 g m^{-3} for the next 5 days from 6th to 10th day, there is a significant increase in the removal efficiency which is ranging from 89% to as high as 93%. The results confirm the adaptability of biofilter column in handling lower MIBK concentration as validated by Kim et al. (2008) for hydrogen sulphide removal. During the later period from 11th to 15th day, the inlet MIBK concentration is further increased to as high as 0.81 g m^{-3} at an air flow rate of 0.3 m^3 h^{-1}. The decrease in the removal efficiency from 93% to 71 – 73% can be seen from Fig. 5.51. It may be due to the fact that the microbial culture is not well acclimated for the degradation of high inlet pollutant concentration (MIBK) even after 70 days of biofilter operation. In the last five days of shock loading conditions from 16th to 20th day, removal

efficiency of around 82% for an inlet MIBK concentration of 0.41 g m^{-3} is achieved. The biofilter is observed to perform well and also found to respond well to the different shock loading conditions. The plot of elimination capacity vs inlet load is shown in Fig. 5.52 where elimination capacity is found to increase with increase in the inlet load from 37 to 177 g m^{-3} h^{-1}. This also shows the stability of the biofilter column.

In the first three days of biofilter operation for IPA removal under shock loading conditions, the inlet IPA concentration is maintained in the range of 0.3 – 0.36 g m^{-3} which corresponds to the inlet load of 45.83 – 55 g m^{-3} h^{-1} at air flow of 0.21 m^3 h^{-1} (Fig. 5.53). The removal efficiency is obtained in the range of 82.11 – 87.01% and corresponding elimination capacity is 37.64 – 47.86 g m^{-3} h^{-1}. These high values of removal efficiency and obtained values of elimination capacity indicate the high stability of biofilter column. For the 4^{th} to 6^{th} day of biofilter operation, the inlet concentration is increased in the range of 0.41 – 0.43 g m^{-3} and air flow rate is maintained at 0.24 m^3 h^{-1}. The inlet IPA load is in the range of 69.85 – 75.08 g m^{-3} h^{-1} for which the elimination capacity is obtained in the range of 53.95 – 60.15 g m^{-3}. The removal efficiency is found in the range of 77.23 – 80.11% which showed good efficiency under high inlet load. For the next four days of biofilter operation, the inlet concentration is suddenly decreased in the range of 0.2 – 0.23 g m^{-3} to check the stability of biofilter column by maintaining the air flow rate of 0.18 m^3 h^{-1}. The removal efficiency is found to be maximum in the range of 90.01 – 93% which indicates that the microbial culture present inside the biofilter column is well acclimatized with IPA and could be used for the IPA removal at different inlet loads. The plot of elimination capacity vs inlet load is shown in Fig. 5.54 for IPA

where elimination capacity is found to increase with increase in the inlet load from 46 to 75 g m^{-3} h^{-1}. This also shows the stability of the biofilter column.

The inlet EA concentration is maintained in the range of 0.25 – 0.27 g m^{-3} for the first 3 days at a flow rate of 0.21 m^3 h^{-1}. The EA removal efficiency obtained is in the range of 85.11 to 88.02% (Fig. 5.55). The inlet load is maintained in the range of 38.19 – 41.25 g m^{-3} h^{-1} and the elimination capacity is found in the range of 32.51 – 36.31 g m^{-3} h^{-1}. In the next 3 days of biofilter operation, the air flow rate is increased to 0.24 m^3 h^{-1} by keeping the inlet EA concentration in the same range. The removal efficiency slightly decreases in the range of 82.11 – 85.12% which shows that there is no significant effect of changing the operating conditions on the performance of biofilter column. During the last four days of biofilter operation, the inlet concentration is decreased to the range of 0.18 – 0.192 g m^{-3} and air flow rate to 0.18 m^3 h^{-1}. The removal efficiency increases with a decrease in inlet EA concentration and air flow rate and reaches to a maximum value of 91.11% which indicate that the biofilter is performing well and also to the different shock loading conditions for EA removal. The plot of elimination capacity vs inlet load is shown in Fig. 5.56 where increasing trend is observed with increase in the inlet load from 38 to 52 g m^{-3} h^{-1}. This also shows the stability of the biofilter column for removal of EA.

In the present study, the biofilter is operated continuously for all VOCs during shock loading conditions which is also reported by Kim et al. (2008). They varied the inlet concentration and gas flow rate after 4 days of biofilter operation. They found that there was a significant change in the removal efficiency on first day of any shock load but it stabilizes with increase in time. Similar trends are obtained in the present study (Fig. 5.49 – Fig. 5.56).

The results of the shock loading conditions indicate that the biofilm developed in the biofilter is quite stable for all VOCs. The better removal efficiency achieved for different VOCs during all phases show the stability of biofilter column and thus substantiates the fact that biofiltration experiments can be successfully applied industrially where pollutant loads vary from lower to medium values. Similar fluctuations in the performance of biofilter are observed for the removal of IPA and ACE by Chang and Lu (2003). The shock loads effect on biofilter performance can be avoided, if the inlet load changes are made gradually and it will not significantly affect the performance of biofilter column. This means that by providing proper control, shock loads can be filtered out.

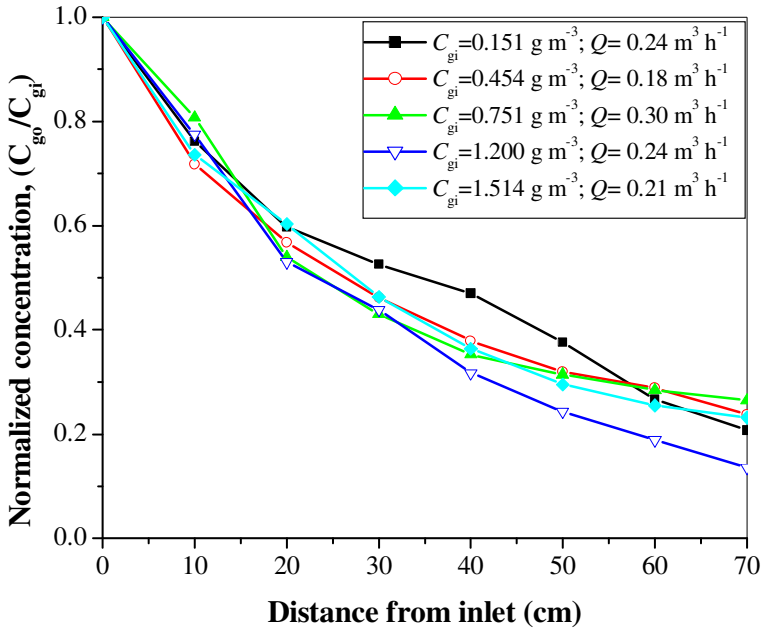

Fig. 5.45. Normalized MEK gas concentration profiles as a function of the biofilter height

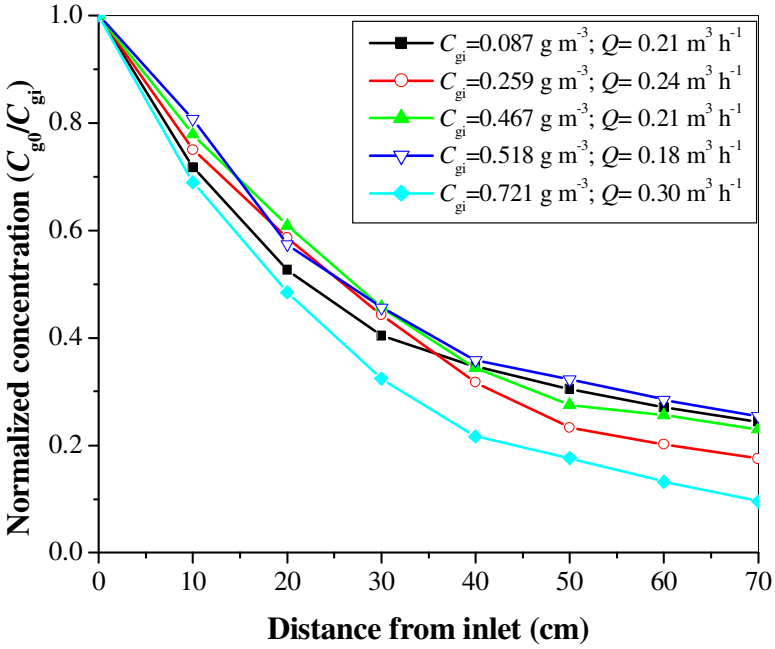

Fig. 5.46. Normalized MIBK gas concentration profiles as a function of the biofilter height

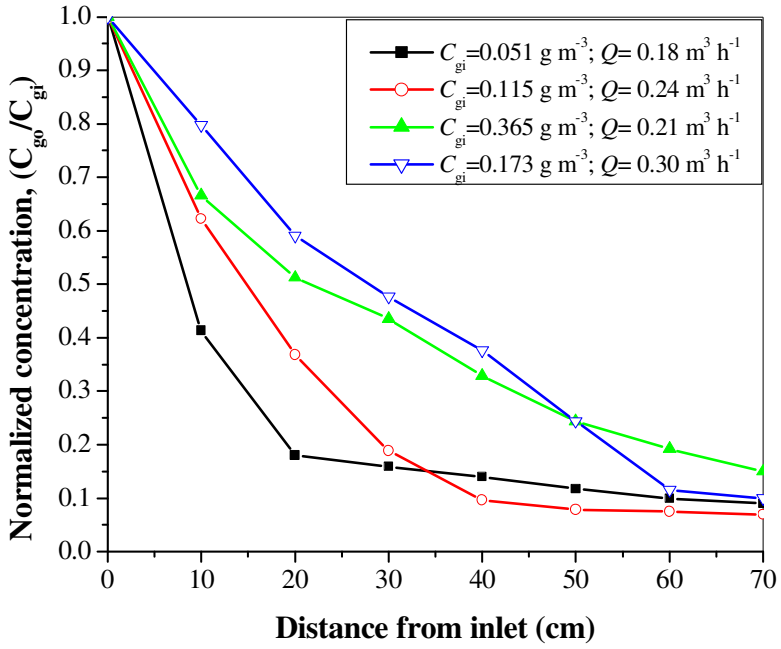

Fig. 5.47. Normalized IPA gas concentration profiles as a function of the biofilter height

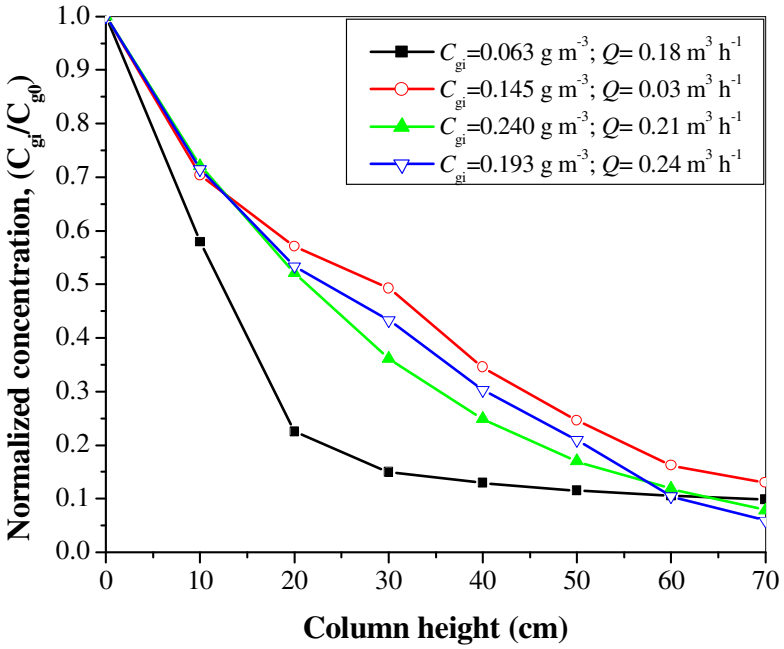

Fig. 5.48. Normalized EA gas concentration profiles as a function of the biofilter height

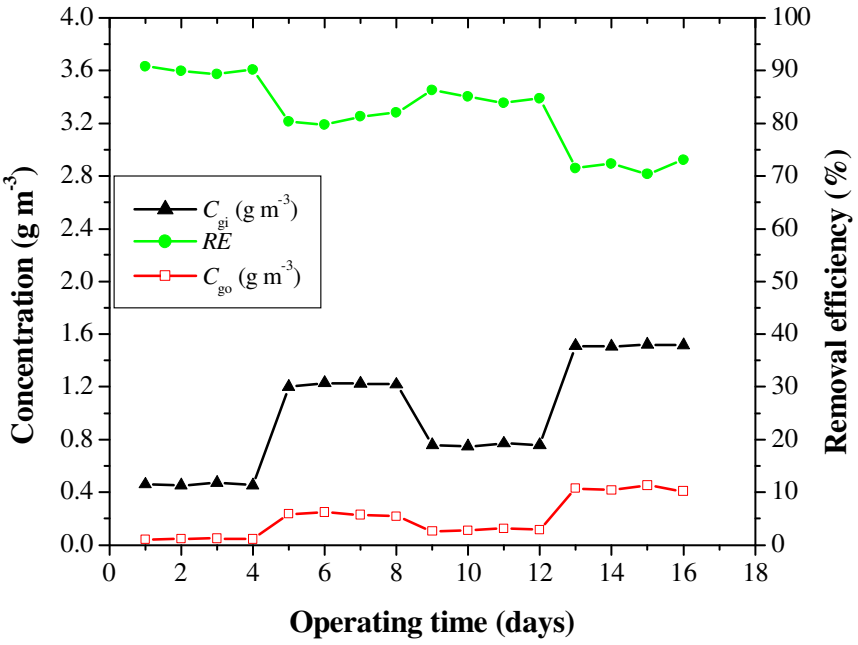

Fig. 5.49. Performance of biofilter with change in air flow rate and inlet MEK concentrations for shock loading conditions

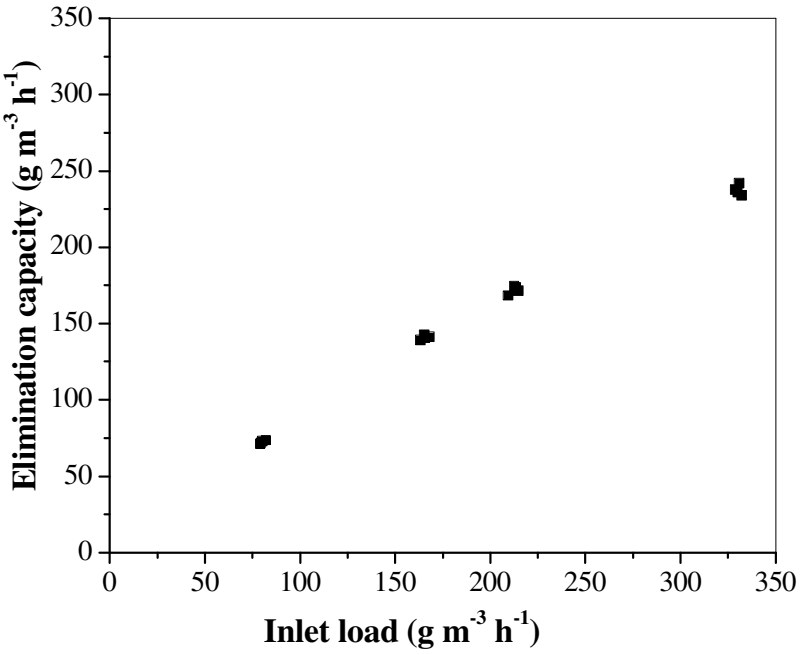

Fig. 5.50. Variation in elimination capacity with change in inlet load of MEK for shock loading conditions

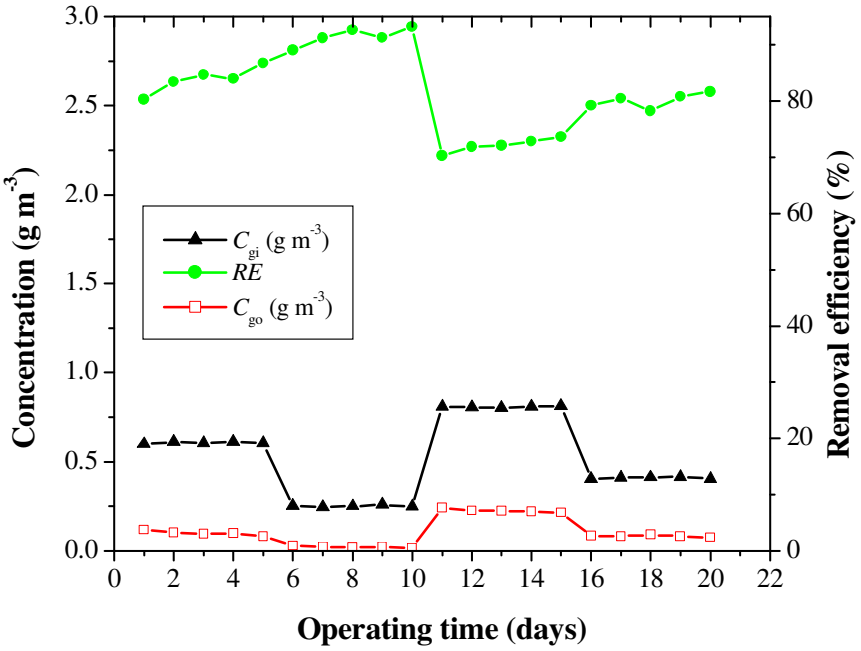

Fig. 5.51. Performance of biofilter with change in air flow rate and inlet MIBK concentrations for shock loading conditions

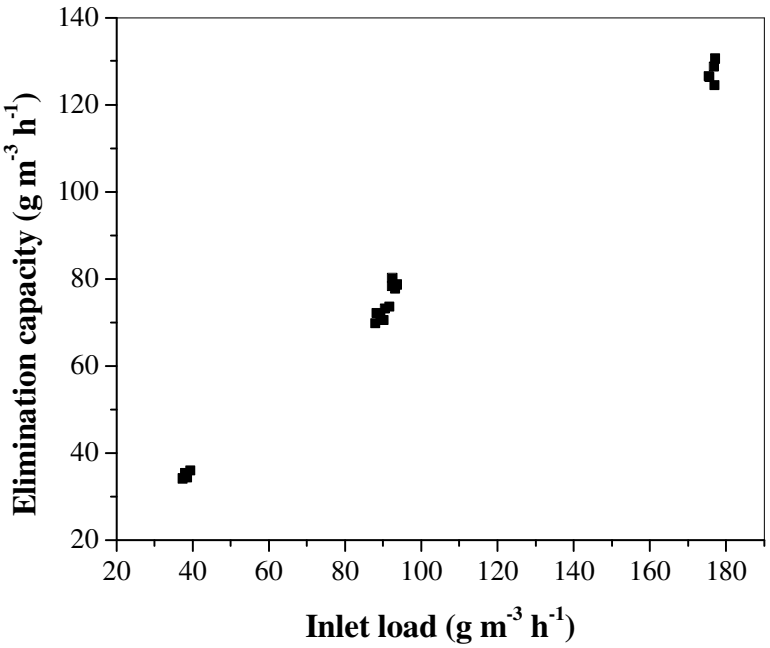

Fig. 5.52. Variation in elimination capacity with change in inlet load of MIBK for shock loading conditions

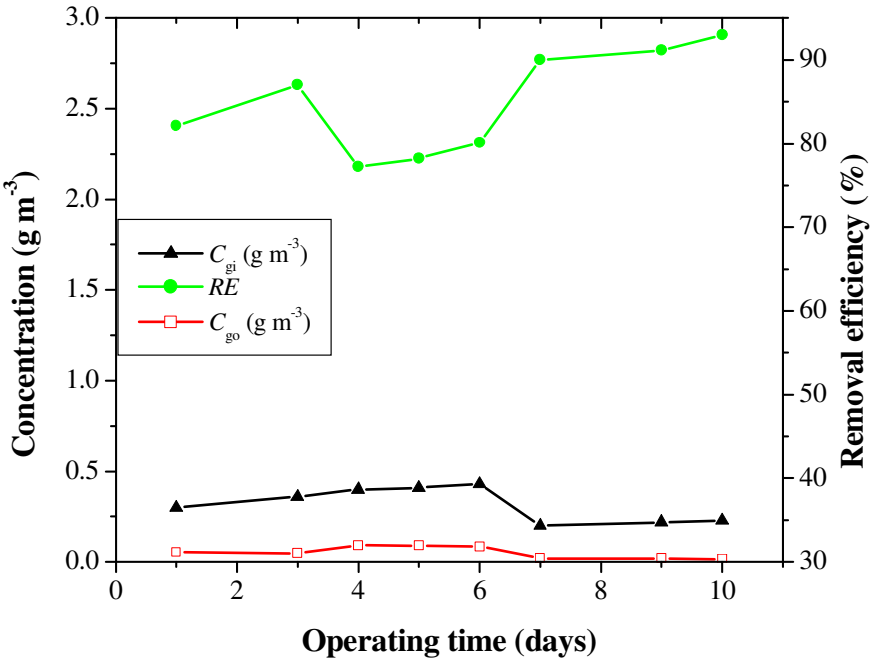

Fig. 5.53. Performance of biofilter with change in air flow rate and inlet IPA concentrations for shock loading conditions

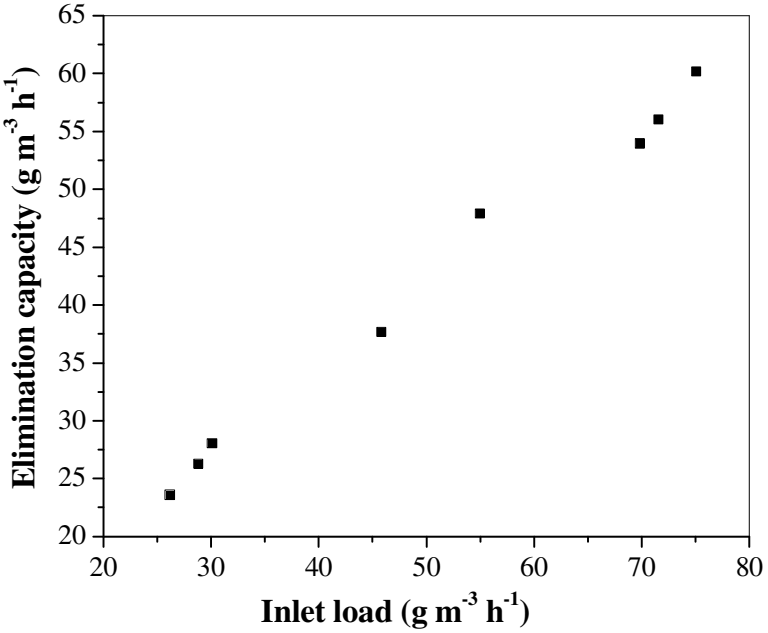

Fig. 5.54. Variation in elimination capacity with change in inlet load of IPA for shock loading conditions

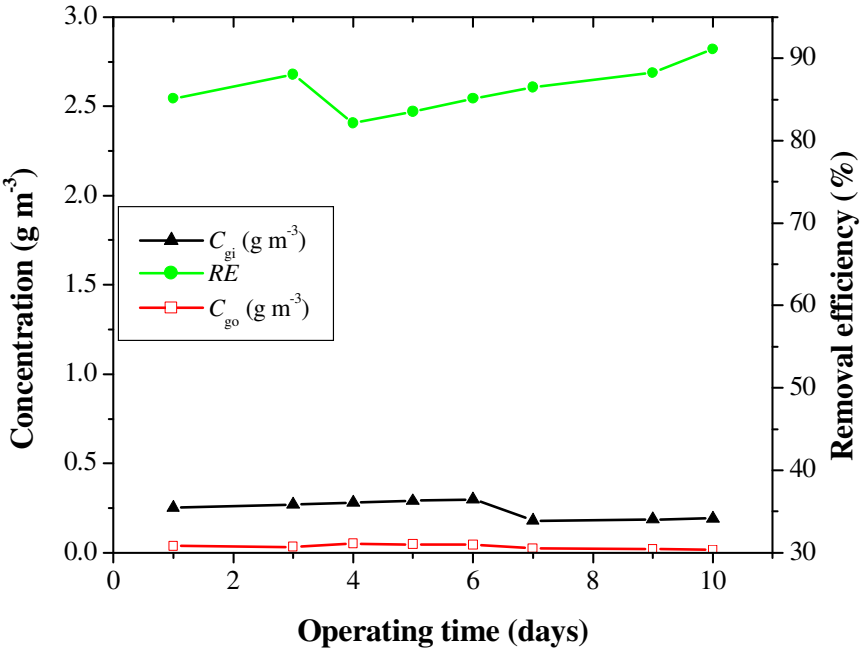

Fig. 5.55. Performance of biofilter with change in air flow rate and inlet EA concentrations for shock loading conditions

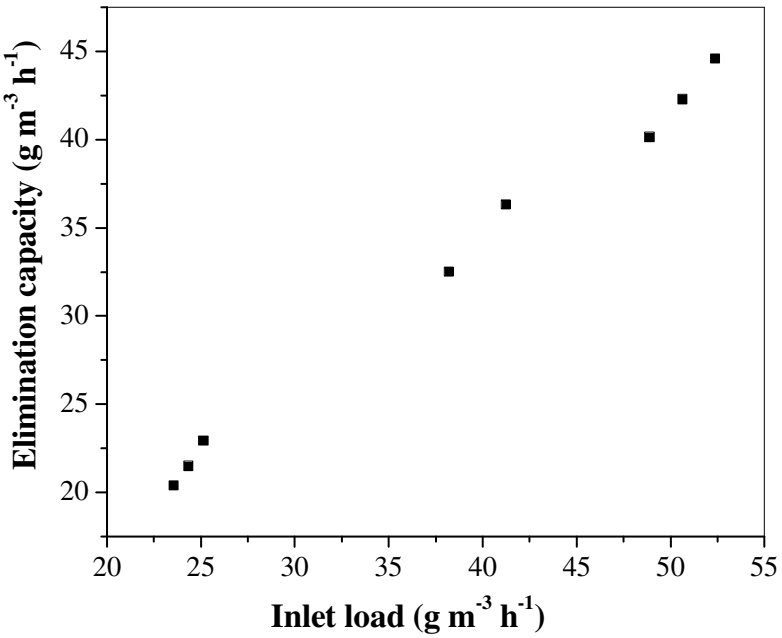

Fig. 5.56. Variation in elimination capacity with change in inlet load of EA for shock loading conditions

5.2.4. Determination of Michaelis–Menten kinetic constants

This study includes the estimation of kinetic constants using Michaelis–Menten kinetic model. The maximum degradation rate per unit filter volume, r_{max} (g m^{-3} h^{-1}) and saturation constant, K_S (g m^{-3}) for the gas phase are obtained by plotting [(V / Q) (C_{gi} – C_{g0})] versus (1/ C_{ln}) from Michaelis-Menten model (Eq. 4.26) which gives a straight line and shown in Figs. 5.57, 5.58, 5.59, and 5.60 for MEK, MIBK, IPA, and EA removal. The steady state value (final data point) for each phase of all VOCs is taken for the evaluation of kinetic constants. The slopes of the straight lines give the maximum degradation rate per unit filter volume (r_{max}) as 0.086, 0.115, 0.11, and 0.092 g m^{-3} h^{-1} and the intercepts of the straight lines give the saturation constant (K_S) as 0.577, 1.046, 1.226, and 1.061 g m^{-3} for MEK, MIBK, IPA, and EA respectively and are listed in Table 5.20. The coefficient of determination (R^2) obtained for MEK, MIBK, IPA, and EA are 0.99, 0.993, 0.996, and 0.991 respectively which are quite good and shows the applicability of Michaelis-Menten model for the biodegradation of MEK, MIBK, IPA, and EA. The values of r_{max} and K_s obtained in the present study are in the same order of magnitude as reported by Mathur and Mazumder (2008) for different VOCs (methyl ethyl ketone, toluene, n-butyl acetate, and *o*-xylene) (r_{max} = 0.024 – 0.16 g m^3 h^{-1} and K_s = 0.679 – 2.305 g m^{-3}) under different operating conditions (Operating time = 41 – 149 days, flow rate = 1 – 2.5 L min^{-1}, inlet load = 0.148 – 0.414 g m^{-3}.

The Michaelis-Menten kinetics can be simplified to either first-order kinetics or zero-order kinetics depending on the values of inlet concentration of pollutant and saturation constant. When inlet VOCs concentration is very less than the saturation constant ($K_S >> C_{gi}$), the reaction rate is simplified to the first-order kinetics. The other situation is when

the inlet MEK concentration is much more than the saturation constant ($K_S << C_{gi}$), the reaction rate is simplified to the zero-order kinetics with the reaction rate limitation. In the present study, the obtained values of K_S are 0.577, 1.046, 1.226, and 1.061 g m^{-3}, which are comparable with inlet concentrations of MEK (0.151 – 1.514 g m^{-3}), MIBK (0.07 – 0.73 g m^{-3}), IPA (0.04 – 0.365 g m^{-3}), and EA (0.05 – 0.24 g m^{-3}) respectively. This indicates that the biodegradation kinetics for MEK, MIBK, IPA, and EA can neither be explained by first-order nor by zero-order kinetics. In such situations, the applicability of zero-order kinetics with diffusion limitation (Ottengraf-Van den Oever model) proposed by Ottengraf and Van-den Oever (1983) can be regarded as the most appropriate biodegradation kinetic model.

5.2.5. Modeling with Ottengraf-Van den Oever model

The Ottengraf-Van den Oever model (Eq. 4.30) is validated with the obtained experimental data during steady state operation for all the phases except for the acclimation phase (Phase I) of MEK, MIBK, IPA, and EA removal. The constant, K_1, is obtained by the linear regression of 1- $(C_{g0} / C_{gi})^{0.5}$ versus $1/(C_{gi})^{0.5}$ and slope of this line represents the value of K_1. The values of K_1 for MEK, MIBK, IPA, and EA at different phases of biofilter operation are estimated and reported in Tables 5.21, 5.22, 5.23, and 5.24 respectively. The value of K_0 corresponds to the maximum elimination capacity in the respective phase which is also reported in Tables 5.21, 5.22, 5.23, and 5.24 for MEK, MIBK, IPA, and EA respectively for different phases of biofilter operation. The critical inlet concentration ($C_{critical}$) is defined as the limiting inlet concentration at which the biodegradation mechanism changes from diffusion-controlled to reaction-rate controlled. The critical inlet concentration ($C_{critical}$) and critical inlet load ($IL_{critical}$) are obtained at

different phases for MEK, MIBK, IPA, and EA and are reported in Tables 5.21, 5.22, 5.23, and 5.24 respectively. The critical inlet concentration obtained is more than the inlet concentration of all VOCs used in present study for all the phases (Tables 5.21 – 5.24). It conforms that the data used to fit the zero order diffusion limited kinetics are comprised of diffusion limited region. This indicates that the biodegradation of MEK can be better explained by the zero-order diffusion limited kinetic model. The Ottengraf-Van den Oever model (Eq. 4.30) is also used to predict the elimination capacity at different phases (different inlet loads) for different VOCs using the obtained kinetic parameters (K_0 and K_1). The predicted model results for elimination capacity are plotted with the experimentally calculated elimination capacity values at different phases with inlet loads for MEK, MIBK, IPA, and EA removal and are shown in Figs. 5.61, 5.62, 5.63, and 5.64 respectively.

The Ottengraf model (zero-order diffusion limitation) predicts the performance of the biofilter well for phase II, phase III and phase V of MEK removal with the standard deviation (s.d.) obtained as 3.004, 3.85, and 3.977 respectively. The standard deviation obtained for phase IV of MEK removal is 7.66 which is more as compared to the standard deviation of the other phases. The may be due to the lower value of *EBRT* because of which assumption of the plug flow of gases does not hold true.

It can be seen from Fig. 5.62 that the biofilter`s performance can be predicted well for phase II, III and V with the Ottengraf-Van den Oever model for MIBK with standard deviation (s.d) values of 2.32, 2.476 and 1.945 respectively. The standard deviation value of phase IV is obtained as 4.815 which is on the higher side when compared with the s.d

values of other phases. The EBRT value is 16.5 s during phase IV, and this may be one of the reasons for the variation of model results with the experimental results.

The standard deviation values obtained at different phases of IPA removal for predicted elimination capacity using Ottengraf-Van den Oever model and experimentally obtained elimination capacity are 1.734, 4.25, and 2.541 for phase II, phase III, and phase IV respectively. The standard deviation values are less for all phases of IPA removal which confirms the suitability of Ottengraf-Van den Oever model.

The Ottengraf Van den Oever model predicts the performance of the biofilter for phase II, phase III and phase IV of EA removal with the standard deviation values obtained as 2.137, 2.37, and 2.209 respectively. Alvarez-Hornos et al. (2008) also used Ottengraf-Van den Oever model to fit the experimental data obtained for the removal of ethylbenzene using fibrous peat and soil amendment biofilter. The values of the obtained constants show the similar trends as obtained in the present study.

The biofilm thickness (δ) is also calculated for different phases using Eq. (4.29) by taking the values of effective diffusivity of biofilm (D_e) and Henry's constant (m) for MEK, MIBK, IPA, and EA as reported in Table 5.25. The values of biofilm thickness are reported in Table 5.25 for different VOCs at different phases of biofilter operation. The biofilm thickness calculated using obtained constant values for MEK, MIBK, IPA, and EA are ranging from 384 – 656 µm, 410.67 – 570.8 µm, 17.99 – 29.5 µm, and 2.137 – 2.67 µm respectively.

The usual range for the biofilm thickness assumed by other authors to obtain biokinetic constants is 100 µm (Deshusses et al., 1995 a, b)**.** In the present study, biofilm thickness is calculated using the zero-order diffusion limited kinetic model for which some of the

parameters are used as per the values reported in the literature. So it is possible to obtain higher values of biofilm thickness using the kinetic model. In this study, the pressure drop is assumed to be constant as a combination of coal particles and compost is used as packing material which does not result in significant pressure drop.

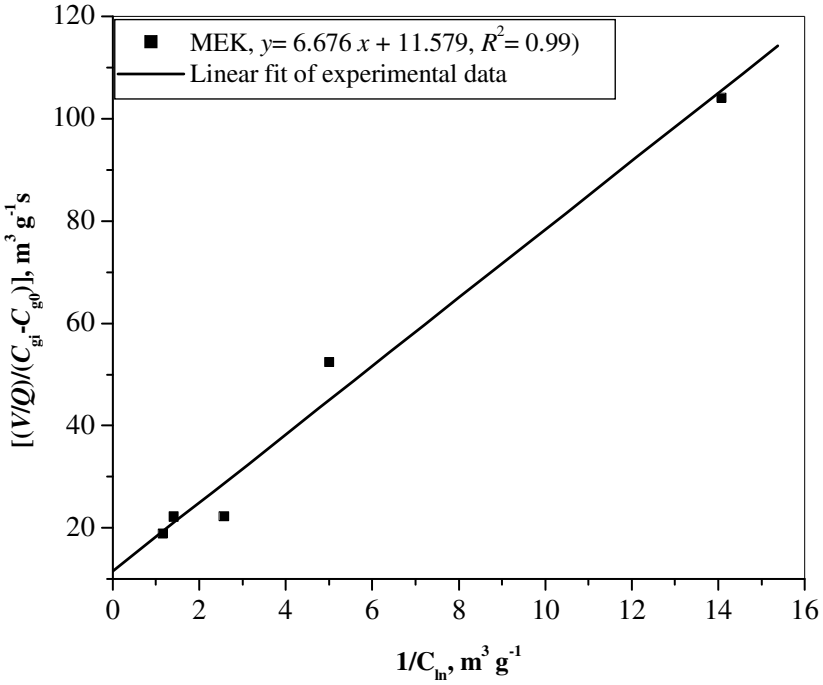

Fig. 5.57. Bio kinetic constants obtained for MEK using Michaelis-Menten equation

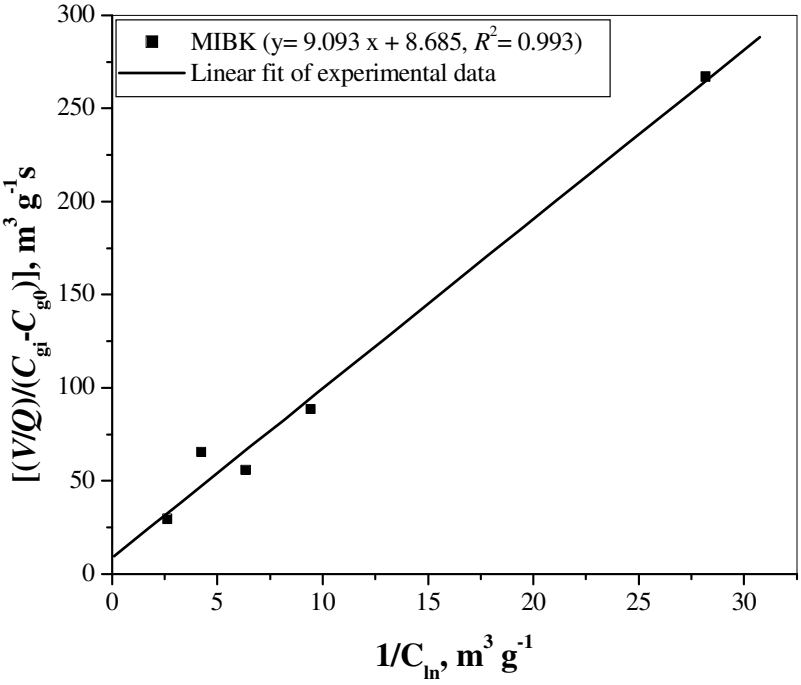

Fig. 5.58. Bio kinetic constants obtained for MIBK using Michaelis-Menten equation

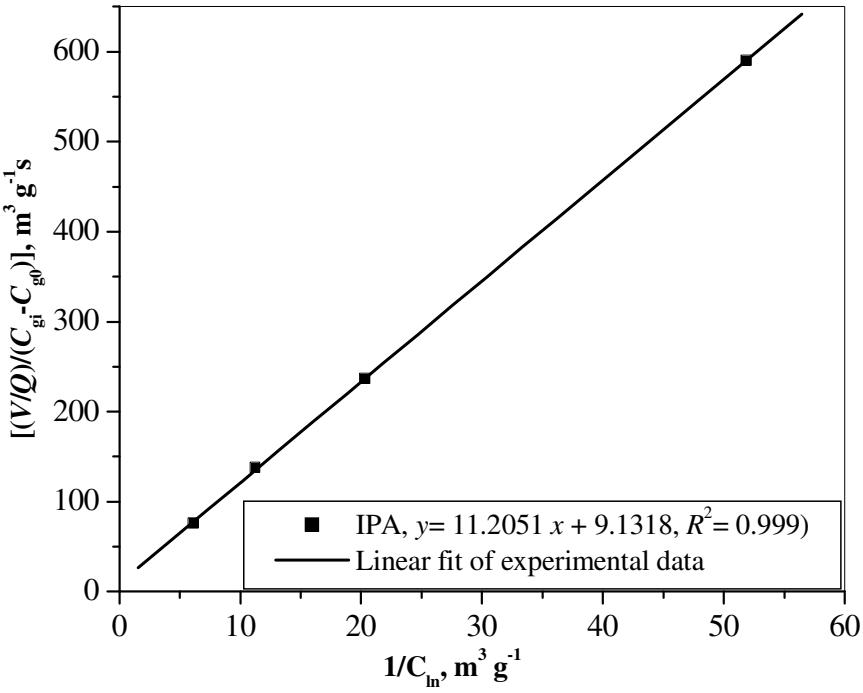

Fig. 5.59. Bio kinetic constants obtained for IPA using Michaelis-Menten equation

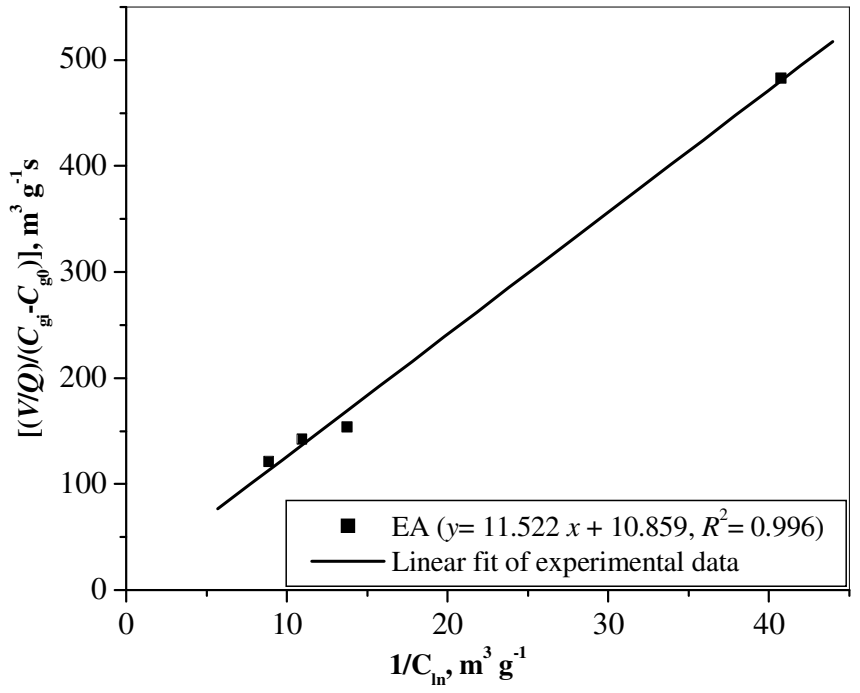

Fig. 5.60. Bio kinetic constants obtained for EA using Michaelis-Menten equation

Table 5.20. Values of Michaelis-Menten constants obtained for different VOCs at different operating conditions

S No	Compound	Michaelis–Menten Constants		Coefficient of determination, R^2
		r_{max} (g m^{-3} h^{-1})	K_s (g m^{-3})	
1	MEK	0.086	0.577	0.990
2	MIBK	0.115	1.046	0.993
3	IPA	0.110	1.226	0.996
4	EA	0.092	1.061	0.991

Table 5.21. Predicted model parameters of Ottengraf-Van den Oever model at different phases for MEK removal

Phase	C_{gi}, (g m^{-3})	IL, (g m^{-3} h^{-1})	K_0, (g m^{-3} h^{-1})	K_1, (g m^{-3} h^{-1})	$C_{critical}$ (g m^{-3})	$IL_{critical}$, (g m^{-3} h^{-1})	s.d.
II	0.45 – 0.6	59 – 78	73.723	62.73	0.683	89.724	3.004
III	1.19 – 1.33	207 – 233	168.338	90.73	1.409	246.328	3.85
IV	0.75 – 0.88	163– 195	164.801	113.92	0.969	211.485	7.66
V	1.51 – 1.64	231– 249	190.842	95.784	1.712	262.295	3.977

Table 5.22. Predicted model parameters of Ottengraf-Van den Oever model at different phases for MIBK removal

Phase	C_{gi}, (g m^{-3})	IL, (g m^{-3} h^{-1})	K_0, (g m^{-3} h^{-1})	K_1, (g m^{-3} h^{-1})	$C_{critical}$ (g m^{-3})	$IL_{critical}$, (g m^{-3} h^{-1})	s.d.
II	0.251 – 0.26	44 – 46	40.70	50.165	0.302	52.656	2.32
III	0.5 – 0.51	66 – 68	56.36	50.183	0.559	73.262	2.478
IV	0.71 – 0.73	156 -159	124.43	87.305	0.833	66.209	4.815
V	0.45 – 0.46	69 - 71	65.65	69.938	0.486	74.302	1.945

Table 5.23. Predicted model parameters of Ottengraf-Van den Oever model at different phases for IPA removal

Phase	C_{gi}, (g m^{-3})	IL, (g m^{-3} h^{-1})	K_0, (g m^{-3} h^{-1})	K_1, (g m^{-3} h^{-1})	$C_{critical}$ (g m^{-3})	$IL_{critical}$, (g m^{-3} h^{-1})	s.d.
II	0.101 –0.115	17 – 21	18.68	34.93	0.135	23.57	1.734
III	0.352 –0.365	53 – 56	47.41	47.05	0.432	66.19	4.25
IV	0.162 –0.173	35 – 38	33.99	51.01	0.202	44.12	2.541

Table 5.24. Predicted model parameters of Ottengraf-Van den Oever model at different phases for EA removal

Phase	C_{gi}, (g m^{-3})	IL, (g m^{-3} h^{-1})	K_0, (g m^{-3} h^{-1})	K_1, (g m^{-3} h^{-1})	$C_{critical}$ (g m^{-3})	$IL_{critical}$, (g m^{-3} h^{-1})	s.d.
II	0.131 –0.145	28 – 32	27.54	44.64	0.169	36.81	2.137
III	0.231 –0.240	35 – 37	33.77	44.19	0.277	42.44	2.37
IV	0.18– 0.193	31 – 34	31.72	47.26	0.221	38.63	2.209

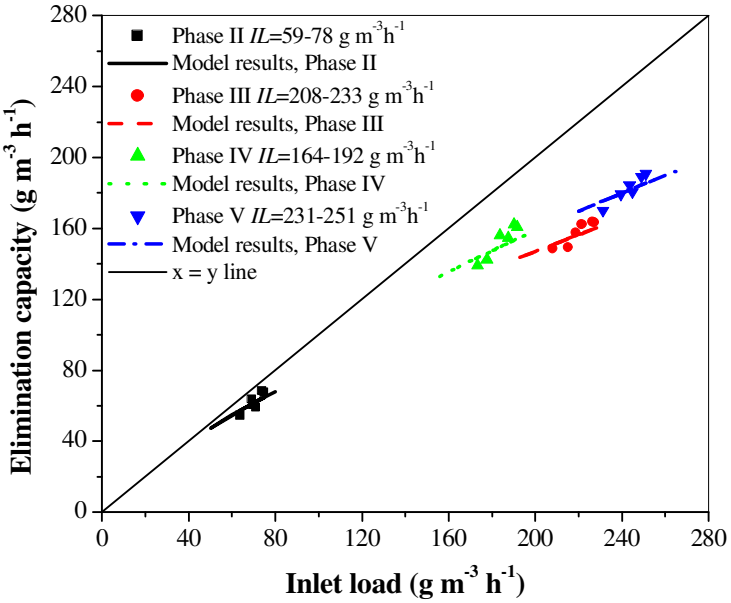

Fig. 5.61. Comparison of experimental elimination capacity values with predicted values of elimination capacity from Ottengraf-Van den Oever model for MEK at different phases

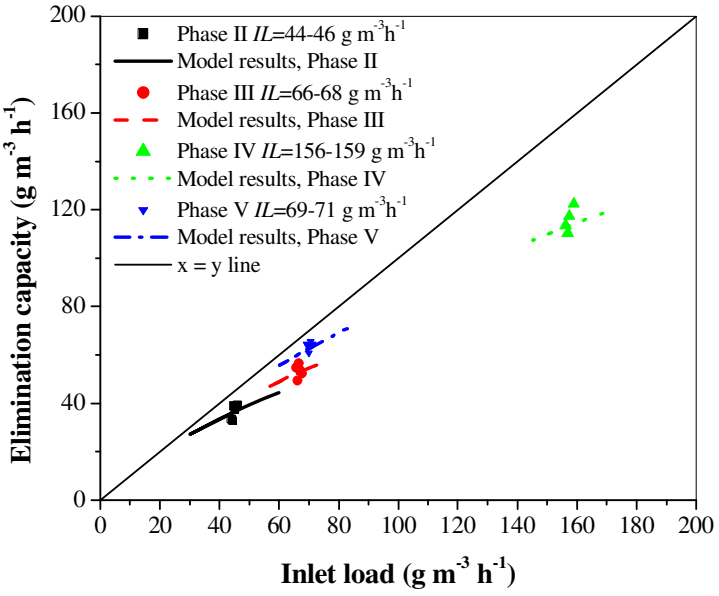

Fig. 5.62. Comparison of experimental elimination capacity values with predicted values of elimination capacity from Ottengraf-Van den Oever model for MIBK at different phases

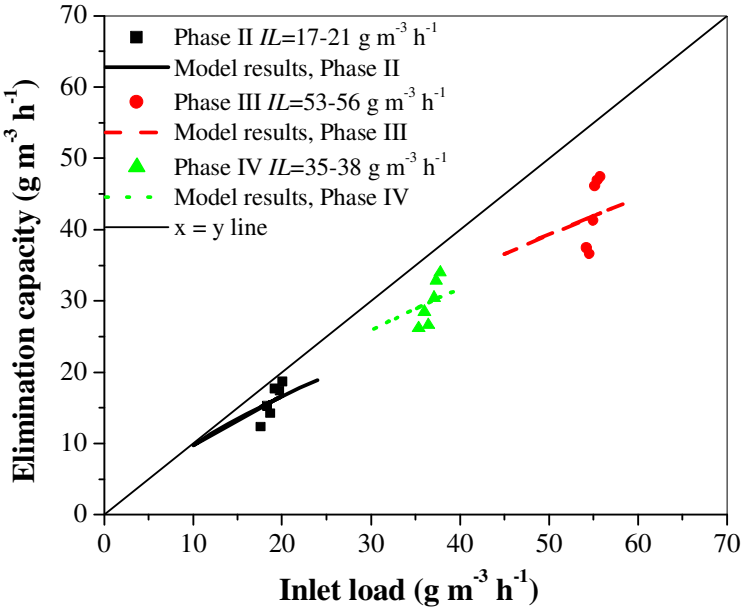

Fig. 5.63. Comparison of experimental elimination capacity values with predicted values of elimination capacity from Ottengraf-Van den Oever model for IPA at different phases

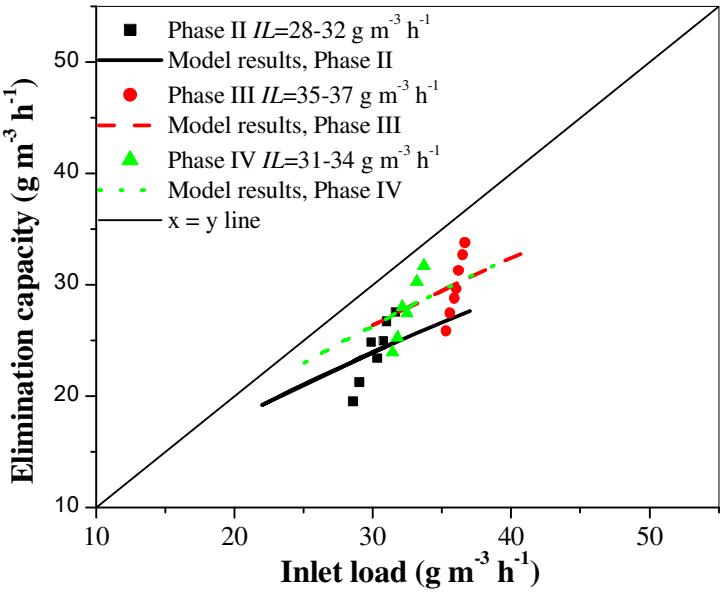

Fig. 5.64. Comparison of experimental elimination capacity values with predicted values of elimination capacity from Ottengraf-Van den Oever model for EA at different phases

Table 5.25. Reported values of Henry's constant and effective diffusion coefficient for different VOCs and predicted biofilm thickness using Ottengraf-Van den Oever model at different phases for VOCs removal

S No	Compound	m (-)	$D_e \times 10^6$ ($m^2 h^{-1}$)	Biofilm thickness, δ (µm)			
				Phase II	Phase III	Phase IV	Phase V
1	MEK	0.00235	1.026	520	626	384	656
2	MIBK	0.00571	1.933	410.67	554.27	414.52	570.8
3	IPA	0.098	1.8	21.08	29.5	17.99	-
4	EA	1.676	3.46	2.137	2.67	2.196	-

5.3. Mathematical modeling and simulation

Mathematical models are developed for the transient biofilter. In the present work, transient biofilter operated in periodic mode and continuous mode is considered for the modeling and simulation. The present model is validated with the experimental and modeling results of Chmiel et al. (2005) as the present data were not sufficient enough to validate the present model.

5.3.1. Transient biofilter operated in periodic mode

In this work, periodic operation of biofilter is considered. A mathematical model is developed that describes the results in the form of breakthrough curves, which represent the outlet VOCs concentration at different times based on different operating conditions. The performance of present model is carried out by comparing the results obtained with the experimental and modeling results given by Chmiel et al. (2005) in Fig. 5.65. Same parameters as given by Chmiel et al (2005) are used and the values of D_L is taken from Deshusses et al. (1995 a, b) for MEK and Cussler (1997) for butanol (Table 5.26). The standard deviation for MEK and butanol are obtained as 0.00242 and 0.000537 for the present model and 0.00414 and 0.002187 for Chmiel et al. (2005) model respectively, which are less as compared to the model represented by Chmiel et al (2005). It is evident from the results obtained that the present model gives better results as compared to the reported model. Based on the good agreement of the proposed model predictions with the experimental results, simulations are carried out for a wide range of concentration for MEK (0.04 -0.1 g m^{-3}) and butanol (0.02 – 0.05 g m^{-3}), respectively. The simulations are also carried out to understand the influence of various important parameters such as inlet

VOC concentration, bed height and gas velocity on the biofiltration process operated in the periodic mode.

5.3.1.1. Effect of inlet concentration

The effect of the inlet concentration of VOCs (MEK and butanol) on the performance of biofilter in terms of breakthrough curves is shown in Fig. 5.66. The breakthrough curves are obtained for the inlet VOC concentration ranging from 0.04 to 0.1 g m^{-3} for MEK and 0.02 to 0.05 g m^{-3} for butanol respectively. It is observed that as the inlet VOC concentration increases, the break point time (the time of biofiltration process when the outlet concentration of VOC reaches to 3–5% of the inlet VOC concentration) decreases. For MEK, as the inlet concentration increases from 0.04 to 0.1 g/m^3, the breakpoint time decreases from 90 to 15 sec. For butanol, as the inlet concentration increases from 0.02 to 0.05 g/m^3, the breakpoint time decreases from 1400 to 1280 sec. These trends could be explained with the fact that at higher value of concentration, the driving force for mass transfer is higher which results in attaining the equilibrium faster.

5.3.1.2. Effect of bed height

The effect of bed height on the effluent VOCs concentration is presented in Fig. 5.67 for the bed height from 0.4 m to 0.6 m. It is observed that as the bed height increases from 0.4 m to 0.6 m, the values of breakpoint time for MEK and butanol increase from 9 to 18 sec and 940 to 1800 sec, respectively. Higher bed height corresponds to the large amount of packing material which indicates that more biofilm surface and adsorbent surface are available for biodegradation and adsorption of VOCs respectively. Hence, the VOC concentration at outlet of the column decreases for the larger bed heights.

5.3.1.3. Effect of gas velocity

The breakthrough curves obtained for MEK and butanol at different gas velocities are plotted in Fig. 5.68. During these simulations, other parameters such as inlet VOC concentration and bed height are kept constant. It is observed that as the gas velocity increases from 0.02 to 0.04 m s^{-1}, the breakpoint times for MEK and butanol decrease from 43 to 10 sec and 2200 to 900 sec, respectively. This is due to the lesser residence time available for the VOCs for undergoing adsorption or biodegradation. So equilibrium gets delayed at higher gas velocities.

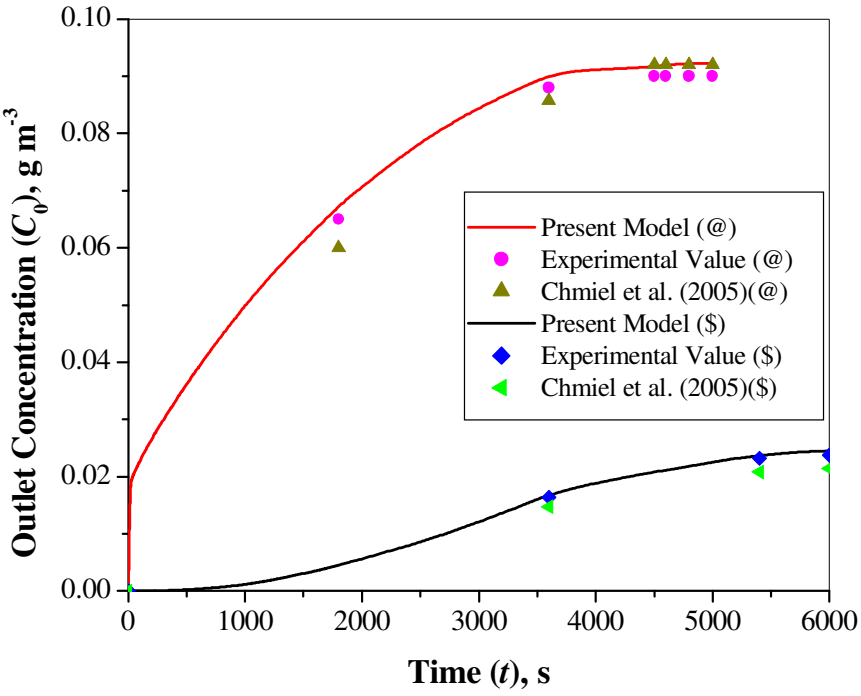

Fig. 5.65. Comparision between the present model, experimental value and model reported by Chimel et.al (2005) for MEK (@) and Butanol ($)

Table 5.26. Model parameters value for the simulation of mathematical model for periodically operated biofilter

S No	Parameter	Butanol	MEK
1.	$k_{ig\text{-}ads}$ (1/s)	0.001	0.003
2.	N (-)	1.5	1.35
3.	μ ($g^{2\text{-}N}/m^{3\text{-}N}s$)	$1.25x10^{-3}$	$0.4x10^{-3}$
4.	K_m (g/m^3)	0.555	0.025
5.	D_L (m^2/s)(*)	$8.7x10^{-6}$	$5x10^{-4}$
6.	m_2 (-)	$4x10^{-4}$	$2x10^{-3}$
7.	ε (-)	0.65	0.58

*The values are taken from Deshusses et al. (1995) and Cussler (1997) as these values are not reported in Chmiel et al. (2005).

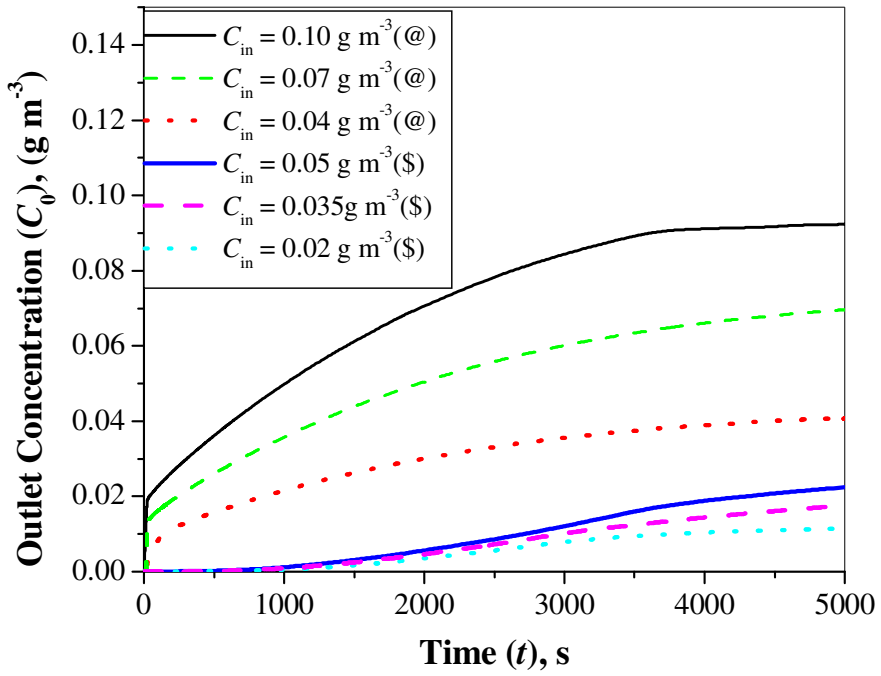

Fig. 5.66. Effect of inlet VOCs concentration on breakthrough curves for MEK (@) and Butanol ($)

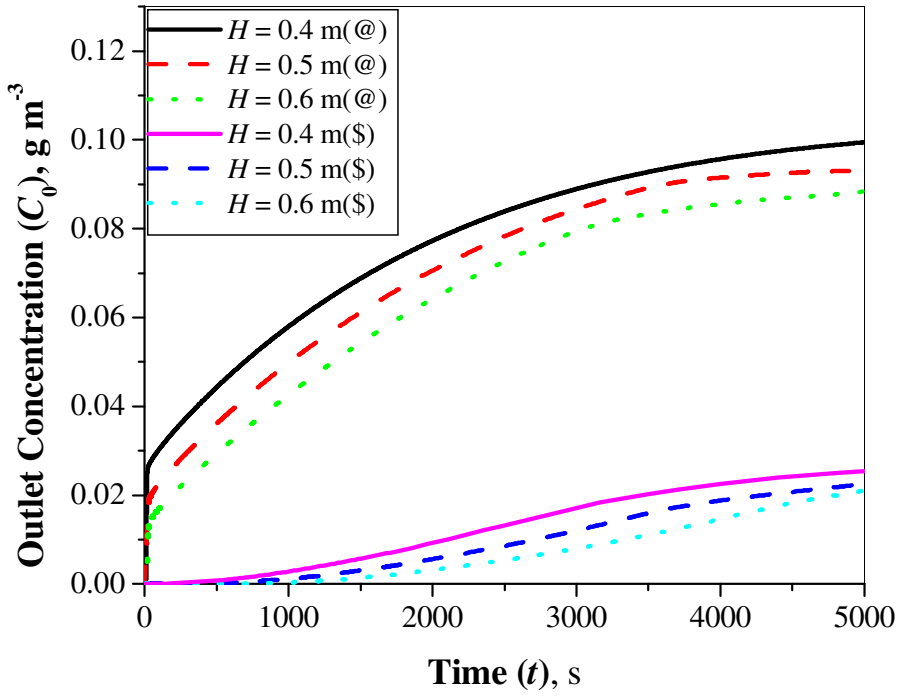

Fig. 5.67. Effect of bed height on breakthrough curves for MEK (@) and Butanol ($)

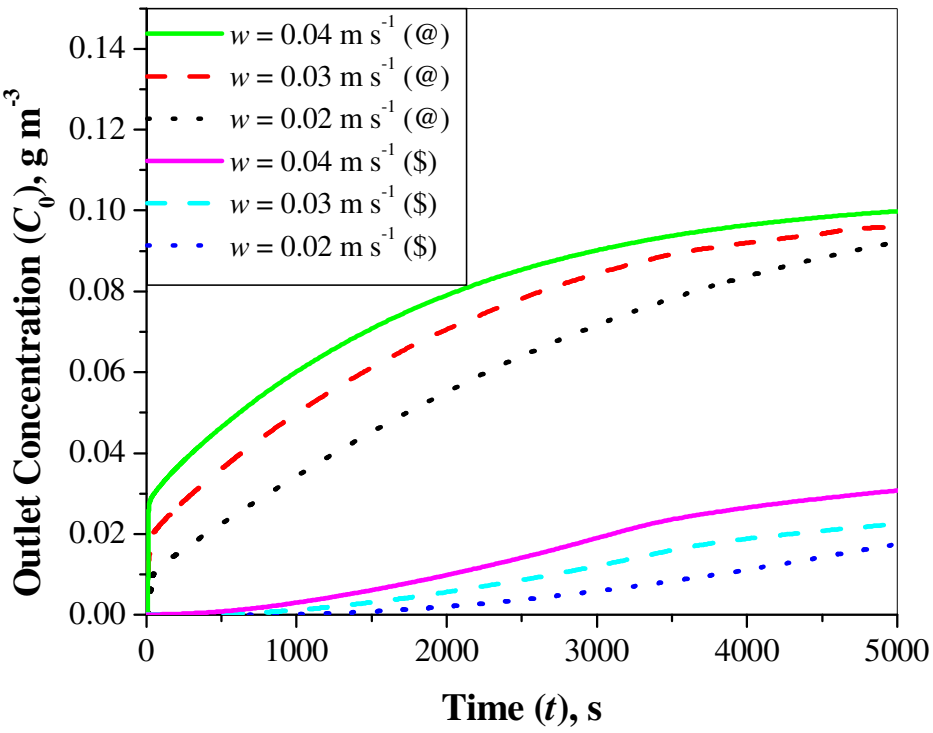

Fig. 5.68. Effect of gas velocity on breakthrough curves for MEK (@) & Butanol ($)

5.3.2. Transient biofilter operated in continuous mode

A generalized mathematical model is proposed for the transient biofilter operated in continuous mode. The details of modeling equations are given in chapter 4 (section 4.4.2). The proposed mathematical model incorporates the effects of gas biofilm resistances, possible extent of reaction in pores on biofilter, gas-phase mass transfer coefficient, and axial diffusion coefficient which were neglected in earlier studies. The model equations are solved numerically using explicit finite difference technique. The model parameters reported by Chmiel et al. (2005) are used for the simulation in the present study. The value of D_L is taken from Deshusses et al. (1995) for MEK and Cussler (1997) for butanol and other design parameters, that are not reported by Chmiel et al. (2005) are assumed based on the ranges given in the literature (Ottengraf and Van Den Oever, 1983; Shareefdeen et al., 1994; Deshusses et al. 1995 (a, b); Hodge and Devinny, 1995; Abumaizar et al., 1998) (see Table 5.27). The obtained simulation results are compared with the experimental and modeling results reported by Chmiel et al. (2005) at different operating conditions and shown in Figs. 5.69 – 5.73. The modeling in the biofiltration operation is very difficult to carry out as the process involves many physical, chemical and microbiological phenomena. During the initial stage of biofilter operation, the model shows that the steady state is reached while experimentally steady state takes several hours. So, it is difficult to validate the present model with the obtained biofiltration experimental results in the present study. The standard deviation values are calculated for the modeling results obtained by Chmiel et al. (2005) and the model proposed in present study and are given in Table 5.28. The standard deviation values indicate that proposed model fits the experimental data better than the model reported by

Chmiel et al. (2005) at all operating conditions. The proposed model in the present study includes the important aspects such as gas biofilm resistances, possible extent of reaction in pores on biofilter and gas-phase mass transfer coefficient which were neglected in the previous model proposed by Chmiel et al. (2005). Due to this reason, the proposed model in the present study gives the better results as compared to model reported by Chmiel et al. (2005).

Based on the successful validation of proposed model with the experimental and modeling results available in the literature, the simulations are carried out to study the effect of significant parameters such as initial concentration, residence time (flow velocity), and bed height in the performance of biofilter column. Fig. 5.74 shows the effect of the inlet concentration of MEK on the performance of biofilter in terms of breakthrough curves. The breakthrough curves are obtained for the inlet MEK concentration ranging from 0.1 to 0.7 g m^{-3}. It is found that the increase in MEK concentration decreases the breakpoint time. The breakthrough curves are obtained at different values of residence time (τ_k = 5.4 to 10.8 s) and are plotted in Fig. 5.75. It is observed that as the residence time increases, the breakpoint time delays. This is due to the more time available for the VOCs for undergoing adsorption or biodegradation. The effect of bed height on the breakthrough curve is presented in Fig. 5.76. The breakthrough curves are obtained for the bed height ranging from 40 to 60 cm by keeping the other parameter values constant. It is observed that the breakpoint time achieved earlier with decrease in bed height. Small height corresponds to the less amount of packing materials which results in less biofilm surface available for biodegradation.

Table 5.27. Model parameter values for simulation of mathematical model for biofilter operated in continuous mode

S.No.	Parameters	Butanol	MEK
1.	$k_{ig\text{-}ads}$ (s^{-1})	0.001	0.003
2.	α (-) (#)	0.3	0.3
3.	$r_{max,i}$ (g cm^{-3} s^{-1}) (#)	1.25×10^{-3}	5.88×10^{-2}
4.	$r_{max,o}$ (g cm^{-3} s^{-1}) (#)	6.25×10^{-4}	1.23×10^{-3}
5.	$K_{m,i}$ (g/m^3)	0.555	1.23
6	$K_{o,i}$ (g/m^3) (#)	0.26	0.26
7.	D_L (m^2/s)(*)	8.7×10^{-6}	5×10^{-5}
8.	m_2 (-)	4×10^{-4}	2×10^{-3}
9.	ε (-)	0.65	0.58
10.	K_I (g/m^3) (#)	56.73	78.94
11.	A_s (cm^2 cm^{-3}) (#)	1.9	1.9
12.	D_i (m^2/s) (#)	2.85×10^{-10}	2.0×10^{-10}
13.	D_o (m^2/s) (#)	4.7×10^{-10}	4.7×10^{-10}
14.	L (m)	0.5	0.5
15	$k_{rxn,i}$ (s^{-1}) (#)	9.72×10^{-7}	9.72×10^{-7}

*The values are taken from Deshusses et al. (1995) and Cussler (1997) as these values are not reported in Chmiel et al. (2005).

Assumed values based on the usual ranges reported in the literature (Ottengraf and Van Den Oever, 1983; Shareefdeen et al., 1994; Deshusses et al. 1995; Hodge and Devinny, 1995; Abumaizar et al., 1997).

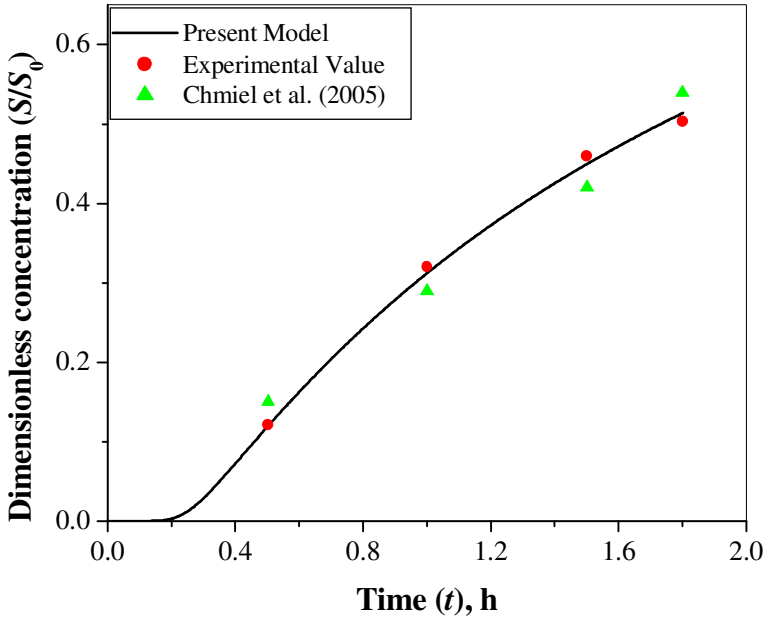

Fig. 5.69. Comparision between the present model, experimental value and model reported by Chimel et.al (2005) for Butanol (S_0 = 50 mg m^{-3} and τ_k = 3.6 s)

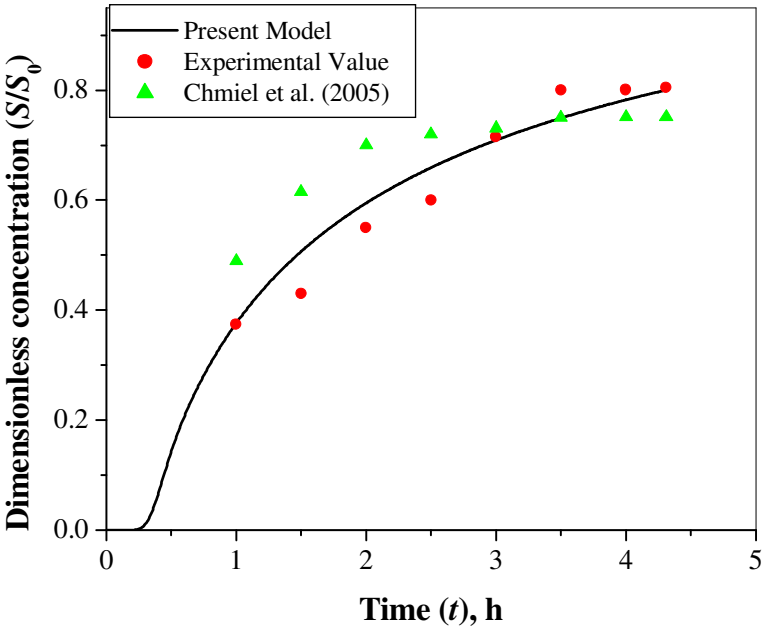

Fig. 5.70. Comparision between the present model, experimental value and model reported by Chimel et.al (2005) for Butanol (S_0 = 100 mg m^{-3} and τ_k = 2.7 s)

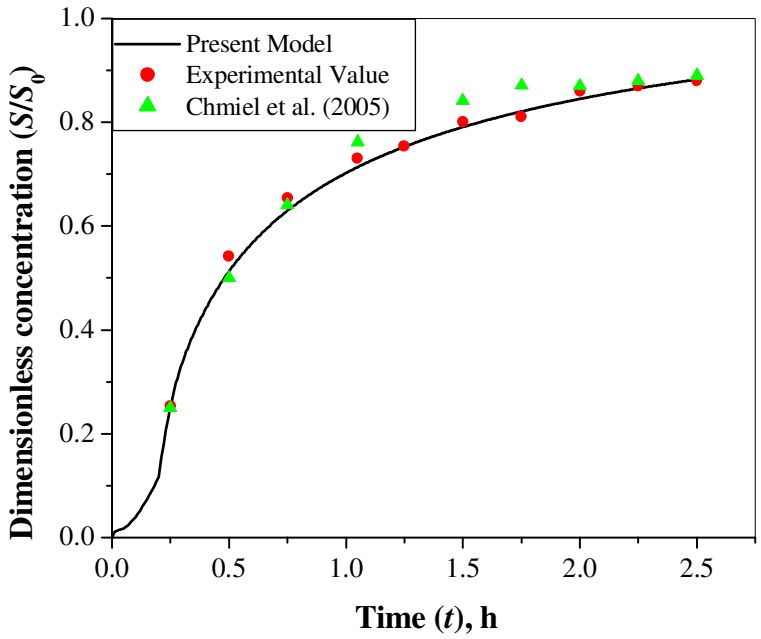

Fig. 5.71. Comparision between the present model, experimental value and model reported by Chimel et.al (2005) for MEK (S_0 = 40 mg m^{-3} and τ_k = 5.4 s)

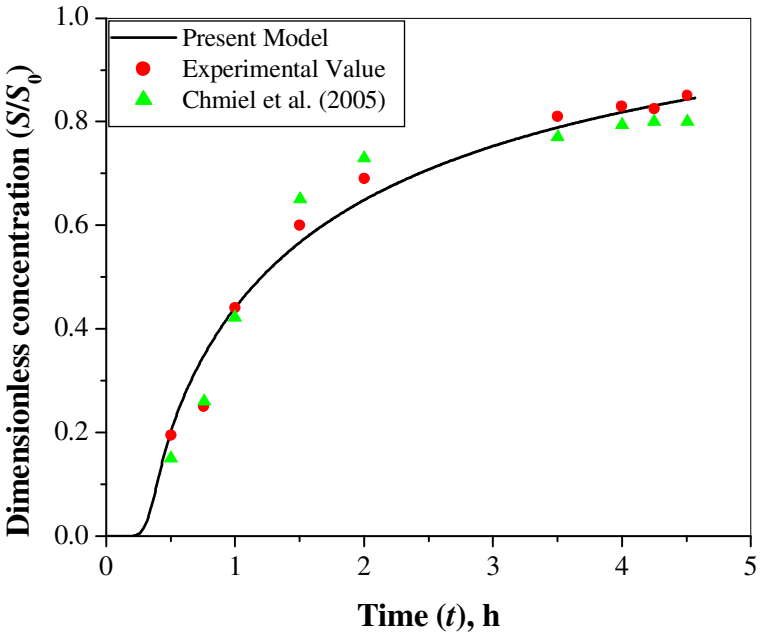

Fig. 5.72. Comparision between the present model, experimental value and model reported by Chimel et.al (2005) for MEK (S_0 = 40 mg m^{-3} and τ_k = 10.8 s)

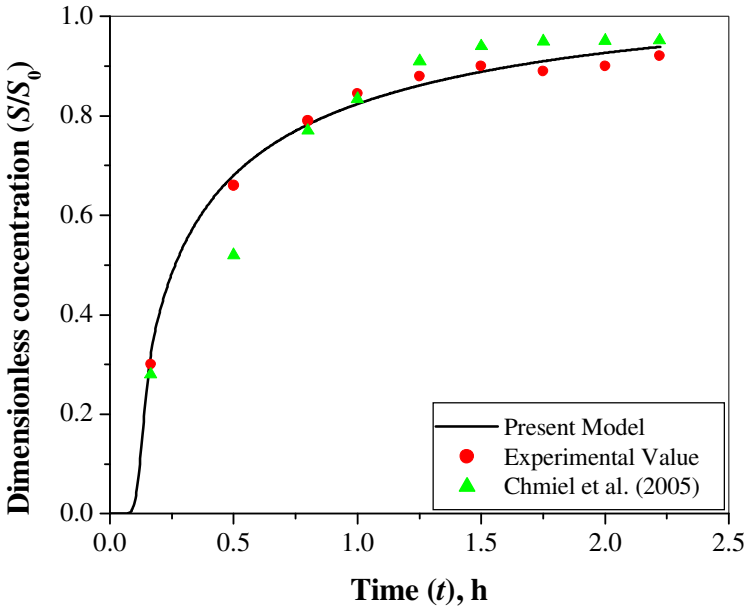

Fig. 5.73. Comparision between the present model, experimental value and model reported by Chimel et.al (2005) for MEK (S_0 = 100 mg m^{-3} and τ_k = 5.4 s)

Table 5.28. Standard deviation values for the model reported by Chimel et.al (2005) and present model for MEK and butanol at different operating conditions

S No	Compound	S_0 (mg m^{-3})	τ_k (s)	Standard deviation	
				Model reported by Chmiel et al. (2005)	Present model
1	Butanol	50	3.6	0.0396	0.0098
2	Butanol	100	2.7	0.0454	0.0119
3	MEK	40	5.4	0.0365	0.0157
4	MEK	40	10.8	0.0410	0.0409
5	MEK	100	5.4	0.0614	0.0198

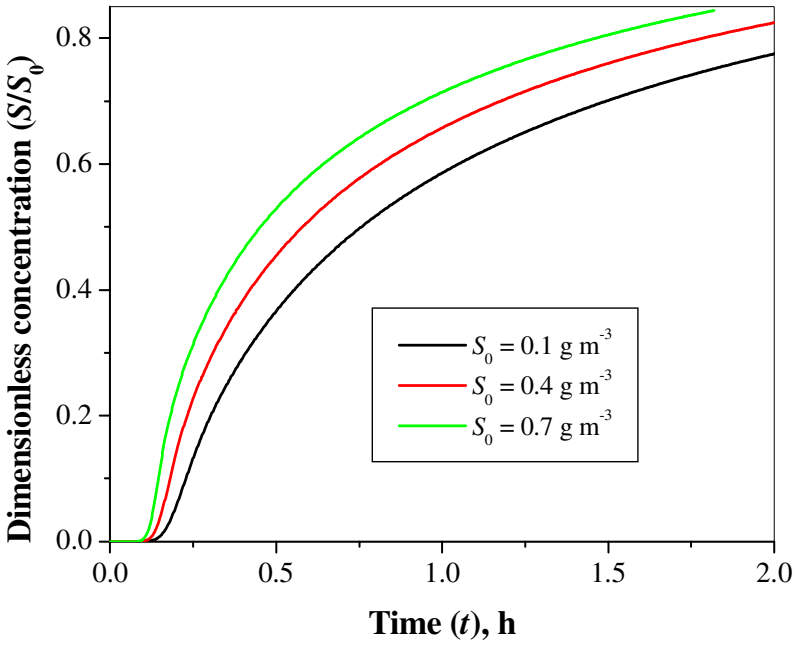

Fig. 5.74. Effect of inlet MEK concentration on breakthrough curves

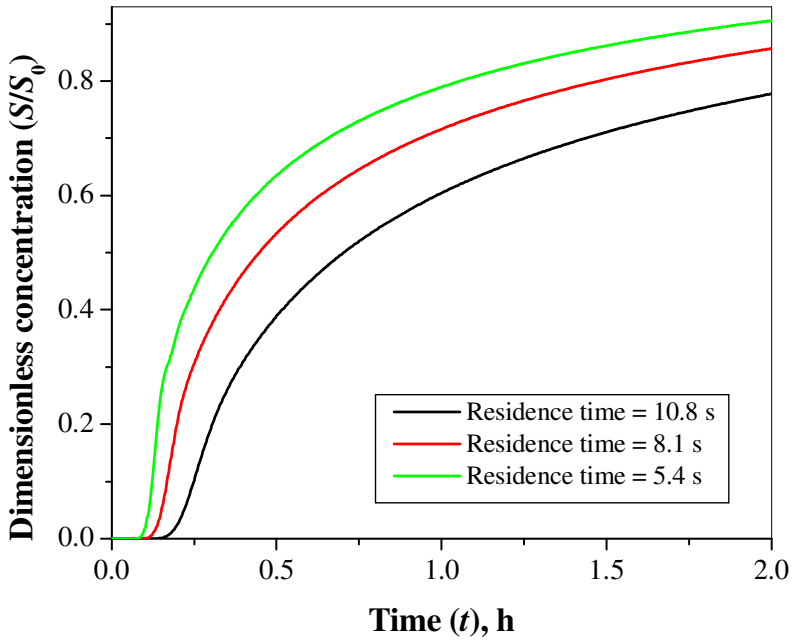

Fig. 5.75. Effect of residence time (gas velocity) on breakthrough curves for MEK

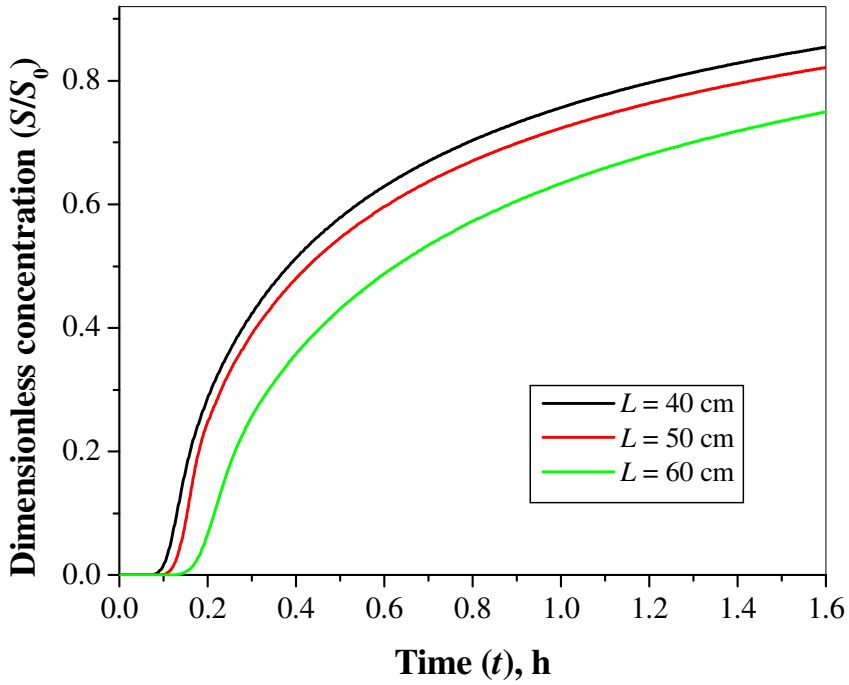

Fig. 5.76. Effect of bed height on breakthrough curves for MEK

CHAPTER – 6
CONCLUDING REMARKS

In the present study, biodegradation and biofiltration methods are used for the removal of different VOCs such as MEK, MIBK, IPA, MA, EA, and BA from polluted water and air streams. Batch and continuous experiments are successfully conducted and the removal efficiency of different VOCs is evaluated. Various growth and rate kinetic models are applied with the obtained experimental results during biodegradation studies. Biofiltration experiments are performed to obtain the performance of biofiltration column at different operating conditions. Kinetic modeling is carried out using Ottengraf-Van den Oever model for the data obtained during biofiltration studies. Mathematical models for the transient biofilter column operated in periodic mode and continuous mode are proposed and validated with the literature and obtained experimental results. This chapter presents a brief summary of the present work followed by conclusions, major contributions and future scope for research.

6.1 Summary

6.1.1. Introduction

The major impact of industrial systems on the environment is the emission of gaseous, liquid and particulate materials in the atmosphere which leads to air pollution. The emissions include hazardous pollutants such as Volatile Organic Compounds (VOCs), ammonia (NH_3), hydrogen sulfide (H_2S), etc. along with other pollutant. VOCs are

released into the atmosphere from various process industries such as chemical, petrochemical, pharmaceutical, food processing, pulp and paper mills, color printing and coating, paint, rubber, fragrance, etc. The impact of a VOC on the environment depends upon the concentration and properties of individual compounds. The harmful effects of VOCs include the headache, nausea, dizziness, nose and throat discomfort, eye irritation, and allergic skin reaction. Certain studies have reported that several VOCs such as toluene, methyl ethyl ketone, methyl iso butyl ketone, isoprene, trichloroethylene, benzene and chloroform are carcinogenic in nature. It has also been found that the vast majority of VOCs have the potential to contribute to the global warming by absorbing infrared radiations. Hence there is a greater need to control the emissions of these harmful VOCs.

Various treatment methods that are used for the abatement of VOCs from wastewater streams include stripping, absorption, pervaporation, biodegradation, etc. The air pollution control techniques include thermal incineration, catalytic incineration, adsorption, absorption, condensation, membrane separation and biofiltration. Out of these methods, biodegradation and biofiltration are the cost efficient processes to control water and air pollution respectively.

Biodegradation, carried out using well acclimated culture, offers numerous advantages for the removal of toxic VOCs from wastewater streams. Biofiltration is a relatively new environmental pollution control technique where microbial biomass is static and the treated fluid is mobile. The performance of biofilter column depends on the selection of microbial culture, packing material, inlet load of VOCs, empty bed resistance time (EBRT), nutrient composition and its flow rate, temperature and moisture content.

The modeling carried out in such technique includes the estimation of growth kinetic constants using growth kinetic models such as Monod, Powell, Haldane, Luong, and Edward models and rate kinetic constants using rate kinetic models such as zero-order model and three-half-order model. The kinetic models such as Michaelis–Menten model, Ottengraf – Van den Oever model are used for the estimation of several biokinetic constants in order to understand the behavior of microorganisms in the biofiltration experiments. The generalized biofiltration models are developed for the prediction of concentration profiles with time and also useful in validating with the experimental data generated through the experiments.

6.1.2. Gaps in literature

The reported studies for the biodegradation of VOCs are limited to certain specific compounds such as phenol, trichlorophenol, dichlorophenol, benzene, toluene, xylene, dichlorobenzene, and trichloroethylene. Very few studies have reported the biodegradation of other widely used compounds such as methyl ethyl ketone, methyl isobutyl ketone, isopropyl alcohol, esters etc. These compounds are used as solvents in many industrial applications and are toxic in nature. The few experimental studies carried out for the biodegradation of these compounds are not sufficient to understand the mechanism of biodegradation. Past studies on biodegradation growth kinetics are mainly focused on Monod kinetic model which does not give the complete insight of the mechanism of biodegradation because it does not include the substrate inhibition effect. Some studies have reported the application of Haldane model which considers the effect of substrate inhibition. But it is not sufficient to explain the growth kinetics of all

compounds. Other substrate inhibition models such as Luong model and Edward model are not studied in the previous works.

The literature on biofiltration experimental studies suggested that very few researchers have carried out the biofiltration experiments (continuous column studies) for the removal of certain high priority toxic VOCs such as MEK, MIBK, IPA and ethyl acetate etc. Biofiltration experiments for these compounds are needed to understand the effect of significant parameters such as bed height, inlet load, and stability of the biofilter column. Biofiltration column studies are essential for the design of biofilter column at pilot plant scale as well as at an industrial scale.

The modeling of biofilter column is always considered to be quite challenging task as it incorporates the microbial degradation which is quite complex to understand. The existing literature on modeling of biofilter column point out good attempts have been made in understanding the modeling aspects of biofiltration column. Few studies have focused on the kinetic modeling (Michaelis–Menten model, Ottengraf – Van den Oever model, etc.) of biofilter column which is useful in the estimation of bio-kinetic constants that are required for the design of biofilter column. The mathematical models for biofiltration column, which are available in the literature, neglected some of the important physical aspects of biofiltration process. The effect of radial dispersion is excluded in several studies reported in the literature. The effect of gas biofilm resistances and the adsorption of VOCs on the uncovered portion of the packing material by biofilm have not been incorporated in the modeling of biofilter column. Because of the complexity of substrate inhibition growth kinetic models, most of the studies have

described the growth kinetics by the Monod model only in the modeling of biofiltration column.

6.1.3. Scope of work

There is a need to carry out the batch studies for the biodegradation of volatile organic compounds such as methyl ethyl ketone, methyl isobutyl ketone, isopropyl alcohol and esters in order to understand the mechanism of biodegradation. In this study, biodegradation experiments are performed in order to generate the data to obtain various growth kinetic models such as Monod, Haldane, Luong and Edward model. The obtained growth kinetic models help in understanding the behavior of microorganisms in degrading the VOCs.

There is a lot of scope to carry out the biofiltration column studies for the removal of organic pollutants such as methyl ethyl ketone, methyl isobutyl ketone, isopropyl alcohol and ethyl acetate by changing various parameters. The biofiltration experiments (column studies) are carried out to get an idea about the adaptability of the microorganisms in the changed operating conditions and thus obtaining the required removal efficiency. Such studies will thus help in the estimation of required parameters needed for the design of the biofilter column on pilot plant and on industrial scale.

The work also deals with the development of the Michaelis-Menten kinetic model and the Ottengraf-Van den Oever model from the biofiltration experiments carried out for the removal of methyl ethyl ketone, methyl isobutyl ketone, isopropyl alcohol and ethyl acetate for the estimation of biokinetic constants. The present work also includes the development of the mathematical model for the biofilter column incorporating the

limitations of the earlier studies. The performance of the developed model is tested with the available data from the literature and with the data generated in the present study.

6.1.4. Experimental studies

The acclimated culture is obtained for different VOCs using enrichment procedure. The biodegradation experiments are performed in a BOD incubator shaker. The experimental set-up is fabricated to perform the biofiltration experiments. The biodegradation studies are carried out for various VOCs such as MEK, MIBK, IPA, MA, EA, and BA and biofiltration studies are conducted using MEK, MIBK, IPA, and EA. The concentration of VOCs in liquid phase and gas phase are analyzed by gas chromatograph. The biomass concentration in liquid phase is measured in terms of optical density at 540 nm with respect to MSM using UV-VIS Spectrophotometer. The batch biodegradation experiments are conducted to study the effect of time on initial substrate concentration and biomass concentration. Continuous biofiltration experiments are carried out to see the performance and stability of biofiltration column under varying operating conditions.

6.1.5. Mathematical modeling and simulation

The biodegradation growth kinetic models explain the mechanism of biodegradation of the biological processes and predict the VOCs concentration in various treatment systems. The growth kinetic models such as Monod model (Monod 1949), Powell model (Powell 1967), Haldane model (Andrew 1968), Luong model (Luong 1986) and Edwards model (Edwards 1970) are reported in the literature and studied in the present work to explain the behavior of biodegradation process. The rate kinetics for the biodegradation of VOCs is demonstrated in the present study using zero-order and three-half-order kinetic models in order to understand the rates of growth, substrate utilization and

product formation. The kinetic behavior of biofilter system is described by Michaelis–Menten model and Ottengraf – Van den Oever model and the kinetic parameters are calculated to relate the kinetic behavior to the biodegradation rate kinetics.

During biofiltration process, various phenomena such as convection, dispersion, adsorption, diffusion and reaction affect the level of pollutant (VOC) removal. The mathematical model for the transient biofilter column proposed in this study describes transport, physical and biological processes that occur during biofiltration. In the present work, transient biofilter operated in periodic mode and continuous mode is considered. The proposed mathematical model incorporates the effects of gas biofilm resistances, possible extent of reaction in pores on biofilter, gas-phase mass transfer coefficient, and axial diffusion coefficient which are neglected in earlier studies considered for the modeling and simulation. The dimensionless form of mathematical modeling equations are solved numerically using explicit finite difference technique.

6.1.6. Results and discussion

In the following sections, the results obtained for batch and continuous experimental studies are summarized. This section discusses the kinetic modeling results estimated using Ottengraf-Van den Oever model. The simulated results which are obtained by validating the proposed mathematical model using literature data and obtained experimental data are also presented.

6.1.6.1. Batch studies

The rate of biodegradation studies are investigated for VOCs such as MEK, MIBK, IPA for the concentration range of 200 – 700 mg L^{-1} while the range for MA, EA and BA is

from 200 – 800 mg L^{-1}. The work is carried out for the parameters such as effect of time on initial concentration, effect of time on biomass concentration and specific growth rate. The concentration of VOCs is found decreasing with time which shows that the microbes consumed the VOCs as they utilize it as a carbon source. The increase in the initial VOCs concentration is attributed to the increase in lag time which delays the total time for biodegradation.

It is observed that the biomass concentration increases with time. The maximum value of biomass concentration is obtained as 0.5, 0.294, 0.155, 0.435, 0.45, and 0.465 g L^{-1} for MEK, MIBK, IPA, MA, EA, and BA at 400, 500, 400, 600, 500, and 500 mg L^{-1} of initial concentration respectively. The growth curve (biomass concentration versus time) obtained for all VOCs show the lag, log, stationary and decay phases.

The specific growth rate for different initial concentration of MEK, MIBK, IPA, MA, EA, and BA are estimated using the data obtained for log phase. The maximum value of specific growth rate is obtained as 0.391, 0.128, 0.210, 0.134, 0.137, and 0.141 h^{-1} for MEK, MIBK, IPA, MA, EA, and BA at 400, 600, 400, 600, 500, and 500 mg L^{-1} of initial concentration respectively.

Various theoretical models such as Monod kinetic model, Powell kinetic model, Haldane model, Luong model and Edwards model are used in the present study to express the growth kinetics of different VOCs. It is found that the substrate affinity constant (K_s) values obtained for MEK, MIBK, IPA, MA, EA, and BA using Powell model are 5.176, 2.344, 5.610, 15.674, 1.920, and 2.1741 mg L^{-1} which are quite lesser than the initial concentration of different VOCs (200 – 800 mg L^{-1}). This confirms the self inhibition effect for VOCs used in the present study. It is important to get an accurate

inhibition growth kinetic model to define the relationship between the specific growth rate and substrate concentration. The obtained results for different growth kinetic models indicate that the growth kinetics of acclimated mixed culture for biodegradation of MEK and IPA is better understood by Edward model but the biodegradation kinetics of MIBK, MA, EA, and BA are better described by Luong model. These results also show that the acclimated mixed culture can be used for the treatment of MEK, MIBK, IPA, MA, EA, and BA from effluent streams using biodegradation method.

The rate kinetic analysis is performed using zero-order and three-half-order kinetic models. The values obtained for coefficient of determination (R^2) for zero-order (0.929 – 0.999) and three-half-order kinetics (0.951 – 0.999) indicate that the three-half-order kinetic model is suitable to explain the biodegradation rate kinetics for different VOCs using acclimated mixed culture over a wide range of operating conditions. This may be due to the fact the three-half-order model incorporates an additional term for explaining the biomass formation during biodegradation of VOCs.

6.1.6.2. Continuous column studies

The biofiltration experiments are carried out using the matured coal and compost as the packing material and acclimated culture as the seeding culture for MEK, MIBK, IPA and EA. The operation time for biofilter column is 60, 60, 40, and 45 days for MEK, MIBK, IPA, and EA removal respectively. The operating conditions for the biofilter operation such as inlet concentration and air flow rate are varied during the entire biofilter operation. It is observed that the removal efficiency at the initial period of acclimation is low which further increases with time and reaches to more than 90% removal efficiency for VOCs used in the present study. The sudden change in the operating conditions of

biofilter column resulted in the sudden decrease in the removal efficiency. Further increase in operation time (2 – 3 days) with the same operating conditions, the steady state value of removal efficiency is achieved. The maximum steady state removal efficiencies obtained are 95%, 91.6%, 93.22% and 90.12 % for MEK, MIBK, IPA and EA respectively. The microbial concentration is found to increase in phases I to V for the removal of all the pollutants treated in the biofiltration process. The dynamics of biofiltration is understood by the measurement of normalized concentration profiles along the biofilter column height for MEK, MIBK, IPA and EA. It is observed that the decrease in normalized concentration is large for initial 50% height of the biofilter column but it is less in remaining height of the column. The increase in inlet VOCs concentration, C_{g0} / C_{gi} increase at the same height of biofilter column. This may be due to the fact that more amount of VOC is available for the same quantity of microbial culture in the column. The elimination capacity is found to be increasing with the increase in the inlet loads of MEK, MIBK, IPA and EA.

The industrial application of biofilter column is more justified when lab scale column undergoes sudden change in pollutant loads and response to such change in inlet loads is calculated in terms of removal efficiency of the biofilter column. The stability of the biofilter column is assessed by subjecting the column to shock loading conditions for a period of 16 days for MEK, 20 days for MIBK and 10 days for IPA and EA immediately after the 60 days of biofilter operation for MEK and MIBK, 40 days for IPA and 45 days for EA. The results of the shock loading conditions indicate that the biofilm developed in the biofilter is quite stable for all VOCs. It is noted that the better removal efficiency achieved for different VOCs during all phases show the stability of biofilter column and

thus substantiates the fact that biofiltration experiments can be successfully applied industrially where pollutant loads vary from lower to medium values. The trend of elimination capacity (utilization of VOCs) is found to be increasing with the increase in the inlet loads of MEK, MIBK, IPA and EA which confirms the applicability of biofilter column for the removal of VOCs in industrial operations.

This study includes the estimation of kinetic constants using Michaelis–Menten kinetic model. The steady state value (final data point) for each phase of all VOCs is taken for the evaluation of kinetic constants. The obtained values of kinetic constants such as maximum degradation rate per unit filter volume (r_{max}) are 0.086, 0.115, 0.11, and 0.092 g m^{-3} h^{-1} and the saturation constant (K_S) are 0.577, 1.046, 1.226, and 1.061 g m^{-3} for MEK, MIBK, IPA, and EA respectively. It is observed that the values of K_S are comparable with inlet concentration ranges of MEK (0.151 – 1.514 g m^{-3}), MIBK (0.07 – 0.73 g m^{-3}), IPA (0.04 – 0.365 g m^{-3}), and EA (0.05 – 0.24 g m^{-3}). This indicates the applicability of zero-order kinetics with diffusion limitation (Ottengraf-Van den Oever model) as the most appropriate biodegradation kinetic model.

The Ottengraf-Van den Oever model (Eq. 4.24) is validated with the obtained experimental data during steady state operation for all the phases except for the acclimation phase (Phase I) of MEK, MIBK, IPA, and EA removal. The predicted model results for elimination capacity are plotted with the experimentally calculated elimination capacity values at different phases with inlet loads for MEK, MIBK, IPA, and EA removal. The standard deviation (s.d.) values are found in the range of 3.004 – 7.66 for MEK, 1.945 – 4.815 for MIBK, 1.734 – 2.541 for IPA, and 2.137 – 2.37 for EA which confirms the suitability of Ottengraf-Van den Oever model to explain the kinetic behavior

of biofilter column. The biofilm thickness is calculated using obtained constant values for MEK, MIBK, IPA, and EA are ranging from 384 – 656 µm, 410.67 – 570.8 µm, 17.99 – 29.5 µm, and 2.137 – 2.67 µm respectively.

6.1.6.3. Mathematical modeling and simulation

Mathematical models are developed for the transient biofilter operated in periodic and continuous modes that describe the results in the form of breakthrough curves, which represent the outlet VOCs concentration at different times based on different operating conditions. The applicability of proposed mathematical models for transient biofilter is confirmed by comparing the experimental and modeling results reported by Chmiel et al. (2005). The standard deviation for MEK and butanol are obtained as 0.00242 and 0.000537 for the present model of periodic mode operated biofilter and 0.00414 and 0.002187 for Chmiel et al. (2005) model respectively, which are less as compared to the model represented by Chmiel et al (2005). The simulations results are obtained to understand the influence of various important parameters such as inlet VOC concentration, bed height and gas velocity on the biofilter column performance operated in the periodic mode.

A generalized mathematical model is proposed for the transient biofilter operated in continuous mode which incorporates the effects of gas biofilm resistances, possible extent of reaction in pores on biofilter, gas-phase mass transfer coefficient, and axial diffusion coefficient. The calculated standard deviation values are in the range of 0.0365 – 0.0614 for the modeling results obtained by Chmiel et al. (2005) and 0.0098 – 0.1193 for the model proposed in the present study. This indicates that the proposed

model of this study fits the experimental data better than the model reported by Chmiel et al. (2005) at all operating conditions.

6.2. Conclusions

Based on the results obtained in the present study, the following conclusions are drawn:

1. The batch biodegradation studies for the removal of MEK, MIBK, IPA, BA, EA and MA are important for understanding the related design aspects.
2. The rate of biodegradation is greatly affected by the initial concentration of VOCs.
3. All compounds are completely consumed by the microorganisms in the biodegradation studies and obtained growth curves show the lag, log, stationary and decay phases.
4. With an increase in the initial concentration of VOCs, the time taken by microorganisms for fully degradation of VOCs increases due to the self inhibition effect of the compounds.
5. At higher initial concentration of VOCs, there is an increase in the lag phase.
6. The increase in biomass concentration with respect to time is exponential during log phase duration.
7. The maximum value of specific growth rate is obtained as 0.391, 0.128, 0.210, 0.134, 0.137, and 0.141 h^{-1} for MEK, MIBK, IPA, MA, EA, and BA at 400, 600, 400, 600, 500, and 500 mg L^{-1} of initial concentration respectively.

8. It is found that the substrate affinity constant (K_s) values obtained for all VOCs using Monod and Powell models are quite lesser than the initial concentration of different VOCs which confirms the self inhibition effect for VOCs.
9. Upon testing the experimental data with the various inhibition models such as Haldane, Luong, and Edwards model, it is obtained that the growth kinetics of acclimated mixed culture for biodegradation of MEK and IPA is better explained by Edward model but the biodegradation kinetics of MIBK, MA, EA, and BA are better described by Luong model.
10. The higher value obtained for critical inhibitor concentration for all VOCs used in the present study indicated that the higher efficiency of the microbial culture to grow in the presence of VOCs.
11. Biodegradation rate kinetics using zero-order and three-half-order kinetic models are tested with rate kinetic data and three-half-order kinetic model is found suitable for the biodegradation of VOCs used in the present study.
12. The effects of time in the biofilter performance for different values of operating parameters such as inlet VOC concentration, air flow rate, and shock loading is studied for MEK, MIBK, IPA and EA.
13. The maximum steady state removal efficiencies are obtained as 95%, 91.6%, 93.22% and 90.12 % for MEK, MIBK, IPA and EA respectively.
14. The results obtained establish the fact that the biofilter performed well for lower to medium inlet loads of MEK, MIBK, IPA and EA.
15. The elimination capacity is found to increase with the increase in the inlet load for all VOCs studied.

16. It is found that the decrease in normalized concentration is large for initial 50% height of the biofilter column but it is less in the remaining height of the column.
17. The results of the shock loading conditions indicate that the biofilm developed in the biofilter is quite stable for all VOCs.
18. The biokinetic constants are estimated using the Michaelis–Menten kinetics for the obtained results in biofiltration studies and the values of K_S are observed comparable with inlet concentration ranges of VOCs which indicates the applicability of zero-order kinetics with diffusion limitation (Ottengraf-Van den Oever model) as the most appropriate biodegradation kinetic model.
19. The obtained experimental results for biofiltration studies are validated with the Ottengraf-Van den Oever model and important design parameters such as critical inlet concentration, critical inlet load and biofilm thickness are found from the model predictions.
20. The mathematical model for periodic mode operated biofilter proposed in the present study (s.d. = 0.00242 and 0.000537 for MEK and butanol respectively) is found suitable for explaining the dynamic behavior of biofilter column as compared to the model proposed by Chmiel et al. (2005) (s.d. = 0.00414 and 0.002187 for MEK and butanol respectively).
21. The obtained simulation results indicate that the important parameters such as inlet VOC concentration, bed height and gas velocity have significant influence on the biofilter column performance operated in the periodic mode.
22. A generalized mathematical model proposed for the transient biofilter operated in continuous mode by incorporating the effects of gas biofilm resistances, possible

extent of reaction in pores on biofilter, gas-phase mass transfer coefficient, and axial diffusion coefficient, fits the experimental data (s.d. = 0.0365 – 0.0614) better than the model reported by Chmiel et al. (2005) (s.d. = 0.0098 – 0.1193) at all operating conditions.

6.3. Major contributions

1. Exhaustive batch biodegradation experiments are conducted for MEK, MIBK, IPA, BA, EA and MA removal for a wide range of initial concentration to check the applicability of biodegradation process for the removal of these compounds from industrial effluent streams.
2. The obtained biodegradation results for MEK, MIBK, IPA, BA, EA and MA are fitted with the growth kinetic models such as Monod, Powell, Haldane, Luong and Edwards unlike most of the studies where Monod and Haldane models dominates the description.
3. The biofilter column experiments are performed for the removal of MEK, MIBK, IPA, and EA under different operating conditions and results obtained at different phases are analyzed in terms of removal efficiency and elimination capacity.
4. The stability of the biofilter column is assessed by subjecting the column to shock loading conditions for all the four VOCs showing that the column can be used in industrial practice where the inlet load varies.
5. The Michaelis-Menten kinetic constants are estimated and Ottengraf-Van den Oever model is validated with the obtained experimental data during steady state operation for MEK, MIBK, IPA and EA removal.

6. The biofilm thickness is predicted using Ottengraf-Van den Oever model for MEK, MIBK, IPA and EA degradation at different operating conditions which is not reported in the previous studies.
7. A generalized mathematical model is developed for the transient biofilter operated in continuous mode which incorporates the limitation of earlier studies such as effects of gas biofilm resistances, possible extent of reaction in pores on biofilter, gas-phase mass transfer coefficient, and axial diffusion coefficient and validated with experimental results and modeling results reported in the literature.

6.4. Future scope

The future scope of this work is enumerated below:

1. The batch biodegradation studies can be carried out for the other VOCs such as benzene, toluene, xylene, butanol, etc. and it can be extended to the inorganic compounds such as heavy metals, hydrogen sulfide, etc.
2. The batch biodegradation studies can be performed to see the effect of other influencing parameters such as pH, concentration of nutrients, etc.
3. The biofiltration experiments can be conducted to study the effect of other important parameters such as pH, concentration of nutrients, particle size of packing materials, etc.
4. The proposed mathematical model for the transient biofilter can be further improved by incorporating the variation of velocity along the biofilter column length.

5. The biofiltration experimental studies and mathematical model proposed in the present work can also pave the way for designing the biofilter column for the pilot plant studies, and subsequently to the industrial scale operation.

REFERENCES

Abuhamed, T., Bayraktar, E., Mehmetoglu, T., Mehmetoglu, U., 2004. Kinetics model for the growth of *Pseudomonas putida* F1 during benzene, toluene and phenol biodegradation. Process Biochemistry, 39, 983–988.

Abumaizar, R. J., Kocher, W., Smith E.H., 1998. Biofiltration of BTEX contaminated streams using compost-activated carbon filter media. Journal of Hazardous Materials, 60, 111-126.

Acuna, M.E., Villanueva, C., Cardenas, B., Christen, P., Revah, S., 2002. The effect of nutrient concentration on biofilm formation on peat and gas phase toluene biodegradation under biofiltration conditions. Process Biochemistry, 38. 7-13.

Agarwal, G.K., Ghoshal, A.K., 2008. Packed bed dynamics during microbial treatment of wastewater: Modelling and simulation. Bioresource Technology, 99, 3765-3773.

Alvarez-Hornos, J., Gabaldon, C., Martınez-Soria, V., Martın, M., Marzal, P., Penya-roja, J.M., 2008. Biofiltration of ethylbenzene vapors: Influence of the packing material. Bioresource Technoogy, l99, 269-276.

Amanullah, M., Viswanathan, S., Farooq, S., 2000. Equilibrium, Kinetics, and Column Dynamics of Methyl Ethyl Ketone Biodegradation. Industrial Engineering and Chemistry Research, 39, 3387-3396.

Andreoni, V., Baggi, M., Cavalca, M., Zangrossi, M., Bernasconi, S. 1998. Degradation of 2,4,6-trichlorophenol by a specialized organism and by indigenous soil microflora: bioaugmentation and self-remediability for soil restoration. Letters in Applied Microbiology, 27, 86–92.

Andrews, J.F., 1968. A mathematical model for the continuous culture of microorganisms utilizing inhibitory substance. Biotechnology and Bioengineering, 10, 707-723.

Aranda, C., Godoy, F., Becerra, J., Barra, R., Martinez, M., 2003. Aerobic secondary utilization of a non-growth and inhibitory substrate 2,4,6-trichlorophenol by *Sphingopyxis chilensis* S37 and *Sphingopyxis*-like strain S32. Biodegradation. 14, 265–274.

Arulneyam, D., Swaminathan, T., 2000. Biodegradation of ethanol vapors in a biofilter. Bioprocess Engineering, 22, 63-70.

Atoche, J. C., Moe, W. M., 2004. Treatment of MEK and Toluene Mixtures in Biofilters: Effect of Operating Strategy on Performance During Transient Loading. Biotechnology and Bioengineering, 86, 468-481.

Auria, R., Frere, G., Morales, M., Acuna, M. E., Revah, S., 2000. Influence of mixing and water addition on the removal rate of toluene vapors in a biofilter. Biotechnology & Bioengineering, 68, 448-455.

Babu, B.V., Chaurasia, A.S., 2003a. Modeling for Pyrolysis of Solid Particle: Kinetics and Heat Transfer Effects. Energy Conversion and Management, 44, 2251-2275.

Babu, B.V., Chaurasia, A.S., 2003b. Modeling, Simulation, and Estimation of Optimum Parameters in Pyrolysis of Biomass. Energy Conversion and Management, 44, 2135-2158.

Babu, B.V., Chaurasia, A.S., 2004a. Dominant Design Variables in Pyrolysis of Biomass Particles of Different Geometries in Thermally Thick Regime. Chemical Engineering Science, 59, 611-622.

Babu, B.V., Chaurasia, A.S., 2004b. Heat Transfer and Kinetics in the Pyrolysis of Shrinking Biomass Particle. Chemical Engineering Science, 59, 1999-2012.

Babu, B.V., Chaurasia, A.S., 2004c. Parametric Study of Thermal and Thermodynamic Properties on Pyrolysis of Biomass in Thermally Thick Regime. Energy Conversion and Management, 45, 53-72.

Babu, B.V., Chaurasia, A.S., 2004d. Pyrolysis of Biomass: Improved Models for Simultaneous Kinetics & Transport of Heat, Mass, and Momentum. Energy Conversion and Management, 45, 1297-1327.

Babu, B.V., Gupta, S., 2005. Modeling and Simulation of Fixed Bed Adsorption Column: Effect of Velocity Variation. Journal on Engineering & Technology, 1, 60-66.

Babu, B.V., Sheth, P.N., 2006. Modeling and Simulation of Reduction Zone of Downdraft Biomass Gasifier: Effect of Char Reactivity Factor. Energy Conversion and Management, 47, 2602-2611.

Banerjee, I., Modak, J.M., Bandopadhyay, K., Das, D., Maiti, B.R., 2001. Mathematical model for evaluation of mass transfer limitations in phenol biodegradation by immobilized Pseudomonas putida. Journal of Biotechnology, 87, 211–223.

Bates, J., Cadman, J., Holland, M., 2003. Environmental burden measures for air: global warming, stratospheric ozone depletion, photochemical ozone creation and airborne acidification. EA R&D Technical Report P6-015/TR2.

Bibeau, L., Kiared, K., Brzezinski, R., Viel, G., Heitz, M., 2000. Treatment of air polluted xylenes using a biofilter reactor. Water, Air, and Soil Pollution, 118, 377-393.

Bridie AL, Wolff M & Winter CJM (1979) BOD and COD of some petrochemicals. Water Res. 13: 627–630.

Brunner, W., Focht, D.D., 1984. Deterministic three-half order kinetic model for microbial degradation of added carbon substrates in soil. Applied and Environmental Microbiology. 47, 1211-1216.

Buitron, G., Gonzalez, A., 1996. Characterization of the microorganisms from an acclimated activated sludge degrading phenolic compounds. Water Science and Technology, 34, 289–294.

Buitron, G., Gonzales, A., Lopez-Marin, L.M., 1998. Biodegradationof phenolic compounds by an acclimated activated sludge and isolated bacteria. Water Science and Technology, 37, 371–378.

Cai, Z., Kim, D., Sorial, G.A., 2004. Evaluation of trickle-bed air biofilter performance for MEK removal. Journal of Hazardous Materials, 114, 153-158.

Chan, W. C., Peng, K. H., 2008. Biofiltration of ketone compounds by a composite bead biofilter. Bioresource Technology, 99, 3029-3035.

Chan, W. C., Su, M. Q., 2008. Biofiltration of ethyl acetate and amyl acetate using a composite bead biofilter. Bioresource Technology, 99, 8016-8021.

Chang, K., Lu, C., 2003. Biofiltration of isopropyl alcohol and acetone mixtures by a trickle bed air biofilter. Process Biochemistry, 39, 415-423.

Chang, K., Lu, C., Lin, M. R., 2001. Treatment of Volatile Organic Compounds from Polyurethane and Epoxy Manufacture by a Trickle-Bed Air Biofilter. Journal of Bioscience Bioengineering, 92, 126-130.

Chmiel, K., Konieczny, A., Palica, M., Jarzebski, A. B., 2005. Periodic Operation of biofilters. A concise model and experimental validation. Chemical Engineering Science, 2005, 2845-2850.

Clean Air Act Amendment (CAAA), To amend the Clean Air Act to provide for attainment and maintenance of health protective national ambient air quality standards, and for other purposes. 101st CONGRESS, 2nd Session, S. 1630 USA, (1990).

Cohen, Y., 2002. Biofiltration – the treatment of fluids by microorganisms immobilized into the filter bedding material: a review. Bioresource Technology, 77, 257-274.

Cox, H. H. J., Sexton, T., Shraeefdeen, Z, Deshusses, M., 2001. Thermophilic Biotrickling Filtration of Ethanol Vapors. Environmental Science and Technology 35, 2612-2619.

Cussler, E. L., 1997. Diffusion: mass transfer in fluid systems. 2nd edition, Cambridge University Press, United Kingdom.

Charter on Corporate Responsibility for Environmental Protection (CREP), 2003. Development of Minimal National Standards (MINAS) for Rubber products Manufacturing Industries. CPCB India.

Dapena-Mora A., Fern´andez, I., Camposa, J.L., Mosquera-Corral, A., M´endez, R., Jetten, M.S.M., 2007. Evaluation of activity and inhibition effects on Anammox process by batch tests based on the nitrogen gas production. Enzyme and Microbial Technology 40, 859–865.

Dehghanzadeh, R., Torkian, A., Bina, B., Poormoghaddas, H., Kalantary, A., 2005. Biodegradation of styrene laden waste gas stream using a compost-based biofilter. Chemosphere**,** 40, 434–439.

Delhomenie, M. C., Bibeau, L., Bredin, N., Roy, S., Broussau, S., Brzezinski, R., Kugelmass, J. L., Heitz, M., 2002. Biofiltration of air contaminated with toluene on a compost-based bed. Advances in Environmental Research, 6, 239-254.

Den, W., Pirbazari, M., 2002. Modeling and design of vapor-phase biofiltration for chlorinated volatile organic compounds. AIChE Journal, 48, 2084-2103.

Derwent, R. G., Nelson, N., 2002. Development of a reactivity index for the control of the emissions of organic compounds. EA R&D Technical Report P4-105 RC8309.

Deshusses, M. A., 1994. Biodegradation of mixtures of ketone vapours in biofilters for the treatment of waste air. Ph D Thesis, Swiss Federal Institute of Technology, Zurich, Switzerland.

Deshusses, M. A., Hamer, G, Dunn, I. J., 1995a. Behavior of Biofilters for Waste Air Biotreatment. 1. Dynamic Model Development. Environmental Science & Technology, 29, 1048-1058.

Deshusses, M. A., Hamer, G, Dunn, I. J., 1995b. Behavior of Biofilters for Waste Air Biotreatment. 2. Experimental evaluation of a Dynamic Model. Environmental Science & Technology, 29, 1059-1068.

Devinny, J. S., Deshusses, M. A., Webster, T. S., 1999. Biofiltration for air pollution control. Lewis Publishers, CRC Press.

Dwyer, D. F., Krumme, M. L., Boyd, S. A., Tiedje, J. M., 1986. Kinetics of phenol biodegradation by an immobilized methanogenic consortium. Applied and Environmental Microbiology, 52, 345-351.

Edwards, V.H., 1970. The influence of high substrate concentrations on microbial kinetics. Biotechnology and Bioengineering, 12, 679-712.

Folsom, B.R., Chapman, P.J., Pritchard, P.H., 1990. Phenol and Trichloroethylene Degradation by *Pseudomonas cepacia* G4: Kinetics and Interactions between Substrates. Applied and Environmental Microbiology, 56, 1279-1285.

Fortin, N.Y., Deshusses, M.A., 1999. Treatment of Methyl tert- Butyl Ether Vapors in Biotrickling Filters. 2. Analysis of the Rate-Limiting Step and Behavior under Transient Conditions. Environmental Science & Technology, 33, 2987-2991.

Kotturi, G., Robinson, C.W., Inniss, W.E. 1991. Phenol degradation by a psychrotrophic strain of *Pseudomonas putida*, Applied Microbiology and Biotechnology, 34, 539–543.

Geoghegan, D.P., Hamer, G., Dehusses, M.A., 1997. Effects of unsteady state conditions on the biooxidation of methyl ethyl and methyl isobutyl ketone in continuous flow liquid phase cultures. Bioprocess Engineering, 16, 315-322.

Goudar, C., Strevett, K., Grego. J., 1999. Competitive substrate biodegradation during surfactant-enhanced remediation. Journal of Environmental Engineering, 125, 1142-1148.

Goudar, C.T., Delvin, J.F., 2001. Nonlinear estimation of microbial and enzyme kinetic parameters from progress curve data. Water Environment Research. 73, 260-265.

Gupta, S., Babu, B.V., 2009. Modeling, simulation, and experimental studies for continuous Cr(VI) removal from aqueous solutions using sawdust as an adsorbent. Bioresource Technology, 100, 5633-5640.

Hinwood, A.L., Berko H. N., Farrar, D., Galbally, I.E., Weeks, I.A., 2006. Volatile organic compounds in selected micro-environments, Chemosphere, 63, 421–429.

Ho, K.L., Chung, Y.C., Lin, Y.H., Tseng, C. P., 2008. Biofiltration of trimethylamine, dimethylamine, and methylamine by immobilized *Paracoccus sp*. CP2 and *Arthrobacter sp*. CP1. Chemosphere, 72, 250–256.

Hodge, D., Devinny, J., 1995. Modeling removal of air contaminants by biofiltration. Journal of Environmental Engineering, 121, 21-32

Hwang, S. C. J., Lee, C.M., Lee, H. C., Pua, H. F., 2003. Biofiltration of waste gases containing both ethyl acetate and toluene using different combinations of bacterial cultures. Journal of Biotechnology, 105, 83-94.

Kanaly, R.A., Harayama, S., 2000. Biodegradation of High-Molecular-Weight Polycyclic Aromatic Hydrocarbons by Bacteria. Journal of Bacteriology, 182, 2059-2067.

Kim, J.H., Oh, K.K., Lee, S.T., Kim, S.W., Hong, S.I., 2002. Biodegradation of phenol and chlorophenols with defined mixed culture in shake-flasks and a packed bed reactor. Process Biochemistry. 37, 1367–1373.

Kim, J.H., Rene, E.R., Park, H., 2008. Biological oxidation of hydrogen sulfide under steady and transient state conditions in an immobilized cell biofilter. Bioresource Technology, 99, 583-588.

Kirk-Othmer, 2005. Encyclopedia of Chemical Technology. 5th Edition, Volume 2-14, John Wiley & Sons, Newyork.

Klecka, M., Maier, W. J., 1985. Kinetics of Microbial Growth on Pentachlorophenol. Applied and Environmental Microbiology, 49, 46-53.

Kumar, A., Kumar, S., Kumar, S., 2005. Biodegradation kinetics of phenol and catechol using *Pseudomonas putida* MTCC 1194. Biochemical Engineering Journal, 22, 151–159.

Kumaran, P., Paruchuri, Y.L., 1996. Kinetics of phenol biotransformation. Water Research 31, 11–22.

Larson, R.J., 1980. Role of biodegradation kinetics in predicting environmental fate. In: A Maiki AW, Dickson KL, Cairns J Jr (Eds) Biotransformation and the fate of chemicals in the aquatic environment. American Society for Microbiology, Washington, DC, pp. 67 – 86.

Liu, Y., Quan, X., Sun, Y., Chen, J., Xue, D., Chung, J. K., 2002. Simultaneous removal of ethyl acetate and toluene in air streams using compost-based biofilters. Journal of Hazardous Materials, B95, 199-213.

Lodge, J. P., 1989. Methods of Air Sampling and Analysis, Lewis Publishing Inc., New York.

Lu, C., Chang, K., Hsu, S., Lin, J., 2004. Biofiltration of butyl acetate by a trickle-bed air biofilter. Chemical Engineering Science, 59, 99-108.

Luong, J.H.T., 1986. Generalization of monod kinetics for analysis of growth data with substrate inhibition. Biotechnology and Bioengineering, 29, 242-248.

Mackay, D., Wan, S.Y., Kuo, M.C., 1990. Illustrated Handbook of Physical-chemical Properties and Environmental Fate for Organic Chemicals. Vol. III., Lewis Publishers, USA.

Martin, M. A., Keuning S., Janssen, D.B., 1998. Handbook on biodegradation and biological treatment of hazardous organic compounds, 2nd ed., Dordrecht, Academic Press.

Mathur, A.K., Majumder, C.B., 2008. Biofiltration and kinetic aspects of a biotrickling filter for the removal of paint solvent mixture laden air stream. Journal of Hazardous Materials. 152, 1027–1036.

Mathur, A.K., Mazumder, C.B., Chatterjee, S., 2007. Combined removal of BTEX in air stream by using mixture of sugar cane bagasse, compost and GAC as biofilter media, Journal of Hazardous Materials, 148, 64–74.

Moe, W.M., Irvine, R.L., 2001. Effect of nitrogen limitation on performance of Toluene degrading biofilters. Water Research, 35, 1407-1414.

Monod, J., 1949. The growth of bacterial cultures. Annual Review of Microbiology 3, 371–394.

Monteiro, A.A.M.G., Boaventura, R.A.R., Rodrigues, A.E., 2000. Phenol biodegradation by Pseudomonas putida DSM 548 in a batch reactor. Biochemical Engineering Journal 6, 45–49.

Murata, M., Tsujikawa, M., Kawanishi, S.,1999. Oxidative DNA damage by minor metabolites of toluene may lead to carcinogenesis and reproductive dysfunction. Biochemical and Biophysical Research Communications, 261, 478–483.

Neal, A.B., Loehr, R.C., 2000. Use of biofilters and suspended-growth reactors to treat VOCs. Waste Management, 20, 59-68.

Nelson, M.J.K., Montgomery, S.O., Neill, E.J., Pritchard, P.H., 1986. Aerobic metabolism of trichloroethylene by a bacterial isolate. Applied and Environmental Microbiology. 52, 383-384.

Nweke, C. O., Okpokwasili, G. C., 2003. Drilling fluid base oil biodegradation potential of a soil *Staphylococcus* species. African Journal of Biotechnology, 2, 293-295.

Oh, Y.S., Choi, S.C., Kim, Y.K., 1998. Degradation of gaseous BTX by biofiltration with Phanerochaete chrysosporium. Journal of Microbiology, 36, 34-38.

Okpokwasili, G.C., Nweke, C.O., 2005. Microbial growth and substrate utilization kinetics. African Journal of Biotechnology, 5, 305-317.

Ottengraf, S. P. P., 1986. Exhaust gas purification. Biotechnology. 8, 425-452

Ottengraf, S.P.P., Van den Oever, A.H.C., 1983. Kinetics of organic compound removal from waste gases with a biological filter. Biotechnology and. Bioengineering. 25, 3089–3102.

Kumaran, P., Paruchuri, Y.L., 1997. Kinetics of phenol biotransformation. Water Research. 31, 11–22.

Paris D.F., Steen, W.C., Baughman, G.L.,Barnett J.T,Jr., 1981. Second-order model to predict microbial degradation of organic compounds in natural waters. Applied and Environmental Microbiology, 41, 603-609.

Park, O.H., Park, S.H., Han, J.H., 2004. Model Study Based on Experiments on Toluene Vapor Removal in a Biofilter. Journal of Environmental Engineering. 130, 1118-1125.

Pettigrew, C.A., Haigler, B.E., Spain, J.C., 1991. Simultaneous Biodegradation of Chlorobenzene and Toluene by a Pseudomonas Strain. Applied and Environmental Microbiology, 57, 157-162.

Peyton, B.M., Wilson, T., Yonge, D.R., 2002. Kinetics of phenol biodegradation in high salt solutions. Water Research. 36, 4811-4820.

Powell, E. O., 1967. The growth rate of microorganisms as function of substrate concentration. Microbial physiology and continuous culture. Evans CGT, Strange RE, Tempest W Edition, HMSO, London, United Kingdom.

Price, K.S., Waggy, G.T., Conway, R.A., 1974. Brine shrimp bioassay and seawater BOD of petrochemicals. Journal of the Water Pollution Control Federation. 46, 63–77.

Qi, B., Moe, W. M., Kinney, K. A., 2002. Biodegradation of volatile organic compounds by five fungal species. Applied Microbiology & Biotechnology. 58, 684-689.

Quan, X., Shi, H., Wang, J., Qian, Y., 2003. Biodegradation of 2,4-dichlorophenol in sequencing batch reactors augmented with immobilized mixed culture. Chemosphere, 50, 1069-1074.

Quesnel, D., Nakhla, G., 2006. Removal kinetics of acetone and MIBK from a complex industrial wastewater by an acclimated activated sludge. Journal of Hazardous Materials, B132, 253-260.

Reardon, K. F., Mosteller, D. C., Rogers, J. D. B., 2000. Biodegradation kinetics of benzene, toluene, and phenol as single and mixed substrates for *Pseudomonas putida* F1. Biotechnology and Bioengineering, 69, 385-400.

Rene, E. R., Swaminathan, T., 2007. Biological treatment systems for VOC removal. Chemical Weekly, 195-202.

Rene, E. R., Murthy, D.V.S., Swaminathan, T., 2005. Performance evaluation of a compost biofilter treating toluene vapours. Process Biochemistry, 40, 2771–2779.

Report on proposed national emission standards for petrochemical plants, CPCB India, 2007.

Rihn, J.M., Zhu, X., Suidan, M.T., Kim, B.J., Kim, B.R., 1997. The Effect of nitrate on VOC removal in Trickle Bed Air Biofilters. Water Research, 31, 2997-3008.

Robinson, J.A., Tiedje, J.M., 1983. Non linear estimation of Monod growth kinetic parameters from a single substrate depletion curve. Applied Environmental Microbiology, 45, 1453-1458.

Saravanan, P., Pakshirajan, K., Saha, P., 2008. Growth kinetics of an indigenous mixed microbial consortium during phenol degradation in a batch reactor. Bioresource Technoogy, 99, 205-209.

Sahinkaya, E., Dilek, F. B., 2007. Biodegradation kinetics of 2, 4-dichlorophenol by acclimatized mixed cultures. Journal of Biotechnology, 127, 716-726.

Shareefdeen, Z., Baltzis, B. C., 1994. Biofiltration of toluene vapor under steady state and transient conditions: theory and experimental results. Chemical Engineering Science, 49, 4347.

Snape, J. B., Dunn, I. J., Ingham, J., Prenosil, J. E., 2005. Dynamics of Environmental Bioprocesses. Modelling and Simulation, VCH Publications. Federal Republic of Germany.

Snyder, C. J. P., Asghar, M., Scharer, J. M., Legge, R. L., 2006. Biodegradation kinetics of 2, 4, 6-Trichlorophenol by an acclimated mixed microbial culture under aerobic conditions. Biodegradation.17, 535-544.

Sokol, W., 1986. Oxidation of an inhibitory substrate by washed cells (oxidation of phenol by *Pseudomonas putida*). Biotechnology and Bioengineering, 30, 921-927.

Spigno, G., Pagella, C., Fumi, M. D., Molteni, R., Faveri, D. M. D., 2003. VOCs removal from waste gases: gas-phase bioreactor for the abatement of hexane by *Aspergillus Niger*. Chemical Engineering Science, 58, 739-746.

Taghipour, H., Shahmansoury, M. R., Bina B., Movahdian, H., 2008. Operational parameters in biofiltration of ammonia-contaminated air streams using compost–pieces of hard plastics filter media. Chemical Engineering Journal, 137, 198–204.

Tang, W.T., Fan, L.S., 1987. Steady state phenol degradation in a draft tube gas-liquid-solid fluidized bed bioreactor. AIChE J, 33, 239 –249.

Tomei, M.C., Annesini, M.C., Bussoletti, S., 2004. 4-Nitrophenol biodegradation in a sequencing batch reactor: kinetic study and effect of filling time. Water Research, 38, 375-384.

US EPA, Guidance for Estimating Ambient Air Monitoring Costs for Criteria Pollutants and Selected Air Toxic Pollutants. EPA-454/R-93-042, 1993.

US EPA, Control and pollution prevention options for ammonia emissions, EPA-456/R-95-002, 1995.

Van Lith, C., David, S. L., Marsh, R., 1990. Design criteria for biofilters. Process Safety and Environmental Protection. 68, 127–132.

Wright, W. F., 2005. Transient response of vapor-phase biofilters. Chemical Engineering Journal, 113, 161-173.

Yoon, I. K., Park, C. H., 2002. Effects of Gas Flow Rate, Inlet Concentration and Temperature on Biofiltration of Volatile Organic Compounds in a Peat-Packed Biofilter. Journal of Bioscience Bioengineering, 93, 165-169.

Zarook, S. M., Shaikh, A. A., Ansar, Z., 1996. Development, experimental validation and dynamic analysis of a general transient biofilter model. Chemical Engineering and Science, 52, 759-773.

World Health Organization, Methyl Isobutyl Ketone. Environmental Health Criteria 117, World Health Organization, Geneva, Switzerland, (1990), pp. 79.

World Health Organization, Methyl Ethyl Ketone. Environmental Health Criteria 14 , World Health Organization, Geneva, Switzerland, (1993), pp. 161.

LIST OF PUBLICATIONS

International Journals

1. Babu, B.V., Raghuvanshi, S., 2006. Simulation Studies on Transient Model for Biofilter operated in Periodic Mode. Journal on Engineering and Technology, 1, 72-76.
2. Raghuvanshi, S., Babu, B.V., 2009. Experimental Studies and Kinetic Modeling for Removal of Methyl Ethyl Ketone using Biofiltration. Bioresource Technology, 100, 3855 – 3861.
3. Raghuvanshi, S., Babu, B.V., 2010. Biodegradation kinetics of methyl iso-butyl ketone (MIBK) by acclimated mixed culture. Biodegradation, 21, 31 – 42.
4. Raghuvanshi, S., Babu, B.V., 2010. Biofiltration for removal of Methyl Iso Butyl Ketone (MIBK): Experimental Studies and Kinetic Modeling. Environmental Technology, 31, 29 – 40.
5. Raghuvanshi, S., Babu, B.V., 2009. Biodegradation of iso-propyl alcohol (IPA) using acclimated mixed culture: Growth and rate kinetic models. Communicated. International Journal of Environment and Waste Management.
6. Raghuvanshi, S., Babu, B.V., 2009. Growth kinetic models for the biodegradation of methyl ethyl ketone (MEK) using acclimated mixed culture. Communicated. Chemical Engineering & Technology.
7. Raghuvanshi, S., Babu, B.V., 2009. Biodegradation of esters (methyl acetate, ethyl acetate, and butyl acetate): Experimental and kinetic studies. To be communicated.
8. Raghuvanshi, S., Babu, B.V., 2009. Isopropyl aclochol (IPA) removal using biofiltration: Experimental Studies and Kinetic Modeling. To be communicated.
9. Raghuvanshi, S., Babu, B.V., 2009. Biofiltration and kinetic aspects of biofilter column for the removal of ethyl acetate (EA). To be communicated.

International Conference Proceedings

1. Babu, B.V., Raghuvanshi, S., 2004. Biofiltration for VOC Removal: A State-of-the-art Review. Proceedings of International Symposium & 57th Annual Session of IIChE in association with AIChE (CHEMCON-2004), Mumbai, December 27-30, 2004.
2. Raghuvanshi, S., Babu, B.V., 2005. Modeling and Simulation of Trickle Bed Air Biofilter for Removal of VOCs. Proceedings of International Symposium & 58th Annual Session of IIChE in association with International Partners (CHEMCON-2005), New Delhi, December 14-17, 2005.

3. Raghuvanshi, S., Babu, B.V., 2005. Modeling and Simulation of Biofilters Operated in Periodic Mode. Proceedings of International Congress Chemistry and Environment (ICCE-2005), Indore, December 24-26, 2005, pp. 387-390, 2005.
4. Raghuvanshi, S., Babu, B.V., 2006. Biofiltration for the Removal of Methyl Isobutyl Ketone (MIBK). Proceedings of International Symposium & 59th Annual Session of IIChE in association with International Partners (CHEMCON-2006), GNFC Complex, Bharuch, December 27-30, 2006.
5. Raghuvanshi, S., Babu, B.V., 2008. Experimentation and Evaluation of Growth Kinetic Parameters for Biodegradation of Methyl Ethyl Ketone (MEK). Proceedings of 18th International Congress of Chemical and Process Engineering (CHISA-2008), Prague, Czech Republic, August 24-28, 2008.
6. Raghuvanshi, S., Babu, B.V., 2008. Biodegradation Kinetic Studies for the Removal of Iso Propyl Alcohol (IPA). Proceedings of International Symposium & 61st Annual Session of IIChE in association with International Partners (CHEMCON-2008), Panjab University, Chandigarh, December 27-30, 2008.
7. Raghuvanshi, S., Babu, B.V., 2009. Removal of isopropyl alcohol from air stream using biofiltration". Proceedings of International Symposium & 62nd Annual Session of IIChE in association with International Partners (CHEMCON-2009), Andhra University, Visakhapatnam, December 27-30, 2009.

National Conference Proceedings

1. Raghuvanshi, S., Babu, B.V., 2006. Removal of Methyl Ethyl Ketone (MEK) using Biofiltration. Proceedings of National Conference on Environmental Conservation (NCEC-2006), BITS-Pilani, September 1-3, 2006, pp. 665-669, 2006.

BIOGRAPHIES

Biography of the Candidate

Smita Raghuvanshi has completed her B.Tech in Chemical Engineering from Beant College of Engineering and Technology, Gurdaspur in the year 2001. She obtained her M.E. degree in chemical engineering from B.I.T.S. Pilani in the year 2003. She joined B.I.T.S. Pilani as an Assistant Lecturer in Chemical Engineering Group in June 2003 and currently she is working as a Lecturer in this institute. She has 6 years of teaching experience and has guided 2 Professional Practice –II students, 2 Thesis students and around 35 project students. She has taught courses such as Polymer Technology, Environmental Management Systems, Thermodynamics, Structure and Properties of Mateirlas and involved in the tutorials of Process Design Decisions, Chemical Process Calculations, and Heat Transfer Operations. Her research interests include separation processes (biofiltration, membrane techniques, etc.), environmental management, polymer engineering and modeling & simulation. She is the Life member of Indian Institute of Chemical Engineers (IIChE), and Fellow of International Congress of Chemistry and Environment (ICCE).

Biography of Supervisor

Dr B V Babu is Professor of Chemical Engineering and Dean of Educational Hardware Division (EHD) at Birla Institute of Technology and Science (BITS), Pilani. He did his PhD from IIT-Bombay. He is on various academic and administrative committees at BITS Pilani. He is the member of project planning & implementation committees of BITS-Pilani Dubai Campus, BITS-Pilani Goa Campus, and BITS-Pilani Hyderabad Campus. He is the Coordinator for PETROTECH Society at BITS-Pilani Campus. He is external expert member of Board of Studies at Banasthali University and MNIT-Jaipur. He is expert peer committee member of National Assessment and Accreditation Council (NAAC), Banglore, India. He is also member of Peer Review Committee for The Natural Sciences and Engineering Research Council of Canada (NSERC), Canada; and National Research Foundation (NRF), International Research Grants, South Africa.

He has 24 years of Teaching, Research, Consultancy, and Administrative experience. He guided 5 PhD students, 36 ME Dissertation students and 35 Thesis students and around 200 Project students. He is currently guiding 5 PhD candidates and 2 Thesis students. He is on doctoral advisory committee for 10 Ph.D. students. He currently has 4 research and sponsored projects from MHRD, UGC, DST & KK Birla Academy. He is PhD Examiner for 7 candidates and PhD Thesis Reviewer for 6 Candidates.

His research interests include Evolutionary Computation (Population-based search algorithms for optimization of highly complex and non-linear engineering

problems), Environmental Engineering, Biomass Gasification, Energy Integration, Artificial Neural Networks, Nano Technology, and Modeling & Simulation.

He is the recipient of National Technology Day (11th May, 2003) Award given by CSIR, obtained in recognition of the research work done in the area of 'A New Concept in Differential Evolution (DE) – Nested DE'. His paper entitled "Convective and Radiative Heat Transfer in Pyrolysis of a Biomass Particle" authored by A S Chaurasia, B V Babu, Amanpreet Kaur, and V Thiruchitrambalam, published in Indian Chemical Engineer Journal, Vol. 47 (No. 2), pp. 75-80, April-June, 2005 earned the Kuloor Memorial Award, 2006 awarded for the Best Technical Paper published in the Institute's Journal Indian Chemical Engineer" in its issues for 2005. His biography is included in 2005, 2006 & 2007 editions of Marquis Who's Who in the World, in Thirty-Third Edition of the Dictionary of International Biography in September 2006, in 2000 Outstanding Intellectuals of the 21st Century in 2006, and in First Edition of Marquis Who's Who in Asia in 2007.

He is the Life member of Indian Institute of Chemical Engineers (IIChE), Life member of Indian Society for Technical Education (ISTE), Life member of Institution of Engineers (IE), Fellow of International Congress of Chemistry and Environment (ICCE), Life member of Indian Environmental Association (IEA), Life member of Society of Operations Management (SOM), Associate Member of International Society for Structural and Multidisciplinary Optimization (ISSMO), Member of International Institute of Informatics and Systemic (IIIS), Member of International Association of Engineers (IAENG). Nine of his technical papers have been included as successful applications of Differential Evolution (DE: a population based search algorithm for optimization) on their Homepage at http://www.icsi.berkeley.edu/~storn/code.html#appl.

He has around 190 research publications (International & National Journals & Conference Proceedings) to his credit. He completed three consultancy projects successfully and he has been Technical Consultant for Maharashtra Electricity Regulatory Commission (MERC), Mumbai and offering Advisory Services in the "Study relating to Bagasse Based Co-generation". He also has been invited as a consultant by a Bahrain (Middle East) based company for making a complex of chemical factories. He is a Panel Expert for www.chemicalhouse.com the most vibrant and active site for the chemical industry on the net which specializes in exchange of information in a structured way among the chemical world in more than a Hundred Countries and a Million core chemical manufacturers traders scientists etc. He is Technical Consultant for Sangam (India) Limited Textile Industry at Bhilwara for Removal of Color, BOD, and COD from Effluent Treatment Plant.

He has published five books (1) "Process Plant Simulation", EDD, BITS-Pilani, 2002, (2)"New Optimization Techniques in Engineering", Springer-Verlag, Germany, 2004, and (3)"Process Plant Simulation", Oxford University Press, India, 2004, (4) "Environmental Management Systems", EDD, BITS-Pilani, 2005, (5) "Chemical Engineering Laboratory Manual", EDD, BITS-Pilani, 2006. In addition he has written several chapters and invited articles in various books, lecture notes, and International Journals. He was invited to write an editorial and for cover design on Conservation of Natural Resources, for December 2006 Issue of International Research Journal of Chemistry & Environment.

He was the Invited Chief Guest and delivered the Keynote addresses at three international conferences and workshops (Desert Technology–7, Jodhpur; Life Cycle Assessment, Kaula Lumpur; Indo-US Workshop, IIT-Kanpur; Indo-French Workshop, TERI-New Delhi; Indo-US Workshop, Kolkata; Research tools Workshop, BITS Pilani-Goa Campus; Process Modeling and Simulation Workshop, UPES-Dehradun) and three national seminars. He has organized many Seminars & Conferences at BITS-Pilani. He also chaired 20 Technical Sessions at various International & National Conferences. He delivered 43 invited lectures at various IITs and Universities abroad.

He is the Editorial Board Member of five international journals 'Energy Education Science & Technology', 'Research Journal of Chemistry and Environment', 'International Journal of Computer, Mathematical Sciences and Applications', 'Journal on Future Engineering and Technology', and 'International Journal of Applied Evolutionary Computation'. He is the referee & expert reviewer of 59 international journals. He is also on the Programme Committees at many (around 100) International Conferences. He reviewed five books of McGraw Hill, John Wiley & Science, Elsevier, Oxford University Press, and Tata McGraw Hill publishers.

He is the Organizing Secretary for "National Conference on Environmental Conservation (NCEC-2006)" held at BITS Pilani during September 1-3, 2006. He is also the Organizing Committee member (Publicity Chair) and Session Organizer for the Special Session on "Evolutionary Computation" at The Second International Conference on Computational Intelligence, Robotics, and Autonomous Systems (CIRAS-2003), National University of Singapore, Singapore, December 15 – 17, 2003. He is the Session Chair and Organized an Invited Session on "Engineering Applications of Evolutionary Computation Techniques" at "The Eight World Multi-Conference on Systemics, Cybernatics, and Informatics (SCI-2004)", Orlando, Florida, USA, July 18-21, 2004.

APPENDIX I

Code in Mat Lab for the periodic mode operated transient biofilter

% Matlab program for solving modeling equation of periodic mode operated transient biofilter column for the removal of MEK

```
N=1.35;          % power exponent value in biodegradation equation
kig=0.003;       % overall mass transfer coefficent, s^-1
mew=0.4e-3;      % rate constant of biofiltration process, s^-1
Km=0.025;        % saturation constant, g m^-3
m2=2e-3;         % partition coefficient of odor between gas and solid phase,
                 dimensionless
Dl=5e-5;         % dispersion coefficient, m^2 s^-1
eps=0.58;        % porosity of the bed, (-)
w=0.03;          % gas velocity, m s^-1
Cin=0.1;         % inlet VOC concentartion, g m^-3
t=1000;          % time of biofiltration, s
h=0.4;           % height of biofilter column, m
delt=0.05;       % time increment, s
delx=0.0125      % height increment, m
n=round(t/delt); % no. of time increments, (-)
m=round(h/delx); % no. of space increments, (-)
A= ((Dl*delt)/power(delx,2))-(w*delt/delx)
B= ((-2*Dl*delt)/power(delx,2))+(w*delt/delx)+1
D= (Dl*delt)/power(delx,2)

% Initial condition for bulk phase and solid phase biofiltration
for j= 2:m+1
   C(1,j)=0;
   q(1,j)=0;
end

% opening a file exp1 for saving the data in file
fid = fopen('exp1.txt','a+');

% Calculation of liquid phase and solid phase concentration with time and height
for i= 2:n+1
   C(i-1,1)=(w*delx*Cin+Dl*C(i-1,2))/(Dl+w*delx);
   for j= 2:m+1
      C(i-1,m+2)= C(i-1,m+1);
```

```
        C(i,j)= A*C(i-1,j+1)+B*C(i-1,j)+D*C(i-1,j-1)-delt*(((1-eps)/eps)*kig*((C(i-
        1,j)/m2)-q(i-1,j))-mew*(power(q(i-1,j),N)/(Km+q(i-1,j))));
        q(i,j)=delt*kig*(C(i-1,j)/m2)+q(i-1,j)*(1-delt*kig)-(mew*power(q(i-
        1,j),N)*delt)/(Km+q(i-1,j));
    end
    C(i,m+1)
end

for i=2:n+1
 if (mod(i,20)==0)
    fprintf(fid,'%12.8f  %12.8f\n',i*delt,C(i,m+1));
end
end
fclose(fid);
```

APPENDIX II

Code in Mat Lab for the periodic mode operated transient biofilter

% Matlab program for solving modeling equation of periodic mode operated transient biofilter column for the removal of butanol

```
N=1.5;              % power exponent value in biodegradation equation
kig=0.001;          % overall mass transfer coefficent, s^-1
mew=1.25e-3;        % rate constant of biofiltration process, s^-1
Km=0.555;           % saturation constant, g m^-3
m2=4e-4;            % partition coefficient of odor between gas and solid phase,
                    dimensionless
Dl=8.7e-6;          % dispersion coefficient, m^2 s^-1
eps=0.65;           % porosity of the bed, (-)
w=0.03;             % gas velocity, m s^-1
Cin=0.1;            % inlet VOC concentartion, g m^-3
t=1000;             % time of biofiltration, s
h=0.4;              % height of biofilter column, m
delt=0.05;          % time increment, s
delx=0.0125         % height increment, m
n=round(t/delt);    % no. of time increments, (-)
m=round(h/delx);    % no. of space increments, (-)
A= ((Dl*delt)/power(delx,2))-(w*delt/delx)
B= ((-2*Dl*delt)/power(delx,2))+(w*delt/delx)+1
D= (Dl*delt)/power(delx,2)

% Initial condition for bulk phase and solid phase biofiltration
for j= 2:m+1
   C(1,j)=0;
   q(1,j)=0;
end

% opening a file exp1 for saving the data in file
fid = fopen('exp1.txt','a+');

% Calculation of liquid phase and solid phase concentration with time and height
for i= 2:n+1
   C(i-1,1)=(w*delx*Cin+Dl*C(i-1,2))/(Dl+w*delx);
   for j= 2:m+1
      C(i-1,m+2)= C(i-1,m+1);
```

```
        C(i,j)= A*C(i-1,j+1)+B*C(i-1,j)+D*C(i-1,j-1)-delt*(((1-eps)/eps)*kig*((C(i-
        1,j)/m2)-q(i-1,j))-mew*(power(q(i-1,j),N)/(Km+q(i-1,j))));
        q(i,j)=delt*kig*(C(i-1,j)/m2)+q(i-1,j)*(1-delt*kig)-(mew*power(q(i-
        1,j),N)*delt)/(Km+q(i-1,j));
    end
    C(i,m+1)
end

for i=2:n+1
 if (mod(i,20)==0)
    fprintf(fid,'%12.8f  %12.8f\n',i*delt,C(i,m+1));
end
end
fclose(fid);
```

APPENDIX III

Code in Mat Lab for the transient biofilter operated in continuous mode

% Matlab program for solving modeling equation of transient biofilter operated in continuous mode for the MEK removal

```
t=1000;                 %time, s
As= 1.90;               %biofilm suface area per unit volume of the particle, cm^2 cm^-3
cio=0.1*10e-6;          %initial concentration of component i in the gas phase, g cm^-3
coo=2.75*10e-4;         %initial concentration of the oxygen in the gas phase, g cm^-3
DL=5*10e-1;             %dispersion coefficient, cm^2 s^-1
Di=2*10e-6;             %diffusivity of component, i, in the biofilm, cm^2 s^-1
Do=4.70*10e-6;          %diffusivity of oxygen in the biofilm, cm^2 s^-1
kads=3.0*10e-3;         %mass transfer coefficent of compont i between gas and solid
                        media, s^-1
kIi=78.94*10e-6;        %inhibition constant in the specific growth rate expression of
                        culture growing on a compound, g cm^-3
kiads=4.74e-4;          %mass tranfer coefficent of compont i between liquid and solid
                        media, s^-1
kmi=1.23*10e-6;         %constant in the reaction rate expression of culture growing on a
                        compound, g cm^-3
koi=0.26*10e-6;         % Constant in the specific growth rate expression of culture
                        expressing the effect of oxygen, g cm^-3
krxni= 9.72*10e-7;      %first order reaction rate constant of component i in the adsorbant,
                        s^-1
L=0.5;                  % Bed height, cm
m1i=2.70*10e-1;         % distribution coefficent of substance i in air/water system, (-)
m2i=2*10e-3;            %distribution coefficent of substance i in air/solid system, (-)
mo=3.44*10e+1;          %distribution coefficent of oxygen i in air/solid system, (-)
no=1;                   %order of reaction in the adsorbent (-)
rmaxi=0.0588;           %Constant in the reacton rate constant of component i (g cm^-3 s^-1)
rmaxoi=1.2228*10e-3;%Constant in the reacton rate constant of component i (g cm^-3 s^-1)
v=0.4;                  % interstitial gas velocity (cm sec^-1)
T=(v*t/L);              % time, (-)
alpha=3*10e-1;          % percentage coverage of the partical by the biofilm, (-)
del=3.76*10e-3;         % Biofilm thickness, cm
eps=0.58;               % porosity of the bed (-)

%define interval
dT=0.001;
dz=0.005;
dX=0.005;
```

```
% constant values
Pe=(L*v)/DL;
c1= (-2/(Pe*dz^2))+(1/dz)-(((1-eps)/eps)*((1-alpha)*kads*L)/(m2i*v));
c2= ((alpha*As*L*Di)/(m1i*del*v))*((1-eps)/(eps*dX));
c3= ((alpha*As*L*Do)/(mo*del*v))*((1-eps)/(eps*dX));
c4= kmi;
c5= (cio^2)/((m1i^2)*kIi*kmi);
c6= (koi*mo)/coo;
c7= Di*L/(v*del^2);
c8= Do*L/(v*del^2);
c9= cio/m1i;
c10= koi;
c11= coo/mo;
c12= ((1-alpha)*kads*L)/v;
c13= (alpha*kiads*L)/v;
c14= ((krxni*L)/v)*(cio/m2i)^(no-1);
c15= -(m1i*kiads*del)/(alpha*m2i*As*Di);
c16= rmaxi*L/v;
c17= rmaxoi*L/v;
c18= (1/(Pe*(dz^2)))-(1/dz);
c19= (1/(Pe*(dz^2)));
c20=(((1-alpha)*kads*L)/(m2i*v))*((1-eps)/eps);
c21=(-2/(Pe*dz^2))+(1/dz);

%no of intervels in each dimensions
n=round(T/dT);
m=1/dz;
p=1/dX;

% i= time, j= height, k=radius

%opening a file exp for saving the data in file
fid=fopen('exp.txt','a+');

% initial conditions in bulk phase and solid phase
   for j=2:m+1
      xi(1,j)=0;
      xo(1,j)=0;
      zi(1,j)=0;
   end

% boundary conditions in bulk phase
   for i=1:n+1
       xi(i,1)=1;
       xo(i,1)=1;
```

```
    end

% initial conditions for biofilm diffusion
    for j=2:m+1
      for k=1:p+1
          yi(k,j,1)=0;
          yo(k,j,1)=0;
      end
    end

% Calculation of substrate concentration and oxygen concentration in bulk phase, solid
phase, and biofilm
    for i=2:n+1,
      for j=2:m+1,
        yi(p+2,j,i-1)=(c15*dX*(xi(i-1,j)-zi(i-1,j)))+yi(p+1,j,i-1);
         yo(p+2,j,i-1)=yo(p+1,j,i-1);
        for k=2:p+1;
          yi(k,j,i)=(c7*(dT/(dX^2))*(yi(k+1,j,i-1)-2*yi(k,j,i-1)+yi(k-1,j,i-1)))-
          dT*((c16*yi(k,j,i-1)*yo(k,j,i-1))/(((c4*(1+c5*(yi(k,j,i-1)^2)))+(c9*yi(k,j,i-
          1)))*(c6+yo(k,j,i-1))))+yi(k,j,i-1);
          yo(k,j,i)=(c8*(dT/(dX^2))*(yo(k+1,j,i-1)-2*yo(k,j,i-1)+yo(k-1,j,i-1)))-
          dT*((c17*c9*yi(k,j,i-1)*yo(k,j,i-1))/(((c4*(1+c5*(yi(k,j,i-1)^2)))+(c9*yi(k,j,i-
          1)))*(c10+(c11*yo(k,j,i-1)))))+yo(k,j,i-1);
        end
      zi(i,j)=(dT*((c12+c13)*(xi(i-1,j)-zi(i-1,j))-(c14*zi(i-1,j)^no)))+zi(i-1,j);
      xi(i-1,m+2)=xi(i-1,m+1);
      xo(i-1,m+2)=xo(i-1,m+1);
      xi(i,j)=dT*((c18*xi(i-1,j+1))+(xi(i-1,j)*c1)+(xi(i-1,j-1)*c19)+(c2*(yi(2,j,i)-
     yi(1,j,i)))+(c20*zi(i,j)))+xi(i-1,j);
      xo(i,j)=dT*((c18*xo(i-1,j+1))+(xo(i-1,j)*c21)+(c19*xo(i-1,j-1))+(c3*(yo(2,j,i)-
     yo(1,j,i))))+xo(i-1,j);
      end
      yi(1,j,i)=xi(i,j);
      yo(1,j,i)=xo(i,j);
    end


for i=2:n+1
  xi(i,m+1)
  fprintf(fid,'%12.8f %12.8f\n',i*dT,xi(i,m+1));
end
fclose(fid);
```

APPENDIX IV

Code in Mat Lab for the transient biofilter operated in continuous mode

% Matlab program for solving modeling equation of transient biofilter operated in continuous mode for the butanol removal

```
t=1000;                 %time, s
As= 1.90;               %biofilm suface area per unit volume of the particle, cm2 cm-3
cio=0.1e-6;             %initial concentration of component i in the gas phase, g cm-3
coo=2.75*10e-4;         %initial concentration of the oxygen in the gas phase, g cm-3
DL=8.7*10e-2;           %dispersion coefficient, cm2 s-1
Di=2*85e-6;             %diffusivity of component, i, in the biofilm, cm2 s-1
Do=4.70*10e-6;          %diffusivity of oxygen in the biofilm, cm2 s-1
kads=0.001;             %mass transfer coefficent of compont i between gas and solid
                        media, s-1
kIi=56.73*10e-6;        %inhibition constant in the specific growth rate expression of
                        culture growing on a compound, g cm-3
kiads=4.74e-4;          %mass tranfer coefficent of compont i between liquid and solid
                        media, s-1
kmi=0.555*10e-6;        %constant in the reaction rate expression of culture growing on a
                        compound, g cm-3
koi=0.26*10e-6;         % Constant in the specific growth rate expression of culture
                        expressing the effect of oxygen, g cm-3
krxni= 9.72*10e-7;      %first order reaction rate constant of component i in the adsorbant,
                        s-1
L= 0.5;                 % Bed height, cm
m1i=2.70*10e-1;         % distribution coefficent of substance i in air/water system, (-)
m2i=4*10e-4;            %distribution coefficent of substance i in air/solid system, (-)
mo=3.44*10e+1;          %distribution coefficent of oxygen i in air/solid system, (-)
no=1;                   %order of reaction in the adsorbent (-)
rmaxi=1.25e-3;          %Constant in the reacton rate constant of component i (g cm-3 s-1)
rmaxoi=6.25*10e-4;      %Constant in the reacton rate constant of component i (g cm-3 s-1)
v=0.55;                 % interstitial gas velocity (cm sec-1)
T=(v*t/L);              % time, (-)
alpha=3*10e-1;          % percentage coverage of the partical by the biofilm, (-)
del=3.76*10e-3;         % Biofilm thickness, cm
eps=0.65;               % porosity of the bed (-)

%define interval
dT=0.001;
dz=0.005;
dX=0.005;
```

```
% constant values
Pe=(L*v)/DL;
c1= (-2/(Pe*dz^2))+(1/dz)-(((1-eps)/eps)*((1-alpha)*kads*L)/(m2i*v));
c2= ((alpha*As*L*Di)/(m1i*del*v))*((1-eps)/(eps*dX));
c3= ((alpha*As*L*Do)/(mo*del*v))*((1-eps)/(eps*dX));
c4= kmi;
c5= (cio^2)/((m1i^2)*kIi*kmi);
c6= (koi*mo)/coo;
c7= Di*L/(v*del^2);
c8= Do*L/(v*del^2);
c9= cio/m1i;
c10= koi;
c11= coo/mo;
c12= ((1-alpha)*kads*L)/v;
c13= (alpha*kiads*L)/v;
c14= ((krxni*L)/v)*(cio/m2i)^(no-1);
c15= -(m1i*kiads*del)/(alpha*m2i*As*Di);
c16= rmaxi*L/v;
c17= rmaxoi*L/v;
c18= (1/(Pe*(dz^2)))-(1/dz);
c19= (1/(Pe*(dz^2)));
c20=(((1-alpha)*kads*L)/(m2i*v))*((1-eps)/eps);
c21=(-2/(Pe*dz^2))+(1/dz);

%no of intervels in each dimensions
n=round(T/dT);
m=1/dz;
p=1/dX;

% i= time, j= height, k=radius

%opening a file exp for saving the data in file
fid=fopen('exp.txt','a+');

% initial conditions in bulk phase and solid phase
   for j=2:m+1
      xi(1,j)=0;
      xo(1,j)=0;
      zi(1,j)=0;
   end

% boundary conditions in bulk phase
   for i=1:n+1
       xi(i,1)=1;
       xo(i,1)=1;
```

```
    end

% initial conditions for biofilm diffusion
    for j=2:m+1
      for k=1:p+1
          yi(k,j,1)=0;
          yo(k,j,1)=0;
      end
    end

% Calculation of substrate concentration and oxygen concentration in bulk phase, solid
phase, and biofilm
    for i=2:n+1,
      for j=2:m+1,
        yi(p+2,j,i-1)=(c15*dX*(xi(i-1,j)-zi(i-1,j)))+yi(p+1,j,i-1);
         yo(p+2,j,i-1)=yo(p+1,j,i-1);
        for k=2:p+1;
          yi(k,j,i)=(c7*(dT/(dX^2))*(yi(k+1,j,i-1)-2*yi(k,j,i-1)+yi(k-1,j,i-1)))-
          dT*((c16*yi(k,j,i-1)*yo(k,j,i-1))/(((c4*(1+c5*(yi(k,j,i-1)^2)))+(c9*yi(k,j,i-
          1)))*(c6+yo(k,j,i-1))))+yi(k,j,i-1);
          yo(k,j,i)=(c8*(dT/(dX^2))*(yo(k+1,j,i-1)-2*yo(k,j,i-1)+yo(k-1,j,i-1)))-
          dT*((c17*c9*yi(k,j,i-1)*yo(k,j,i-1))/(((c4*(1+c5*(yi(k,j,i-1)^2)))+(c9*yi(k,j,i-
          1)))*(c10+(c11*yo(k,j,i-1)))))+yo(k,j,i-1);
        end
      zi(i,j)=(dT*((c12+c13)*(xi(i-1,j)-zi(i-1,j))-(c14*zi(i-1,j)^no)))+zi(i-1,j);
      xi(i-1,m+2)=xi(i-1,m+1);
      xo(i-1,m+2)=xo(i-1,m+1);
      xi(i,j)=dT*((c18*xi(i-1,j+1))+(xi(i-1,j)*c1)+(xi(i-1,j-1)*c19)+(c2*(yi(2,j,i)-
     yi(1,j,i)))+(c20*zi(i,j)))+xi(i-1,j);
      xo(i,j)=dT*((c18*xo(i-1,j+1))+(xo(i-1,j)*c21)+(c19*xo(i-1,j-1))+(c3*(yo(2,j,i)-
     yo(1,j,i))))+xo(i-1,j);
      end
      yi(1,j,i)=xi(i,j);
      yo(1,j,i)=xo(i,j);
    end


for i=2:n+1
  xi(i,m+1)
  fprintf(fid,'%12.8f %12.8f\n',i*dT,xi(i,m+1));
end
fclose(fid);
```